On the track of cellular ecology. Methodological improvements and contributions of single-cell phosphatase activity on the ecology of phytoplankton in Pyrenean lakes

Seguint el rastre de l'ecologia cel·lular. Millores metodològiques i contribucions de l'anàlisi individual de l'activitat fosfatasa a l'ecologia del fitoplàncton en estanys del Pirineu

Daniel Diaz de Quijano i Barbero

ON THE TRACK OF CELLULAR ECOLOGY. METHODOLOGICAL IMPROVEMENTS AND CONTRIBUTIONS OF SINGLE-CELL PHOSPHATASE ACTIVITY ON THE ECOLOGY OF PHYTOPLANKTON IN PYRENEAN LAKES

SEGUINT EL RASTRE DE L'ECOLOGIA CEL·LULAR. MILLORES METODOLÒGIQUES I CONTRIBUCIONS DE L'ANÀLISI INDIVIDUAL DE L'ACTIVITAT FOSFATASA A L'ECOLOGIA DEL FITOPLÀNCTON EN ESTANYS DEL PIRINEU

Daniel Diaz de Quijano i Barbero

2014

TESI DOCTORAL

Departament d'Ecologia

Universitat de Barcelona

Programa de doctorat: Ecologia fonamental i aplicada

Bienni: 2004-2006

On the track of cellular ecology. Methodological improvements and contributions of single-cell phosphatase activity on the ecology of phytoplankton in Pyrenean lakes.

Seguint el rastre de l'ecologia cel·lular. Millores metodològiques i contribucions de l'anàlisi individual de l'activitat fosfatasa a l'ecologia del fitoplàncton en estanys del Pirineu.

Memòria presentada per en Daniel Diaz de Quijano i Barbero per tal d'optar al grau de doctor per la Universitat de Barcelona

Daniel Diaz de Quijano i Barbero

Sants, juny de 2014

Vist-i-plau de la directora de la tesi

Marisol Felip i Benach

Professora del Departament d'Ecologia

Universitat de Barcelona

“We may be able to substitute nuclear power for coal, and plastics for wood, and yeast for meat, and friendliness for isolation—but for phosphorus there is neither substitute nor replacement.”

ISAAC ASIMOV

***Asimov on chemistry*, 1974**

“El arte de vencer se aprende en las derrotas”

SIMÓN BOLÍVAR

Als meus pares

Als qui estimen

Als ecòlegs que vindran i que també viuran el canvi global

AGRAÏMENTS

Al llarg d'aquests anys de tesi, de tant en tant, pensava en el moment d'escriure els agraïments. "Segur que t'oblides d'algú", pensava. La Marta, un dia em va dir que ella també creia que s'oblidaria d'algú i que havia pensat de fer un dibuix amb molta gent, i que cadascú s'hi sabés trobar. Bé... jo de dibuixar no en sé, així que aquí em llanço, amb les paraules, i perdoneu si m'he descuidat d'escriure algú, en el cor de paper sí que hi sou tots i totes.

Crec que hi ha quatre persones, a més de jo, que han viscut aquesta tesi en primera fila. La Marisol, el Papa (el meu, no el de Roma, és clar!), la Mama, i la Mireia.

Marisol, gràcies per aquests anys. N'hem passat de tots colors, oi? Les campanyes nocturnes maratonianes, de vegades amb en Quim quan encara deia "fita" a la seva manera, amb els vídeos de l'Èlia, amb l'Eliseu. Jo he de dir una cosa. Si no fos per la teva paciència, capacitat de percebre què em passava a cada moment i dedicació professional i personal, és ben segur que no hauríem arribat a acabar la tesi. Amb una altra persona com a directora, és probable que no haguéssim arribat a aquest port. Jo sóc conscient que he estat un doctorand difícil, bé, no sé si n'hi ha gaires que siguin "fàcils", però sigui com sigui, gràcies per acompanyar-me en aquest camí.

Papa! n'hem parlat tantes vegades, de la tesi! Hehe. Quan et vaig dir que ja havia acabat d'escriure i em vas respondre pel whatsapp que t'havien saltat les llàgrimes d'emoció i que estaves conduint, vaig pensar "aix! Que encara tindrem un disgust!" Hehe. Els testos se semblen a les olles... Moltes gràcies pel suport. Incondicional, encara que de vegades no ho he sabut reconèixer. Gràcies pel suport. Gràcies pel suport. I gràcies per l'evolució i per l'amor i la llibertat.

Mama! Bonica! No sé com dir-ho. Estàs tan a dins del meu cor, i sempre has estat tan i tan al costat dels tres germans, recolzant-nos i ajudant-nos en tot, que el que som i el que fem no s'entén sense tu, "que ens ajudes i ens entens en tots els mals, i els bons, moments". Fas els millors somriures que conec, i quan et vaig dir que ja havia acabat d'escriure també me'n vas fer un. Un dels meus éssers de llum.

Mireiutxi, bonica. Moltes gràcies a tu també. Gràcies pel teu amor, com l'aigua de les Païtides, transparent, fresc, abundant, d'un doll que no s'acaba. Són mil coses: el cafè davant de "Il incontro", l'hostal ELF al qual no vam

anar, el teatre fluorescent, Oussouye, Crna Gora i el Karabakh. L'Àvia i el Porto que s'acabava a la sobretaula de diumenge, el Poto, la guitarra i la casa a Palautordera, en Roger, bonic i benvolgut! I en Xavier i la Mireia, i en Francesc i la Carme. Són mil coses, i n'és una de sola: que tu ets casa. Moltes, moltes, moltes, moltes gràcies.

Els germanets. Maria i David, que també porteu aquesta llum. Gràcies per l'exemple de persona, la il·lusió de viure, la consciència, l'atenció, la companyia, l'acollida, les aurelles ben parades per escoltar i els braços oberts per abraçar.

I a l'estany Redon. Gràcies per la teva pau. Sí, ja ho sé que et visiten les tempestes d'aquí i d'allà, del sud i del nord, però tot i així: la pau. I els estels. D'entre els molts moments, en guardo dos de ben guardats. Aquell del principi en què vaig remar entre els estels, en silenci, en una nit d'estiu que no feia vent. El segon va ser al final, acabades les campanyes, i en temps de descompte, et vaig poder venir a visitar i en silenci em vas fitar als ulls i acollidorament em vas dir "va Dani, endavant, continua".

I és clar, la gent del Departament i de més enllà del Departament. Els del principi. La Iraima, la Tura, en Pau, la Núria Cid, en Salva, en Raúl, la Blanca, en Cesc, la Núria S, i l'Oriol, la Gemma i en Carles, amb qui vam estudiar plegats. Que van acceptar que en una festa de fruites jo em sentís més gos que fruita, Bracons, i l'elecció de l'hereu i la pubilla en el dia de Maria, Mare de Déu. La Paula i la Pati, i també la Jordina i tots aquells que hem buscat i que hem dibuixat el nostre camí travessant fronteres que no hem entès mai. Els de l'ARDA-Muntu, l'Armonia, en Ferran, el Miquel i la colla, i el sentit de la vida. La Bartrons, la Gemma, en Javi, i la Neus i els ànims que transmet, els marrecs i en Jarone,. Els del mig. La Bet, amb les seves paraules sempre positives, confident en els meus mals tràngols a la vora de la mort, l'Eusebi i els seus consells, el Julio i l'eco-antropologia religiosa de cada dia, la Lidia, l'Esther i les cerveses als xinesos, el Jaime, l'Alba, la Mary, la Isis i la Suen San. I la Marta dels Roscons quadrats i la consciència nítida, i en Gonzalo, que em va somriure i em va acompanyar a carregar 30 Kg de microbis, sense bateria al cotxe, i em va salvar la vida. La Leticia i l'Àngels, i les seves converses de nit en tornar a casa. L'Olga i la seva energia, la vida, el cafè licor i el que és capaç de fer amb els colors del blau, els pic-nics sota el Sol entre setmana, el Pallars, les places de diumenge i els carrers plens d'esperances. La Gemma Cots, periodista, en Ferran i en Jordi i els caps de setmana *chingons* i les nits

llargues. La Maria Barretina i la Laia, que em van dur al Pallars a una missa amb gintònic quan a mi més em calia, la Marta i la força de riure, la gent circum-CREAF i l'Amanda, l'Helena, l'Alicia, i totes les de la coope. I també els de més cap al final, en Pau transparent i simpàtic, l'Ada que és tota bondat, la Sílvia sempre a punt, quin riure, la Núria C, la de C, en Lluís, en Pol, l'altre Pol, l'Eneko, en Max, la Txell, la Redolta, l'altra Txell, l'Aurora, la Lupon, la Mari, els hapi ouers, la Claudia, i tota la colla. Els de Kung Fu i les seves històries. El Jordi, l'Elisenda, i la tropa. Taký děkujeme moc všechno lidé z České Budějovice: Vojta děkuju moc moc pro tvoje pomoc s Favorit červené kolem a pro všechno, Jana, Jirka, Znachy, Jitka, Jitka a Jan, Karlos děkuju že ty vyučoval mě MAR a ukázal mě taký Šumavký topinky, Alena a Martina. Děkujeme Karel a Jarda. Máte hezký věd kolektiv. Děkujeme moc Alena pro velikonoční vejce, pro tvoje velký nitro. A ještě jednou, omlouvám se že moc nemluvím český. Doufejme já budu jednou!! I... en un altre pla, gràcies també tots els àngels de la guarda que habiten el CRAM, sense els quals, la immortalització de l'activitat fosfatasa del Pirineu no hagués pogut ni començar. Lluís, Marc, Carlos, et dec unes cerveses, Ramón, Montse, Maddi, i tota la resta.

Amén.

Sants, vila assetjada, Barcelonès, Països Catalans

Maig de 2014

TABLE OF CONTENTS

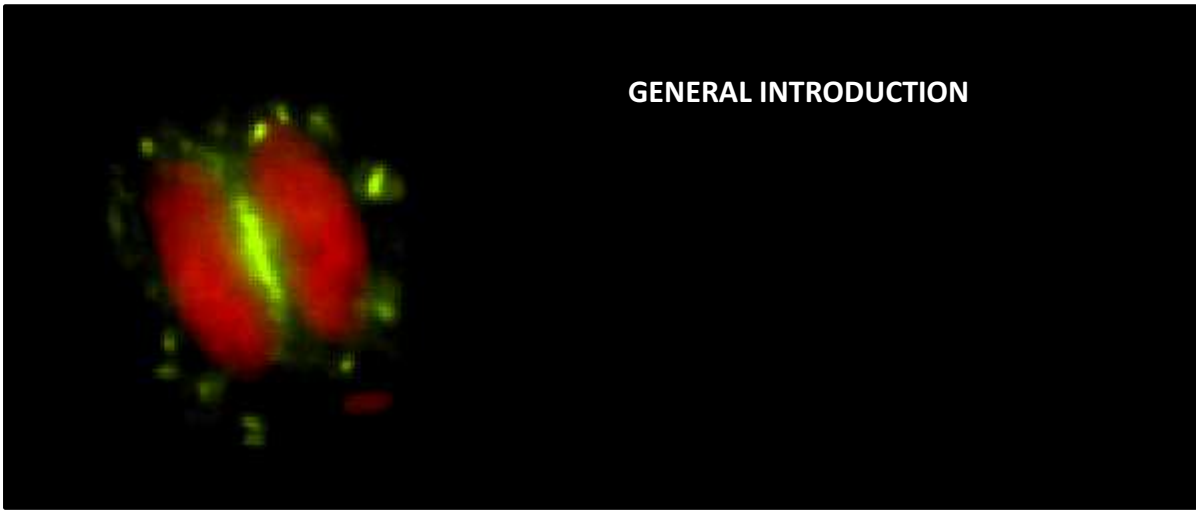

GENERAL INTRODUCTION

1. PHOSPHORUS.

1.1 The limiting factor concept. What governs the primary production and biomass of phytoplankton?

The determination of the factors that limit primary production and the biomass of primary producers has occupied aquatic and terrestrial ecologists since the early times of their disciplines. The concept of a factor limiting populations' growth was developed by the agronomist Carl Philipp Sprengel, who formulated the first law of the minimum: "…when a plant needs 12 substances to develop, it will not grow if any one of these is not available in a sufficiently large amount as required by the nature of plants" (1828). Embedded in a cultural environment like the one that Max Weber described in *Die protestantische Ethik und der Geist des Kapitalismus* (1905), the aim of this German evangelist was to use the agricultural chemistry to lead the agriculture *to the highest perfection*. The law of the minimum was later popularised by the also German evangelist and agronomist Justus von Liebig, who used the simile of a barrel with staves of different length to explain the law of the minimum. The barrel's capacity (plant growth potential) was limited by the length of the shortest stave (the scarcest nutrient or limiting factor). By lengthening it, the barrel's capacity increases until the following shortest stave. Liebig completed the mineral theory of plant nutrition, added non-nutrient factors like light and temperature to a reformulated law of the minimum (von Liebig, 1855) and established the early industry of mineral fertilizers. Some decades later, the oceanographer Karl Brandt proposed that the growth of oceanic phytoplankton was ruled by the law of the minimum (Brandt, 1899). Based on very scant nutrient values, he mimicked terrestrial conclusions and proposed nitrogen (N) as the limiting factor.

The history of research on the limiting factors of phytoplankton passed through the distinction of growth and biomass, the debate about how many limiting factors are there, the contributions of different methodological approaches, and the determination of the limiting factor(s). Firstly, the biomass increase is the net primary production (photosynthesis minus algal respiration) minus loss terms (grazing, sedimentation and cell death), so the study of factors limiting primary production work in an ecophysiological sphere whereas the limitation of biomass involves a wider range of ecological processes. The use of the expression *growth rate* led to confusion in the first studies and beyond. Regarding the number of limiting factors,

Liebig's law of the minimum states there is just a single nutrient (or factor) limiting growth in a certain moment. This contributed to focus efforts in understanding the role of certain key nutrients. Nevertheless, since the early application of the law of the minimum to phytoplankton growth, critical voices like that of Gebbing arose to say that *one singular cause does not exist in Nature* (Gebbing, 1910). A generalised co-limitation of oceanic phytoplankton by phosphorus (P) and N was accepted by the scientific community in 1929 thanks to the data collected with a new generation of chemical analysis (see Harvey, Atkins, Wattenberg and Brandt *in* de Baar, 1994). Finally, a multiple limitation hypothesis, based in microeconomic analogies and cost-benefit analysis, suggested that all resources limit growth at the same time (Bloom *et al.*, 1985; Gleeson & Tilman, 1992). According to this hypothesis, a plant (or algae) limited by one resource invests more efforts in acquiring it and less in the others, which leads to a dynamic balance where all the resources are equally limiting. Here, a carbon-limited or light-limited plant would invest in the aerial part whereas a N-limited plant would develop the roots. Although the interest of such hypothesis, it is not strictly met because different nutrients have specific biological functions that make them not easily interchangeable and because a limited number of resource acquisition strategies, that usually affect more than one resource at the same time, hinders a perfect co-optimization for the multiple required resources. Nowadays, the Liebig's law of the minimum is still used due to its simplicity to design experiments on the role of nutrients in phytoplankton growth, and to transfer simple and concrete advices to the managers of aquatic ecosystems. Nevertheless, it is generally accepted that the concept of a single limiting factor is an oversimplification of a complex combination of co-limiting factors. The occurrence of multiple co-limitation at the community and population level is explained by the fact that: (1) different species may have different structural nutrient requirements, different activities of nutrient procurement, different strategies like dormancy and encystment, and different capabilities to substitute one nutrient for another to achieve the same function (Van Mooy *et al.*, 2009), and (2) different individuals in a population may also be in different stages of the cell cycle, or have different nutritional histories. Therefore, it is thinkable that the answer to "how many nutrients are limiting phytoplankton growth?" may depend on the level of analysis (community, population or individual cell).

1.2 Methods for assessing nutrient limitation

Phytoplankton is responsible of a half of the primary production in the world, which makes it a key agent in the regulation of aquatic food webs and biogeochemical cycles (Falkowski *et al.*, 2004). Therefore, the understanding of the factors limiting phytoplankton has been a topic in aquatic ecology and has promoted the development of different methodological approaches: chemical analyses of nutrients, nutrient additions and biochemical or molecular indicators (Goldman, 1972; Petersson, 1980; Falkowski *et al.*, 1992; Beardall *et al.*, 2001). Chemical analyses of dissolved nutrients in water have been used to identify limiting macronutrients in meso-eutrophic ecosystems. Unfortunately, this nutrient supply approach doesn't inform about the bioavailability of the measured nutrients, sometimes lacked an assessment of nutrient turnover times, and used to face problems in the detection levels of certain nutrients or micronutrients in oligotrophic waters. In those cases, aquatic ecologists tended to consider undetectable nutrients as limiting, although the high affinity for determinate nutrients estimated in some phytoplankton species indicates they could supply their requirements even under the detection limits of chemical analyses (Catalan, 2000). The content of nutrients of the phytoplankton fraction in natural ecosystems has been compared to that of cultured algae known to be P-starved, but different species have different minimum quotas and not all the species are cultivable, so extrapolations to the bulk community are tricky. Additionally, luxury consumption and storage of nutrients, or adsorption of certain nutrients in the phytoplankton fraction may alter its values regardless of biological limitation (Sañudo-Wilhelmy *et al.*, 2004). Finally, nutrient ratios between dissolved and particulate (as an estimate of living particulate matter) fractions have also been used to identify the limiting factors and key trophic strategies of organisms (e.g. Hassett *et al.*, 1997; Teubner, 2003; Teubner *et al.*, 2003).

A second family of methods for the study of nutrient limitation is the enrichment experiment. They are more sensitive than the previous approach when nutrients are below the detection limits and include a notion of the metabolic activity. Different levels of assays have been used, from the most artificial (incubation of a cultured standard organism in the filtered water sample with a nutrient addition), through nutrient enrichment of natural phytoplankton communities in the laboratory or in mesocosms, and to the most complex experimental nutrient addition to a whole lake. On the one

hand, the higher the level of the enrichment experiment, the more applicable it is to natural ecosystems, but on the other hand longer incubation times used in these mesocosm or ecosystem-wide enrichments hinder the interpretation of results because changes in the composition of phytoplankton communities occur. A variety of response variables has been used in enrichment experiments with different sensitiveness and results: cell abundance, oxygen, pH or pigment evolution, and ^{14}C incorporation.

A series of different biochemical or molecular indicators believed to be specific to a certain nutrient limitation have been explored in the last decades: enzymatic activities, nutrient uptake kinetics (Rhee, 1978), pigment ratios, nucleic acids (protein:RNA, RNA:DNA, DNA:Carbon, etc.), membrane transporters or other kinds of proteins synthesized under a certain nutrient starvation, and nutrient-induced fluorescence transients (NIFTs). A discussion on the pros and cons of the different indicators could focus on its sensitivity, nutrient specificity, capability to provide quantitative and/or taxon-specific information, and taxonomic range of applicability (Scanlan & Wilson, 1999; Beardall *et al.*, 2001). For example, the most used P-limitation indicator until the date is probably phosphatase activity because it was early suggested (Kuenzler & Perras, 1965), it is present in a wide range of phylogenetic lineages, it's relatively simple to assess, provides quantitative data, and species-specific information.

1.3 So, which factors are limiting?

Going back to the identity of the limiting factor(s), N was believed to limit oceanic phytoplankton at the beginning of the XXth century, and a N and P co-limitation was proposed later (1929). In 1934, Redfield published an impressive seminal paper where the seston of the Atlantic, Pacific and Indic oceans followed a constant C:N:P ratio of 106:16:1 (Redfield, 1934). Later on, it was found that the synthesis of proteins and rRNA in prokaryotes and eukaryotes converges to a homeostatic ratio that implies an N:P ratio very close to 16:1 under non-limiting conditions (Loladze & Elser, 2011). The generalised use of pentasodium triphosphate in detergents after World War II (Gilbert & De Jong, 1977) caused increasing problems of eutrophication and a renewed interest for the understanding of phytoplankton limiting factors. Limnological studies flourished in the late 1960's until the mid-1970's without any clear consensus. Commercial interests supported C as the

limiting factor in lakes, but by the late 1970's there was so much evidence of P limitation in lakes, that it was considered by management policies. Observational studies compared multiple lakes and analysed trends in certain lakes, nutrient enrichment experiments were performed at different levels, and deductive reasoning about general biogeochemical cycles led to consider lakes to be generally P-limited. Studies in the Experimental Lake Area (ELA), such as whole lake enrichment experiments (Schindler *et al.*, 1974; Schindler, 1975) or correlations found between mean annual chlorophyll and P concentrations independently of the N:P (Schindler, 1977), left their stamp on this topic. At that time, the accepted paradigm recognised lake and marine phytoplankton to be P- and N-limited respectively (Ryther & Dunstan, 1971; Schindler, 1977; Hecky & Kilham, 1988). Following studies improved the marine part of the paradigm in geographical resolution: P-limited areas were identified in the Mediterranean, the North Pacific Sub-tropical Gyre, the Sargasso Sea and the central, and northwestern Atlantic (Krom *et al.*, 1991; Thingstad *et al.*, 1998; Karl, 1999; Guildford & Hecky, 2000; Wu *et al.*, 2000; Sañudo-Wilhelmy *et al.*, 2001; Vidal *et al.*, 2003), and Fe-limited areas in the collar of the Antarctic Ocean, subarctic Pacific and equatorial Pacific. Although little is known about Fe limitation in inland waters, it deserves a special comment. Decades of research passed from the first suggestion that Antarctic phytoplankton was Fe-limited (Gran, 1931) to the workshop of the US National Research Council, in 1989, where Fe fertilization of the high nutrient low chlorophyll areas (HNLC) regions was suggested to remove fossil fuel CO_2 from the atmosphere. Such controverted episode in the history of phytoplankton limiting factors motivated a formal resolution of the special 1991 ASLO symposium calling on all the governments not to consider such a policy (Chisholm & Morel, 1991, p. viii).

Deconstruction of the lake phosphorus limitation paradigm.

The position of P as the first order limiting factor in lakes has been challenged by two groups of candidates: N and the other macro- and micronutrients. Prior to the establishment of the P limitation paradigm for lakes, a series of studies had already highlighted micronutrient limitation in oligotrophic lakes of high altitude or latitude (molybdenum; Goldman, 1960, 1972) and a marl lake (iron; Schelske, 1962), as well as silicon limitation in diatoms (Lund *et al.*, 1963). Additionally, freshwater phytoplankton living

under extreme pH conditions was found to be C-limited (Stumm & Morgan, 1970; Ohle, 1981). This set of findings printed a range of tones to the picture of P-limited lakes –and N-limited oceans, as far as they were also applicable to oceans (Nelson & Tréguer, 1991; Reinfelder *et al.*, 2000; Spilling, 2007). Although they all are important, Si limitation is not universal (diatoms and chrysophytes), C may limit only in concrete situations with extreme pH, and unfortunately, micronutrient limitation in lakes has not been sufficiently explored yet (despite available data suggest it plays an important role; Chang *et al.*, 1992; Evans & Prepas, 1997; Vrede & Tranvik, 2006). On the other hand, the role of N as a possible limiting factor in lakes was never completely abandoned. Despite defending that P was ultimately limiting the primary production, Margalef early highlighted that a lag in the adjustment of N to P cycles led to N limiting situations and occurrence of cyanobacteria in lakes, so that N had to be considered too (Margalef, 1983). According to him, the P limitation was a specific case in the Canadian lakes, not to be extrapolated Earth-wide. For instance, tropical lakes are known to be usually N-limited (Talling & Lemoalle, 1998). Supporting the double limitation, most of the enrichment experiments in the literature attained maximum phytoplankton growth when P and N were added at the same time (e.g. Elser *et al.*, 1990). Moreover, the sigmoidal correlation between TP and TN in lakes (high TP lakes are not met with sufficient TN to keep the TN:TP) defines a range of TP between 10 $\mu g \cdot l^{-1}$ and $1 mg \cdot l^{-1}$, where lakes can be P-limited, N-limited or both (Sterner, 2008). Note that according to this stoichiometric approach, oligotrophic lakes with TP < 10 $\mu g \cdot l^{-1}$ are the sort of ecosystem where the P limitation paradigm is more easily met. Finally, the general notion that primary producers are limited by P and N has been successfully contrasted across freshwater, marine and terrestrial ecosystems (Guildford & Hecky, 2000; Elser *et al.*, 2007).

Influence of the atmospheric nutrient deposition

An interesting turn in the debate of nutrient limitation was set when Bergström and Jannsson proposed that the anthropogenic increase in the deposition of atmospheric N shifted many European and North American lakes from historical N limitation to contemporary P limitation (Bergström & Jansson, 2006). Dinitrogen (N_2) is the most abundant component in the atmosphere, but it has a low reactivity. More reactive forms include oxidized

NO_x, N_2O, and reduced NH_x, which are emitted by fossil fuel combustion, industrial agriculture and livestock production. These components are the protagonists of a wide-range atmospheric communication that is established between emitting areas and terrestrial and aquatic ecosystems that receive them via rain, snow and dry deposition. Then, the deposition map depends on the geographical distribution of emitting areas, changes in the wind, rain and snow regimes, and the magnitude of emissions (Lamarque *et al.*, 2013). The effects of this deposition are also dependent on the receiving ecosystem: N-limited ecosystems would increase their productivity whereas oligotrophic ecosystems would need smaller amounts of atmospheric N to suffer changes in their stoichiometries and nutrient dynamics. Synergistic effects between atmospheric N deposition and other elements of the global change rely on the facts that N deposition depends on the rain and snow distribution, and that oceanic oligotrophy due to a reinforcement of the thermocline is being expanded with climate warming (Sarmiento *et al.*, 2004). In conclusion, oligotrophic lakes, sensitive to increases in temperature and placed in the northern hemisphere, such as high mountain lakes in the Pyrenees, are amongst the target ecosystems where classic P limitation may be a reflection of N deposition (Elser *et al.*, 2009). Nevertheless, an intermediate situation between N and P limitation rules the Pyrenean lakes due to regional deposition of P-rich Saharan dust in the Pyrenees (Camarero & Catalan, 2012), which evidences the importance of atmospheric deposition in changing the nutrient limitation dynamics in lakes.

1.4 The phosphorus cycle in lakes

The interest of ecologists in the P cycle is based on the important biological functions it plays and on the relatively scarcity of P in the ecosystems. Phosphorus is a component of different molecules that are essential to all the living organisms and play different roles along the whole cell cycle. These functions include: the transmission of genetic information (DNA), genetic expression (RNA), cellular energy exchange (ADP, ATP, etc.), transport of reducing power in the cell (e.g. NADPH), signal transduction (cAMP, cGMP, phosphorylated forms of phosphatidylinositol, etc.), activation, inhibition and general regulation of receptors and enzymes (phosphoproteins), diverse functions as vitamins and cofactors, constituting membranes

(phospholipids), or just as storage forms and phosphorylated intermediate compounds of different metabolic pathways (sugar phosphates).

Phosphorus is present in lakes in a wide variety of chemical forms that can be classified as organic or inorganic, and dissolved, colloidal or particulate forms. Particulate P forms may be organic (mainly living and dead cells) or inorganic (minerals mainly based on ferric phosphate and calcium phosphate –but also combined with aluminium, fluorine and chlorine- and eventually adsorbed onto clays or organic material). Colloidal or condensed P also has an inorganic (pyro- meta- and polyphosphates) and an organic fraction (e.g. ATP, phosphonates, etc.). Finally, dissolved forms include strict dissolved inorganic phosphorus (DIP) or orthophosphate (PO_4^{3-}, HPO_4^{2-}, $H_2PO_4^-$), and a variety of dissolved organic phosphorus molecules (DOP). Phosphorus in organic molecules may be directly bounded to a C atom (C-P) forming a phosphonate (either biogenic like phosphonoproteins and membrane phosphonolipids and phosphonoglycolipids, or synthetic like e.g. glyphosate) or by one, two or three ester bounds (C-O-P) forming phosphomonoesters (e.g. ATP), phosphodiesters (e.g. nucleic acids and phospholipids) and phosphotriesters (Fig. 1). Nevertheless, P in lakes is usually assessed using chemical analyses that distinguish dissolved from particulate forms and its reactiveness to acidic hydrolysis, but do not perfectly match the previous classification. The routinely measured compartments are: total phosphorus (TP), total dissolved phosphorus (TDP), and soluble reactive phosphorus (SRP) (Fig. 2). Strictly, the two measurements of the dissolved phase also include some colloidal P that passes through the filter into the filtered sample, and SRP uses the term “reactive” because although it is mostly dissolved inorganic orthophosphate (DIP), some organic molecules also directly react with molybdate and are included into the SRP value, while some inorganic (like polyphosphates) do not. Soluble unreactive phosphorus (SUP) is calculated as SUP= TDP-SRP, and includes most of the dissolved organic phosphorus (DOP) and polyphosphates. Particulate phosphorus (PP) is calculated as PP=TP-TDP, and includes all the organic and inorganic particulate and colloidal P that was retained on the filter. In Redon lake, in the Pyrenees, the annual average P fractionation in the water column is PP (70%) and TDP (30%), of which 41% is DOP and 59% is SRP. To sum up, the filtration of a solution of molecules distributed along a continuum of sizes, and the specific characteristics of the digestion to extract non-reactive P provides analytical compartments that are different to strict DIP and DOP,

and that do not reflect bioavailable P (Boström *et al.*, 1988). Only some studies, usually focused on phosphatase activity, used enzymatic digestions or incubations to assess the pool of either organic or inorganic, colloidal and dissolved phosphomonoesters (Strickland & Solórzano, 1966; Chróst *et al.*, 1986). Up to a 10-50% of the SUP was found to be hydrolysable by phosphomonoesterases in the sea and lakes (Strickland & Solórzano, 1966; Herbes *et al.*, 1975). Other studies used phosphorus-31 nuclear magnetic resonance (^{31}P NMR) to characterize the proportions of dissolved P other than orthophosphates in the sea (phosphate esters, 80-85%; phosphonates, 5-10%; and polyphosphates, 8-13%) (Young & Ingall, 2010).

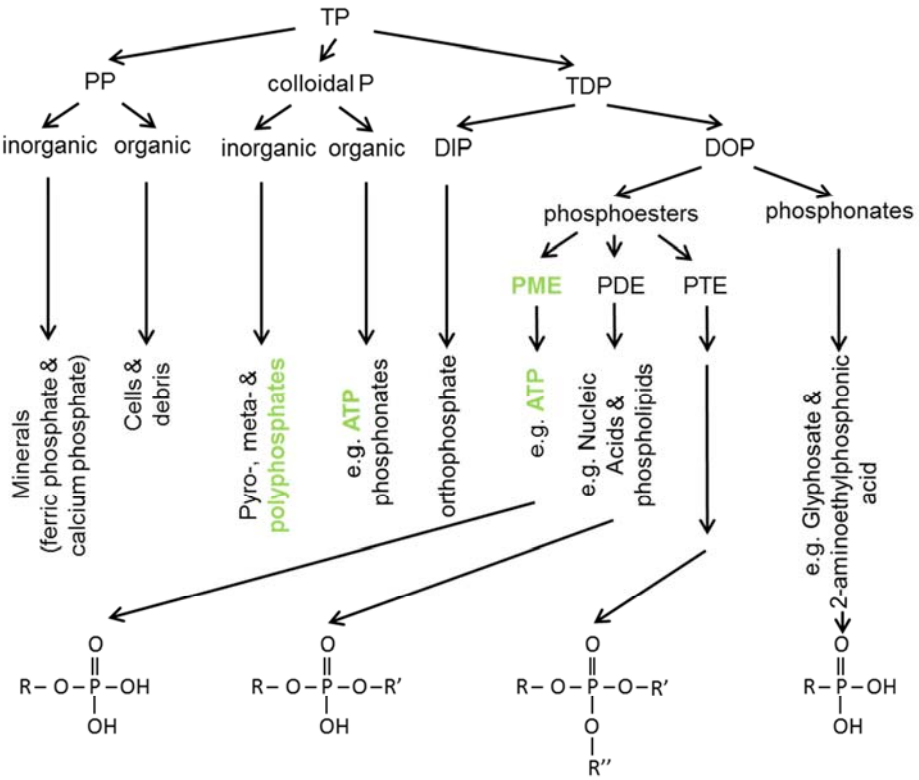

Fig. 1 Phosphorus fractions in lake water. Phosphomonoester (PME),phosphodiester (PDE), phosphotriester (PTE) and phosphonate general formulas.

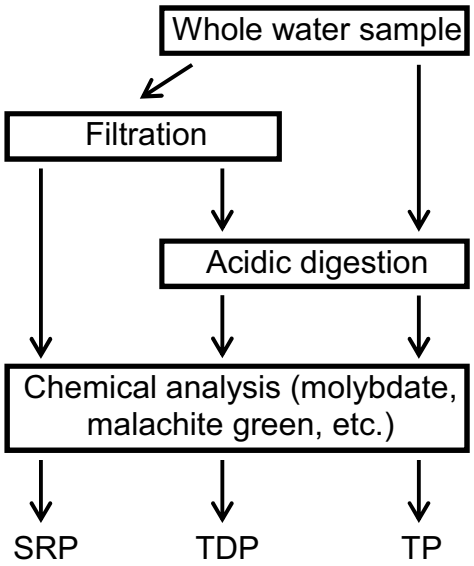

Fig. 2 Basic schema of the protocol for the routine analyses of P in lake waters.

One of the arguments raised to support the P limitation paradigm was based on an essential characteristic of the P cycle: P, unlike N and C, does not have any significant pool in the atmosphere for the primary producers to draw on (Wetzel, 1975; Schindler, 1977). This implies that P in lakes needs to be efficiently recycled and that it was ultimately originated via weathering of rocks and then transported by water across terrestrial ecosystems, soils and streams, or flown into the atmosphere as dust. External P inputs in the lake water are streams, runoff, aquifer, rain, snow and dry deposition. Generally, the majority of P in the epilimnion of lakes is particulate because dissolved forms are rapidly recycled. Zooplankton consumes particulate P and releases dissolved P, and phytoplankton releases low molecular weight organophosphates (organic compounds with P), which may condense into colloidal P. Colloidal P and DOP may be hydrolysed (either inorganically, catalysed by enzymes or in a combination of both) into dissolved orthophosphate that is rapidly incorporated by phyto- and bacterioplankton (Francko & Heath, 1979, 1982; Boavida & Wetzel, 1998; Tank *et al.*, 2005). Bacterioplankton has a double function: on the one hand as a source of remineralized DIP, and on the other hand as a means to recovering DOP and DIP into a PP pool bioavailable via bacterivory, i.e. the microbial loop (Pomeroy, 1974; Azam *et al.*, 1983). The slow losses of colloidal and

particulate P into the hypolimnion are replenished back via mixing of the water column, release from the sediments and the abovementioned external inputs (Wetzel, 1975). Another main difference between N and P cycles is that P species are almost always phosphates (valence +5) and it can only be reduced into PH_3 in a few concrete ecosystems (Margalef, 1997). Then, the chemical reactions affecting P species in the aquatic ecosystems involve basically the synthesis and hydrolysis of covalent bounds between phosphates and different (organic) molecules. This chemical reactivity and the fact that the source bedrock is usually poor in P makes happen that the bioavailability of P is determined by both, the recycling of organic P and the hydrolysis of organic into inorganic P (Schlesinger, 2000).

2. **PHOSPHATASE ACTIVITY IN PHYTOPLANKTON**

2.1 Introduction

Enzymes are proteins synthesized by the living beings to catalyse or accelerate biochemical reactions of synthesis and hydrolysis at rates sufficiently fast to sustain life. The presence of enzymes in the environment was firstly noted by Woods, who presented his studies in soils in the 1899 Annual Meeting of the American Association for the Advancement of Science (Skujiņš, 1978). This observation of enzymes, concretely proteolytic enzymes, was rapidly generalised to water pools (Fermi, 1906), but the lack of appropriate methodologies and basic knowledge on enzymes delayed the appearance of new studies of enzymes in the environment. Oxidases, catalases and catalysts of nitrate reduction and ammonia oxidation were suspected to be active in sea water (Harvey, 1925; Kreps, 1934). The presence and activity of phosphatases released by zooplankton and supporting phytoplankton blooms in lakes was firstly deducted and empirically demonstrated by the German biochemist Maximilian Steiner (Steiner, 1938). Phosphatases are a group of enzymes that hydrolyse esters and anhydrides of phosphoric acid, producing an orthophosphate and an organic (or inorganic) moiety. Steiner's idea of zooplankton recycling P via phosphatase activity (PA) was recovered by Margalef (Margalef, 1951), but the modern study of environmental phosphatases, with more appropriate techniques, was started by Jürgen Overbeck when he reported his early studies focused on the P metabolism of phytoplankton in the 1959 congress of the International Association of Theoretical and Applied Limnology

(*Societas Internationalis Limnologiae*; SIL). A series of rigorous studies in Overbeck's lab assessed bacterial and phytoplankton contributions to PA (reviewed in Overbeck, 1991), and culminated in the reference paper "free dissolved enzymes in lake waters" (Reichardt *et al.*, 1967). The following literature on PA has covered different environments (lakes, oceans, soils, biofilms, thermally extreme environments, etc.) and a diversity of ecological questions like for example the role of phosphatases in eutrophic ecosystems or its convenience as an indicator of P limitation. Changing methodological approaches combined with evolving interests and questions of the scientific community has triggered a series of different attributions and interpretations of PA.

In this study we will use the term phosphatase, as it has usually been used, to refer to the most studied subgroup of phosphatases: phosphomonoesterases or phosphomonoesterhydrolases. Phosphodiesterases (including nucleases) are a similar but different subgroup of phosphatases. Finally, phosphonate hydrolases are enzymes that also produce orthophosphoric acid but whose substrates are phosphonates (see Fig. 1 for general substrate formulas). As mentioned, the scientific community has basically focused on phosphomonoesterases due to a combination of available methods and evidence suggesting they play the main role. Phosphonates represent only the 3% of P in the plankton assemblage, but they are a 5-10% of dissolved molecules containing orthophosphate in marine environments, which indicates that their hydrolysis is less efficient than that of other organophosphates (Clark *et al.*, 1998; Young & Ingall, 2010). Nucleases (like RNase and DNase) are phosphodiesterases that cooperate together with 5'-nucleotidases and general phosphatases to recycle P from nucleic acids in aquatic ecosystems. RNase is thought to be very efficient because even if RNA constitutes about 10-20% of cell biomass, no dissolved RNA has been detected in lake water. On the other hand, DNA may contribute to a 10-60% of DOP in lakes, and although 5'-nucleotidases were found to be one or two orders of magnitude faster than general phosphatases, it is likely that this enzymatic pathway is limited by slow DNase rates (Chróst & Siuda, 2002). In conclusion, because phosphonates are scarce and phosphonate hydrolases and DNases are relatively slow, phosphatases are thought to be a keystone agent in the cycling of P, where they control most of its remineralization step. Only the

contribution of RNases could be comparable, but unfortunately much less is known about that.

2.2 Classification

Phosphatases could be classified according to a variety of criteria (molecular structure, phylogenetic distances, kinetic and thermodynamic parmeters, etc.), but we would like to comment two possible classifications that are relevant to the present study, in order to avoid misinterpretations. Phosphatases present in the environment have been roughly classified as alkaline or acidic, according to the pH range where they have their optimum activity rate. Because early studies found alkaline phosphatases to be more important in the studied algae and ecosystems (Kuenzler & Perras, 1965), the term alkaline phosphatase has been indiscriminately used in literature. Nevertheless, acidic phosphatases in the environment are sometimes important too, so that specific evidence should be provided to justify the term alkaline phosphatase. Our objective was to study PA at environmental pH, so (i) we did not perform assays at high pH (let's say above 8.0-9.0) to inhibit acidic phosphatases, (ii) we did not incubate the same sample at different pH to distinguish acidic from alkaline phosphatases, and (iii) we did not sequence phosphatase genes to compare them with genes of known pH optimum. For these reasons, and because many samples were at circumneutral pH, both, acidic and alkaline phosphatases have been studied and we will consequently use simply the term phosphatase and phosphatase activity (PA).

The second classification criterium is the position of phosphatases in the cell, which is important because it determines the biological and ecological functions they can do. Intracellular phosphatases have multiple structures, positions (e.g. in the cytoplasm and digestive organelles) and functions. Ectophosphatases are periplasmic or cell-surface-bound (on the cell membrane or cell wall) and interact with organophosphates outside the cell. These are the catalysts involved in the ecological interactions between the living organisms and their immediate environment. Finally, extracellular phosphatases are actively excreted or released by cell lysis to the environment, where they can be dissolved or adsorbed to mineral and/or organic seston (Chróst & Siuda, 2002). Both, extracellular and ectophosphatases share the same ecological role (hydrolyse

organophosphates) but have different implications for different organisms and it's interesting to treat them as separate phenomena. To mention two opposite cases, the relative distribution of PA in a typical eutrophic lake was 75% ectophosphatases, ~15% extracellular, and ~10% intracellular phosphatases (Chróst & Siuda, 2002), whereas the extracellular fraction, mostly originated by prokaryote excretion, dominated PA in the open ocean (57-97%), especially in the deep dark waters (Baltar *et al.*, 2010, 2013).

Although current data supports the idea that all combinations are possible (Wetzel, 1991; Nicholson *et al.*, 2006), it has been suggested that prokaryotes (especially when Gram-positive or associated to marine or lake snow) are prone to produce extracellular phosphatases whereas phytoplankton (and some planktonic or Gram-negative prokaryotes) rather tend to present ectophosphatases (Cembella *et al.*, 1984a; Azam & Smith, 1991; Overbeck, 1991). The high surface-to-volume ratio (S/V) in most prokaryotes makes them competitive in the uptake of dissolved hydrolysed phosphates, whereas the low S/V in phytoplankton may force them to retain phosphatases around the cell boundaries and improve their affinity for phosphate uptake (Fuhs *et al.*, 1972; Wetzel, 1975; Bentzen & Taylor, 1991). Finally, it is also thinkable that "dissolved" phosphatases excreted by prokaryotes were a strategy to avoid diffusional resistances and that either they remained associated to the original prokaryote cell by viscosity properties at such small scales (Lemke *et al.*, 1995; Catalan, 1999), or that they worked in a cooperative manner at the community level (Wetzel, 1991). The distribution of PA in some mountain lakes of the Pyrenees is summarized in table 1.

lake	**habitat**	**dissolved PA (nM/min)**	**particulate PA (nM/min)**	**dissolved PA (%)**	**particulate PA (%)**
Redon	water column (Summer)	1.115 (0.634-1.615)	1.537 (0.302-2.433)	54 (21-72)	46 (28-79)
Bassa d'Oles		0.684	0.015	98	2
Muntanyó d'Àrreu	DCM	0.033	0.782	4	96
Filià		0.167	0.073	70	30
Llauset		0.671	0.418	62	38
Botornàs		0.261	0.074	78	22
Redon	neuston	0.213	0.091	70	30
Bassa d'Oles		1.866	0.155	92	8
Redon	slush	0.819 (0.083-10.408)	0.559 (0.09-15.468)	57 (29-96)	43 (4-71)

Table 1. Distribution of dissolved and particulate PA in miscellaneous lake samples from the Central Pyrenees measured using a saturating concentration of substrate ([MUFP] = 300µM) and *in situ* pH and temperature conditions between 2005 and 2009. Median (minimum-maximum) values are reported for cases with multiple samples (Redon lake summer water: n=4; Redon lake slush: n=10).

2.3 The methodological prism.

Bulk methods

A series of evolving methods, original from the field of enzymology, have been transferred to the study of enzymes in the environment (see the Methods in Enzymology series for a complete exposition), but those most relevant for the study of phosphatases in aquatic ecosystems have been radioisotope methods, spectrophotometric and fluorometric methods. Radioisotope methods provide very valuable information that other methodologies don't provide: the influence of the molecular structure of the substrate is evaluable because a diversity of molecules that are relatively similar to natural substrates may be used and compared (e.g. glucose-6-phosphate, ATP, phytic acid, etc.; Hoppe, 2003), the actual uptake of hydrolysed phosphate is assessed (as a drawback its enzymatic hydrolysis is assumed rather than observed), and the fate of the organic moiety is also traceable. The colorimetric and fluorometric methods became popular thanks to their suitability to assess kinetic (and thermodynamic) parameters of enzymes, low price, low time consume and safer conditions for the users. The chromogenic substrate p-nitrophenyl phosphate (p-NPP) was early available and commonly used in aquatic ecosystems in the 1970s and 1980s, although some authors are still using it (Bessey *et al.*, 1946; Dignum *et al.*, 2004a; Mateo *et al.*, 2010). It supposed an easy way to assess PA via spectrophotometry. The advent of fluorogenic substrates improved the sensitivity of the former colorimetric substrates, which made possible to detect lower PA and to perform assays with short incubation times and substrate concentrations ranging from high saturating concentrations to low and close to *in situ* concentrations (Pettersson & Jansson, 1978). This avoided problems of contamination, synthesis of enzymes during the incubation, lack of signal at low activities or low substrate concentrations, and background at high substrate concentrations. Traditionally, the most

used fluorogenic substrates have been 3-O-methylfluorescein-phosphate (MFP) predominantly in marine environments (Hill *et al.*, 1968; Perry, 1972; Healey & Hendzel, 1979) and 4-methylumbelliferyl-phosphate (MUF-P or MUP) in both, freshwater and marine (Pettersson & Jansson, 1978).

Single-cell methods

The Enzyme Labelled Fluorescence (ELF; Molecular Probes Inc.) is a group of fluorogenic substrates for enzyme activity assays including PA. The ELF substrate for PA is based on a soluble colourless molecule, 2-(5'-chloro-2'-phosphoryloxyphenyl)-6-chloro-4-(^{3}H)-quinazolinone, also called CPPCQ or ELF-phosphate (ELFP) (Huang *et al.*, 1992, 1993). When the ELFP reacts with phosphatases, the phosphate group is hydrolysed and the organic moiety (called [(2-(5'-chloro-2'-hydroxyphenyl)-6-chloro-4-(^{3}H)-quinazolinone, CHPQ, ELF-alcohol or ELFA) becomes highly insoluble and yellow-green fluorescent, which makes it precipitate and label the phosphatase-active cells at the site of enzymatic reaction (Fig. 3). This hydrolytic reaction from ELFP to ELFA involves an intermediate step where an intramolecular hydrogen bond is formed, which implies two consequences. Firstly, this step makes the reaction to be pH sensitive. A high and constant fluorescence was obtained at pH from below 2 to 8, with a relative peak around pH~8.3 or 8.4 and a sharp decrease in fluorescence above these values (Huang *et al.*, 1992). Secondly, a lag time is observed between the beginning of the reaction and the moment when the ELFA product, with the intramolecular hydrogen bond, reaches local concentrations sufficiently high (~0.1mM) to precipitate (Huang *et al.*, 1993). Nevertheless, other mechanisms like nucleation have been proposed to explain the observed lag times because the lag time was not tightly related to reaction rate (Nedoma *et al.*, 2003).

The ELF technique, also called fluorescence labelled enzyme activity (FLEA), was early applied to cultures of autotrophic protists (González-Gil *et al.*, 1998), natural phytoplankton samples (González-Gil *et al.*, 1998; Rengefors *et al.*, 2001), rotifers (Štrojsová & Vrba, 2005), and, albeit with difficulties, in bacteria (Ommen Kloeke & Geesey, 1999; Ommen Kloeke *et al.*, 1999; Carlsson & Caron, 2001; Nedoma & Vrba, 2006; Van Wambeke *et al.*, 2008; Stibal *et al.*, 2009). It is fair to say that if our knowledge of PA at the species level used to be reduced to cultivable species (i.e. a minority of species that when cultivable, probably evolved into strains that behave differently to

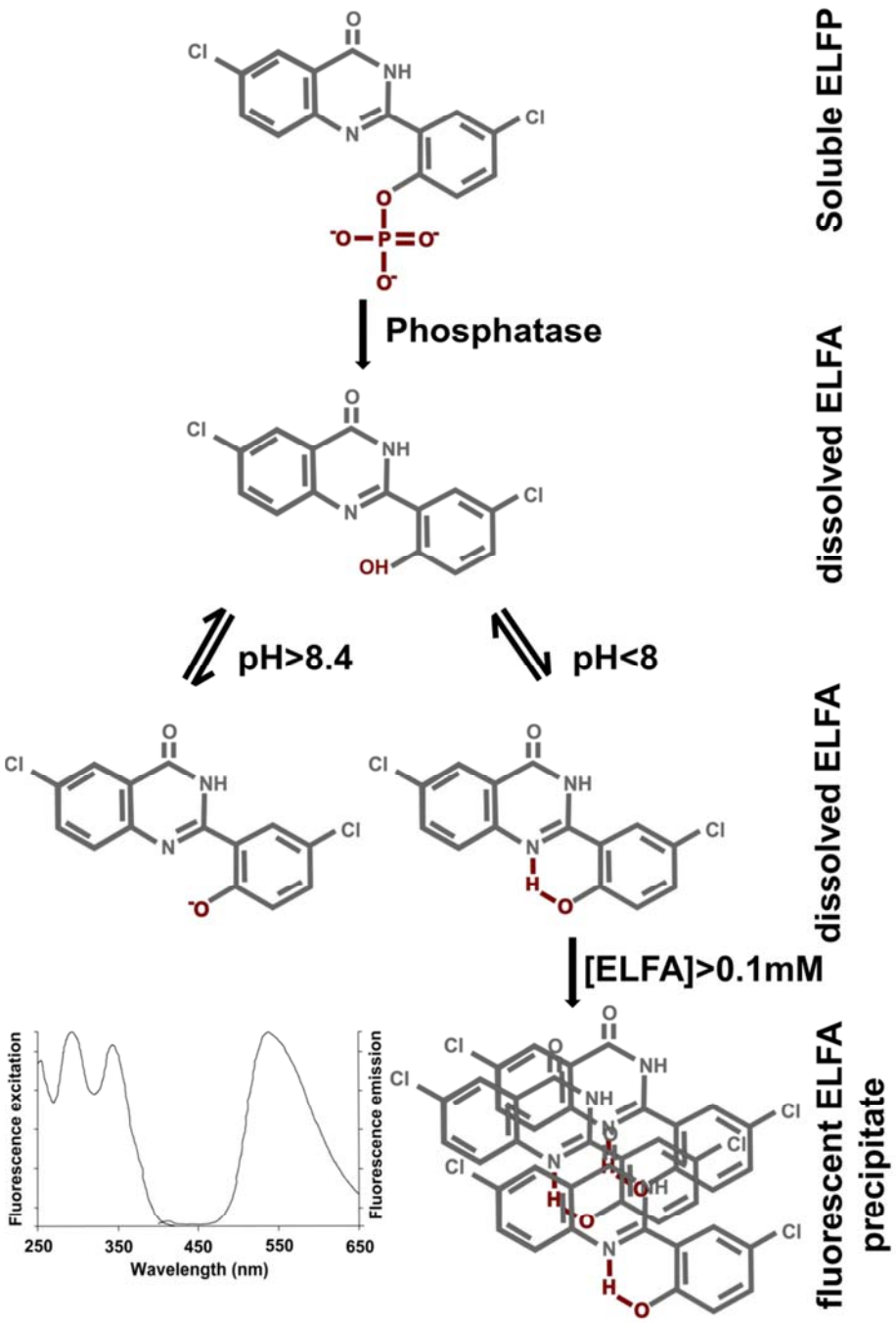

Fig. 3 Hydrolysis reaction of the Enzyme labelled fluorescence phosphate (ELFP) substrate and following reaction leading to the fluorescent precipitate.

those in the natural environment), the ELF technique has provided data of PA for all the species present in the assessed natural communities at conditions closer to those in nature. The first and most robust evidence showed by the ELF technique was that not all the species in a community nor all the cells in a population are phosphatase active, but the contributions and potentialities of this culture-free and single-cell technique are much broader than that (Štrojsová & Vrba, 2006). The ELF technique to assess phytoplanktonic PA is the central methodology studied and used in this thesis, and we will discuss their contributions, limitations and potentialities in the following words.

Without regard of the fact that fluorescent substrates provide bulk or single-cell information, they all share some limitations. Firstly, the assays are based on a single and artificial substrate that may not reflect the diversity of substrates in nature. Secondly, very different incubation conditions have been used, according to the aims, possibilities and sometimes the quality of the studies: Since phosphatases in the environment are not in their optimum conditions, an early debate was open on the convenience of measuring the maximum potential or the actual PA (i.e. as close as possible to *in situ* conditions of temperature, pH, ionic strength, cofactors, and substrate concentration) (Chróst & Siuda, 2002), but many measurements were performed at intermediate conditions. Additionally, it has been widely assumed that these substrates only react with ecto- and extracellular phosphatases (Marxsen & Schmidt, 1993; Espeland & Wetzel, 2001; Nedoma *et al.*, 2006; Štrojsová *et al.*, 2008; Novotná *et al.*, 2010) although some evidences challenged this point of view (Dyhrman & Palenik, 1999; Diaz-de-Quijano, 2006; Skelton *et al.*, 2006; Ou *et al.*, 2010). Finally, there are two more challenges that remain unresolved: how to avoid temporal aliasing (i.e. the artefact where the reconstructed signal is different to the original continuous signal due to undersampling), and how to handle with species-specific information. Many studies including phosphatase measurements were often based on monthly or weekly samplings (Haupert, 2000; Štrojsová *et al.*, 2003; Nedoma *et al.*, 2006; Tanaka *et al.*, 2006; Ivancić *et al.*, 2010), whereas the scarce attempts to characterize daily variability have shown that PA may respond to phenomena occurring at much shorter time scales (Rivkin & Swift, 1979; Wynne, 1981; Chróst *et al.*, 1984; Štrojsová & Vrba, 2009). Regarding the second point, questions posed during the times when only bulk substrates were available (PA contribution to P demands, PA regulation, bacteria-phytoplankton competition, etc.) lacked species-specific resolution

and this probably hided a crucial factor for a correct understanding. Nowadays, the ELF assay should be able to offer a better insight, but most studies are limited to confirm differences between (and within) species without exploring multilevel relationships between bulk and single-cell PA (SCPA) nor the relationship between quantitative SCPA and cell-level factors (e.g. cell nutrient stoichiometry, cell cycle phase, nutritional history of the cell, etc.).

The limitations specific to the ELF technique at the beginning of this thesis concerned some methodological aspects. A diversity of protocols including some dubious recommendations was available and the choice of the method could not be based on any clear and rational comparison. This mainly affected the way to stop the reaction and its consequences (loss of fragile cells), and the used fixative. The single-cell quantification presented two limitations: the convenience for a more fitted conversion factor between relative fluorescence units and the actual ELFA concentration (Nedoma *et al.*, 2003), and the fact of measuring 3D objects on the basis of 2D images. Other gaps of knowledge about the incubation included the causes and meaning of a lag time between the beginning of the reaction and the first signal detection, and the chemical properties of the commercially available kit were not provided by the company Molecular Probes (although it was later resolved; Nedoma *et al.*, 2007). Nevertheless, the main limitation related to the ELF technique would rather be the fact that most studies only quantify bulk PA with traditional bulk substrates and limit the use of ELF to identify the species responsible for the bulk PA rates, so ELF remains as a dummy or percentage variable, instead of quantitative. In the best cases, when ELF is quantified, data is merged into population models, but unfortunately it is not analysed with individual or mixed models.

In this thesis we followed the philosophy of incubating at conditions as close as possible to the in situ conditions, we improved the ELF technique, we applied it to check the actual localization of phosphatases reacting with the substrate and we explored the potential of the quantitative ELF technique to address general and species-specific ecological questions from a species-resolution point of view.

2.4 Relevance and meaning of PA.

Ecto- and extracellular phosphatases are seen as an important P scavenging strategy for bacterio- and phytoplankton in oligotrophic and other P-limited aquatic ecosystems. Although only a few studies have directly assessed the relationship between PA, the uptake of hydrolysed P, and planktonic P demand, it is known that the contribution of phosphatase-hydrolysed P to the total P demand is highly variable: between <1% of the total phytoplanktonic P demand (Heath, 1986; Boavida & Heath, 1988; García-Ruiz *et al.*, 2000) to >40% (Bentzen *et al.*, 1992; Hernández *et al.*, 1996). The common fact that PA concentrates in certain species or individuals in the phytoplankton community (Rengefors *et al.*, 2001, 2003; Štrojsová *et al.*, 2003), makes it conceivable that much more than a 40% of cellular P demands were met by PA in the active cells (e.g. Aaronson & Patni, 1967).

Phosphatase in the eye of the beholder. From P limitation indicator to functional trait.

In the same way as different generations of historians construct different speeches on the basis of the similar pieces of evidence, according to the questions of interest at the moment they perform their studies, microbial ecologists have also been measuring phosphatases in the environment during the last five to six decades under the eyes of different questions. Consequently, different meanings, roles and applications have been attributed to phosphatases in the environment in a process where new contributions did not displace previous conceptions. The seminal Overbeck's works already understood phosphatases as a P scavenging activity that allowed phyto- and bacterioplankton to access DOP in the absence of orthophosphate (Provasoli, 1958; Overbeck, 1991), and so as a step in the P cycling. The modern study of extracellular enzyme activities in the environment was contemporary to societal concerns on eutrophication and the search for the limiting nutrients that had to offer the key for a proper management. Phosphatase activity was suggested as an indicator of P limitation prior to the consensus that P was the limiting nutrient in many lakes and the element responsible for many eutrophication cases. The role of phosphatases and other extracellular enzymatic activities (EEA) were studied along ecological successions (Kjøller & Struwe, 2002; Frossard *et al.*, 2011, 2013a, 2013b), in litter decomposition (Sinsabaugh *et al.*, 1993), in ecosystem biogeochemical cycles (Arnosti, 2011), etc. The sensitiveness of

phosphatases and the other EEA makes them a good indicator not only of P deficiency but also of ecosystem response to multiple factors. Primarily, enzymatic activities are dependent on pH, temperature, ionic strength, cofactors, inhibitors, and substrate and enzyme concentrations, which makes them a component of the ecosystems sensitive to global warming, acidification and chemical changes (Sinsabaugh *et al.*, 2002; Allison & Treseder, 2008; Piontek *et al.*, 2010; Maas *et al.*, 2013). As a consequence, EEA may be used as a bioindicator of nutrient limitation, trophic state (Kiersztyn *et al.*, 2002), quantity and quality of organic matter (Romaní i Cornet, 2001), soil health, degradation and recovery (Killham & Staddon, 2002; Speir & Ross, 2002), harmful algal blooms (Dyhrman, 2008), etc. Other applications included the biocontrol of plant pathogens and pests (Chernin & Chet, 2002), geoengineering (Freeman *et al.*, 2012), and the bioremediation of organic pollutants, heavy metals and metalloids (Dungan & Frankenberger, 2002; Gianfreda & Bollag, 2002), although credited opinions like Speir's tend to evaluate more positively the bioindicator than the bioremediation applications (Speir, 2011).

It is worth to take the time to comment the use of PA as an indicator of P limitation because it is a controverted but widely used interpretation, and because it has influenced many of the questions posed to PA in the environments (origin of phosphatases, regulation mechanisms, bacteria-phytoplankton competition, etc.). The observation that many algae were able to grow on the expenses of organophosphates in the absence of orthophosphate (Provasoli, 1958) led some authors to check the responsible mechanism. PA was proposed as an indicator of P limitation in phytoplankton because (1) many phytoplankton species synthesized ecto- and extracellular phosphatases under P limitation to hydrolyse DOP, absorb the orthophosphate ion and leave the organic moiety in the water (Kuenzler & Perras, 1965; Fitzgerald & Nelson, 1966; Pettersson, 1980), (2) high orthophosphate concentrations repressed phosphatase synthesis (Perry, 1972; Cembella *et al.*, 1984b; Elser & Kimmel, 1986) and diminished PA via competitive inhibition (Jansson *et al.*, 1988), (3) PA was related to extracellular and intracellular P concentrations (Jansson *et al.*, 1988; Litchman & Nguyen, 2008), and (4) was coherent with other indicators of P limitation in freshwaters (Healey & Hendzel, 1979; Pettersson, 1980; Vrba *et al.*, 1995). The repression-derepression mechanism is the core reason that makes PA a possible indicator of P limitation, and it seems to be a robust

mechanism: only a few phosphatases of constitutive (non-regulated) were detected (and were probably acidic and intracellular; Jansson *et al.*, 1988). Some studies found some species to be always phosphatase active when present in a data set (e.g. Rengefors *et al.*, 2001; Štrojsová *et al.*, 2003; Cao *et al.*, 2005), but it is dubious to consider it sufficient evidence of constitutive expression of their phosphatase gene. Nevertheless, a comparison between nutrient addition experiments and PA in phytoplankton showed that PA was a reliable indicator only for P limitation, but not for NP or N limitations (Rose & Axler, 1998). The criticisms to the use of PA as indicator of P limitation can be structured at two levels. Firstly, measured PA has commonly been attributed to a certain group of organisms without having the certainty that they produced the measured enzyme activity. This occurred when measuring dissolved PA and size fractions of particulate PA. The origin of dissolved phosphatases (excretion in metazoans, autotrophic or heterotrophic protists, prokaryotes, release by cell lysis and external inputs; Stevens & Parr, 1977; Jansson *et al.*, 1988; Cao *et al.*, 2009, 2010) is almost always undetermined, and the PA of a size fraction, let's say that corresponding to phytoplankton, is also questionable because phosphatases associated to other types of organisms (big prokaryotes and heterotrophic protists) or non-living particles may contribute to the PA values (Cao *et al.*, 2010) and because conclusions tend to be drawn for the average phytoplankton whilst PA and P limitation may concentrate in a few or a single species. The use of the ELF technique would overcome these drawbacks (Štrojsová & Vrba, 2009), but here the second level of criticisms would come into play. False positives (presence of PA not indicating P deficiency) would include cases where PA was enough to meet the P demands, PA was intended for the use of the organic moiety rather than phosphate (Cotner & Wetzel, 1991; Nicholson *et al.*, 2006; Cao *et al.*, 2010). Uncertainty and false negatives are conceivable as well because different P-limitation degrees are needed to activate PA in different species and some may even be unable to use phosphatases as a P scavenging activity (Graziano *et al.*, 1995), and because other activities and strategies to avoid P limitation exist in phytoplankton species (polyphosphate reserves, dormancy, phagocytosis, substitution of phospholipids by sulfolipids, etc.).

The studies of EEA received a new impulse with the formulation of the microbial loop concept. The fact that small phytoplankton (<60µm) was responsible for more than 90% of the total authoctonous primary production attracted the attention of ecologists for the microbial dynamics (Pomeroy,

1974). Dissolved and particulate organic matter original from all the trophic levels was incorporated by prokaryotes that were grazed by protists and then connected to the upper trophic levels (Azam *et al.*, 1983) in a complex web of trophic interactions (Sherr & Sherr, 1988). The concept of the enzymatic pathway highlighted the crucial role of EEA in the ability of prokaryotes to recycle organic matter from the whole ecosystem (Azam & Smith, 1991), and the interest in this mechanism permeated to the neighbouring microorganisms, the protists, who contributed to exploit organic matter resources as well. In fact, the enzymatic pathway may be seen as one of the two strategies that microorganisms may present to utilize organic matter. In the absence of (compact) cell walls, microorganisms may engulf dissolved and particulate organic matter via pinocytosis and phagocytosis respectively with subsequent enzymatic digestion within the vacuoles. In the opposite case, ecto- and extracellular enzymes catalyse a kind of digestion (hydrolysis) outside the cytoplasm to produce low molecular weight molecules transportable across the cell wall and membrane (Chróst & Siuda, 2002). One and another strategies have been studied recently as functional traits because they define the manner in which a species relates to its biotic and abiotic environment, and because it significantly affects the fitness of the species (Litchman & Klausmeier, 2008; Novotná *et al.*, 2010; Rottberger *et al.*, 2013), and in this thesis we focused on their role as P scavenging activities. This alternative point of view seems to be much more related to the ecological sense of such activities and less influenced by an anthropocentric will to give a human meaning, use or application to natural phenomena like PA. Traditionally, the phagotrophy of bacteria (bacterivory) rather than general phagotrophy has been more studied, probably because trophic relationships between living organisms attracted more the attention of scientists. In the case of phytoplankton, both activities, PA and bacterivory, have been reported to play a double role: as a source of P for the photoautotrophic metabolism, and as a source of matter and energy for the chemoheterotrophic metabolism. PA has mainly been considered to provide P to phytoplankton but some species (e.g. *Chlamydomonas acidophila*) and phytoplankton in determinate environments may use it as a source of carbon and energy (Joseph *et al.*, 1995; Tittel *et al.*, 2005; Spijkerman *et al.*, 2007; Cao *et al.*, 2010). Equally, bacterivory spans along a continuum of mixotrophic species and metabolic statuses that include different degrees of photoautotrophy and chemoheterotrophy, and subsequent roles of bacterivory itself. For these

reasons we found it interesting to assess PA together with at least another trophic activity related to P acquisition, like bacterivory (Pernthaler, 2005) (Fig. 4 and 5).

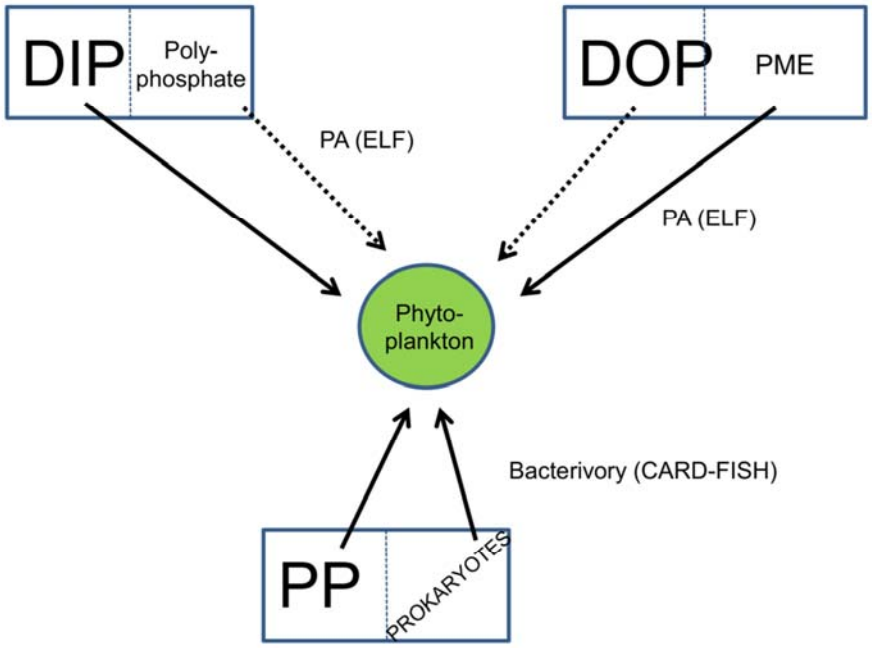

Fig. 4 Sources of P for phytoplankton. The assessed mechanisms are named. Dotted arrows show less important processes.

Therefore, the study of the microbial food web promoted a rushing development and application of techniques capable to link the structure or identity of microorganisms (who they are) to their function (what they do) at the single-cell analysis level (Kemp, 1994), which provided the adequate tools for the study of functional traits in microbes. In this thesis, we took our time to identify the gaps in the use, quantification, interpretation and applications of the ELF technique and to contribute to resolve some of them. This effort is justified by the potentialities of the ELF technique. Quantitative single-cell data is comparable to previous and present rates of bulk EEA, allowing for a multi-level approach (individual, population and community) using mixed models, which would integrate from the cell ecology to the ecosystem ecology of EEA. The ELF technique has the potential to follow opposite and complementary philosophies: to deepen into the details of environmental EEA via determining kinetic and thermodynamic parameters

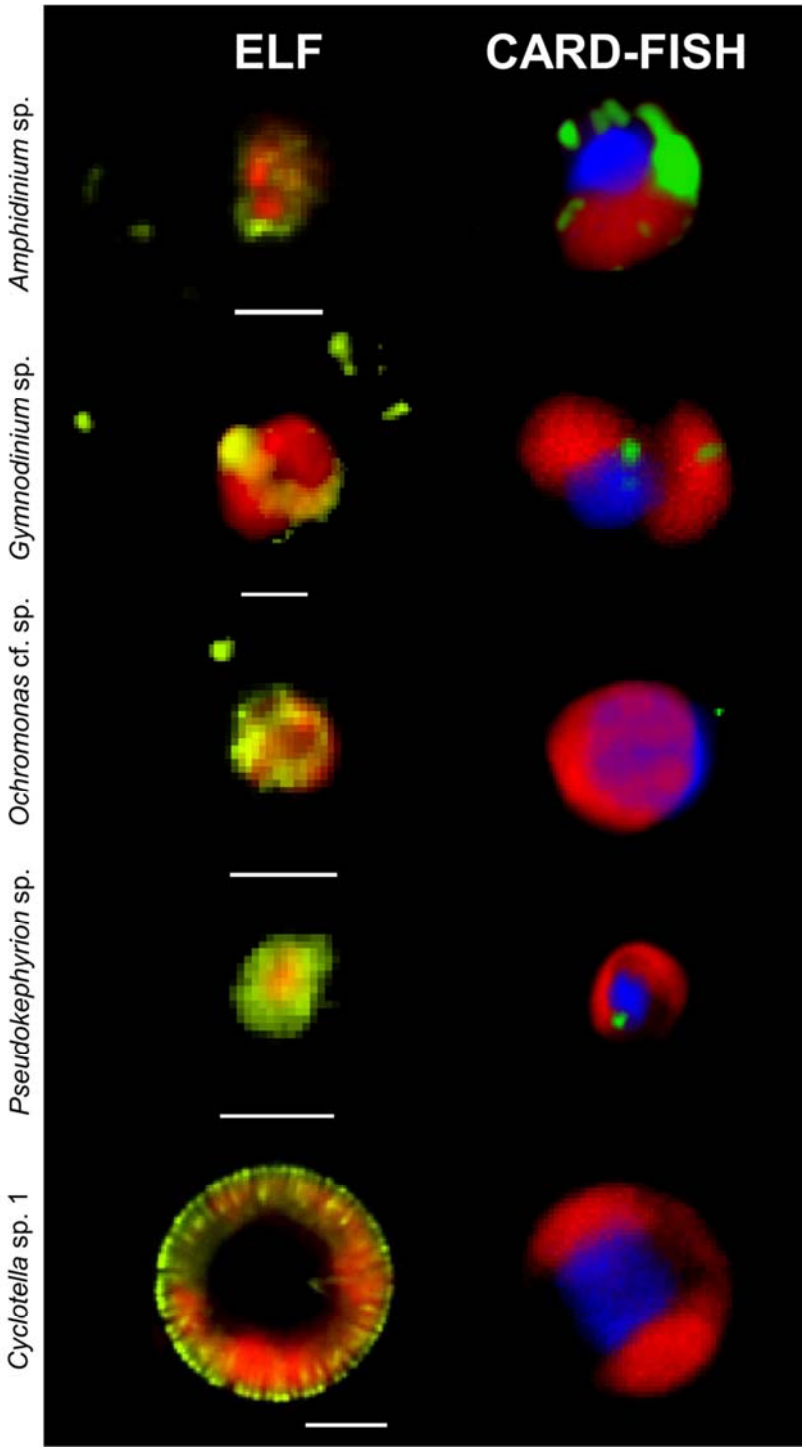
ELF
CARD-FISH
Amphidinium sp.
Gymnodinium sp.
Ochromonas cf. sp.
Pseudokephyrion sp.
Cyclotella sp. 1

Fig. 5 Microimages of fluorescence microscopy of different dinoflagellates, chrysophytes and a diatom species. The first column corresponds to the PA assay with the ELF technique (autofluorescent chloroplasts in red; ELFA precipitates indicating PA in green), the second column corresponds to the bacterivory assay using catalysed reporter deposition fluorescence in situ hybridisation or CARD-FISH (autofluorescent chloroplasts in red; DAPI-stained nuclei in blue; CARD-FISH hybridised prokaryotes in green). White bars in the ELF images are 5 µm long.

at the species level, and to become a high-throughput technique using flow cytometry, automatic image acquisition and analysis routines, and data bases (Dignum *et al.*, 2004b; Swedlow *et al.*, 2009; Zeder & Pernthaler, 2009; Zeder *et al.*, 2010, 2011; Allan *et al.*, 2012; Spidlen *et al.*, 2012). Additionally, the use of the ELF technique has shown that different phytoplankton species had different spatial patterns of PA, whose meaning is to be addressed. Moreover, the ELF technique is currently the most appropriate methodology to study phosphatases as a functional trait because it can be used in close to in situ conditions, on natural phytoplankton communities, and with information of its position in the cell. Under this prism, we used the ELF technique to compare PA and bacterivory, and we discussed the role of PA as a functional trait in shaping some phytoplankton paleo-records.


OBJECTIVES

As we mentioned in the introduction, high mountain lakes from the Pyrenees lay mostly in the oligotrophic to ultraoligotrophic range and tend to be P limited, in a dynamic combination with N limitation enhanced by P inputs of air-transported Saharan dust (Catalan, 1987; Camarero & Catalan, 2012). We chose this ecological theatre to observe the play of P scavenging activities in phytoplankton species. Apart from this general objective, specific objectives may be divided into two groups:

Methodological objectives:

A critical reading of literature on the ELF technique was the starting point of our will to improve the ELF protocol and single cell PA quantification.

1. Our first aim was to contribute to standardize the protocol via avoiding possible false negative results (Van Wambeke *et al.*, 2008) and possible false positive results (Lomas *et al.*, 2004), design or select a protocol that conserved as much as possible the most fragile phytoplankton species and the original aspect of chloroplasts, and design or select a protocol that maximised the ectoenzyme activity labelling whilst minimizing the intracellular signal.

2. A second objective was to compare the quantification of fluorescence using two dimensions (2D) and 3D microscopic images (microimages), in order to detect whether the use of 2D images of actual 3D objects was triggering any bias and whether such a bias would be dependent on the cell size, to eventually refine the quantification resolution, and to explore 3D images as a possible way to improve the fitting of the conversion factor between relative fluorescence units and the concentration of hydrolysed organophosphates.

Ecological objectives:

3. The following objective was to determine whether was there a trade-off between phosphatase and bacterivory, as P scavenging activities, in phytoplankton species and communities, to compare the relative importance of both activities in making available non orthophosphate phosphorus to phytoplankton, and explore phylogenetic and allometric patterns in the investment in these two activities and the selection of one activity or the other. In this sense, we tested the hypothesis that species with high cell surface to volume ratios (S/V) would proportionally invest more efforts in PA whereas low S/V species would lean towards bacterivory because it also needs intracellular space for digestion.

4. Finally, we had as an objective to define a part of the functional niche of a variety of phytoplankton species from Pyrenean mountain lakes and to apply this information to any ecological question involving these species, which we did to interpret the take-off and expansion of *Cyclotella* spp. registered in paleolimnological records of alpine and sub-arctic lakes during the last ~150 years (Rühland *et al.*, 2008).

Chapter 1

A comparative study of fluorescence-labelled enzyme activity methods for assaying phosphatase activity in phytoplankton. A possible bias in the enzymatic pathway estimations.

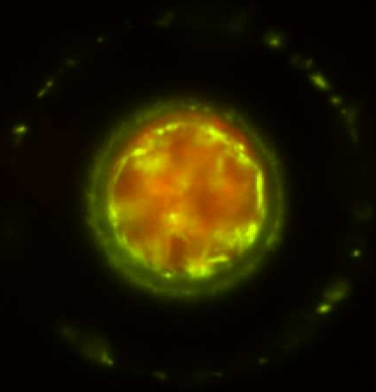

Journal of Microbiological Methods 86 (2011):104-107

AUTHORS

Daniel Díaz-de-Quijano[a*] and Marisol Felip[a]

[a]Unitat de Limnologia, Departament d'Ecologia i Centre de Recerca d'Alta Muntanya, CEAB-CSIC-Universitat de Barcelona, 645 Diagonal Av. 08028, Barcelona, Catalonia, Spain.

ABSTRACT

We compared different fluorescence-labelled enzyme activity (FLEA) methods for assaying phosphatase activity in phytoplankton. Unfixed and liquid incubations are devised. We demonstrated that the presence of intracellular labelling was persistent, which could point out a source of bias in ectoenzymatic activities measurements based either on the FLEA or classical methods.

KEY WORDS

Phosphatase; Ectoenzyme; Phytoplankton; ELF97-phosphate; Single cell analysis

TEXT

The published protocols of the enzyme-labelled fluorescence (ELF) or FLEA technique differ widely in the fixative used, the way the incubation is performed and the final support of the sample (liquid or filter). These differences have been shown to affect not only cell integrity, but also labelling efficiency (Rengefors et al., 2001; Young et al., 2010). Additionally, the presence of intracellular labelling is a problem that has not yet been solved. We compared published and new protocols for the phosphatase activity assay in natural phytoplankton communities, using the criterion that ectophosphatase (surface-bound) FLEA labelling should be maximised because these are the phosphatases playing the ecological role of catalysing reactions around the lipid boundary, where life and the surrounding environment come into contact.

Phytoplankton communities were sampled from Crous Pond (41º40'37''N, 2º35'2''E) and Redon Lake (42º38'33''N, 0º46'46''E), in Catalonia. We tested several protocols that were defined by a combination of two factors: step order and fixative (Table 1). The step order had two levels: B (Bottle) and F (Filter). B consisted in incubating the sample in a bottle, fixing it and stopping the reaction by filtration. It was based on the protocol devised by Nedoma et al. (2003). F consisted in fixing the sample, filtering it, and incubating the filters in a Petri dish. This was a modification of the protocol drawn up by Lomas et al. (2004). B or F was placed in first position in our protocol code. The fixative factor had five levels, whose initial letters were placed in the second position in our code: $HgCl_2$ (H), no fixative (X), LFT (L), ethanol + DMSO (E), and liquid N_2 (N). $HgCl_2$ 4mM f.c. was added to samples and immediately filtered. LFT fixation was performed by adding alkaline Lugol 0.5% (vol/vol), formaldehyde 2% f.c. (pH 7) and several drops of 3% sodium thiosulfate (Sherr and Sherr, 1993). Ethanol 70% + DMSO 10% were added to the samples and left for 30 minutes before filtration (Lomas et al., 2004). In the case of the FN protocol, samples were placed in plastic vials and sunk into the liquid N_2, removed, and left to thaw prior to filtration. All the incubations were performed in the dark for 1 hour at room temperature and with a substrate concentration of 20 µM ELF97-phosphate (ELFP) (Molecular Probes, E6589). Three replicates and one negative control (without ELFP) of 30 ml each were filtered through 25 mm diameter and 2 µm pore polycarbonate filters (Millipore). Very gentle pressure (<20 KPa) was used to avoid cell disruption. Filters were left to dry on cellulose paper and stored at -20 ºC. Finally, they were thawed and mounted on microscope slides using Citifluor AF1.

			Fixative				
			$HgCl_2$	No fixative	LFT	Ethanol +DMSO	Liquid N_2
Step order	Bottle	Crous	BH (n=2)	BX (n=2)	BL (n=2)	BE (unc)	-
	Filter		FH (unc)	FX (n=2)	FL (n=2)	FE (n=2)	-
	Bottle	Redon	BH (n=3)	BX (n=3)	BL (n=2)	-	-
	Filter		FH (n=3)	FX (n=3)	FL (n=3)	-	FN (n=3)

Table 1. Experimental design and codes used in this study; n = number of available replicates; unc = uncountable filters.

The composition of the phytoplankton community was determined by the Utermöhl method. Particular attention was paid to the size and shape of chloroplasts, as these characters would subsequently be used to identify taxa under the epifluorescence microscope. The different FLEA filters were analysed under a Nikon Eclipse E600 epifluorescence microscope and the percentage of ELFA-labelled cells was determined. A cell was only considered positive when a clear ELFA object was observed on or in the cell, whatever its size or intensity. Some of the experimental conditions (FH and BE in the Crous sample) resulted in non-measurable filters (Fig. 1 a and b). One replicate per experimental condition and sample was analysed with a Leica SP II spectral detection confocal microscope to determine the location of ELFA bodies. The percentage of cells with only external labelling (EXT), only internal labelling (INT), and both external and internal labelling (EXT and INT) (Fig. 1 c, d, e and f) were determined by counting more than 100 cells per filter. Within each taxon, we discarded location patterns that were based on less than 5% of taxon total counts. One-way and two-way ANOVAs were performed with Statgraphics Plus 5.1 (Statistical Graphics Corp.) and STATISTICA 6.0 (Statsoft, Inc., OK, USA).

The percentage of ELFA-labelled cells in the entire phytoplankton differed significantly between protocols in both Redon (p-v<0.0000) and Crous (p-v = 0.0153) samples. The step order (Crous p-v= 0.035781 and Redon p-v= 0.001377) was always more significant than the fixative (Crous was not significant and Redon p-v= 0.0025) (Fig. 2, first row), and this result was consistent across most of the studied taxa. In all the cases, liquid-incubation protocols (B) significantly maximised ELFA labelling. B and F protocols differed in two factors that could explain this result: (1) the status of cells and enzymes during incubation (alive/unfixed (B) or fixed (F)), and (2) the physical support of the incubation (liquid (B) or on-filter (F)). If we consider the low labelling results of FX protocol, where cells were incubated live but on filter, as in Van Wambeke's method (Van Wambeke et al., 2008), we may conclude that apart from the expected effect of incubating fixed or unfixed samples, a physical obstruction that prevents ELFP from reaching enzymes may occur. Reasonable explanations would be either because in F protocols some phosphatases are in contact with the filter itself, or because ELFP cannot diffuse fast enough within the drop, which creates a low concentration of ELFP in the volume surrounding the cell.

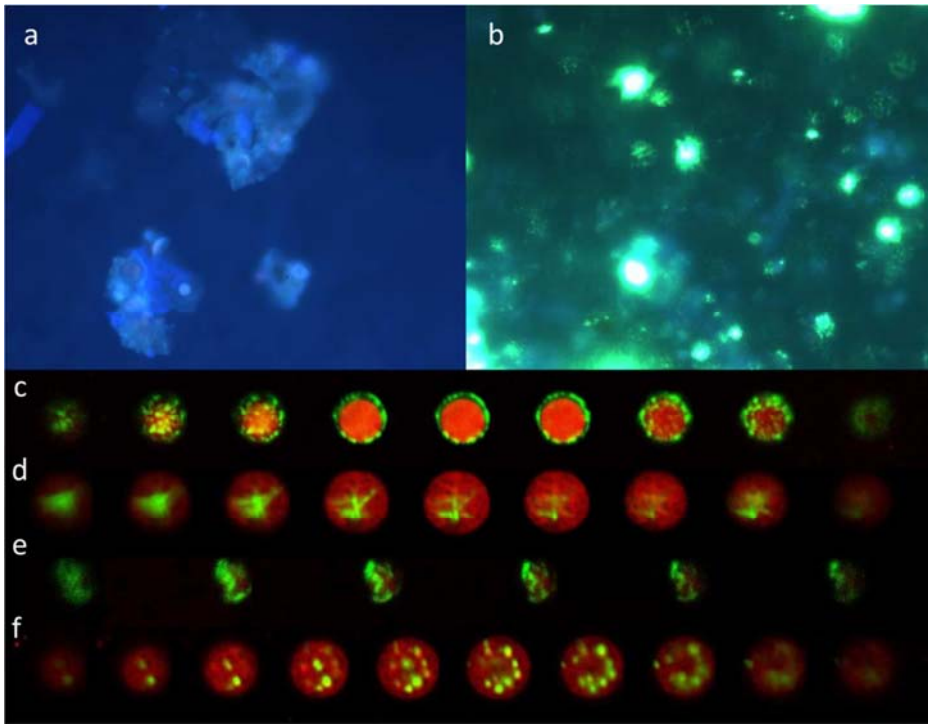

Fig. 1. Colour epifluorescent images: a and b; a) general view of protocol FH, with aggregates (Crous); b) general view of protocol BE, with extremely high unspecific ELFA labelling and non-recognisable chloroplasts (Crous). Pseudocolour optical sections at different depths through a unicellular *S. schroeteri* (c, d and f) or a small flagellated (e). Red is chloroplast and green are ELFA precipitates. c) EXT labelling; d) INT labelling; e and f) EXT and INT labelling.

The percentage of ELFA-labelled cells showed four acceptable protocols: BH, BX, BL and FH. Of these options, BH was the best in terms of the percentage of ELFA-labelled cells, but consistently performed the worst in terms of ELFA-labelling location. It was therefore an undesirable option. BX and BL had good percentage of labelled cells and good labelling location in all the cases except that BX had low EXT location in Redon sample and BL had a low percentage of labelled cells in Crous. Finally, FH had good results in both variables when the protocol worked (in Redon), but it could be unreliable as it developed huge particle aggregates in Crous. To sum up, BX and BL would be reasonably good options, BH could provide positive but ecologically uncertain results, and FH seems to be a good but unstable option.

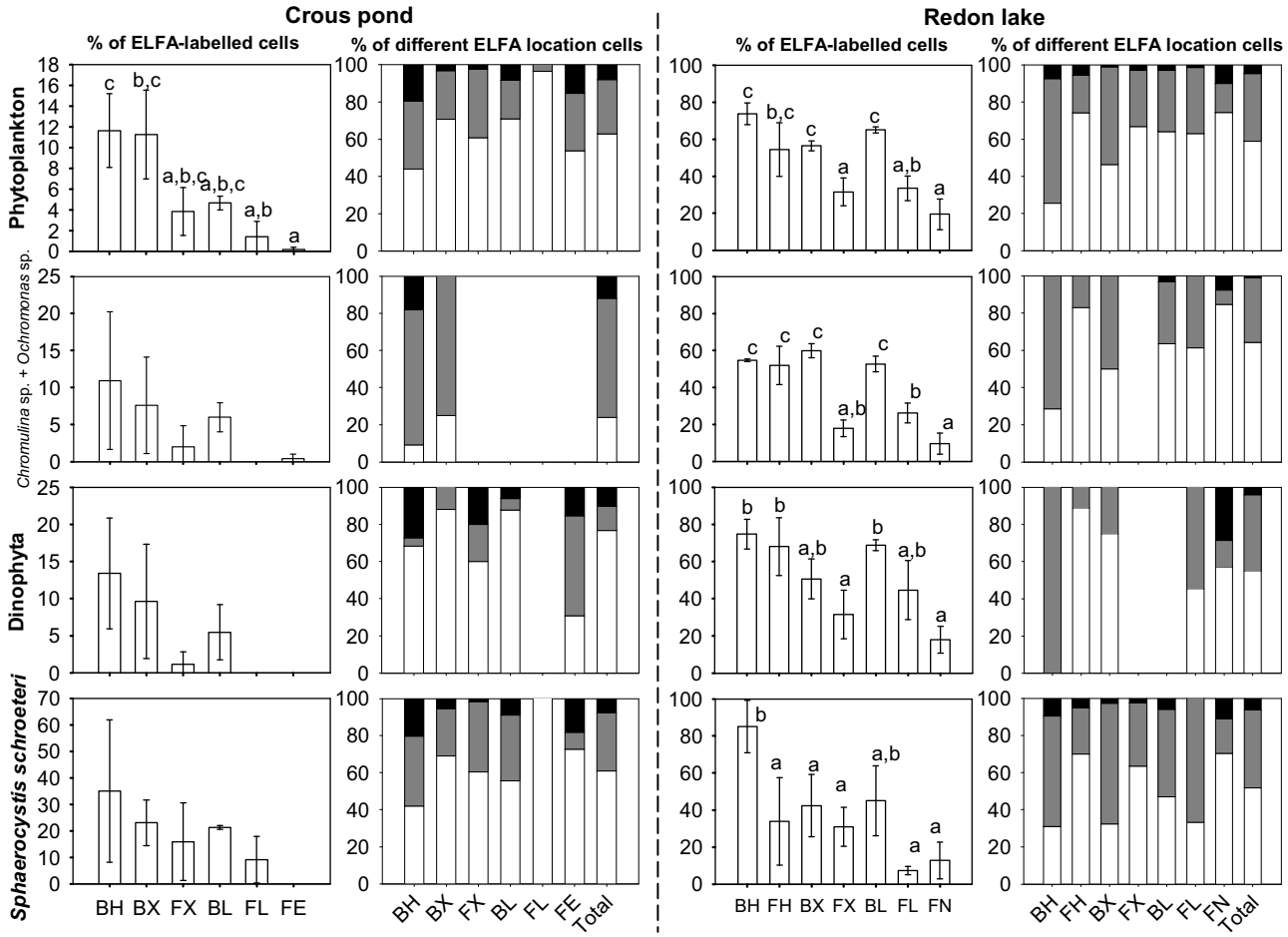

Fig. 2. Simple bars: Percentage of ELFA-labelled cells. Letters on bars (a, b, and c) show homogeneous groups, as found by Tukey HSD multiple range tests (p-v<0.05), when one-way ANOVA showed significant differences (p-v<0.05). Stacked bars: Percentage of different ELFA-labelling location cells. Black = INT labelling, grey = EXT and INT labelling, white = EXT labelling. TOTAL column = sum of all the cells counted in all the protocols.

Traditional total enzyme activity substrates (MUF-P, MFP, p-NNP, etc.) have been thought to label dissolved and/or ectoenzymes as they have physical and chemical characteristics that make it impossible for them to get into the cells by membrane transport (Chróst, 1991). The ELF substrate shares the same physical and chemical characteristics. In addition, there is evidence that ELFP and MUFP substrates react with the same set of phosphatases

within a certain sample (Štrojsová et al., 2003; Nedoma et al., 2007). Therefore, we could conclude that the ELF substrate should normally react with ectoenzymes, but not with intracellular enzymes. However, the optical dissection of FLEA-incubated cells by confocal microscopy confirmed that intracellular PA was labelled by any of the tested protocols (Fig. 2, first row), as previously observed (Dyhrman and Palenik, 1999; Skelton et al., 2006; Ou et al., 2010). The extent of INT together with EXT and INT labelling shows that this problem should be taken into consideration. The hypothesis that the detection of intracellular labelling is a problem that is exclusive to ELF substrate should be experimentally tested in the future. If this hypothesis was rejected, all of our substrate reaction-based knowledge about environmental PA, and maybe the general enzymatic pathway, would have been biased to some extent by interaction with intracellular enzymes.

Previous observations have found ELFA labelling patterns to vary in different species (e.g. linear structures, dots, evenly labelled whole cell surfaces, etc.) (Pers. Obs., Štrojsová et al., 2003). Therefore, we expected the location of ELFA labelling to be species-specific. In contrast, we found the taxon effect to be secondary to the protocol effect: the range of variability within protocols was significantly narrower than within taxa (p-v=0.0003). Nonetheless, more diverse species than those used here (in terms of cell aggregation, morphology, wall properties, etc.) should be considered to generalise this result. In any case, many hypotheses (including taxon-specific ones) could be made to explain intracellular labelling. In Dinophyta and small flagellated Crysophyta intracellular labelling could be due to the internalisation of ELFP together with phagocytosed particles, as these taxa have been described as potential bacterivores (Jones, 2000). However, this does not explain other intracellular labelling, such as that found in *Sphaerocystis schroeteri* (CHOD) (Fig. 2 c), *Monoraphidium* sp., *Oocystis parva*, *Stichogloea doederleinii* (SCHMIDLE) (data not shown), which are the first non-mixotrophic phytoplankton observed with intracellular ELFA. In this case, we hypothesise that cell membrane disruption may be the reason for intracellular labelling. There may be three different causes of membrane disruption: natural cell death (Bidle and Falkowski, 2004), sample manipulation, and accumulation of ELFA crystals, which may damage the cell membrane and make it collapse, resulting in ELFA penetrating the cell.

In conclusion, the FLEA technique protocols should incubate unfixed and liquid samples. BX and BL may be the best trade-offs amongst the tested

protocols, between FLEA signal maximisation and the EXT location of the signal. The FLEA technique results are mainly determined by the protocol, and the possible taxon dependence is secondary. Finally, we demonstrated the presence of intracellular fluorescence-labelled PA when the FLEA technique is used, which highlights the need to further understand the origin of this signal.

ACKNOWLEDGMENTS

We thank Jiři Nedoma for critically reading the manuscript and for valuable suggestions, the Scientific-Technical Services of the University of Barcelona (SCT-UB) for technical assistance in confocal microscopy, and Maria Diaz de Quijano and Eglantine Chappuis for assistance in the field. This research was carried out by the Limnology Group CEAB-UB and was supported by the Spanish Ministry of Science and Technology, projects CGL2004-02989 and CGL2007-64177/BOS.

REFERENCES

Bidle, K. D., Falkowski, P. G., 2004. Cell death in planktonic, photosynthetic microorganisms. Nat. Rev. Micro. 2, 643-655.

Chróst, R.J., 1991, Environmental control of the synthesis and activity of aquatic microbial ectoenzymes. In: Chróst R.J. (Ed.), Microbial Enzymes in Aquatic Environments, Springer-Verlag New York Inc., New York, pp. 29-59.

Dyhrman, S.T., Palenik, B., 1999. Phosphate Stress in Cultures and Field Populations of the Dinoflagellate Prorocentrum minimum Detected by a Single-Cell Alkaline

Jones, R.I., 2000. Mixotrophy in planktonic protists: an overview. Freshwat. Biol. 45, 219-226.

Lomas, M.W., Swain, A., Shelton, R., Ammerman, J.W., 2004. Taxonomic variability of phosphorus stress in Sargasso Sea phytoplankton. Limnol. Oceanogr. 49, 2303-2310.

Nedoma, J., Van Wambeke, F., Štrojsová, A., Štrojsová, M., Duhamel, S., 2007. Affinity of extracellular phosphatases for ELF97 phosphate in aquatic environments. Mar. Freshwat. Res. 58, 454-460.

Nedoma, J., Štrojsová, A., Vrba, J., Komárková, J., Šimek, K., 2003. Extracellular phosphatase activity of natural plankton studied with ELF97 phosphate: fluorescence quantification and labelling kinetics. Environ. Microbiol. 5, 462-472.

Ou, L., Huang, B., Hong, H., Qi, Y., Lu, S., 2010. Comparative alkaline phosphatase characteristics of the algal bloom dinoflagellates *Prorocentrum donghaiense* and *Alexandrium catenella*, and the diatom *Skeletonema costatum*. J. Phycol. 46, 260-265.

Rengefors, K., Pettersson, K., Blenckner, T., Anderson, D.M., 2001. Species-Specific Alkaline Phosphatase Activity in Freshwater Spring Phytoplankton: Application of a Novel Method. J. Plankton Res. 23, 435-443.

Sherr, E.B., Sherr, B.F., 1993. Preservation and storage of samples for enumeration of heterotrophic protists. In: Kemp PF, Sherr BF, Sherr EB, Cole JJ (Eds.), Handbook of Methods in Aquatic Microbial Ecology, Lewis publishers, Boca Raton, Florida, U.S.A., pp. 207-212.

Skelton, H.M., Parrow, M.W., Burkholder, J.M., 2006. Phosphatase activity in the heterotrophic dinoflagellate Pfiesteria shumwayae. Harmful Algae 5, 395-406.

Štrojsová, A., Vrba, J., Nedoma, J., Komárková, J., Znachor, P., 2003. Seasonal study of extracellular phosphatase expression in the phytoplankton of a eutrophic reservoir. Eur. J. Phycol. 38, 295-306.

Van Wambeke, F., Nedoma, J., Duhamel, S., & Lebaron, P., 2008. Alkaline phosphatase activity of marine bacteria studied with ELF 97 substrate: success and limits in the P-limited Mediterranean Sea. AME 52, 245-251.

Young, E.B., Tucker, R.C., Pansch, L. A., 2010. Alkaline phosphatase in freshwater *Cladophora*-epiphyte assemblages: regulation in response to phosphorus supply and localization. J. Phycol. 46, 93-101.

Chapter 2

3D restoration microscopy improves quantification of enzyme-labelled fluorescence (ELF)-based single-cell phosphatase activity in plankton

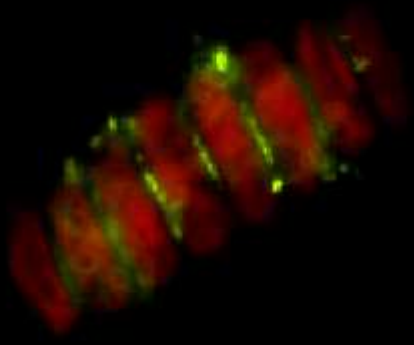

Cytometry Part A

DOI: 10.1002/cyto.a.22486

AUTHORS

Daniel Diaz-de-Quijano[a*], Pilar Palacios[b], Karel Horňák[c], Marisol Felip[a]

[a]Unitat de Limnologia, Departament d'Ecologia i Centre de Recerca d'Alta Muntanya, CEAB-CSIC-Universitat de Barcelona, Av. Diagonal 643, 08028 Barcelona, Catalonia, Spain.

[b]Centro Nacional de Biotecnología-CSIC, Darwin 3, Campus de Cantoblanco, 28049 Madrid, Spain.

[c]Biology Centre of the Academy of Sciences of the Czech Republic, Institute of Hydrobiology, Na Sádkách 7, CZ-370 05 České Budějovice, Czech Republic.

RUNNING HEADLINE

3D ELF single-cell phosphatase quantification

KEY WORDS

3D fluorescence microscopy, deconvolution, ELF phosphate, phosphatase activity, phytoplankton

CREDITS FOR RESEARCH SUPPORT

The study was supported by the Spanish Ministry of Science and Technology, projects NITROPIR (CGL2010-19373), ECOFOS (CGL2007-64177/BOS) and GRACCIE (CDS2007-00067).

ABSTRACT

The ELF or fluorescence-labelled enzyme activity (FLEA) technique is a culture-independent single-cell tool for assessing plankton enzyme activity in close-to-*in situ* conditions. We demonstrate that single-cell FLEA quantifications based on two-dimensional (2D) image analysis were biased by up to one order of magnitude relative to deconvolved 3D. This was basically attributed to out-of-focus light, and partially to object size. Nevertheless, if sufficient cells were measured (25 to 40 cells), biases in individual 2D cell measurements were partially compensated, providing useful and comparable results to deconvolved 3D. We also discuss how much caution should be used when comparing the single-cell enzyme activities of different sized bacterio- and/or phytoplankton populations measured on 2D images. Finally, a novel method based on deconvolved 3D images (wide field restoration microscopy; WFR) was devised to improve the discrimination of similar single-cell enzyme activities, the comparison of enzyme activities between different size cells, the measurement of low fluorescence intensities, the quantification of less numerous species, and the combination of the FLEA technique with other single-cell methods. These improvements in cell enzyme activity measurements will provide a more precise picture of individual species' behaviour in nature, which is essential to understand their functional role and evolutionary history.

INTRODUCTION

Phosphorus recycling in ecosystems is driven by different processes involving various enzyme activities. Phosphatases (including phosphoesterases, nucleases and nucleotidases) hydrolyse oxygen–phosphorus bonds in phosphoesters, the dominant form of dissolved organic phosphorus (1–4), whereas C-P lyases and hydrolases hydrolyse carbon–phosphorus bonds in phosphonates (5). These enzymes may play a key role in those ecosystems in which P is temporarily or permanently a limiting factor, as is the case of some freshwater, marine and terrestrial ecosystems (6–10). Notably, P limitation is expected to increase as the deposition of atmospherically transported anthropogenic N modifies the N:P stoichiometry of ecosystems all over the world (11). A number of studies have already assessed the shifts in environmental enzyme activity driven by anthropogenic atmospheric N deposition (12,13) and by other parameters related to climate change that

can modulate enzymatic activity, such as pH (14,15), temperature (16,17), and UV radiation (18–21). These studies have demonstrated the importance of enzyme activity in the response of ecosystems to global climate change. However, a more accurate characterization of the link between taxonomic identity and *in situ* enzymatic activity is essential to understand and to predict enzyme dynamics in nature.

Phosphomonoesterases are one of the most widely studied enzymes in aquatic ecosystems, and to date the only ones that can be assessed using the enzyme-labelled fluorescence-phosphate (ELFP) substrate, via the so-called FLEA technique. Upon enzymatic hydrolysis, the ELFP substrate is converted to a fluorescent ELF alcohol (ELFA) that precipitates at the site of enzyme activity (22). Therefore, the FLEA technique constitutes a powerful and culture-independent tool with which to study the contribution of this functional trait to the species trophic strategy (23,24) at the single-cell level, and in close-to-*in situ* conditions. Simultaneously, this technique also enables the preservation of useful cell structures required for adequate taxonomic identification (autofluorescent chloroplasts and stained DNA), mainly in phyto- and bacterioplankton communities (25–28). Moreover, Nedoma and colleagues (29) developed a method to quantify the ELFA precipitate based on epifluorescence microscopy and 2D image analysis. Thus, the FLEA technique has provided the opportunity to open the “black box” of environmental enzyme activity in phyto- and bacterioplankton. Knowledge of single-cell enzymatic activity, if accurate enough, is essential for the proper definition of functional niches, the reconstruction of the evolution of functional traits associated with certain trophic strategies (30,31), and better modelling and understanding of the dynamics of enzyme activity in nature (32). Nonetheless, the 2D images on which most quantifications have been based to date are distorted representations of real 3D cells. Therefore, we hypothesized that (i) 2D image-based measurements might be significantly biased, and (ii) cell size might modulate this bias, which could invalidate comparisons between different size cells, such as phytoplankton and bacterial cells.

To test these hypotheses, a 3D imaging system was required. Amongst the different modalities of fluorescence microscopy (wide-field, structured light illumination, confocal, and confocal-derived techniques), 3D wide-field restoration microscopy (WFR) was chosen for several reasons. Blurring of light is a common phenomenon in all the abovementioned 3D microscopy

techniques but it is especially important in 3D wide-field microscopy, where light blurs mainly along the Z axis and more moderately in the XY plane (33). This problem may be solved in one of two ways or via combination of approaches. On the one hand, mechanical devices may be used to reduce the amount of out-of-focus light (confocal and structured light illumination microscopy). On the other hand, out-of-focus light may be considered informative light and any of the mentioned techniques, including wide-field, may be combined with image restoration by deconvolution to relocate out-of-focus light to its source (34). Secondly, the WFR imaging system requires a wide-field microscope with a motorized Z axis, a cooled digital CCD camera and deconvolution software for image restoration. This WFR set up is cheaper than that required for the other techniques and makes it affordable for a larger number of laboratories. Moreover, WFR microscopy is the most suitable technique for our fluorescence intensity quantification purposes and for microplankton samples (thin and with no or small amounts of fluorescent material out of focus). This technique has a higher signal-to-noise ratio (SNR) than laser scanning confocal microscopy (LSCM) for samples <30 µm thick (33,35), and uses CCD detectors with a quantum efficiency of ~60%, contrasting with that of photomultiplier (PMT) detectors normally used in confocal microscopy which used to have a quantum efficiency of ~10% (36). WFR microscopy also has the shortest acquisition time, which makes this technique a better option for fluorescence quantification and the imaging of living cells, as photobleaching of fluorophores and cell damage are minimized. Finally, WFR microscopy has also been found to be more sensitive and accurate than LSCM when measuring low fluorescence intensity objects (35,36), although ELFA labellings are usually intense enough for both techniques. So, although structured light illumination could be an alternative option (it meets most of the requirements mentioned above and has been reported to be reliable (37)), WFR is an appropriate choice for fluorescence quantification in phyto- and bacterioplankton samples.

In WFR, image formation can be described by the 3D mathematical model:

$$\text{image} = \text{object} \otimes \text{psf} \quad (1)$$

where *image* is the acquired image, *object* is the real specimen and *psf* is the point spread function of the microscope (all the elements in the equation are 3D arrays). The *psf* describes the way an infinitely small point would be imaged, and distorted, by the microscope (in fact, it is a 3D photograph of a

subresolution fluorescent bead) (38). By the mathematical operation of convolution ($\otimes$), i.e. by applying the psf to every single point in the real 3D object, we would get the blurred image. Inversely, an estimate of the object can be calculated by deconvolution of the distorted image. Two kinds of deconvolution algorithms have been implemented: deblurring and restoration algorithms (38–40). The first operate separately on each focal plane of the 3D image to estimate and eliminate its blur. In contrast, restoration algorithms consider all the 3D data simultaneously to reassign light to its source in its original in-focus plane. The result in both cases is a contrast improvement but only the latter algorithms respect all the acquired information and are, therefore, suitable for improving fluorescence intensity measurements (33,35,41).

In this study, we describe and propose a novel method for accurate FLEA quantification in phytoplankton cells based on WFR. We characterize the improvement in performance and accuracy of the proposed imaging system, and we compare, for the first time in the literature, 2D and 3D WFR fluorescence intensity quantifications. This is an important contribution because on the one hand 3D fluorescence microscopy is considered superior to 2D and is thus widely used for many different purposes (41–43), but on the other hand, 2D imaging may still be used given its various advantages: simplicity, faster acquisition and analysis times, cheaper equipment and lower storage memory requirements. With this in mind, we describe the errors associated with the current 2D wide-field method and the relative distorting effect of cell size on these measurements, and discuss how to correctly interpret 2D-based data.

MATERIALS AND METHODS

Study sites and sampling

Data were collected from phytoplankton cells from eight high mountain lakes of the Central Pyrenees in order to have a wide range of phosphatase activity and cell sizes.

FLEA phosphatase protocol

Samples were sieved in the field to remove zooplankton and processed upon arrival at the laboratory (always within 6 hours after sampling in summer and

within 18 hours in winter and spring). An aliquot per sample was fixed with alkaline Lugol for phytoplankton determination. The FLEA technique was performed as previously described by Diaz-de-Quijano & Felip (44). Liquid samples were incubated in the dark, at *in situ* temperature, buffered at *in situ* pH with 0.1M HCl/Tris, citric or acetic acid buffers depending on sample pH, and using 10 µM of ELFP (Molecular Probes, E6589) substrate to achieve a compromise concentration above K_M for almost all samples. The time courses of the incubations were always monitored by fluorimeter to ensure that we sampled the incubation during its linear phase, as previously recommended (29). Incubation of the samples was stopped by gentle filtration (<20 KPa) through 2 µm pore polycarbonate filters, following which the samples were stored at -20ºC until they were mounted with CitiFluor AF1, and covered with 0.17 µm thick cover slides for microscope analysis.

Beads

Different sets of fluorescent beads were quantified: 2.5 µm diameter fluorescence intensity calibrated beads (In Speck™ Green (505/515) Microscope Image Intensity Calibration Kit, 2.5 µm, Invitrogen, Molecular Probes, I7219), 6 µm beads (FocalCheck Fluorescent Microspheres Kit, 6 µm, Slide C, Invitrogen, Molecular Probes, F24633), and 15 µm beads (FluoSpheres polystyrene microspheres, 15 µm, yellow-green fluorescent (505/515), Invitrogen, Molecular Probes, F8844). A drop of each intensity and size set of beads was spread separately on a slide, air-dried, and mounted with CitiFluor AF1 as in the case of phytoplankton cells except for the 6 µm beads, which were commercially mounted in optical cement.

Beads were used to check for size and intensity effect. First, we measured 193 fluorescent 2.5 µm diameter latex beads stained with six different calibrated intensities ranging between three orders of magnitude by flow cytometry (as a reference) and by quantitative microscopy (2D raw, and 3D raw or deconvolved). We compared differences in relative fluorescence measurements between the different methods and checked for linearity of the fluorescence intensity measurements using simple linear regression, within the R environment. The percentages of FU were log transformed to meet the assumptions of normality and homoscedasticity. Secondly, we used linear regression to relate 2D and 3D measurements of different size beads. Sample sizes were n=30 for 15 µm beads, n=52 for 6 µm beads and n=140 for

2.5 µm beads. We estimated the regression slopes and calculated their two-sided and nonparametric bootstrapped 95% confidence intervals with the boot.ci function in R, based on 10000 replicates (samplings of data) each. The bias-corrected accelerated percentile (BCa) interval type was chosen (45,46).

Flow cytometry

Intensity calibrated fluorescent beads (as detailed above) diluted in 1 ml of fresh 0.2 µm-filtered Milli-Q water were measured using the FACSCalibur flow cytometer (Becton Dickinson, USA) equipped with an air-cooled argon ion laser (15 mW, 488 nm). Beads were identified based on their fluorescent intensity signatures in a plot of 90° angle light scatter versus green fluorescence (515 nm) using the flow cytometry analysis software CELLQuest Pro (Becton Dickinson) (the gating strategy is shown as Supporting Information). To avoid particle coincidence, the rate of particle passage was kept at <1000 events s^{-1} during analyses.

Image acquisition

Samples were imaged with a Huygens restoration microscope (Scientific Volume Imaging b. v., Hilversum, The Netherlands) built around a Nikon Eclipse 90i epifluorescence microscope (Nikon, Tokyo, Japan). The microscope was equipped with a monochromatic Vosskühler COOL-1300Q CCD camera with a pixel size of 6.45 μm^2 (Vosskühler GmbH, Osnabrück, Germany) and a Xenon-arc illumination. Bead images were acquired with a Plan Apo 40X/1.0 NA oil immersion objective lens and a fluorescein filter block (ex. 450–490 nm, em. >515 nm). Cell images were acquired using a Plan Fluor 20X/0.75 NA MI objective lens with the collar adjusted to immersion with oil, and two different filter blocks: an ELFA-specific filter block (ex. 360–370 nm, em. 520–540 nm) and a chlorophyll-specific filter block (ex. 510–550 nm, em. >590 nm) for species determination. A 9.4% w/v fluorescein standard solution was used for shading correction, and to determine an inter-session correction factor (*Icf*) (47). Gain was fixed to 1 but exposure time was modified for each image acquisition to avoid image clipping (no voxel saturation was allowed) and also to collect as much information as possible from weakly bright voxels. Modulation of exposure time between images did not hinder comparability because CCDs generate a

linear response over time (48). The three parameters were recorded in metadata for further calculations. Collected 3D images were a stack composed of 35 2D slides spaced at a distance similar to the depth of field (DOF) (1.4 µm at the 20X objective and 0.7 µm at the 40X objective), and had the object of interest centred on the Z axis.

Deconvolution

Image restoration (deconvolution) was performed using the Classic Maximum Likelihood Estimation algorithm implemented in Huygens Professional 3.3.2p1, which includes a batch processor. Images were translated from nd2 to ICS file format to import them into the deconvolution software. They were cropped, respecting the volume dimensions of out-of-focus light, to speed up deconvolution. A set of images with known SNR of 40, 30, 20 and 10 was visually compared with our raw images to determine their SNR index. A SNR index of 35 was used according to our data, the maximum number of iterations was set to 40, and bleaching correction was activated. In order to select a point spread function (PSF) we deconvolved an image of a 2.5 µm fluorescent bead using both, experimental and theoretical PSF. The latter was able to reconstruct the known spherical shape of the fluorescent bead whereas the former produced a distorted shape (double banana-shaped artefact at the top and bottom edges). Moreover, the grey values of the deconvolved images showed a quantitatively more efficient deconvolution when using theoretical PSF (minimum, mean and maximum) (0, 38.03, 40807) than experimental PSF (0.002, 16.55, 13481). Therefore, we decided to use the theoretical PSF for both reasons: it triggered a better shape and fluorescence intensity restoration. The output format file had to be scaled 16 bit TIFF because the NIS-Elements software used to quantify the images only supports up to 16 bit images, whereas voxel intensities reached values above 16 bits after deconvolution.

Image analysis and calculations

Fluorescence intensity was measured using NIS-Elements AR 2.34 software (Laboratory Imaging, Praha, Czech Republic). We used two macros to semi-automate the quantification routine: the macro described by Nedoma *et al*. (29) for 2D images, and an adapted version for 3D images. In the latter

macro, the user is able to set an optimum contrast enhancement and move across the different slides of the stack to properly select the area of the object and the area of the background to be measured. These areas are projected across the whole stack defining two irregular prisms (the Volumes of Interest, VOIs). Finally, the macro measured the following variables per slide in the stack: area of the object (*Area*; μm^2), mean grey value of the object (*Mgv*; dimensionless), and mean grey value of the background (*BgMgv*; dimensionless). These measurements were automatically exported to an Excel file for semi-automated calculation together with the following metadata: distance between slides in a stack (*Zstep*; µm), number of slides (*ns*; dimensionless), camera exposure time (*expT*; ms), camera gain (*Gain*; dimensionless), intersession correction factor (*Icf*; dimensionless), and image file identity. The relative fluorescence of the object (*RFobject*; fluorescence units –FU) was calculated as follows:

$$RFobject = \frac{Icf}{\exp T \cdot Gain} \cdot \sum_{i=1}^{ns} Area \cdot Zstep \cdot (Mgv_i - BgMgv_i) \quad (2)$$

A conversion factor to relate the amount of ELFA to FU (*ConvF*; fmol ELFA·FU^{-1}) was obtained from the comparison of fluorimeter and microscope raw 2D measurements. The increase in ELFA fluorescence of several phosphatase incubations from an independent set of samples was measured by both methods in parallel. Microscope measurements were expressed in FU whereas fluorimeter measurements were translated to fmol ELFA using a calibration line based on a dilution of commercially available ELFA standard. See Nedoma *et al*. (29) for more details. To obtain the *ConvF* for the raw 3D and deconvolved 3D modes, we compared the fluorimeter measurements (fmol ELFA) and predicted raw and deconvolved 3D fluorescence intensity values corresponding to the raw 2D measurements of the independent set of samples. This prediction was based in two partial regressions (built on the 212 raw, or 175 deconvolved, cells measured in this study) that related raw 2D fluorescence intensity and object area to the raw (or deconvolved) 3D fluorescence intensity. *ConvF* values were 0.013553 fmol ELFA·FU^{-1} (raw 2D), 0.000124 fmol ELFA·FU^{-1} (raw 3D), and 0.000014 fmol ELFA·FU^{-1} (deconvolved 3D). In the case of phytoplankton cells, the single cell hydrolysed phosphate (*SCHP*; fmol ELFA·$cell^{-1}$) was calculated as:

$$SCHP = RFobject \cdot ConvF \quad (3)$$

Finally, the single cell phosphatase activity (SCPA; fmol ELFA·cell^{-1}·h^{-1}) was calculated by dividing SCHP by the number of hours in the linear phase before incubation was stopped.

Statistics

Linear least-squares regression, partial correlation, partial regression, graphics and variation partitioning were carried out in the R environment (49). Comparison of least-squares regression slopes and comparison of slopes to a theoretical value for the different intensity beads were performed using GraphPad Prism 5.01 for Windows (GraphPad Software, Inc., San Diego, CA, USA). K-means analysis was performed within the Ginkgo multivariate analysis system (http://biodiver.bio.ub.es/ginkgo/index.html, Barcelona, Catalonia).

We used an iterative approach in the R environment to find the minimum number of cells that must be counted in raw 2D to obtain the most similar results to deconvolved 3D. For each group (a species or a set of several species), the first loop involved removing one cell per iteration, sampled stochastically without replacement, and testing if the new set of sampled data: (i) maintained the homogeneity of variances between raw 2D and deconvolved 3D, and (ii) had the same difference in raw 2D and deconvolved 3D means as calculated using all observations. The macro recorded the number of remaining cells (sample size) when conditions (i) or (ii) were not met. The second loop restarted the first one 10000 times and recorded the results. For each species (or set of several species), we considered the minimum sampling size to be the number of cells that did not significantly alter the original mean and SD results in 99.99% of iterations.

RESULTS

Measurement of beads of different fluorescence intensity

We measured 193 fluorescence intensity calibrated latex beads of 2.5 µm diameter using three image analysis (IA) methods: raw 2D, raw 3D and deconvolved 3D (Table 1). These measurements were compared with flow cytometry measurements with adjusted R-squared values between 0.994

and 0.9969 and slopes between 0.9830 and 1.0199. These slopes were significantly different from 1 (p-value<0.05), but approached 1 in 3D imaging (raw or deconvolved). Therefore, the tested quantitative microscopy methods provided comparable but slightly different relative fluorescence intensity measurements to those obtained by flow cytometry (Fig. 1 a).

We also compared the previously used raw 2D IA method to the two 3D methods. Raw 3D provided the same relative fluorescence measurements as raw 2D (slope=1, α=0.05) (Fig. 1 b). Deconvolved 3D did not fit a linear regression (runs test p-value<0.0001) but did fit a quadratic one when low intensity beads were included (Fig. 1 c). This was due to a difference between the two methods when measuring low intensity objects. If the latter objects were excluded, the relationship became linear (Fig. 1 d). Deconvolved 3D measurements provided the most similar percentage fluorescence to that obtained by flow cytometry in these dimmest fluorescent beads (although not in the intermediate intensity beads) (Table 1).

Measurement of different size fluorescent beads

Fluorescence intensities of 2.5, 6 and 15.4 µm diameter beads were quantified by the raw 2D, raw 3D and deconvolved 3D methods. The slopes of simple regression lines that related 2D and 3D methods increased along with the diameter of the bead, which suggests that object size might determine the relationship between the raw 2D and the 3D measurements. This tendency was clearer when comparing raw 2D vs. raw 3D than raw 2D vs. deconvolved 3D, because the 95% confidence intervals of the regression's slopes overlapped in the latter case (Table 2).

Measurement of phytoplankton cells

We quantified SCHP (fmol·cell^{-1}) in lake phytoplankton cells using the previously outlined quantitative microscopy methods. Cells were divided into three size groups by a K-means analysis. The plots relating the current

n	Manufacturer Fluorescence Intensity (%)	Flow cytometry Fluorescence Intensity (%)	Raw 2D		Raw 3D		Deconvolved 3D	
			Fluorescence Intensity (FU) and (SD)	Fluorescence Intensity (%)	Fluorescence Intensity (FU) and (SD)	Fluorescence Intensity (%)	Fluorescence Intensity (FU) and (SD)	Fluorescence Intensity (%)
37	100	100	19719 (1879)	100	202750 (26123)	100	18226411 (16718390)	100
29	38	36	6068 (541)	30.11	64803 (6959)	30.91	9467089 (1966014)	29.47
36	14	13	2110 (172)	10.57	22033 (1828)	10.66	2637021.8 (1333435)	9.83
22	3.3	3.1	547 (28.3)	2.75	5739 (431)	2.81	636586 (437252)	2.73
36	0.96	0.9	157 (14.7)	0.79	1679 (149)	0.82	168243 (114843)	0.75
33	0.25	0.22	25.6 (4.9)	0.18	371 (49.1)	0.18	65583 (32185)	0.24

Table 1. Average fluorescence intensities of the different groups of fluorescence intensity standard beads. Values are in percentage relative to the most fluorescent group, and in fluorescence units (FU). Note that values, in FU, increase one order of magnitude from raw 2D to raw 3D, and two orders of magnitude more from raw 3D to deconvolved 3D. The statistics of flow cytometry measurements are available as Supporting Information.

Slopes	2.5 µm	6 µm	15.4 µm
Raw 2D vs. Raw 3D	10.23 (10.09, 10.41)	15.31 (13.98, 16.92)	20.77 (20.51, 21.04)
Raw 2D vs. Dec. 3D	18.92 (18.07, 19.71)	23.98 (16.43, 30.99)	43.31 (22.53, 56.88)

Table 2. Slopes of linear regressions relating 2D and 3D measurements of fluorescent beads of different sizes. In brackets are the bootstrapped 95% confidence intervals of these slopes. The bootstrapped confidence intervals are of the bias-corrected accelerated percentile (Bca) type and are based on 10,000 bootstrap replicates (see materials and methods for more detail).

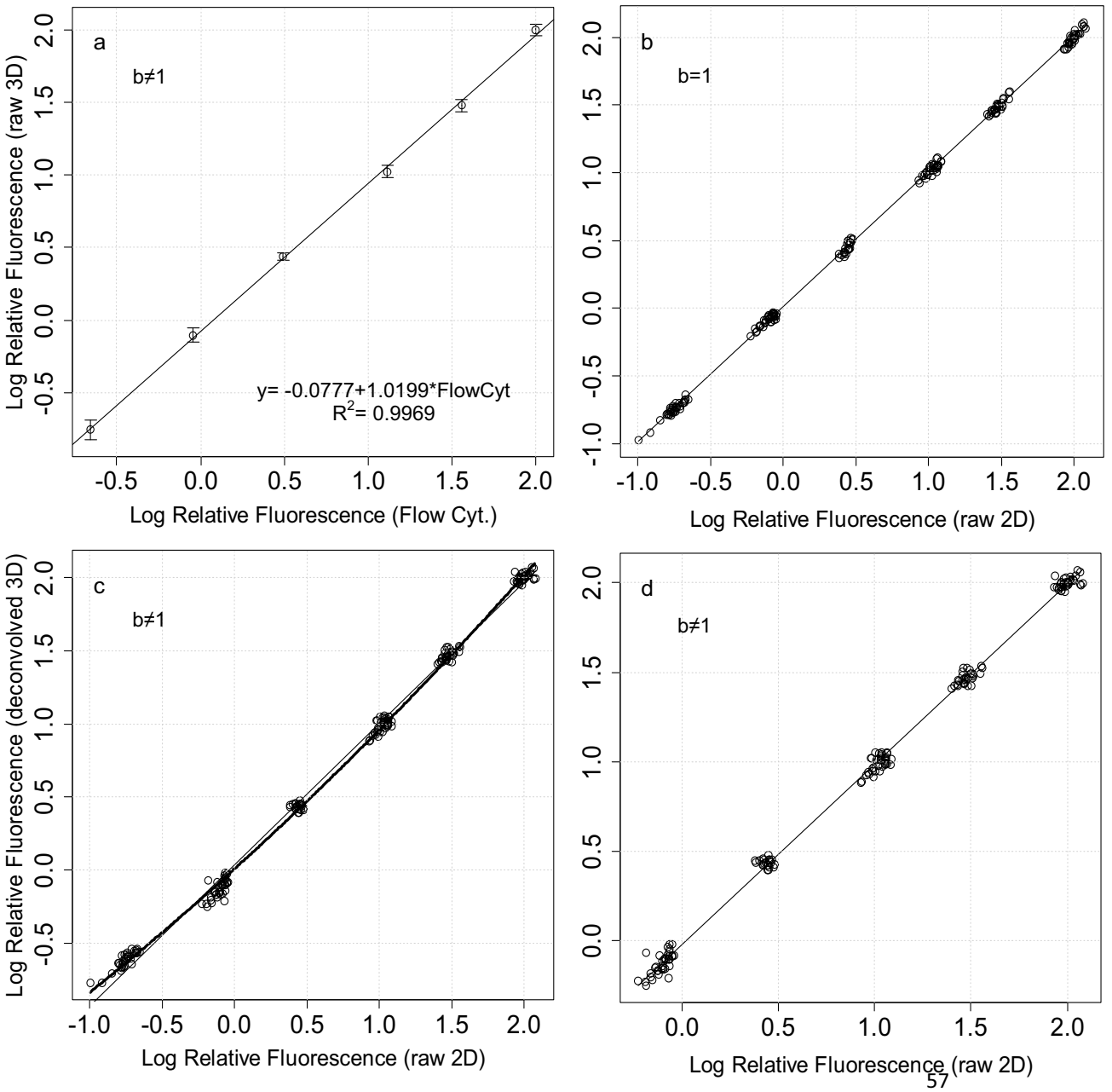

Fig. 1. Comparison of standard fluorescence intensity bead measurements performed using different methods (flow cytometry and quantitative microscopy: raw 2D, raw 3D and deconvolved 3D). Thin lines are linear regressions, thick line in Figure c is quadratic regression. Figure d presents the same data as c, but excluding the lowest intensity fluorescent beads.

method (raw 2D) to the 3D methods (Fig. 2 a,b) confirmed the results obtained by measuring different size beads. The relationship between raw 2D and 3D gave regression lines for the different cell size groups with clearly different intercepts (Fig. 2 a), whereas that of raw 2D against deconvolved 3D was not as clearly affected by cell size. In this case, the increase in dispersion may mask any eventual cell size effect.

To understand the dispersion difference between Fig. 2 a and b we may consider an ideal cell (Fig. 2 right). Three-dimensional measurements are based on the sum of voxel intensities within a volume of interest (VOI). This volume is a prism whose irregular base is user-defined following the silhouette of the cell projected on the XY plane. Besides, the restoration algorithm that we used respects the total amount of energy that belonged to a cell in the raw image and simply relocates it to its source, in such a way that the sum of energy inside ($_i$) and outside ($_o$) the VOI before ($_r$) and after deconvolution ($_d$) is identical, i.e.:

$$E_{ir}+E_{or}=E_{id}+E_{od} \quad (4)$$

which can be expressed as:

$$E_{or}-E_{od}=E_{id}-E_{ir} \quad (5)$$

The dispersion difference between Fig. 2 a and b indicates that for two cells with a very similar raw 2D measurement, the difference for each cell between deconvolved 3D (E_{id}) and raw 3D (E_{ir}) values may be quite substantial. Taking into account equation 5, this dispersion difference also means that the difference of energy outside the VOI in the raw image (E_{or}) minus energy outside the VOI in the deconvolved image (E_{od}) differs between cells. Because the first element of the difference (E_{or}) is proportional to the degree of out-of-focus light and the second (E_{od}) is inversely proportional to the efficiency of deconvolution, we argue that the increase in dispersion observed when deconvolving could be due to either the original amount of acquired out-of-focus light, the efficiency of deconvolution or a combination

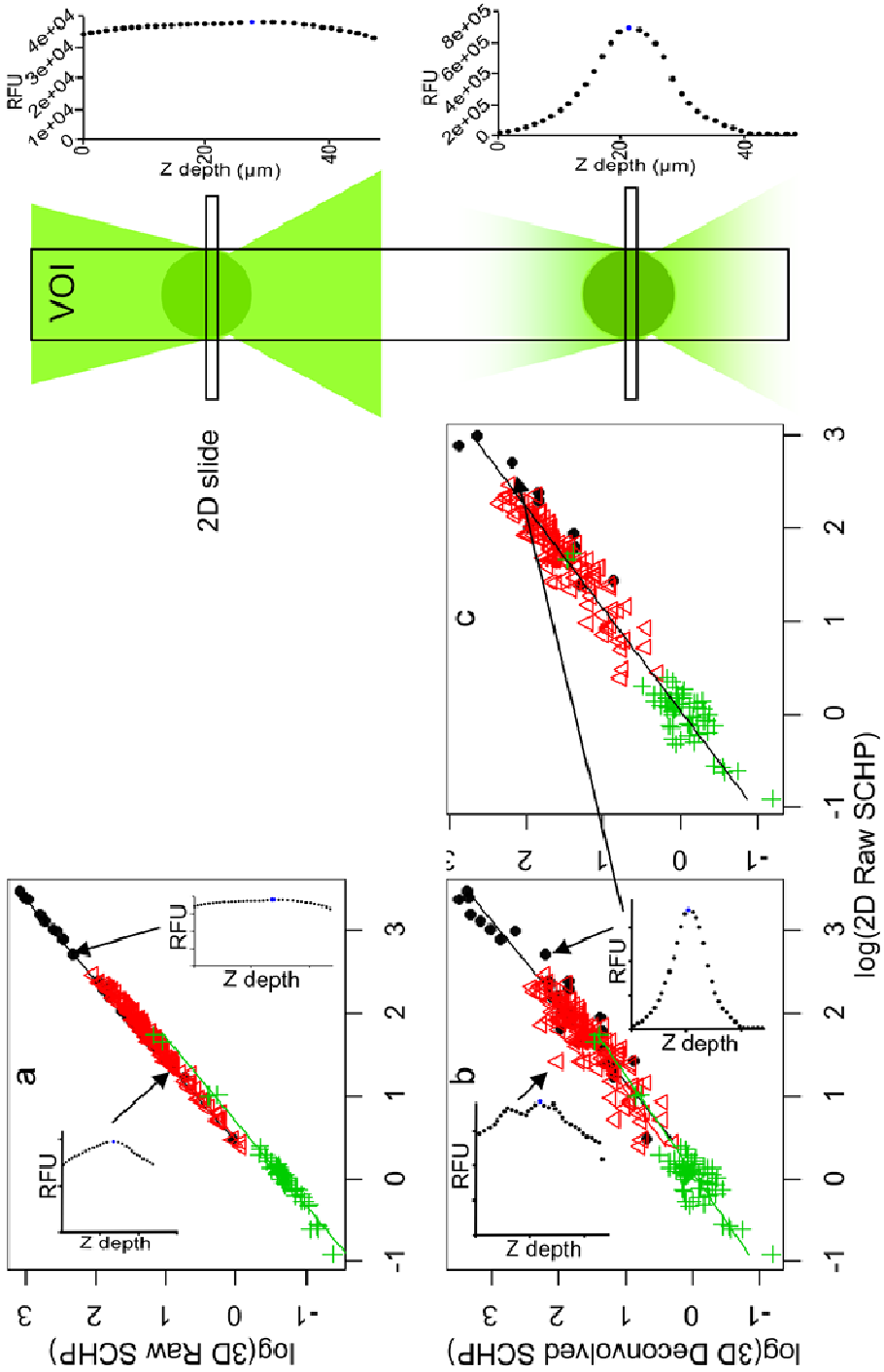

Fig. 2. Right: Schema of the lateral view of a raw cell (top) and a well deconvolved cell (bottom), and their respective intensity profiles. Horizontal rectangles represent in-focus 2D slides, the vertical one represents the volume of interest (VOI) for 3D

fluorescence measurements. Left: Comparison of three different IA fluorescence quantification methods using the log of SCHP (fmol ELFA·cell^{-1}) of phytoplankton cells (a and b). Graph c is the same as graph b but excludes inefficient deconvolved cells. Small +, medium △, and large cells ●. The intensity profiles of a well deconvolved cell and an inefficiently deconvolved cell are embedded in graphs a (raw) and b (deconvolved profiles). The arrows point out the position of these two example cells.

of both. To further deepen our knowledge on this subject, we conducted a cell-by-cell inspection of the intensity profile of their VOI along the Z axis (Fig. 2). Only cells with sharp profiles, indicative of efficient deconvolution, were considered while those with inefficient deconvolution were excluded from the analysis (Fig. 2 c). (A total of 175 cells out of 212 were analysed). Thus, the increase in dispersion can be caused by actual differences in the amount of out-of-focus light between individual cells and not by any artefact introduced by deconvolution. As the magnitude of dispersion was virtually identical (Fig. 2 b and c), we were able to confirm that for a given value in raw 2D (or 3D), a range of values spanning one order of magnitude was recorded by deconvolved 3D. Therefore, raw SCHP measurements (used to calculate the population averages reported in recent studies) may be biased by up to one order of magnitude since out-of-focus light was not taken into account.

Because we used mismatching immersion oil (n=1.516 at 23ºC) and embedding Citifluor AF1 (n=1.4628 at 22ºC), it could be hypothesized that the increase in dispersion observed between raw and deconvolved results (Fig. 2 a and b) was also explained by the fact of having imaged under spherical aberration (SA) conditions. SA implies both, a strong decay in signal intensity as the focal plane is moved into the sample (depth aberration) and a challenge to efficient deconvolution. Nevertheless, only the former effect was to be taken into account because efficient deconvolutions triggering sharp and symmetric fluorescence intensity profiles where achieved thanks to a series of pre-deconvolution treatments (accurate image cropping to accommodate all the out-of-focus light, instable illumination correction, and correction of bleaching- and SA-induced fluorescence intensity decline in depth) together with a SA correction mechanism in Huygens Professional software (where the PSF was resized, and the whole image stack was splitted into a series of bricks along the Z axis to be able to apply different PSF to

them). In the case that such dispersion was induced by SA the cells with high residuals in the 2D vs deconvolved 3D regression should be those closer to the coverslide because the loss of fluorescence intensity with depth is steeper there, and hence the pre-deconvolution bleaching (and SA) correction may increase more the whole 3D image intensity. Sample depth was recorded just for big and small beads, and we found that fifteen µm fluorescent beads also showed this increase in dispersion when deconvolved but there wasn't any significant correlation between sample depth and the residuals (Fig. 3). Therefore, difference in the dispersion between raw and deconvolved data does not seem to be caused by SA, either.

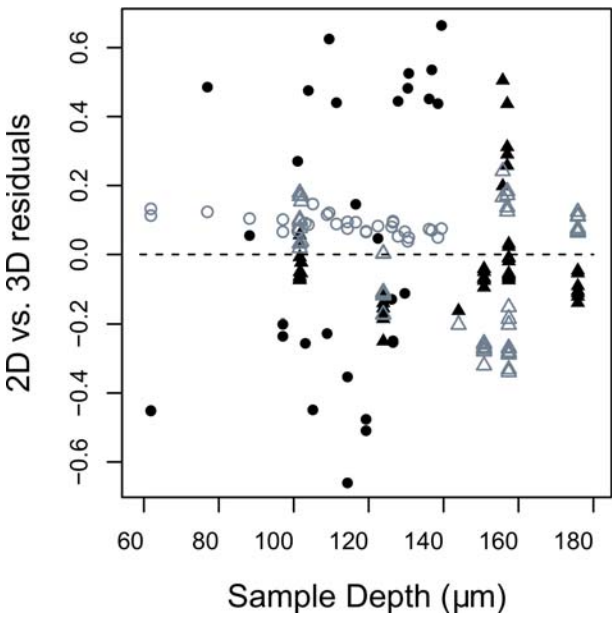

Fig. 3 Relationship between sample depth (or distance to the coverslide) of 2.5 µm (triangles) and 15 µm (circles) fluorescent beads, and the residuals of linear regressions relating their raw 2D and raw 3D (grey) or raw 2D and deconvolved 3D (black) fluorescence intensities.

Additionally, we compared beads and cells to check whether morphology could be responsible for some of the unexplained variation. The adjusted R-squared of linear regressions relating 2D and 3D measurements decreased when 3D was deconvolved, i.e. the unexplained variation increased. Concretely, the unexplained variation increase was high for 15µm beads, intermediate in the three populations of cells (large, medium and small) with diverse morphology (including diatoms, dinoflagellates, chrysophytes and chlorophytes), and small in the case of 2.5µm beads. Hence, morphology might not be an important driver of unexplained variation.

To assess the impact of the cell area on the relationship between 2D and 3D fluorescence intensity measurements, we developed a specific model. Since 2D and 3D measurements are different ways of measuring fluorescence intensity, these variables were highly correlated. Log of area vs. log of raw 3D fluorescence intensity and log of area vs. log of deconvolved 3D fluorescence intensity had partial correlation coefficients of 0.997 and 0.93, respectively. Due to this high degree of collinearity, partial regression was selected as the best approach to forecast raw ($Raw3D_0$) or deconvolved ($Dec3D_0$) 3D measurements from new area ($Area_0$) and 2D measurements ($Raw2D_0$). The e subindices ($_e$) correspond to estimated intermediate variables necessary to resolve the equation system. The functions we obtained, as the log of area (μm^2) and log of fluorescence intensity expressed as SCHP (fmol ELFA·$cell^{-1}$), were:

$$Raw2D_e = Raw2D_0 - (-1.482449 + (1.329476 \cdot Area_0))$$

$$Raw3D_e = 1.255279 \cdot 10^{-17} + (1.026991 \cdot Raw2D_e)$$

$$Raw3D_0 = Raw3D_e + (-2.406128 + (1.514223 \cdot Area_0))$$

(6)

And in the case of deconvolved 3D:

$$Raw2D_e = Raw2D_0 - (-2.259155 + (1.725148 \cdot Area_0))$$

$$Dec3D_e = 2.037851 \cdot 10^{-17} + (8.952034e\text{-}01 \cdot Raw2D_e)$$

$$Dec3D_0 = Dec3D_e + (-2.145553 + (1.600514 \cdot Area_0))$$

(7)

Then, we calculated adjusted R-squared to clarify whether the addition of object size (*Area*) provided any improvement in the explanation of variation relative to a simple linear regression that excluded object size. The results showed that for the forecast of raw 3D, we explained 99.5% of the variation when using a linear regression without the *Area* variable, whereas the explained variation increased to 99.7% when the *Area* variable was included in the partial regression. In contrast, for the forecast of deconvolved 3D, the inclusion of the *Area* variable slightly decreased the explained variation (from 95.4% to 95.3%). The partitioning of variation is summarized in Table 3,

	Variation explained by Raw 2D	Variation explained by Raw 2D and Area	Variation explained by Area	Unexplained variation
Raw 3D	33.5%	66.1%	0.2%	0.2%
Deconvolved 3D	28.9%	66.6%	0.03%	4.5%

Table 3. Proportions of variation of raw and deconvolved 3D values (R^2).

unexplained variation (4.5–0.2), which is attributable to deconvolution, is almost 150 times greater than the variation explained by object size alone (0.03).

Here again, we could hypothesize that the slight impact of the cell area on the relationship between 2D and 3D fluorescence intensity measurements (Fig. 2 a) was influenced by the fact of having imaged under SA conditions. To test this hypothesis, we used *in silico* modelling. The behaviour of the ratio between raw 2D and raw 3D fluorescence intensity values (2D/3D) was observed for typical intensity profiles of small and big objects at different distances to the coverslide. As we mentioned above, the decline of fluorescence intensity in depth caused by SA is steeper in the first micrometers and more moderate at deeper positions in the sample. This triggered two observable phenomena: (i) the 2D/3D was slightly smaller than in the cases where the decline was lineal or where there wasn't any decline, and (ii) the 2D/3D relationship diminished more intensely when the non-aberrated intensity profile of the object was flatter (not sharply unimodal), but mainly diminished when the imaged object was closer to the coverslide (steeper loss of intensity). Because big cells usually have flatter intensity profiles than small cells, it was expectable that big cells had smaller 2D/3D than small cells (as it was observed in Fig. 2 a), and especially when the cells were close to the coverslide. Therefore, it is possible that SA contributed to some extent to the apparent size effect, although it would be quantitatively modest according to the model (to a maximum of about 5% in an extreme case).

To assess the bias induced by cell size in raw 2D single-cell enzyme activity measurements, raw 2D SCHP were determined for five ideal spherical cells ranging from 2 to 32 µm diameter and having the same deconvolved 3D SCHP value by using equation 7. The different raw 2D values of these cells

	32 µm	16 µm	8 µm	4 µm	2 µm
32 µm	100	109	119	130	142
16 µm	92	100	109	119	130
8 µm	84	92	100	109	119
4 µm	77	84	92	100	109
2 µm	71	77	84	92	100

Table 4. Percentage between the apparent raw 2D SCHP simulated for five ideal spherical cells (from 2 to 32 µm diameter) with the same deconvolved 3D SCHP value. The table is to be read from columns to rows. For instance: in raw 2D SCHP values, a 2 µm diameter cell seems to have a 142% of the ELFA of a 32 µm cell with the same deconvolved 3D SCHP value. Inversely, a 32 µm cell seems to have the 71% of the ELFA of a 2 µm cell with the same deconvolved 3D SCHP value.

were compared in pairs and the comparison was expressed as a percentage (Table 4). If cells with 2 and 32 µm in diameter were compared in raw 2D (the most extreme case), it could seem that the larger cell had 71% of the SCHP of the small cell (i.e. the small cell had 142% of the SCHP of the large cell), while they would have the same value in deconvolved 3D according to our model.

Species level analysis

In the analysis of natural populations or species, it is interesting to assess the population- or species-specific functional variability as well as the average SCPA. Three selected species of lake phytoplankton were analysed for SCHP to estimate enzymatic functional variability by the three techniques (raw 2D and raw or deconvolved 3D) (Fig. 4). Similar dispersions were recorded and the homogeneity of variances between raw 2D and deconvolved 3D measurements was statistically confirmed using Levene's test (Table 5). Although the medians were similar in raw 2D and deconvolved 3D, the means were significantly different in most cases (Wilcoxon test; Table 5). Raw 3D provided clearly lower values (Fig. 4). The mean SCPA measured by the classic raw 2D method was 17.23 fmol·cell^{-1}·h^{-1} in *Amphidinium* sp., 0.3786 fmol·cell^{-1}·h^{-1} in *Cyclotella* sp.1, and 32.43 fmol·cell^{-1}·h^{-1} in *Cyclotella* sp.2.

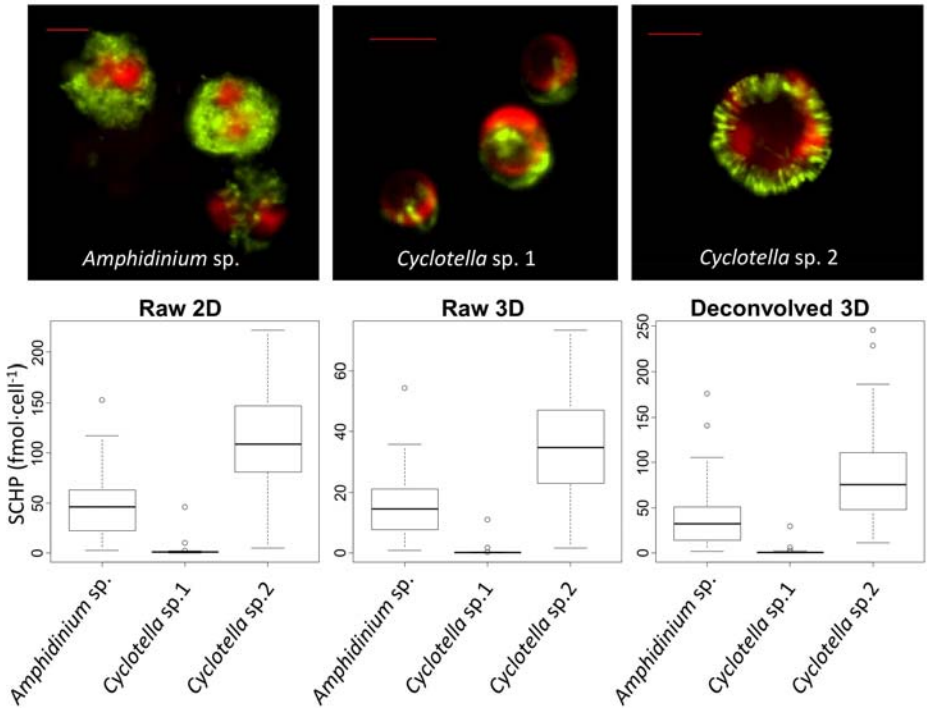

Fig. 4. Epifluorescence microimages of three phytoplankton species. Red: chloroplasts; Yellow-green: ELFA precipitates indicating phosphatase activity. Scale bars are 5 µm long. Single cell hydrolysed phosphate (SCHP) of the three separate phytoplankton populations, measured using the three IA quantification methods.

n	Species	Size	Mean (p-v)	SD (p-v)	Minimum sampling size (number of cells)
175	All	All	≠ (3.075×10^{-14})	= (0.4598)	141
53	*Amphidinium* sp.	Medium (14µm)	≠ (0.0004)	= (0.8421)	39
54	*Cyclotella* sp.1	Small (~6µm)	= (0.0761)	= (0.6858)	37
35	*Cyclotella* sp.2	Medium (14µm)	≠ (1.106×10^{-9})	= (0.1360)	26

Table 5. Wilcoxon and Levene tests for comparison of means and homogeneity of variances between raw 2D and deconvolved 3D fluorescence intensity measurements in the three selected species and the whole set of efficiently deconvolved cells.

DISCUSSION

Deconvolved 3D is the best estimate

Deconvolved 3D was considered our best estimate of fluorescence intensity because it generally improved the management of out-of-focus light (which significantly increases the total measured fluorescence intensity) without introducing any detectable error. On the one hand, the biggest difference driven by deconvolution in fluorescence intensity measurements was a substantial increase in the dispersion of 2D vs. 3D measurements (Fig. 2 b relative to 2 a). Therefore, dealing with out-of-focus light (performing restorative deconvolution) is more important than correcting the eventual size effect or using raw 3D microscopy alone. The contribution of out-of-focus light to total variation in the 2D vs. 3D measurements was visibly more important (changes in overall dispersion from Fig. 2 a relative to 2 b) than that due to size effect (changes in 2D to 3D relationship between size groups in Fig. 2 a and b). Specifically, out-of-focus light may account for 4.3% of the total variation on top of the 0.03% or 0.2% due to object size. On the other hand, we showed that this difference in dispersion mainly reflected real changes in the amount of out-of-focus light per cell and therefore should not be regarded as a deconvolution artefact or a spherical aberration effect (Fig. 2 b and c, Fig 3). In summary, absolute and relative values (magnitude and dispersion) obtained by deconvolved 3D should be considered as the most reliable estimate of real values.

Raw 2D and deconvolved 3D are equivalent methods in the case of population characterization

We found that since current raw 2D quantifications do not take out-of-focus light into account, they may produce single-cell measurements that are half an order of magnitude above or below our best estimate of fluorescence intensity via deconvolved 3D. Nevertheless, these individual errors in raw 2D measurements were partially compensated when we attempted to describe mean cell activity and functional variability of one or several species (Fig. 4) or groups of cells (Fig. 2). If 25–40 cells per species were measured in raw 2D, the obtained SD did not differ significantly from that of deconvolved 3D, and the slight (but significant) difference in means was not significantly affected by sample size either, with a confidence level of 99.99% (Table 5) (see methods for more detail). A minimum of 141 cells had to be measured to

achieve a reliable result in groups of more heterogeneous cells (like a community). Thus, the measurement in raw 2D of a minimum of 25–40 cells per species provides sufficiently similar average values and ranges to deconvolved 3D.

Cell size modulates 2D measurement bias

Although deconvolved 3D was the best method tested, the results from raw 3D are also interesting since they show that cell size contributed substantially to the overall bias recorded by the raw 2D method. When object size was introduced into the model of raw 3D depending on raw 2D, adjusted R-squared (total explained variability) improved from 0.995 to 0.997. This suggests that object size modulates the raw 2D bias in relation to raw 3D. The apparent paradox is that when we modelled deconvolved 3D depending on raw 2D, the inclusion of object size did not increase the adjusted R-squared. As pointed out in the first paragraph of the discussion, we interpret this as showing that object size contributes to the fluorescence intensity bias measured in raw 2D but is clearly a less important source of variability when compared to deconvolution. These observations were essentially not undermined by having imaged under SA. According to our partial regression, comparison of raw 2D ELFA values of different species or populations of different cell sizes should be carefully interpreted: for instance, a 16 µm diameter cell could appear to have 84% of the ELFA of a 4 µm cell in raw 2D, while they would be identical in deconvolved 3D (Table 4).

If we take raw 3D as a reference (Fig. 2 a), we can graphically observe the effect of object size on 2D fluorescence intensity measurements even when we consider this variable in discrete groups of small, medium and large cells. The simple regression lines of the three size groups showed different intercepts (relationship between 2D and 3D measurements depended on cell size). Moreover, we observed a non-linearity in this size effect: the distance between the intercepts of the regression lines of small and medium cells was greater than that between the medium and large cells (~6 µm, 14 µm and 40 µm of object diameter respectively). (Note that object sizes –the projection in the XY plane of the defined VOI– are always proportional but slightly larger than the actual cell size). Having said that object size was not the major biasing factor, we must note that most of the phytoplankton cells in oligotrophic marine and freshwater systems are frequently of small to

medium size (50–52), a range in which object size bias might be more important.

Finally, deconvolution did not affect all cell sizes in the same way. When we deconvolved, the simple linear regression intercepts of all three size groups moved towards zero, but the smaller the cell, the bigger the effect of deconvolution. In this respect, the percentage of inefficient deconvolutions was the highest in larger cells. These results suggest that deconvolution may be more efficient for small and medium cells than for very large ones. Nevertheless, after checking for deconvolution efficiency, all the values of efficiently deconvolved cells were equally reliable whatever their size.

Future quantification of cells with low phosphatase activity

The fluorescence intensity measurements of weakly fluorescent objects were the most affected by deconvolution. This resulted in a quadratic relationship between deconvolved 3D and raw 2D (Fig. 1 c and d), but deconvolved 3D was the method that measured the most similar values to flow cytometry and manufacturer values for the standard 0.22% (weak fluorescence) intensity beads (Table 1). Deconvolved 3D was also reported as the most accurate quantification method for low intensity objects in the literature (35), although we did not observe such improvement. In practice, the 0.22% intensity beads recorded average fluorescence intensities (FU) like those that would produce the low ELFA amounts of: 0.35±0.07 fmol in raw 2D, 0.05±0.01 fmol in raw 3D, or 0. 92±0.45 fmol in deconvolved 3D (0.071±0.014 fmol·μm^{-2}, 0.010±0.002 fmol·μm^{-2}, and 0.187±0.092 fmol·μm^{-2} respectively). Therefore, non-linearity is a phenomenon that is restricted to the smallest values of SCHP, which constitutes a minor problem in the current state-of-the-art. Although reported SCHP values ranged from 0 to 1831 fmol·$cell^{-1}$ (53), including the non-linear range of fluorescence intensity, in current state-of-the-art, small amounts of fluorescence originating from fluorochromes in the sample other than ELFA (DAPI, degraded chlorophyll autofluorescence, etc.) may show overlap of their emission tails with the ELFA emission peak window and may account for a significant proportion when object ELFA intensity is very low. Therefore, the cells with the lowest amount of activity cannot be accurately quantified nor distinguished from completely inactive cells when DAPI or degraded chlorophyll is present in the sample. To avoid this problem, we suggest that raw 3D images should be

deconvolved with an algorithm that, apart from modelling light blur, also models the spectral overlap of different fluorochromes (41). In that scenario, the question why is there a rupture of linearity between the dimmest and the intermediate fluorescent beads when measured via deconvolved 3D in comparison to the other methods should be addressed. Such phenomenon seems to be robust because it was not only observed in this study but also in Swedlow *et al*. (35).

Improvement of the FLEA technique

One of the weaknesses that Nedoma and colleagues detected in the FLEA technique (29) was the intercalibration of a microscope with a fluorimeter, i.e., the conversion of microscope FU to fmols of ELFA. The conversion factor is the slope of a linear regression that relates the rate of ELFA formation during the linear phase of an incubation measured by a fluorimeter (in $fmol \cdot l^{-1} \cdot h^{-1}$, on the X axis) and by raw 2D image analysis (in $FU \cdot l^{-1} \cdot h^{-1}$, on the Y axis). Thus, each point on the graph represents a single incubation. The problem is that the r^2 of the regression line is about 0.65. Since the range of ELFA formation rates is already quite wide, we argue that there are other sources of the dispersion of the different incubations in the mentioned graph. Firstly, quantitative microscopy may underestimate ELFA particles <0.2 µm because the incubated sample is filtered by polycarbonate (PC) filters of the same pore size, whereas ELFA particles of all sizes are measured by fluorimetry. Thus, dispersion could be due to differences in the proportion of small ELFA particles between different incubated samples. Secondly, using raw 2D images may be another source of variability. Current raw 2D images of filters acquired to calculate the conversion factor (ConvF) are focused to the plane with the highest amount of fluorescence, but this compromise undersamples fluorescence for three reasons: only one optical slice of large objects is acquired, only one optical slice of the out-of-focus light of objects (usually >10 µm deep) is acquired, and not all objects in a frame are usually well focused because some may detach from the PC filter during sample mounting, and more important, because rippling or mispositioning (not strictly orthogonal) of the PC filter may occur. The proposed deconvolved 3D method for FLEA quantification is expected to significantly improve this critical step in the FLEA technique.

In conclusion, deconvolved 3D FLEA measurements provide superior analytical power and are recommended to distinguish cells with SCPA differing by less than an order of magnitude. They also avoid problems of comparability between different size cells and, finally, they are the most appropriate option in those cases where the value of each single cell is important rather than the average of a population of cells. This is the case for measurements of activity in less numerous species and in the combination of the FLEA technique with other single-cell techniques. The deconvolved 3D FLEA technique alone will provide accurate information about a relevant component of trophic strategy, the enzymatic pathway, which should be incorporated into studies of biological traits that could be important for the fitness of species (54). This will aid in reconstructing the evolutionary history of the trophic strategy, defining the functional niche of many microplanktonic species, and better understanding and modelling of the dynamics of enzyme activity in nature. In addition, the deconvolved 3D FLEA technique improves the accuracy of the FLEA technique at the cell level enough to make it combinable with microautoradiography or MAR-FISH for single-cell nutrient incorporation, and with FLBs or CARD-FISH for single-cell bacterivory assessments. Such technical integrations may provide information about detailed biogeochemical processes such as the link between hydrolytic enzyme activity and nutrient uptake at the cellular level and in close-to-*in situ* conditions, but also about functional shifts in trophic strategies within mixotrophic populations of the microbial loop.

ACKNOWLEDGEMENTS

This research involved collaboration between the Limnology Group (CEAB-UB) and the Aquatic Microbial Ecology Department (HBI, CAS). We thank Dr. Jiři Nedoma for technical support during image acquisition and image analysis, and Mrs. Mireia Utzet and Dr. Francesc Carmona for statistical advice. All the authors state that we do not have any conflict of interests to declare.

REFERENCES

1. Clark LL, Ingall ED, Benner R. Marine phosphorus is selectively remineralized. Nature 1998;393:426.

2. Kolowith LC, Ingall ED, Benner R. Composition and cycling of marine organic phosphorus. Limnol. Oceanogr. 2001;46:309–320.

3. Reitzel K, Ahlgren J, Gogoll A, Jensen HS, Rydin E. Characterization of phosphorus in sequential extracts from lake sediments using P-31 nuclear magnetic resonance spectroscopy. Can. J. Fish. Aquat. Sci. 2006;63:1686–1699.

4. Bai X, Ding S, Fan C, Liu T, Shi D, Zhang L. Organic phosphorus species in surface sediments of a large, shallow, eutrophic lake, Lake Taihu, China. Environ. Pollut. 2009;157:2507–2513.

5. Luo H, Zhang H, Long R, Benner R. Depth distributions of alkaline phosphatase and phosphonate utilization genes in the North Pacific Subtropical Gyre. Aquat. Microb. Ecol. 2011;62:61–69.

6. Schindler DW. Evolution of Phosphorus Limitation in Lakes. Science 1977;195:260–262.

7. Thingstad TF, Rassoulzadegan F. Nutrient limitations, microbial food webs, and biological C-pumps - Suggested interactions in a P-limited Mediterranean. Mar. Ecol. Prog. Ser. 1995;117:299–306.

8. Perry MJ. Phosphate utilization by an oceanic diatom in phosphorus-limited chemostat culture and in the oligotrophic waters of the central North Pacific. Limnol. Oceanogr. 1976;21:88–107.

9. Vidal M, Duarte CM, Agustí S, Gasol JM, Vaqué D. Alkaline phosphatase activities in the central Atlantic Ocean indicate large areas with phosphorus deficiency. Mar. Ecol. Prog. Ser. 2003;262:43–53.

10. Reich PB, Oleksyn J. Global patterns of plant leaf N and P in relation to temperature and latitude. Proc. Natl. Acad. Sci. U. S. A. 2004;101:11001–11006.

11. Elser JJ, Andersen T, Baron JS, Bergström A-K, Jansson M, Kyle M, Nydick KR, Steger L, Hessen DO. Shifts in lake N:P stoichiometry and nutrient limitation driven by atmospheric nitrogen deposition. Science 2009;326:835–837.

12. Sinsabaugh RL, Carreiro MM, Repert DA. Allocation of extracellular enzymatic activity in relation to litter composition, N deposition, and mass loss. Biogeochemistry 2002;60:1–24.

13. Edwards I, Zak D, Kellner H, Eisenlord S, Pregitzer K. Simulated Atmospheric N Deposition Alters Fungal Community Composition and Suppresses Ligninolytic Gene Expression in a Northern Hardwood Forest. PLoS One 2011;6:1-10.

14. Yamada N, Tsurushima N, Suzumura M. Effects of Seawater Acidification by Ocean CO(2) Sequestration on Bathypelagic Prokaryote Activities. J. Oceanogr. 2010;66:571–580.

15. Piontek J, Lunau M, Haendel N, Borchard C, Wurst M. Acidification increases microbial polysaccharide degradation in the ocean. Biogeosciences 2010;7:1615–1624.

16. Sardans J, Penuelas J, Estiarte M. Seasonal patterns of root-surface phosphatase activities in a Mediterranean shrubland. Responses to experimental warming and drought. Biol. Fertil. Soils 2007;43:779–786.

17. Wallenstein M, Allison S, Ernakovich J, Steinweg JM, Sinsabaugh R. Controls on the Temperature Sensitivity of Soil Enzymes: A Key Driver of In Situ Enzyme Activity Rates. Soil Biol. 2011;22:245–258.

18. Boavida M-JJ, Wetzel RG. Inhibition of phosphatase activity by dissolved humic substances and hydrolytic reactivation by natural ultraviolet light. Freshw. Biol. 1998;40:285–293.

19. Espeland EMM, Wetzel RGG. Complexation, stabilization, and UV photolysis of extracellular and surface-bound glucosidase and alkaline phosphatase: Implications for biofilm microbiota. Microb. Ecol. 2001;42:572–585.

20. Tank SE, Xenopoulos MA, Hendzel LL. Effect of ultraviolet radiation on alkaline phosphatase activity and planktonic phosphorus acquisition in Canadian boreal shield lakes. Limnol. Oceanogr. 2005;50:1345–1351.

21. Steen AD, Arnosti C. Long lifetimes of beta-glucosidase, leucine aminopeptidase, and phosphatase in Arctic seawater. Mar. Chem. 2011;123:127–132.

22. González-Gil S, Keafer BA, Jovine RVM, Aguilera A, Lu S, Anderson DM. Detection and quantification of alkaline phosphatase in single cells of phosphorus-starved marine phytoplankton. Mar. Ecol. Prog. Ser. 1998;164:21–35.

23. Lauro F, McDougald D, Thomas T, Williams T, Egan S. The genomic basis of trophic strategy in marine bacteria. Proc. Natl. Acad. Sci. U. S. A. 2009;106:15527–15533.

24. Christie-Oleza JA, Piña-Villalonga JM, Bosch R, Nogales B, Armengaud J. Comparative proteogenomics of twelve Roseobacter exoproteomes reveals different adaptive strategies among these marine bacteria. Mol. Cell. proteomics 2012;11:1–12.

25. Ou L, Huang B, Lin L, Hong H, Zhang F, Chen Z. Phosphorus stress of phytoplankton in the Taiwan Strait determined by bulk and single-cell alkaline phosphatase activity assays. Mar. Ecol. Ser. 2006;327:95–106.

26. Carlsson P, Caron DA. Seasonal variation of phosphorus limitation of bacterial growth in a small lake. Limnol. Oceanogr. 2001;46:108–120.

27. Nedoma J, Vrba J. Specific activity of cell-surface acid phosphatase in different bacterioplankton morphotypes in an acidified mountain lake. Environ. Microbiol. 2006;8:1271–1279.

28. Duhamel S, Gregori G, Van Wambeke F, Nedoma J. Detection of Extracellular Phosphatase Activity at the Single-Cell Level by Enzyme-Labeled Fluorescence and Flow Cytometry: The Importance of Time Kinetics in ELFA Labeling. Cytom. Part A 2009;75A:163–168.

29. Nedoma JJ, Štrojsová A, Vrba J, Komárková J, Šimek K, Strojsova A, Komarkova J, Simek K. Extracellular phosphatase activity of natural plankton studied with ELF97 phosphate: fluorescence quantification and labelling kinetics. Environ. Microbiol. 2003;5:462–472.

30. Litchman E, Klausmeier CA. Trait-Based Community Ecology of Phytoplankton. Annu. Rev. Ecol. Evol. Syst. 2008;39:615–639.

31. Litchman E, Klausmeier CA, Schofield OM, Falkowski PG. The role of functional traits and trade-offs in structuring phytoplankton communities: scaling from cellular to ecosystem level. Ecol. Lett. 2007;10:1170–1181.

32. Allison SD. A trait-based approach for modelling microbial litter decomposition. Ecol. Lett. 2012;15:1058–1070.

33. Andrews PD, Harper IS, Swedlow JR. To 5D and beyond: Quantitative fluorescence microscopy in the postgenomic era. Traffic 2002;3:29–36.

34. Verveer PJ, Gemkow MJ, Jovin TM. A comparison of image restoration approaches applied to three-dimensional confocal and wide-field fluorescence microscopy. J. Microsc. 1999;193:50–61.

35. Swedlow JR, Hu K, Andrews PD, Roos DS, Murray JM. Measuring tubulin content in Toxoplasma gondii: A comparison of laser-scanning confocal and wide-field fluorescence microscopy. Proc. Natl. Acad. Sci. 2002;99:2014–2019.

36. Murray JM, Appleton PL, Swedlow JR, Waters JC. Evaluating performance in three-dimensional fluorescence microscopy. J. Microsc. 2007;228:390–405.

37. Barlow AL, Guerin CJ. Quantization of widefield fluorescence images using structured illumination and image analysis software. Microsc. Res. Tech. 2007;70:76–84.

38. Wallace W, Schaefer LH, Swedlow JR. A workingperson's guide to deconvolution in light microscopy. Biotechniques 2001;31:1076–1097.

39. McNally JG, Karpova T, Cooper J, Conchello JA. Three-Dimensional Imaging by Deconvolution Microscopy. Methods 1999;19:373–385.

40. Swedlow JR. Quantitative fluorescence microscopy and image deconvolution. Methods Cell Biol. 2007;81:447–465.

41. Hoppe AD, Swanson J a., Shorte SL. Three-dimensional FRET microscopy Periasamy A, So PTC, editors. Proc. SPIE--the Int. Soc. Opt. Eng. 2006;6089:1–9.

42. Selinummi J, Niemisto A, Saleem R, Carter G, Aitchison J, Yli-Harja O. A case study on 3D reconstruction and shape description of peroxisomes in yeast. 2007 IEEE Int. Conf. Signal Process. Commun. 2008:672–675.

43. Huang K, Murphy RF. From quantitative microscopy to automated image understanding. J. Biomed. Opt. 2004;9:893–912.

44. Diaz-de-Quijano D, Felip M. A comparative study of fluorescence-labelled enzyme activity methods for assaying phosphatase activity in phytoplankton. A possible bias in the enzymatic pathway estimations. J. Microbiol. Methods 2011;86:104–7.

45. Davison AC, Hinkley D V. Bootstrap methods and their application. Cambridge: Cambridge University Press; 1997:582.

46. Crawley MJ. Regression. Bootstrap with regression. In: R B. Chichester: John Wiley & Sons, Ltd.; 2007. p 418–421.

47. Model MA, Burkhardt JK. A standard for calibration and shading correction of a fluorescence microscope. Cytometry 2001;44:309–316.

48. Hiraoka Y, Sedat JW, Agard DA. The use of a charge-coupled device for quantitative optical microscopy of biological structures. Science 1987;238:36–41.

49. R_Development_Core_Team. R: A Language and Environment for Statistical Computing Team RDC, editor. R Found. Stat. Comput. 2011;1:409.

50. Duarte CM, Agustí S, Canfield DE. Size plasticity of fresh-water pytoplankton: Implications for community structure. Limnol. Oceanogr. 1990;35:1846–1851.

51. Sarmento H. New paradigms in tropical limnology: the importance of the microbial food web. Hydrobiologia 2012;686:1–14.

52. Chen B, Liu H. Relationships between phytoplankton growth and cell size in surface oceans: Interactive effects of temperature, nutrients, and grazing. Limnol. Oceanogr. 2010;55:965–972.

53. Novotná J, Nedbalová L, Kopáček J, Vrba J. Cell-specific extracellular phosphatase activity of Dinoflagellate populations in acidified mountain lakes. J. Phycol. 2010;46:635–644.

54. Green JL, Bohannan BJM, Whitaker RJ. Microbial biogeography: From taxonomy to traits. Science 2008;320:1039–1043.

Chapter 3

Phytoplankton adaptations to oligotrophy: A trade-off between two nutrient scavenging activities

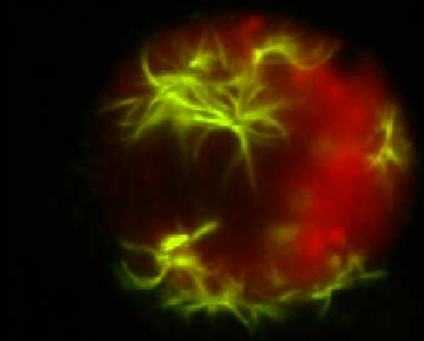

AUTHORS

Diaz-de-Quijano Daniel[a]; Ballén, Miguel[a,b]; Felip, Marisol[a]

[a]Unitat de Limnologia, Departament d'Ecologia i Centre de Recerca d'Alta Muntanya, CEAB-CSIC-Universitat de Barcelona, Av. Diagonal 643, 08028 Barcelona, Catalonia, Spain.

[b]Escuela de Ciencias Exactas e Ingeniería en Universidad Sergio Arboleda

KEY WORDS

Phytoplankton, phosphatase activity, bacterivory, trade-off, functional traits, surface to volume ratio

ABSTRACT

1. The relationship between phosphatase and bacterivory activities (considered as tracers of dissolved and particulate organic phosphorus utilization) was investigated in phytoplankton communities and species of oligotrophic high mountain lakes.
2. A trade-off between phosphatase and bacterivory activities was observed at the bulk community level. Phosphatase activity (PA) was preferred in acidic lakes, whereas bacterivory was selected in deep stratified lakes, with shallow lakes in an intermediate position. In non-acidic lakes, the investment in these phosphorus scavenging activities correlated to high chlorophyll and low nutrients availability, which suggests an increase of investment with nutrient competition gradient. Albeit the recorded PA were low in relation to bibliography, communities with relatively high levels of investment mobilized up to 3.6 or 26.1 times more organic phosphorus by PA than by bacterivory.
3. An inter-specific trade-off between phosphatase and bacterivory activities was also observed. Chlorophytes and diatoms only used PA, chryptophytes almost only used bacterivory, and dinoflagellates and chrysophytes combined both.
4. Species-specific analyses showed two different trophic phenomena. Bacterivory rate per biomass unit separated the trophic niches of three close dinoflagellate species, and concave trade-off curves between PA and bacterivory were observed in two chrysophytes (*Pseudokephyrion* sp. and 5 µm *Chromulina-Ochromonas*). Thus, different populations within a same genus may respond increasing either one or another activity.
5. No allometric relationship was found between surface-to-volume ratio (S/V) and the selection of PA or bacterivory. Nevertheless, we identified a S/V threshold at 1.24 above which the investment in both phosphatase and bacterivory decreased in absolute terms. In spite of the scarce use of phosphatase and bacterivory by these small-celled populations, relatively important rates per biovolume unit could be reached.

INTRODUCTION

Primary producers living in oligotrophic environments face specific challenges to their survival and development. In the same way as some plants adopted carnivory to acquire alternative nutrients under oligotrophic conditions (Givnish 1989), the phytoplankton of large oligotrophic areas of the oceans and freshwaters adapted biological traits such as phagotrophy and extracellular enzyme activities to access alternative sources of nutrients from organic matter (particulate and dissolved). Because it is clearly recognised that phytoplankton may acquire essential nutrients independently through different trophic pathways, trophic plasticity is nowadays considered in trait-based plankton studies (Barton *et al.* 2013).

A functional trait is defined as an organism characteristic that determines its fitness through its effects on growth, reproduction, and survival (Violle *et al.* 2007). For phytoplankton, functional traits include light and nutrient acquisition and use, predator avoidance, morphological variation, temperature sensitivity and reproductive strategies (Litchman & Klausmeier 2008). Traits should vary strongly between species and be measurable in a continuous scale (McGill *et al.* 2006), it should be emphasized the value of quantifying functional traits in order to detect interspecific variation in ecological strategies. Albeit trade-offs play a fundamental role in ecology and evolution, there is still little understanding of which trade-offs maintain phytoplankton diversity and very few is known about the trade-offs among traits (one species cannot be optimal at everything) in natural conditions. This little knowledge is largely due to the lack of species-specific quantifications in the environment, so that laboratory-measured functional traits are typically used to explain interspecific variation (Edwards, Litchman & Klausmeier 2013a b). Our goal was to compare *in situ* trophic activities across phytoplankton species or groups, to ask how niches vary across them, and to ask whether there are important trade-offs between different nutrient acquisition activities.

Mixotrophic algae combine autotrophy and heterotrophy (either osmotrophy or phagotrophy) and may become an essential way of life of phytoplankton in oligotrophic conditions (Zubkov & Tarran 2008; Hansen 2011; Hartmann *et al.* 2012; Sanders & Gast 2012; Moore 2013). By the principle of opportunity costs (Stephens & Krebs 1987), the scarcity of resources in oligotrophic conditions favours this generalist mixotrophic

activity, which although being physiologically less efficient has wider resource opportunities (Tittel *et al.* 2003). The trophic characterization of these organisms would need at least two kinds of concerns. Firstly, there is the trophic strategy or the type of source of matter and energy. In the case of phytoplankton it means the degree to which this matter and energy is acquired by phototrophy, heterotrophy or a combination. Moreover, different levels of detail may be distinguished: for instance, heterotrophy may be divided into osmo- and phagotrophy, and phagotrophy may be divided in assimilation of organic detritus, bacterivory or predation on other living organisms. Secondly, there are those mechanisms, behaviours, activities and characteristics that define the mode these trophic strategies are executed. A non-exhaustive list could include the amount of chlorophyll a and other pigments that determine the exploitable wavelength range and minimum intensity of light, the photosynthetic efficiency, the inorganic carbon fixation metabolism, the kinetics of different nutrients uptake, kinetic and thermodynamic parameters of extracellular enzymatic pathways , dissolved organic matter uptake and organic particles ingestion rates, prey selection criteria, etc. Complexity is assured because not only different mixotroph phytoplankton species may distribute along a mixotrophic gradient, from almost only autotroph to almost only heterotroph (Jones 1994), but it is also thinkable that different individuals within a population may present different levels of mixotrophy and that it may change in time (Ballén Segura 2012). The understanding of this complex trophic behaviour of mixotrophic phytoplankton species is essential to predict changes in the efficiency of the microbial loop shortcut, which affects the biogeochemistry of aquatic ecosystems (Jones 2000; Hartmann *et al.* 2012).

In this study we focused on bacterivory and extracellular phosphatase activity, which we considered as organic phosphorus scavenging activities although they also play other roles. Bacterivory has been described useful to obtain organic carbon and energy in light limiting conditions, to obtain nutrients (phosphorus, nitrogen, etc.) in oligotrophy, just to obtain micronutrients, vitamins and growing factors to support photosynthesis, to eliminate prokaryote competitors for nutrients or to profit from prokaryote advantage in inorganic nutrients uptake affinity (Thingstad *et al.* 1996; Jones 2000; Medina-Sanchez, Villar-Argaiz & Carrillo 2004). Phosphatase activity has also been reported as an osmotrophy contributing mechanism that hydrolyses dissolved organic phosphorus to facilitate the uptake of both, the

liberated orthophosphate (Provasoli 1958; Kuenzler & Perras 1965) and eventually the organic moiety (Tittel *et al.* 2005; Cao *et al.* 2005, 2009; Cao, Song & Zhou 2010; Spijkerman *et al.* 2007). Many subtleties exist in the variability between taxa on the presence and regulation of PA (e.g. Dyhrman and Ruttenberg, 2006) and bacterivory (e.g. Sanders and Gast, 2012). Thus, bacterivory and phosphatase activity (PA) are some of the functional traits that define the mode of trophic activity, contribute to the autotrophic and/or heterotrophic components of the trophic strategy of the phytoplankton populations and individuals that struggle to survive in oligotrophy, but also can be considered as tracers of the main organic phosphorus scavenging activities.

Unfortunately, only a few studies assessed these two co-occurring activities at the same time (Nagata & Kirchman 1992; Chróst & Siuda 2006; Cao *et al.* 2010), and little is known about the relationship between them. Since important differences in the bacterivory and PA were observed between congeneric species, we used single-cell techniques to evaluate them. This way, we obtained not only bulk activity information but also activity information at the population level, at close-to-*in-situ* conditions of natural and uncultured phytoplankton communities. Moreover, the use of microscopy-based single-cell techniques on diverse natural phytoplankton communities allowed us to assess the relationship between phosphatase and bacterivory activities, and a wide enough range of cell size and of surface-to-volume ratios (S/V). We hypothesized that since surface-bound phosphatases occupy a physical space on the cell membrane or wall, species with high S/V could proportionally invest more in PA. On the other hand, low S/V species would invest more in bacterivory because it doesn't only need a certain cell surface area for ingestion, but also a sufficient intracellular space for the digestion machinery.

To sum up, the goal of this study was to answer the following questions: (i) Is there a trade-off between bacterivory and PA in phytoplankton communities? (ii) Does the investment in one and another activity depend on the resource (phosphomonoesters or prokaryotes) availability, on nutrient limitation, or on the species (phyletic) identity? And (iii) would that trade-off be direct (so, generally due to metabolic restrictions) or indirect (e.g. modulated by cell size or S/V)?

MATERIALS AND METHODS

Study sites and sampling

Fifteen oligotrophic high mountain lakes from the Central Pyrenees were sampled from the 15th of July to the 3rd of August 2008. The lakes ranged from 1600 to 2450 m.a.s.l. and were selected to cover the diversity of Pyrenean lakes. A summary of their morphological and environmental parameters are presented in Table 1. A Ruttner's bottle was used to sample the deep chlorophyll maximum (DCM), determined as 1.5 times the Secchi disk depth (Catalan *et al.* 2006), at the deepest lake location. Shallower lakes were sampled at one meter above the bottom. Samples were sieved in the field (40 µm pore-size net) to remove large zooplankton and further treated upon arrival to the laboratory (always within 6 hours after sampling).

Chemical analyses

A subsample was separated for environmental data analysis. Alkalinity was assessed by acidimetric titrations. Total dissolved phosphorus (TDP) was extracted with an oxidative persulfate digestion, and analysed by spectrophotometry using the malachite green method (Camarero. 1994). Total dissolved nitrogen (TDN) was extracted with an oxidative persulfate digestion in the autoclave. Nitrate (NO_3^-) was determined by UV radiation spectrophotometry (Slanina, Lingerak & Bergman 1976), and nitrite (NO_2^-) by the sulfanylamide and n-naphthyl-ethylenediamide method (Grasshoff, Ehrhamdt & Kremling 1983). Amonium (NH_4^+) was measured by spectrophotometry, using the indophenol method (Fresenius, Kentin & Schneider 1988). Dissolved organic carbon (DOC) was assessed with a Shimadzu TOC5000 analyzer. Finally, Chlorophyll a (Chl*a*) concentrations were measured in 90% acetone extracts (1 L sample filtered on Whatman GF/F filter and extracted by 3 min sonication in 4 mL 90% acetone) according to Jeffrey & Humphrey (Jeffrey & Humphrey 1975).

Phytoplankton composition

Another subsample was preserved with 0.5 % (vol/vol) alkaline Lugol solution to determine phytoplankton abundance and composition (Sournia 1978). Samples were concentrated using an Utermöhl chamber and examined under an inverted microscope (Wild) at 600-1000X magnification.

TDP	TDN	Chla	Bacterial Abundance	Bacterial Production	PA	Bacterivory	activation index	selection index	
(nM)	(nM)	($mg \cdot l^{-1}$)	($cell \cdot ml^{-1}$)	($fg\ C \cdot ml^{-1} \cdot h^{-1}$)	($nmol\ ELFA \cdot l^{-1} \cdot min^{-1}$)	($prok \cdot ml^{-1} \cdot h^{-1}$)			Acronym
294.4	23.5	3.8	7.3.E+05	ND	0.78	1924	0.3	0.8	Bole
94.2	20.7	1.7	3.8.E+05	191543	0.86	35793	0.9	-0.4	Fili
126.4	17.9	5.2	2.2.E+06	172924	1.81	37935	1.3	-0.04	Roi
88.1	8.9	1.3	3.8.E+05	33386	0.24	18099	0.4	-0.6	Gerb
113.2	18.3	1.1	5.9.E+05	53533	0.31	11421	0.3	-0.3	Llau
168.5	19.2	2	5.5.E+05	58524	0.07	14226	0.3	-0.8	Boto
50.5	ND	0.6	4.9.E+05	20724	0.1	10452	0.2	-0.7	Redo
73.7	18	0.6	4.9.E+04	7023	2.39	1620	0.9	0.9	Aixe
150.4	16.8	0.6	5.8.E+05	238016	0.7	10036	0.4	0.2	Ibon
82.2	13.8	2.9	8.6.E+05	158464	0.08	54023	1	-0.9	Pois
49.7	8.8	0.8	2.1.E+05	85736	2.87	5785	1.1	0.8	Pica
273.5	78.8	4.2	1.3.E+06	178220	0.23	55970	1.1	-0.9	Podo
103.4	12.7	2.8	3.3.E+05	67576	1.61	42221	1.3	-0.1	Rome
118.6	26	4.6	1.4.E+06	281801	0.47	18411	0.5	-0.3	Bgra
202.7	ND	1.8	7.3.E+05	212117	0.94	27292	0.8	-0.2	Lleb

Table 1. Basic morphological, physical, chemical, biomass, and trophic strategy (bacterivory and PA) parameters of the studied lakes.

LAKE	Acronym	Altitude (m.a.s.l.)	lake area (ha)	catchm. area (ha)	Max. Depth (m)	Sample Depth (m)	pH	Temp (ºC)	Alkalinity ($\mu eq \cdot l^{-1}$)	DOC ($mg \cdot l^{-1}$)
Bassa d'Òles	Bole	1600	1.3	84.6	1.5	0.5	8.02	15.2	1284	4
Filià	Fili	2140	1.4	147.6	6	2	7.79	8.7	1330	ND
Roi	Roi	2310	3.5	117	10	8.5	7.06	8	161	0.4
Gerber	Gerb	2170	14.9	388.4	63	18	7.13	4.9	148	0.6
Llauset	Llau	2190	44.3	777.5	90	15	7.47	10.3	424	ND
Botornàs	Boto	2340	3.7	289.7	22	18	7.23	4	178	0.2
Redon	Redo	2234	24	154	73	30	6.67	4.5	58	0.2
Aixeus	Aixe	2370	3.4	82.3	16	12.5	4.97	8.3	-13	0.1
Ibonet de Perramó	Ibon	2293	0.7	18	5	4	7.49	13.6	239	0.4
Pois	Pois	2056	3.9	151.3	20	13	8.19	8.1	516	0.3
Pica Palomèra	Pica	2308	4.9	68.9	10	8.5	4.61	11.3	-26	0
Podo	Podo	2450	4.6	33.5	20	14	6.41	4.7	83	0.3
Romedo de Dalt	Rome	2114	14.4	259.8	40	21.5	6.31	4.5	22	0.8
Bassa de les Granotes	Bgra	2330	0.7	2.7	5	3.5	6.45	19.6	20	2.2
Llebreta	Lleb	1620	8	5437.9	12	9.5	7.55	11.2	249	1.1

Table 1. Basic morphological, physical, chemical, biomass, and trophic strategy (bacterivory and PA) parameters of the studied lakes.

Algae were identified at genus level and only in few cases, especially for small soft flagellates, genus assignment was not possible (e.g. *Chromulina-Ochromonas*). If size differences were observed within a species, the individuals of that species were divided into several cell classes so that we could better account the ecological significance of size.

Bacterial production

Bacterial production was measured upon arrival to the laboratory via ^{3}H-leucine incorporation according to the method of Kirchman and colleagues (1985). Briefly, 1.2 ml of quadruplicate live and duplicate killed (5% TCA) subsamples were incubated with ^{3}H-leucine (40 nmol·l^{-1} final concentration) for about 2 h, at the *in situ* temperature, in the dark. Incubations were stopped by addition of 120 ml of cold 50% TCA and then frozen (–20°C) until further processing, by centrifugation and TCA rinsing as described by Smith and Azam (1992). Bacterial production rate was calculated using the conversion factors 3594·10^{-6} µg protein·pmol Leu^{-1} and 0.86 µg C·µg protein^{-1} (Simon & Azam 1989).

Phosphatase activity

Phosphatase activity (PA) was measured upon arrival to the laboratory by the enzyme labelled fluorescence (ELF) bulk and single-cell assay. We incubated samples in the dark, at *in situ* temperature and pH using a 10 µM ELF97-phosphate (ELFP; Molecular Probes E6589) substrate final concentration. This substrate concentration was not saturating the environmental phosphatases but it was typically above the Michaelis-Menten K_M constant. To ensure pH stability, incubations were buffered at lake water pH with different buffers: citric acid (pH 4.6-5.5), acetic acid (pH 5.5-7) or Tris buffer (pH 7-8.2). A modification of the Nedoma *et al*. (2003) ELF protocol was used as described in Diaz-de-Quijano and Felip (2011). Liquid sample was incubated until terminated via gentle vacuum filtering (<20KPa) on 25-mm-diameter 2-µm-pore polycarbonate filters (Millipore). The incubation time course was controlled with a spectrofluorimeter Shimadzu RF-5301PC. Thus, we were sure to sample the incubation within the linear increase phase (Nedoma *et al.* 2003; Duhamel *et al.* 2009). Two incubation samples were obtained: one at the beginning of the linear phase

(initial sample) and another (final sample) after a reasonable increase in the fluorimetrically-detected ELF-alcohol product (ELFA). In this way, incubation times could be adapted to a wide range of PA time kinetics. Dried filters were stored at -20ºC until they were mounted with CitiFluor AF1 (Citifluor Ltd, London, United Kingdom) for microscope analysis. Additionally, parallel incubations at 3, 5, 20 and 40 µM ELFP were also performed in five lakes under the mentioned conditions in order to estimate the kinetic parameters of PA. The K_M and V_{max} parameters were obtained *via* the Linewaver-Burk plot (Lineweaver & Burk 1934).

PA samples were imaged for quantification purposes with a Nikon Eclipse 90i epifluorescence microscope (Nikon, Tokyo, Japan) equipped with a monochromatic Vosskühler COOL-1300Q CCD camera with a pixel size of 6.45 μm^2 (Vosskühler GmbH, Osnabrück, Germany) and a Xenon-arc illumination. Images were acquired using a Plan Fluor 20X/0.75 NA MI objective lens with the collar adjusted to immersion with oil, and two different filter blocks: an ELFA-specific filter block (ex. 360–370 nm, em. 520–540 nm) and a chlorophyll-specific filter block (ex. 510–550 nm, em. >590 nm) for species determination. Protists were identified through chloroplast size and shape observed by the chlorophyll auto-fluorescence. Parallel observations of Lugol fixed subsamples under an inverted light microscope (X600 and X1000 magnifications) facilitated and confirmed protist genera identification under epifluorescence microscope. A 9.4% w/v fluorescein standard solution was used for shading correction, and to determine an inter-session correction factor (*Icf*) (Model & Burkhardt 2001). Gain was fixed to 1 but exposure time was modified for each image acquisition to avoid image clipping (no pixel saturation was allowed) and also to collect as much information as possible from weakly bright pixels. Modulation of exposure time between images did not hinder comparability because CCDs generate a linear response over time (Hiraoka, Sedat & Agard 1987; van Vliet *et al.* 1998).

PA rates

ELFA fluorescence intensity was measured using NIS-Elements AR 2.34 software (Laboratory Imaging, Praha, Czech Republic). Fluorescence was quantified in active or inactive phytoplankton cells of the initial and final filters until a minimum sample size of 30 cells per filter was reached for the

most abundant species. We used the macro described by Nedoma *et al*. (2003) to semi-automate the quantification routine. In this macro, the user is able to set an optimum contrast enhancement and select the area of the background and the object to be measured. Finally, the macro measured the following variables: area of the object (*Area*; μm^2), mean grey value of the object (*Mgv*; dimensionless), and mean grey value of the background (*BgMgv*; dimensionless). These measurements were automatically exported to an Excel file for semi-automated calculation together with the following metadata: camera exposure time (*expT*; ms), camera gain (*Gain*; dimensionless), intersession correction factor (*Icf*; dimensionless), and image file identity. The relative fluorescence of the object (*RFobject*; fluorescence units –FU) was calculated as follows:

$$RFobject = \frac{Icf}{\exp T \cdot Gain} \cdot Area \cdot (Mgv - BgMgv) \quad (1)$$

RFobject of each measured cell was converted to amount of ELFA precipitate (or single cell hydrolysed phosphate, *SCHP*; fmol ELFA·cell^{-1}) by using a conversion factor (*ConvF*) of 0.013553 fmol ELFA·FU^{-1}, determined as described in the literature (Nedoma *et al.* 2003; Diaz-de-Quijano *et al.* 2014). Finally, the single cell phosphatase activity (SCPA; fmol ELFA·cell^{-1}·h^{-1}) per population was calculated as:

$$SCPA = \frac{SCHP_f - SCHP_i}{t_{fi}} \quad (2)$$

Where $SCHP_i$ and $SCHP_f$ are arithmetic means of the *SCHP* of the population cells in the initial and final filters, and t is the incubation time (in hours) between them. In the populations where data followed a lognormal distribution we based SCPA calculation on the expectation of SCHPs (E(SCHP)) instead of arithmetic mean using the following formula:

$$E(SCHP) = e^{\mu + \frac{1}{2}\sigma^2} \quad (3)$$

Where μ and σ are, respectively, the mean and standard deviation of the natural logarithm of SCHP. Thus, we avoided the bias produced when arithmetic mean is used on small size samples (notably when variance is big) of lognormal distributions (Finney. 1941).

Percentage of phosphatase active cells

Percentage of phosphatase active cells in a population was determined via a combination of *de visu* and quantitative approaches. Cells were classified *de visu* into four categories: strongly positive, scarcely positive (usually one or a few well-defined ELFA dot/s), negative and undetermined. Undetermined cells were reassigned to either positive or negative using an R implemented algorithm that calculated the average absolute distance from the undetermined cell to the strongly positive and to the negative cells of the same species that fall in the window of the 4 closest cells in fluorescence to the undetermined cell (2 cells above and 2 below). The routine finally reassigned the undetermined cell to the less distant category (positive or negative). After this step, not only strongly positive but also scarcely positive cells were reassigned as positive, as some previous studies considered (e.g. Girault et al., 2013). Finally, the percentage of phosphatase active cells in the final filter was considered as the population percentage of phosphatase active cells, but for the cases where the initial filter had a higher percentage of active cells and a minimum number of 25 quantified cells, the initial filter percentage was considered.

Bacterivory and bacterioplankton composition

CARD-FISH protocol (catalysed reported deposition-fluorescence *in situ* hybridization) proposed by Medina-Sánchez *et al*. (2005) was applied to visualize some Bacteria groups and/or Archaea cells inside mixotrophic protists, and to characterize bacterioplankton composition. Subsamples were fixed upon arrival to the laboratory with a series of the LFT fixative: 0.5% (vol/vol) alkaline Lugol, pH7 buffered and 0.2-µm-pore-size-filtered 2% Formaldehyde, and several drops of 3% sodium thiosulfate to decolour the Lugol fixative. After 1 h of fixation at room temperature, 16 aliquots of each sample (8 aliquots of 90ml for protists and 8 aliquots of 10ml for prokaryotes) were gently filtered (<100 mm Hg) onto respective 25 mm diameter polycarbonate membrane filters (Millipore). Filters were then rinsed twice with Milli-Q water, allowed to air dry, and stored at -20°C until further processing.

Three different HRP (Horse-Radish-Peroxidase)-labelled probes for the main Bacteria groups found in Pyrenean lakes plankton (Hervàs *et al.* 2009; Llorens-Marès, Auguet & Casamayor 2012) and one for the domain Archaea

were used to hybridize the filters (Table 2; Biomers.net, Germany). Two replicate filters were processed for each probe and lake sample, corresponding to both microbial groups (prokaryotes and protists). Alexa488-labeled tyramide (Molecular Probes) were used for signal amplification and filters were counterstained with DAPI (4´,6´-diamidino-2-phenylindole; 1ug ml^{-1} final concentration), and mounted on glass slides by using Citifluor (Citifluor Ltd., UK). Slides were stored at -20 °C in the dark until subsequent counting.

Probe	**Specificity**	**Sequence (5'-3')**	**%FA***	**Reference**
Arch-915	Archaea	GTGCTCCCCCGC CAATTCCT	40	(Medina-Sanchez, Felip and Casamayor. 2005)
CF319a	*Cytophaga-Flavobacteria of bacteroidetes*	TGGTCCGTGTCT CAGTAC	55	(Ishii, Kousuke Mussmann, Marc MacGregor,Barbara Amann, Rudolf. 2004)
HGC69A	Actinobacteria	TATAGTTACCAC CGCCGT	30	(Warnecke, Falk Sommaruga, Ruben Sekar, Raju Hofer,Julia Pernthaler, Jakob. 2005)
Bet42a	B-proteobacteria	GCCTTCCCACTT CGTTT	55	(Warnecke, Falk Sommaruga, Ruben Sekar, Raju Hofer,Julia Pernthaler, Jakob. 2005)

Table 2. Oligonucleotide probes used in this study. *Formamide concentration in the hybridization buffer.

Slides were examined at X1000 for Bacteria groups, Archaea and smaller protists (<10 µm) and at X400 magnifications for larger protists (>10 µm) under a Zeiss Axio Imager epifluorescence microscope. The microscope was equipped with an X-Cite 120 lamp, appropriate filter sets for DAPI (Zeiss filter set 01: ex. 365/12 nm, em. >397 nm) and Alexa-Fluor488 (Zeiss filter sets 09: ex. 450-490 nm, em. >515 nm; or 24: ex. 485/20 nm + 578/14 nm, em. 515-540 nm + >610 nm), a coupled camera Axio Cam MRm and a PC-based image analysis software Axio Vision 4.8. For prokaryotes, a minimum of 500 cells were counted to establish the total abundance, and the number of hybridized cells for each specific probe in order to estimate their abundance and percentage of hybridization. Protists were identified through chloroplast size and shape in the same way as in the ELF samples. A minimum of 100

individuals of the most abundant protist species were considered, for each individual the number of hybridized prokaryotic cells inside it was counted.

To estimate the average vacuole content of DAPI-stained prokaryotes (VC) in a protist population, we firstly added the average vacuole contents of the four probes, and then we divided it by the proportion of DAPI-stained prokaryotes that were co-stained by the sum of the four probes in bacterioplankton. Estimated VCs were transformed to bacterivory ingestion rates according to the phytoplankton cell size and lake temperature with the formulae of Ballén (2012) and assuming a Q_{10} of 2 (Eppley 1972). We estimated the potential maximum percentage of bacterivory active cells for each phytoplankton population as the sum of the four probes percentages, assuming that protists ingesting prokaryotes labelled with one probe reject ingesting the others.

Calculations on phosphorus scavenging activities

Investment and activity selection indices

Activity investment and activity selection indices were calculated for rates and percentages of phosphatase and bacterivory strategies in lakes or populations. Activity investment index is the sum of standardized to one phosphatase and bacterivory. It spans from 0, when no activity or presence is recorded, to two. Activity selection index equals 0 when neither phosphatase nor bacterivory are positive and in the other cases it is calculated as:

$$\frac{phosphatase - bacterivory}{phosphatase + bacterivory} \quad (4)$$

Where phosphatase and bacterivory are also standardized to one. Thus, activity selection index spans from 1, when only phosphatase is used, to -1, when only bacterivory is used, and equals zero when both strategies are used in the same magnitude.

Phosphorus mobilization

The contribution of phosphatase and bacterivory activities to *in situ* P mobilization (in ng $P \cdot l^{-1} \cdot h^{-1}$) was estimated in those lakes where phosphatase kinetics were measured. To do so, we converted bacterivory rates to ng of

$P \cdot l^{-1} \cdot h^{-1}$ based on the cell size of bacterioplankton in Pyrenean lakes and the average content of P per biovolume unit of planktonic bacteria reported in the literature (Gundersen *et al.* 2002; Felip *et al.* 2007), and we estimated *in situ* PA (in ng $P \cdot l^{-1} \cdot h^{-1}$) from Michaelis-Menten kinetic parameters of PA and assuming environmental DOP concentrations as the substrate for phosphatases:

$$\textit{in situ}\ \text{PA} = \frac{V_{\max} \times [DOP]}{K_M + [DOP]} \quad (5)$$

Statistics

Principal components analysis (PCA) was done using CANOCO 5.01 (Ter Braak & Šmilauer 2012). Missing values were replaced by the arithmetic mean of the variable, data was log transformed, centred and standardized by variables. Mann-Whitney U-test and graphics were done in the R environment (R Development Core Team 2011).

RESULTS

Lake level

A trade-off between phosphatase and bacterivory rates was observed at the ecosystem level (Fig. 1). Whereas lakes with low rates of both activities could be observed, no lake was found with high rates in both activities, and always a high rate in one of them implied a low rate in the other one. Lakes could be grouped into either low or relatively high levels of bacterivory and PA (see ellipses in Fig 1). Typical deep high mountain lakes could be differentiated from shallow ponds and acidic lakes, the former being prone to a more bacterivore strategy.

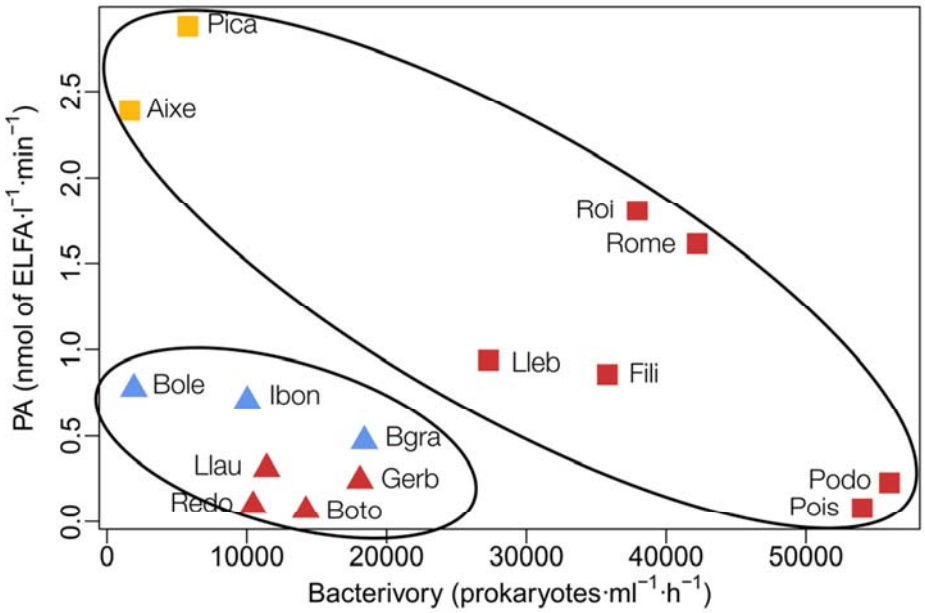

Fig 1. Bulk bacterivory versus phosphatase activity (PA) rates in 15 high mountain lakes. Ellipses group highly and low active sets of lakes (squares and triangles respectively). Acidic lakes (yellow squares), shallow lakes (blue triangles), and deep lakes (red symbols). Lake acronyms are indicated in Table 1

The contribution of phosphatase and bacterivory activities to P mobilization was compared in those lakes where phosphatase kinetics were measured (Fig. 2). Clearly two levels of P mobilization were observed: lakes that

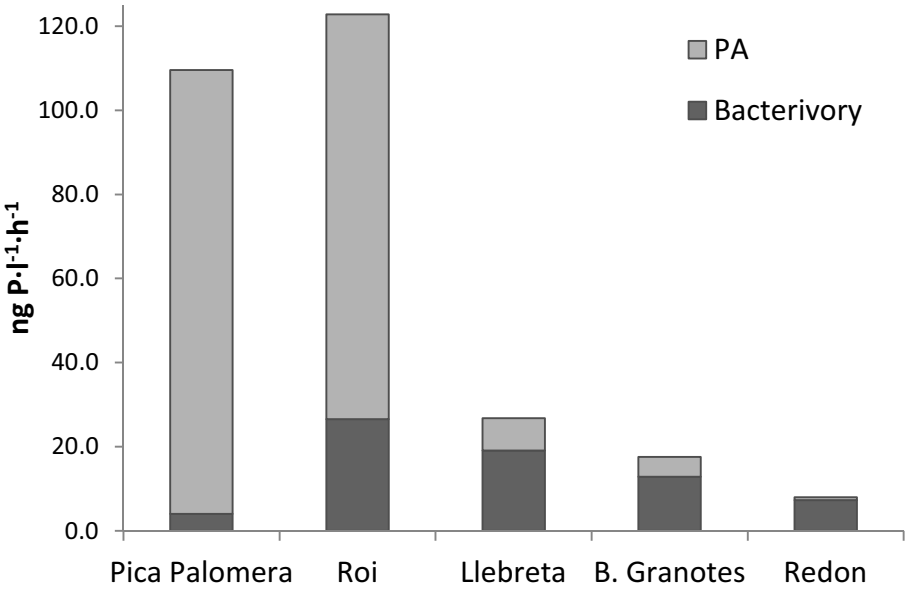

Fig. 2 Amount of phosphorus mobilized by phosphatase (PA) and bacterivory strategies in deep chlorophyll maximum samples of five Pyrenean lakes

mobilized > 100 ng $P \cdot l^{-1} \cdot h^{-1}$ versus lakes that mobilized < 30 ng $P \cdot l^{-1} \cdot h^{-1}$. In the former, PA was capable of mobilizing 3.6 and 26.1 times more P than bacterivory, while in those lakes where a few P is mobilized, bacterivory was more important than PA. In other words, PA was responsible for the highest P mobilization rates measured whereas bacterivory remained less variable between lakes.

Investment in these two activities increased along a trophic gradient in deep high mountain lakes and shallow ponds, where high phytoplankton abundance and low nutrient availability motivated PA and/or bacterivory activities (Fig. 3). The activity selection at the ecosystem level was strongly correlated to lake type, which is represented in Fig. 3 by temperature and DOC availability: shallow lakes had higher DCM temperature, more DOC concentration and positive activity selection index (more PA than bacterivory) whereas deep lakes were in the opposite case (colder, less DOC and more bacterivore). Finally, acidic lakes appeared as an independent typology of lakes. They always had a high activity investment and selection indices (i.e. clearly high PA levels and low bacterivory). Despite being also quite warm lakes, we argue that the main ruling factor was probably pH because (i) the investment in the phosphorus scavenging activities doesn't

respond to the same factors as in other lakes, and (ii) the selection for PA is too strong to be attributed only to temperature or lake type.

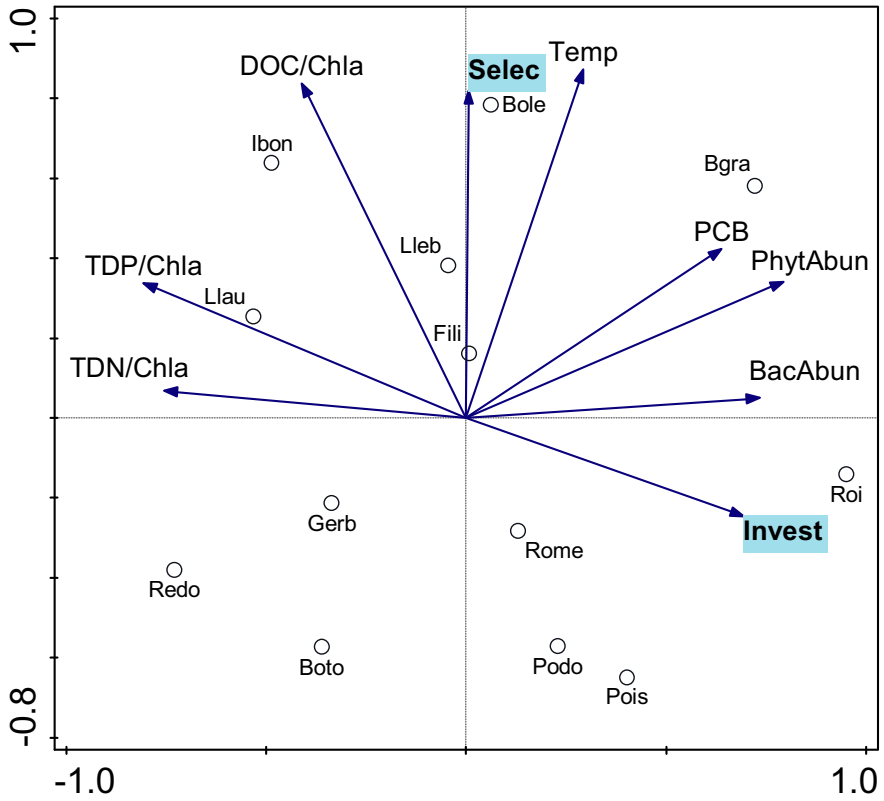

Fig 3. Principal Components Analysis ordination of non-acidic high mountain lakes showing the relationship between some lake variables and the strategy investment (Invest) and strategy selection (Selec) indices at the lake level. Temperature (Temp), Bacterial Carbon Production (PCB), bacterial abundance (BacAbun), phytoplankton abundance (PhytAbun), and availability of nutrients related to Chla: Total Dissolved Nitrogen (TDN), Total Dissolved Phosphorus (TDP), Dissolved Organic Carbon (DOC). All variables were log transformed. Axis 1 explains 42.79% of variance, and 27.16% of variance is explained by axis 2. Lake acronyms are indicated in Table 1.

Population level

Bacterivory and PA rates could be calculated in 71 of the 354 phytoplankton populations explored in the fifteen mountain lakes sampled. The complete set of the assessed populations used at least one of these strategies, and a half of them used both (Table 3 a). Although PA was absent in only 4

a)

		Bacterivory	
		ABSENCE	PRESENCE
PA	ABSENCE	0	4
	PRESENCE	31	36

b)

		Bacterivory rate	
		0	>0
PA rate	0	9	9
	0-0.18	16	19
	>0.18	6	12

Table 3. Number of populations where bacterivory and phosphatase rates were estimated, in terms of activity presence/absence (a) and rates (b). PA rates are in fmol P·cell^{-1}·h^{-1}, and bacterivory rates, in prokaryotes·cell $^{-1}$·h^{-1}.

populations, 14 more populations (with phosphatase presence detected) fell below the PA rate detection limit (Table 3 a and b). Additionally, 35 more populations had detectable PA rates below the 1% of our most phosphatase active population (i.e. below 0.18 fmol P·cell^{-1}·h^{-1}) (Table 3 b). Population data also supports the idea that there might be a trade-off between PA and bacterivory because almost always, when a population had a high rate or high percentage of active cells in one of the mentioned activities, it was low in the other (Fig. 4). Only one of the 71 populations (*Gymnodinium* sp. in Pica Palomèra lake) had both, high percentage of bacterivory and phosphatase *a*ctive cells.

As expected, Chlorophyceae and Bacillarophyceae didn't have bacterivory capacity (Fig. 4), and Bacillarophyceae had significantly higher percentages of phosphatase active cells and higher PA rates per cell (Mann-Whitney U-test p-v=0.0031 and p-v=0.0275, respectively). Cryptophyceae populations had notable bacterivory rates in our lakes, ranging from 5 to 16 prokaryotes·cell^{-1}·h^{-1}, but despite having phosphatase active cells (Fig. 4) PA rates were undetectable except in the case of a small *Rhodomonas* in Llauset Lake, which had a low rate of 0.44 fmol P·cell^{-1}·h^{-1}. Chrysophyceae and Dinophyceae had different populations spread over the possible space of

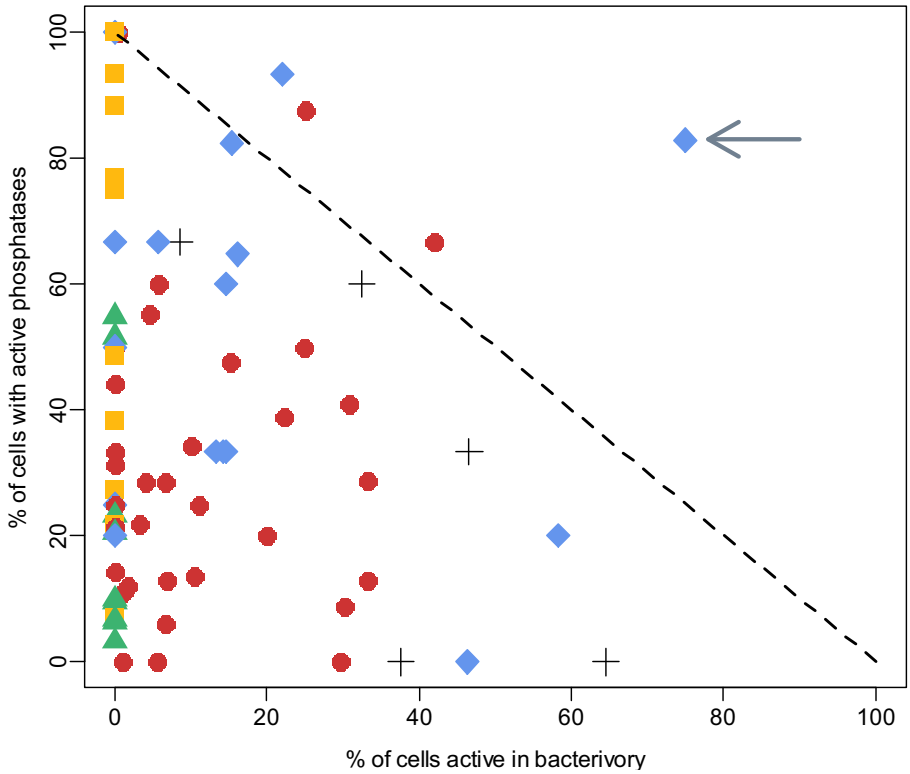

Fig. 4 Percentage of population active cells in bacterivory versus phosphatase. Dotted line indicates y=100-x threshold. Bacillarophyceae (yellow squares), Chlorophyceae (green triangles), Cryptophyceae (black crosses), Chrysophyceae (red circles), Dinophyceae (blue rhombuses). Arrow points out the only population with high percentages of active cells in both activities.

phosphatase and bacterivory values (in percentage of active cells), suggesting differences in the shape of the trade-off curve (more convex for Chrysophyceae and more concave for Dinophycea). In order to go further into this trend, patterns at the species level were plotted for these two groups (Fig. 5). Whereas variability between lakes was low for some species (for instance *Peridinium* spp.), other species, especially Chrysophyceae, showed a wide range of phosphatase and bacterivory active cells (Fig. 5 a,b). In the case of Dinophyceae, *Amphidinium* sp. always had low proportion of bacterivory active cells (<20%) but larger *Amphidinium* cells (8 µm) had higher percentage of phosphatase active cells than the small ones (4 µm). *Gymnodinium* sp. populations were more spread in percentage of active cells (Fig. 5 a). If cell size is considered and rates are related to cell biovolume,

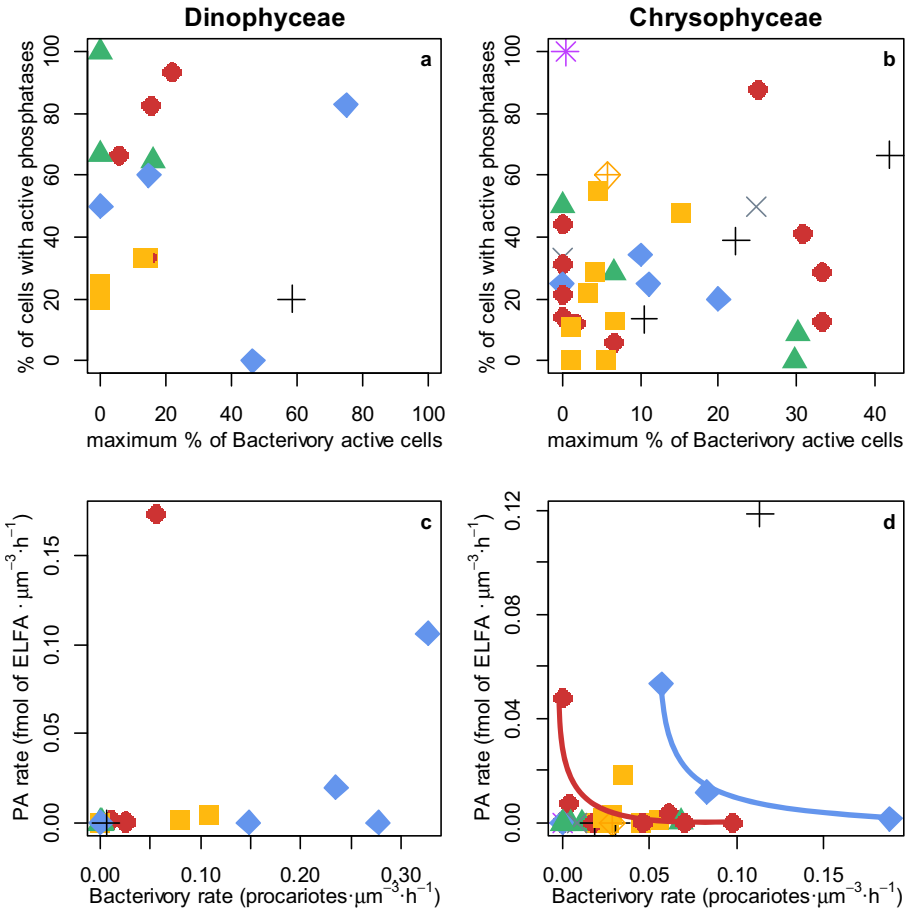

Fig. 5 Percentage of active cells and rates of Bacterivory versus PA in Dinophyceae and Chrysophyceae species. In Dinophyceae, 4 µm (yellow square) and 8 µm *Amphidinium* sp. (red circle), *Gymnodinium* sp. (blue rhombus), *Peridinium* spp. (green triangle), *Wolozynskia* sp. (black cross). In Chrysophyceae, *Pseudokephyrion* sp. (blue rhombus), 3 µm (yellow square), 5 µm (red circle), 7 µm (black cross), and 10 µm *Chromulina-Ochromonas* (grey X), *Crysococcus* sp. (yellow crossed rhombus), *Dinobryon* sp. (green triangle), *Uroglena* sp.(purple star). In figure d, lines draw tradeoff curves for *Pseudokephyrion* sp. (blue) and for 5 µm *Chromulina-Ochromonas* (red).

activity values were very low for *Peridinium* and *Wolozynskia*, but the other populations were clearly separated by bacterivory rate following the order 8 µm *Amphidinium* sp. < 4 µm *Amphidinium* sp. < *Gymnodinium* sp. (Fig. 5 c). On the other hand, specific PA rates were generally low except in an 8 µm *Amphidinium* sp. and a *Gymnodinium* sp. populations. Regarding

Chrysophyceae, *Pseudokephyrion* sp. populations had similar proportions of phosphatase active cells in the various lakes but differed in specific PA rate and in bacterivory percentage of active cells and rate (Fig. 5 b and d).

Relative to other Chrysophyceae, *Pseudokephyrion* sp. populations had intermediate percentages of active cells in both activities, nevertheless, they reached almost the highest rates per biovolume unit due to their small size. They were only surpassed by the highest phosphatase active 7 µm *Chromulina-Ochromonas* population from the acidic lake Pica Palomèra (up to 0.12 fmol ELFA $\mu m^3 h^{-1}$). On the other hand, the small (3 µm) *Chromulina-Ochromonas* had a quite different response. Here, populations differed in the proportion of phosphatase active cells but stayed in a relatively narrow range of PA rate and bacterivory percentage and rate. The 5 µm *Chromulina-Ochromonas* presented a wide range of percentage of phosphatase active cells, and two groups of populations with either low or relatively higher percentage of bacerivory active cells. Overall, the 5 µm *Chromulina-Ochromonas* has a wider range of values than the 3 µm both in specific rates and percentage of active cells. Finally, *Dinobryon* sp. populations differed in bacterivory and in PA percentages of active cells but their specific PA rates were always very low (Fig. 5 b and d). In spite of the fact that 5 µm *Chromulina-Ochromonas* and *Pseudokephyrion* sp. appeared in a low number of lakes, clear concave trade-off curves can be observed in their specific activity rates (Fig. 5 d). Interestingly, the investment in P scavenging activities seemed to be larger for the small loricated cell.

Cell surface-to-volume ratio (S/V) (μm^{-1}) was checked as a possible explanatory variable of both, activity selection and investment in phytoplankton populations. Despite we didn't find any correlation between S/V and activity selection index (Fig. 6 a), it can be observed that populations with the highest investment in phosphatase and bacterivory activities (in rates per cell) fell within the intermediate S/V values (Fig. 6 c). If the rates per biovolume unit were considered, a secondary peak for S/V values between 1.5 and 2 was added to the previous bell-shaped distribution (Fig. 6 d). This indicates that some small cells may reach considerable biovolume specific activities. Additionally, we found that the sum of percentages of active cells in both activities could span from 1% to slightly above 115% for S/V values below 1.24, whereas above this threshold the maximum sum of percentages of active cells decreased linearly with S/V (Fig. 6 b).

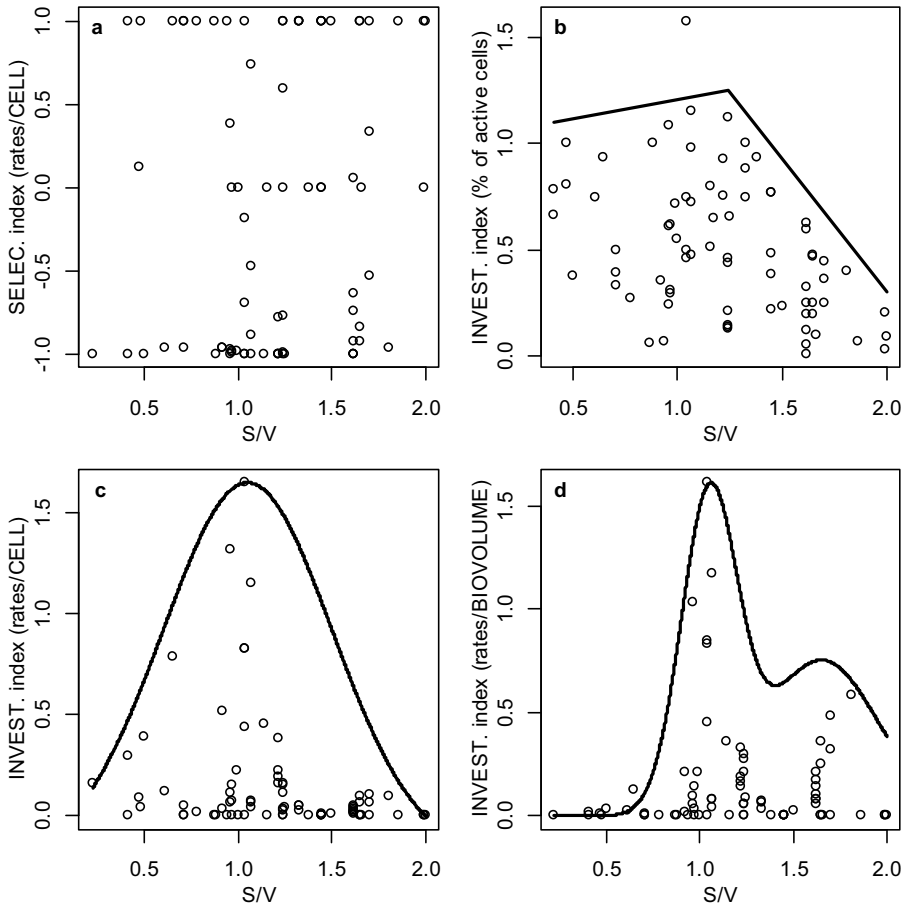

Fig. 6 Surface to Volume ratio (μm^{-1}) of different populations versus phosphorus scavenging activities Investment and Selection indices based on the % of active cells, rates per cell or rates per biovolume unit. Broken, unimodal and bimodal lines are superimposed only for visual purpose.

DISCUSSION

Bulk

PA and Bacterivory in acidic lakes

The behaviour in acidic lakes (with low bacterivory rates but the highest PA rates) appeared to be pH driven, in contrast to the rest of studied lakes. High PA has been recorded in several acidic lakes elsewhere (e.g. Jansson et al., 1981; Olsson, 1988; Bittl et al., 2001) and different mechanisms have been proposed to explain it. On the one hand, acidic phosphatases, i.e.

phosphatases with an acid optimum pH, have been found to be predominant in acidic lakes (Münster 1991; Bittl & Babenzien 1996; Bittl *et al.* 2001), so the enzymes responsible for the high PA rates are probably different from those in lakes with lower PA. On the other hand, a series of biogeochemical processes alter the P cycle in acid lakes. Firstly, different Fe species (ferric hydroxide, Lijklema, 1980; ferric oxide hydroxide, Golterman, 1995; and ferric oxide, Parfitt et al., 1975; Roden and Edmonds, 1997) have the capacity to adsorb orthophosphate and precipitate. Moreover, the capacity of ferric hydroxides to adsorb orthophosphate is maximized in acidic conditions when DOC and ionic strength remain at low levels (Lijklema 1980; Shaw 1994), which is the case in Aixeus and Pica Palomèra. Pica Palomèra lake is next to a disused Zn mine and its watershed is mainly composed of an Inferior Silurian-Devonian rock with black slate rich in pyrite, i.e. in FeS_2 that can be oxidized to sulphate and iron oxides. Aixeus is placed on the top of Vall Ferrera, a traditional iron mining valley, and both lakes had very high sulphate concentrations that indicate oxidized conditions.

Secondly, Al species can also modify the P cycle. Ionic-Al predominates in the pH range between ~4 and ~5 (Driscoll. 1985) and it has been described as a chemical agent capable to form complexes with organic-P (Jansson *et al.* 1981; Bittl *et al.* 2001) but also as a phosphatase inhibitor (probably a non-competitive or allosteric inhibitor) (Bittl *et al.* 2001). But under higher pH (pH>5) ionic-Al hydrolyses and forms colloidal-Al hydroxides (Dickson 1978) that coagulates dissolved organic C and adsorbs orthophosphate from the water column. Thus, it sweeps P out of the water column, increases the sediment capacity to retain P, and reduces P liberation from sediment (Kopáček *et al.* 2000). Lakes with pH around 5 might suffer both Al-mediated P limiting mechanisms. No Fe and Al measurements were performed in our water samples, but their abundance in the sediment (Camarero, pers. comm.) and the substantial airborne Al and Fe deposition (natural lithological dust from Iberian Peninsula and North Africa) demonstrated in the Central Pyrenees (Bacardit & Camarero 2009), suggest that both elements could be relevant in the water. In any case, the contribution of these P limiting mechanisms must be considered with caution.

This Al and Fe reactivity with phosphates in acidic lakes defines a P limiting situation that may be overcome by overproduction of acid PA, as observed. Pica Palomèra and Aixeus not only presented the highest bulk PA rates, but they were also respectively positioned as the 3rd and 1st lakes in

phosphatase-active phytoplankton biomass, with values above 50% of the total phytoplankton biomass. Regarding bacterivory, high levels would be also expected because additionally to P limitation, primary production in acidic lakes may be C-limited as well (Ohle 1981). In such acidic environments, we could expect high mixotroph activity to overcome C limitation, as it was proved in the osmotroph *Chlamydomonas acidophila* of an acidic mining lake (Tittel *et al.* 2005), and/or to overcome P limitation (Joseph, Morel & Price 1995; Vrba *et al.* 2003). Nevertheless, we didn't observe such high levels of bacterivory in our acidic lakes, which must be attributed mainly to their low phytoplanktonic biomass, but also to the scarcity of prey (see lowest bacterial abundance in Table 1). The percentages of bacterivory active biomass were intermediate in Aixeus and Pica Palomèra (they were in the 5^{th} and 10^{th} position out of 15 lakes, respectively), and the species in these lakes had moderate bacterivory rates and percentages of active cells compared to those of the others lakes. In acidic lakes, nutrient limitation, heavy metals toxicity and directly pH may limit phytoplankton biomass (the acidic oligotrophication) but also select for resistant species, reducing the species richness in a similar way to extreme basic waters (Pedersen & Hansen 2003). The restricted amount of biomass and richness of species in Aixeus and Pica Palomèra suggests that a strong species selection may occur. Concretely, selected species (and the final community) are characterized as extraordinary phosphatase active (with exceptional PA per biomass unit).

Investment in P acquiring activities increases along the trophic gradient

Lakes were sampled at the summer DCM, a peak of algae biomass located in the upper hypolimnion during summer stratification, corresponding to one of the main production periods typically present in alpine lakes (Catalan *et al.* 2006). Our study found that investment in PA and especially bacterivory activities increased along a trophic gradient in non-acidic lakes, with maximum investment indices in those lakes where phytoplankton and bacterial abundances and the demand on DOC, TDP and TDN by phytoplankton were higher (Fig. 3), which indicates the importance of both P scavenging activities for phytoplankton growth and DCM development.

Previous studies recorded seasonal peaks of phosphatase activity in nutrient demand conditions, following the Spring phytoplankton bloom and/or in a

more advanced successional stage, in the late Summer (Stevens & Parr 1977; Pettersson 1980; Chróst 1991; Olsson 1991; García-Ruiz *et al.* 2000; Dyhrman & Palenik 2003; Štrojsová *et al.* 2003; Nedoma & Vrba 2006). Our results also agree with previous studies that found significant correlations of total bacterivory with bacterial abundance (Vaqué, Gasol & Marrasé 1994; Pålsson & Daniel 2004) or bacterial production (Sanders, Caron & Berninger 1992; Bergström *et al.* 2003). In conclusion, apart from acidic lakes, a gradual investment in phosphorus scavenging activities along a gradient of lake production can be observed, since both PA active and bacterivore species appear to be favoured under resource competition conditions.

Trade-off. Is there a winning strategy?

A trade-off between PA and bacterivory was observed in the studied mountain lakes. Two groups of lakes could be identified according to their level of investment in P scavenging activities, and the whole set of lakes defined the possible combinations of bulk phosphatase and bacterivory activities: the realizable space (Fig. 1). This suggests that the concrete environmental conditions in each lake may shape the whole phytoplankton community composition and activity to an optimum solution of the trade-off between both P scavenging activities.

Then, which P scavenging activity is most widespread in high mountain lakes, bacterivory or PA? Bacterivory ingestion rates were within the range of values previously reported in the literature (Vaqué *et al.* 1994; Šimek *et al.* 1999; Callieri, Corno & Bertoni 2006; Comte *et al.* 2006; Zubkov & Tarran 2008). Bulk PA in our study should be cautiously compared to other studies because we used ELF substrate, instead of the more common MUP substrate, but anyway our values are strongly lower than in many other studied ecosystems (Hoppe 2003; Sawatzky, Wurtsbaugh & Luecke 2005; Nedoma *et al.* 2006). Nevertheless, we also noticed that in the most P scavenging active planktonic communities, the largest proportion of potentially mobilized P was PA mobilized (Fig. 2). Therefore, we conclude that despite the recorded PA are low in comparison to bibliography, phosphatases appear to be more effective in potentially mobilize amounts of P significant enough for phytoplanktonic needs in some lakes. Besides, bacterivory may supply a more reduced but more constant amount of P, along with other nutrients or micronutrients, in the majority of lakes.

Lake type determines activity selection

In general, two types of high mountain lakes with contrasting biotic characteristics have been distinguished: shallow lakes (maximum depth < 10 -15 m) and deep lakes. This distinction is of broad application to all alpine lakes and constitutes an ecological threshold in the sense that bigger changes in species communities can be found around this lake depth range than above or below it (Catalan *et al.* 2006, 2009). The identity of the main phytoplankton P scavenging activity (PA or bacterivory) seems to be related to such lake types. In our study, activity selection index correlated with lake water temperature and DOC availability, where PA was selected in warmer and higher DOC/Chl*a* waters and bacterivory in colder and lower DOC/Chl*a* systems (Fig. 3).

High temperature lakes correspond to shallow lakes that also have a weaker vertical thermal structure, relatively higher bacterial production and DOC availability, whereas colder lakes correspond to deeper and nutrient-poorer lakes (Table 1). DOC and bacteria resources could be hypothesized as PA and bacterivory enhancers, respectively, but only PA activity was selected in the nutrient-richer shallow lakes. A possible explanation would be that bacteria are available almost everywhere and bacterivory would be selected (and enhanced) only when no more resources are available, in deep lakes. But other factors could also be driving the activity selection. Light limiting conditions have been reported as a bacterivory enhancing factor (Porter 1988; Pålsson & Granéli 2003), but since all lakes were sampled at the DCM (optimum light conditions for the average phytoplankton assembly), we wouldn't expect major differences between lakes regarding light availability. On the other hand, lower turbulence is expected in the DCM of deep lakes, which are mostly at the hypolimnion, below a strong vertical thermal structure. Therefore, we suggest that bacterivory could also be preferred to PA in less turbulent conditions but more experimental data is necessary to test this hypothesis.

Populations

A main law of ecology is the principle of allocation (Levins 1968), which based in the cost-to-benefit approach postulates that not all life functions

can be simultaneously maximized and the use or investment in one option comes at the expense of another option. In an ecological context, trade-offs may arise from conflicting demands and limits, and from costs associated with different benefits, so organisms can choose between a set of optimal situations. This is what we observed in the relationship between the percentages of active cells in both P scavenging activities for the whole phytoplankton species set (Fig. 4). The majority of the 71 analysed populations were situated below the optimal allocation line (% of cells with active phosphatases = 100 - % of cells active in bacterivory) and only one (*Gymnodinium* sp. in Pica Palomèra lake) clearly surpassed this line.

In this study we observed that some classes of phytoplankton only selected PA (Chlorophyceae and Bacillarophyceae) whereas Chryptophyceae almost only used bacterivory (Fig. 4). Therefore, the selection of one or another P scavenging activity depends at some extent on the phylogenetic identity. Nevertheless, the species distribution within Dinophyceae and Chrysophyceae over the bacterivory-PA space draws a more complex allocation pattern. While the first group would reach maximum P scavenging by increasing active cells in one of the two activities (concave trade-off curve), Chrysophyceae would achieve its maximum combining both activities at intermediate percentage of active cells (convex trade-off curve). More data are necessary to analyse the selective advantage that such different allocation pattern could mean, but we hypothesized that more generalist Chrysophyceae species would be favoured under scant resources conditions (Tittel *et al.* 2003).

Although species-specific patterns in the two dimensional space (bacterivory-PA) do not permit us to conclude that a certain species is clearly selecting a certain activity or clearly investing more in these activities (Fig.5), it is worthwhile to note two facts. On the one hand, *Amphidinium* and *Gymnodinium* sp. had separated realized trophic niches in terms of bacterivory rate per biovolume unit, being the largest species up to three times more active than the small ones. On the other hand, two chrysophytes (*Pseudokephyrion* sp. and 5 µm *Chromulina-Ochromonas*) had concave trade-off curves between PA and bacterivory specific rates (Fig. 5 d), which shows that different populations of the same genus may respond increasing either one or another activity, depending on the environmental conditions where they live. We speculate that differences in genetic diversity, physiological status and/or cell cycle phase could also explain this shift between

alternative nutrient acquisition activities in *Pseudokephyrion* sp. and 5 µm *Chromulina-Ochromonas*. The case of these two chrysophytes is also suggestive (and exceptional) in terms of activities investment. *Pseudokephyrion* sp. has a higher investment in bacterivory and PA than their close relatives 5 µm *Chromulina-Ochromonas*. We suggest that the presence of a lorica in *Pseudokephyrion* could make the difference and enhance the efficiency of these two activities. As a conclusion, we would say that phylogenetic Class rather than species identity partly explains the P scavenging activity selection, and that diverse relationships between traits (non-trade-off or trade-off curve shapes) were observed within different species (or genera).

As previously mentioned trade-offs between biological traits can be the expression of direct restrictions such as energetic budget of the organisms (optimal allocation principle), but they can also indirectly emerge when the compared biological traits have opposite allometric relationship with body size, i.e. one biological trait increasing with size and the other decreasing. We checked if the observed trade-off was of direct or indirect type by using S/V instead of biovolume. S/V has been previously used by Reynolds to show a strong allometric relationship between size, shape and replication rate in phytoplankton (Reynolds 2006). Moreover, S/V always spreads along a smaller range than biovolume (Lewis 1976; Reynolds 1984) because larger cells tend to be sufficiently non-spherical and because the cell surface increases slower (as the square of the diameter) than biovolume (as its cube) with cell size. In our case we reduced from three to two orders of magnitude resulting in a more comparable dispersion of the data. Additionally, S/V parameter is ecologically interesting because phosphorus and general nutrient demand is proportional to the cell volume and supply to the cell surface. Our initial hypothesis was that there could be an indirect trade-off where organisms with bigger S/V would have proportionally more cell surface available for surface-bound phosphatases. Similarly, organisms with lower S/V would have more intracellular space available for bacteria digestion. Nevertheless, we didn't observe any significant relationship between the selection of bacterivory or PA and the S/V of the studied species (Fig. 6a).

Surprisingly, we did find a relationship between S/V and the amount of investment in P scavenging activities, where the most investing species had intermediate S/V (Fig. 6c), and the proportion of active cells clearly declined

in smaller sizes (Fig. 6b). We interpret that very small cells with the highest S/V may be more efficient in the uptake of inorganic P (and other nutrients) (Tambi *et al.* 2009), which might make them less dependent on PA and bacterivory to access organic phosphorus. Alternatively, smaller species could also have a relatively lower bacterivory ceiling because of limited intracellular space for prokaryote digestion. The explanation for bigger cells (low S/V) is not so evident: the investment decreases in rates but not in percentages of active cells, which could be related to their lower growth rates and higher temperature dependence (Catalan 2000). Moreover, we think that future observations could modify this picture because we observed some rare big cells with relatively important P scavenging activities that were not included in this study because counts didn't reach a minimum sample size. As a conclusion, we identified a S/V threshold of 1.24 above which bacterivory and PA rates and percentages of cells decreased. This threshold corresponds to a sphere of about 4.8 µm in diameter, a rod of 9.6 x 4 µm, or a pointed dinoflagellate of around 7.6 x 5.4 µm. These sizes are common in high mountain lake phytoplankton (Felip 1997), for whom P scavenging activities appear to be important functional traits. Model simulations of mixotrophic foraging modes also showed changes around 5 µm cell size (Våge *et al.* 2013) but further studies are necessary to properly interpret the threshold significance.

In conclusion, this study showed a direct trade-off relationship between PA and bacterivory in bulk oligotrophic high mountain lakes and in their phytoplankton species. In general, these activities were widely present in high mountain lakes, increased along a gradient of nutrient demand, and the selection of one or another depended on the resources availability, which was determined by the type of lake (acidic lakes apart). In lakes where high amounts of P were mobilised, PA dominated over bacterivory. Thanks to the single-cell *in situ* quantification of these two P scavenging activities, different behaviours were detected at the phylogenetic levels of Class and genus. On the one hand, Chlorophyceae and Bacillarophyceae only presented PA, Chryptophyceae mostly used bacterivory, and Dinophyceae and Chrysophyceae combined both. On the other hand, it is worth to highlight that *Pseudokephyrion* sp. and 5 µm *Chromulina-Ochromonas* populations presented concave trade-off curves, with higher specific activities in the loricated *Pseudokephyrion* sp.. Finally, we detected a S/V threshold of 1.24, above which rates and percentage of cells active in PA and bacterivory

decreased (i.e. approximately in cells below 5 µm of diameter), indicating less dependence on P scavenging activities.

ACKNOWLEDGEMENTS

This research involved collaboration between the Limnology Group (CEAB-UB) and the Institut de Ciències del Mar-CMIMA (CSIC). We thank Lluis Camarero for chemical analyses and Josep M Gasol and Hugo Sarmento for bacterial production analyses. We also thank Lluís Camarero, Berta Fueyo, Josep M Gasol, Hugo Sarmento, Maria Vila, Jean-Christophe Auguet, and Emili O. Casamayor for collaboration in field work; and Jordi Catalan for critically reading the manuscript and for valuable suggestions. The study was supported by the Spanish Ministry of Science and Technology, projects ECOFOS (CGL2007-64177/BOS), GRACCIE (CDS2007-00067) and NITROPIR (CGL2010-19373).

BIBLIOGRAPHY

Bacardit M. & Camarero L. (2009) Fluxes of Al, Fe, Ti, Mn, Pb, Cd, Zn, Ni, Cu, and As in monthly bulk deposition over the Pyrenees (SW Europe): The influence of meteorology on the atmospheric component of trace element cycles and its implications for high mountain lakes. *Journal of Geophysical Research* **114**, G00D02.

Ballén M. (2012) Calibración del contenido vacuolar como tasas de ingestión. In: *Estudio del comportamiento fagotrófico del fitoplancton mediante técnicas de análisis unicelular*. pp. 28–43. Barcelona.

Ballén Segura M.Á. (2012) *Estudio del comportamiento fagotrófico del fitoplancton mediante técnicas de análisis celular*. University of Barcelona.

Barton A.D., Pershing A.J., Litchman E., Record N.R., Edwards K.F., Finkel Z. V, *et al.* (2013) The biogeography of marine plankton traits. *Ecology Letters* **16**, 522–534.

Bergström A.K., Jansson M., Drakare S. & Blomqvist P. (2003) Occurrence of mixotrophic flagellates in relation to bacterioplankton production, light regime and availability of inorganic nutrients in unproductive lakes with differing humic contents. *Freshwater Biology* **48**, 868–877.

Bittl T. & Babenzien H.-D. (1996) Microbial activity in an artificially divided acidic lake. *Ergebnisse der Limnologie*, 113–121.

Bittl T., Vrba J., Nedoma J. & Kopacek J. (2001) Impact of ionic aluminium on extracellular phosphatases in acidified lakes. *Environmental microbiology* **3**, 578–587.

Ter Braak C.J.F. & Šmilauer P. (2012) *Canoco reference manual and user's guide: software for ordination, version 5.0*. Microcomputer Power, Ithaca, USA.

Callieri C., Corno G. & Bertoni R. (2006) Bacterial grazing by mixotrophic flagellates and Daphnia longispina: a comparison in a fishless alpine lake. *Aquatic Microbial Ecology* **42**, 127–137.

Cao X., Song C. & Zhou Y. (2010) Limitations of using extracellular alkaline phosphatase activities as a general indicator for describing P deficiency of phytoplankton in Chinese shallow lakes. *Journal of Applied Phycology* **22**, 33–41.

Cao X., Song C., Zhou Y., Štrojsová A., Znachor P., Zapomělová E., *et al.* (2009) Extracellular phosphatases produced by phytoplankton and other sources in shallow eutrophic lakes (Wuhan, China): taxon-specific versus bulk activity. *Limnology* **10**, 95–104.

Cao X., Štrojsová A., Znachor P., Zapomělová E., Liu G., Vrba J., *et al.* (2005) Detection of extracellular phosphatases in natural spring phytoplankton of a shallow eutrophic lake (Donghu, China). *European Journal of Phycology* **40**, 251–258.

Catalan J. (2000) Primary production in a high mountain lake: an overview from minutes to kiloyears. *Atti Associazione Italiana Oceanologia Limnologia* **13**, 1–21.

Catalan J., Barbieri M.G., Bartumeus F., Bitušík P., Botev I., Brancelj A., *et al.* (2009) Ecological thresholds in European alpine lakes. *Freshwater Biology* **54**, 2494–2517.

Catalan J., Camarero L., Felip M., Pla S., Ventura M., Buchaca T., *et al.* (2006) High mountain lakes : extreme habitats and witnesses of environmental changes. *Limnetica* **25**, 551–584.

Chróst R. & Siuda W. (2006) Microbial production, utilization, and enzymatic degradation of organic matter in the upper trophogenic layer in the pelagial zone of lakes along a eutrophication gradient. *Limnology and Oceanography* **51**, 749–762.

Chróst R.J. (1991) Environmental control of the synthesis and activity of aquatic microbial ectoenzymes. In: *Microbial Enzymes in Aquatic Environments*. (Ed. R.J. Chróst), pp. 29–59. Springer-Verlag New York Inc., New York.

Comte J., Jacquet S., Viboud S., Fontvieille D., Millery a, Paolini G., *et al.* (2006) Microbial community structure and dynamics in the largest natural French lake (Lake Bourget). *Microbial ecology* **52**, 72–89.

Díaz-de-Quijano D. & Felip M. (2011) A comparative study of fluorescence-labelled enzyme activity methods for assaying phosphatase activity in phytoplankton. A possible bias in the enzymatic pathway estimations. *Journal of microbiological methods* **86**, 104–7.

Diaz-de-Quijano D., Horňák K., Palacios P. & Felip M. (2014) 3D restoration microscopy improves quantification of enzyme-labelled fluorescence (ELF)-based single-cell phosphatase activity in plankton. *Cytometry Part A*.

Dickson W. (1978) Some effects of the acidification of Swedish lakes. In: *Internationale vereinigung fuer theoretische und angewandte limnologie verhandlungen. International association of theoretical and applied limnology, Proceedings*. (Ed. V. Sladecek), pp. 851–856. Copenhagen, Denmark.

Duhamel S., Gregori G., Van Wambeke F. & Nedoma J. (2009) Detection of Extracellular Phosphatase Activity at the Single-Cell Level by Enzyme-Labeled Fluorescence and Flow Cytometry: The Importance of Time Kinetics in ELFA Labeling. *Cytometry Part A* **75A**, 163–168.

Dyhrman S.T. & Palenik B. (2003) Characterization of ectoenzyme activity and phosphate-regulated proteins in the coccolithophorid Emiliania huxleyi. *Journal of Plankton Research* **25**, 1215–1225.

Dyhrman S.T. & Ruttenberg K.C. (2006) Presence and regulation of alkaline phosphatase activity in eukaryotic phytoplankton from the coastal ocean: Implications for dissolved organic phosphorus remineralization. *Limnology and Oceanography* **51**, 1381–1390.

Edwards K.F., Litchman E. & Klausmeier C.A. (2013a) Functional traits explain phytoplankton community structure and seasonal dynamics in a marine ecosystem. *Ecology letters* **16**, 56–63.

Edwards K.F., Litchman E. & Klausmeier C.A. (2013b) Functional traits explain phytoplankton responses to environmental gradients across lakes of the United States. *Ecology letters* **16**, 56–63.

Eppley R.W. (1972) Temperature and phytoplankton growth in sea. *Fishery Bulletin* **70**, 1063–1085.

Felip M. (1997) *Ecologia del microplàncton d'un estany profund d'alta muntanya (Redó, Pirineus)*.

Felip M., Andreatta S., Sommaruga R., Straškrábová V. & Catalan J. (2007) Suitability of flow cytometry for estimating bacterial biovolume in natural plankton samples: comparison with microscopy data. *Applied and Environmental Microbiology* **73**, 4508–4514.

Fresenius W., Kentin K.E. & Schneider W. (1988) *Water analysis*. Springer-Verlag, Berlin.

García-Ruiz R., Hernández I., Lucena J. & Niell F.X. (2000) Significance of phosphomonoesterase activity in the regeneration of phosphorus in a

meso-eutrophic, P-limited reservoir. *Soil Biology and Biochemistry* **32**, 1953–1964.

Girault M., Arakawa H. & Hashihama F. (2013) Phosphorus stress of microphytoplankton community in the western subtropical North Pacific. *Journal of Plankton Research* **35**, 146–157.

Givnish T.J. (1989) Ecology and evolution of carnivorous plants. In: *Plant-animal interactions*. (Ed. W.G. Abrahamson), pp. 243–290. McGraw-Hill, New York.

Golterman H.L. (1995) The role of the ironhydroxide-phosphate-sulfide system in the phosphate exchange between sediments and overlying water. *Hydrobiologia* **297**, 43–54.

Grasshoff K., Ehrhamdt M. & Kremling K. (1983) *Methods of sea water analysis*, 2nd editio. Wiley Verlag-Chemie, Weinheim.

Gundersen K., Heldal M., Norland S., Purdie D.A. & Knap A.H. (2002) Elemental C, N, and P cell content of individual bacteria collected at the Bermuda Atlantic Time-series Study (BATS) site. *Limnology and Oceanography* **47**, 1525–1530.

Hansen P.J. (2011) The role of photosynthesis and food uptake for the growth of marine mixotrophic dinoflagellates. *The Journal of eukaryotic microbiology* **58**, 203–14.

Hartmann M., Grob C., Tarran G.A., Martin A.P., Burkill P.H., Scanlan D.J., *et al.* (2012) Mixotrophic basis of Atlantic oligotrophic ecosystems. *Proceedings of the National Academy of Sciences* **109**, 5756–5760.

Hervàs A., Camarero L., Reche I. & Casamayor E. (2009) Viability and potential for immigration of airborne bacteria from Africa that reach high mountain lakes in Europe. *Environmental microbiology* **11**, 1612–1623.

Hiraoka Y., Sedat J.W. & Agard D.A. (1987) The use of a charge-coupled device for quantitative optical microscopy of biological structures. *Science* **238**, 36–41.

Hoppe H.G. (2003) Phosphatase activity in the sea. *Hydrobiologia* **493**, 187–200.

Jansson M., Olsson H. & Broberg O. (1981) Induction of high phosphatase activity by aluminum in acid lakes. *Archiv fü r Hydrobiologie* **93**, 32–44.

Jeffrey S.W. & Humphrey G.F. (1975) New spectrophotometric equations for determining chlorophylls a, b, c1 and c2 in higher plants, algae and natural phytoplankton. *Biochemie und Physiologie der Pflanzen* **167**, 191–194.

Jones R.I. (1994) Mixotrophy in planktonic protists as a spectrum of nutritional strategies. *Marine Microbial Food Webs* **8**, 87–96.

Jones R.I. (2000) Mixotrophy in planktonic protists: an overview. *Freshwater Biology* **45**, 219–226.

Joseph E.M., Morel F.M.M. & Price N.M. (1995) Effects of aluminum and fluoride on phosphorus acquisition by Chlamydomonas reinhardtii. *Canadian journal of fisheries and aquatic sciences/Journal canadien des sciences halieutiques et aquatiques. Ottawa ON* **52**, 353–357.

Kirchman D., Knees E. & Hodson R. (1985) Leucine incorporation and its potential as a measure of protein synthesis by bacteria in natural aquatic systems. *Applied and Environmental Microbiology* **49**, 599–607.

Kopáček J., Hejzlar J., Borovec J., Porcal P. & Kotorová I. (2000) Phosphorus inactivation by aluminum in the water column and sediments: Lowering of in-lake phosphorus availability in an acidified watershed-lake ecosystem. *Limnology and Oceanography* **45**, 212–225.

Kuenzler E.J. & Perras J.P. (1965) Phosphatases of marine algae. *Biological Bulletin* **128**, 271–284.

Levins R. (1968) *Evolution in a changing environment*. Princeton University Press, Princeton, NJ.

Lewis W.M. (1976) Surface/volume ratio – Implications for phytoplankton morphology. *Science* **192**, 885–887.

Lijklema L. (1980) Interaction of orthophosphate with iron(III) and aluminum hydroxides. *Environmental science & technology* **14**, 537–541.

Lineweaver H. & Burk D. (1934) The determination of enzyme dissociation constants. *Journal of the American Chemical Society* **56**, 658–666.

Litchman E. & Klausmeier C.A. (2008) Trait-based community ecology of phytoplankton. *Annual Review of Ecology, Evolution, and Systematics* **39**, 615–639.

Llorens-Marès T., Auguet J.-C. & Casamayor E. (2012) Winter to spring changes in the slush bacterial community composition of a high-mountain lake (Lake Redon, Pyrenees). *Environmental Microbiology Reports* **4**, 50–56.

McGill B.J., Enquist B.J., Weiher E. & Westoby M. (2006) Rebuilding community ecology from functional traits. *Trends in ecology evolution* **21**, 178–185.

Medina-Sánchez J.M., Felip M. & Casamayor E.O. (2005) Catalyzed Reported Deposition-Fluorescence In Situ Hybridization Protocol To Evaluate Phagotrophy in Mixotrophic Protists. *Applied and Environmental Microbiology* **71**, 7321–7326.

Medina-Sanchez J.M., Villar-Argaiz M. & Carrillo P. (2004) Neither with nor without you: A complex algal control on bacterioplankton in a high mountain lake. *Limnology and Oceanography* **49**, 1722–1733.

Model M.A. & Burkhardt J.K. (2001) A standard for calibration and shading correction of a fluorescence microscope. *Cytometry* **44**, 309–316.

Moore L. (2013) More mixotrophy in the marine microbial mix. *Proceedings of the National Academy of Sciences of the United States of America* **110**, 8323–8324.

Münster U. (1991) Extracellular enzyme activity in eutrophic and polyhumic lakes. In: *Microbial enzymes in aquatic environments*. (Ed. R.J. Chróst), pp. 96–122. Springer-Verlag, New York.

Nagata T. & Kirchman D.L. (1992) Release of macromolecular organic complexes by heterotrophic marine flagellates. *Marine Ecology Progress Series* **83**, 233–240.

Nedoma J., GARCIA J.C., COMERMA M., Simek K. & ARMENGOL J. (2006) Extracellular phosphatases in a Mediterranean reservoir: seasonal, spatial and kinetic heterogeneity. *Freshwater Biology* **51**, 1264–1276.

Nedoma J. & Vrba J. (2006) Specific activity of cell-surface acid phosphatase in different bacterioplankton morphotypes in an acidified mountain lake. *Environmental microbiology* **8**, 1271–1279.

Nedoma J.J., Štrojsová A., Vrba J., Komárková J., Šimek K., Strojsova A., *et al.* (2003) Extracellular phosphatase activity of natural plankton studied with ELF97 phosphate: fluorescence quantification and labelling kinetics. *Environmental microbiology* **5**, 462–472.

Ohle W. (1981) Photosynthesis and chemistry of an extremely acidic bathing pond in Germany. *Internationale Vereinigung fuer Theoretische und Angewandte Limnologie Verhandlungen* **21**, 1173–1177.

Olsson H. (1991) Phosphatase activity in an acid, limed, Swedish lake. In: *Microbial enzymes in aquatic environments*. (Ed. R.J. Chróst), pp. 206–219. Springer-Verlag, New York.

Olsson H. (1988) *Phosphatases in lakes – characterization, activity and ecological implications*. Uppsala University.

Pålsson C. & Daniel C. (2004) Effects of prey abundance and light intensity on nutrition of a mixotrophic flagellate and its competitive relationship with an obligate heterotroph. *Aquatic Microbial Ecology* **36**, 247–256.

Pålsson C. & Granéli W. (2003) Diurnal and seasonal variations in grazing by bacterivorous mixotrophs in an oligotrophic clearwater lake. *Archiv für Hydrobiologie* **157**, 289–307.

Parfitt R.L., Atkinson R.J. & Smart R.S.C. (1975) Mechanism of phosphate fixation by Iron oxides. *Soil Science Society of America Journal* **39**, 837–841.

Pedersen M.F. & Hansen P.J. (2003) Effects of high pH on a natural marine planktonic community. *Marine Ecology Progress Series* **260**, 19–31.

Pettersson K. (1980) Alkaline phosphatase activity and algal surplus phosphorus as phosphorus-deficiency indicators in Lake Erken. *Archiv fü r Hydrobiologie* **89**, 54–87.

Porter K.G. (1988) Phagotrophic phytoflagellates in microbial food webs. *Hydrobiologia* **159**, 89–97.

Provasoli L. (1958) Nutrition and ecology of protozoa and algae. *Annual Review of Microbiology* **12**, 279–308.

R Development Core Team (2011) R: A Language and Environment for Statistical Computing. *R Foundation for Statistical Computing* **1**, 409.

Reynolds C. (2006) *Ecology of phytoplankton*. Cambridge University Press, Cambridge, UK.

Reynolds C.S. (1984) *The ecology of freshwater phytoplankton*. Cambridge University Press.

Roden E.E. & Edmonds J.W. (1997) Phosphate mobilization in iron-rich anaerobic sediments: Microbial Fe(III) oxide reduction versus iron-sulfide formation. *Archiv für Hydrobiologie* **139**, 347–378.

Sanders R.W., Caron D.A. & Berninger U.-G. (1992) Relationships between bacteria and heterotrophic nanoplankton in marine and fresh waters: an inter-ecosystem comparison. *Marine Ecology Progress Series* **86**, 1–14.

Sanders R.W. & Gast R.J. (2012) Bacterivory by phototrophic picoplankton and nanoplankton in Arctic waters. *FEMS microbiology ecology* **82**, 242–53.

Sawatzky C.L., Wurtsbaugh W.A. & Luecke C. (2005) The spatial and temporal dynamics of deep chlorophyll layers in high-mountain lakes: effects of nutrients, grazing and herbivore nutrient recycling as growth determinants. *Journal of Plankton Research* **28**, 65–86.

Shaw P.J. (1994) The effect of pH, dissolved humic substances, and ionic composition on the transfer of iron and phosphate to particulate size fractions in epilimnetic lake water. *Limnology and Oceanography* **39**, 1734–1743.

Šimek K., Kojecká P., Nedoma J., Hartman P., Vrba J. & Dolan J.R. (1999) Shifts in bacterial community composition associated with different microzooplankton size fractions in a eutrophic reservoir. *Limnology and Oceanography* **44**, 1634–1644.

Simon M. & Azam F. (1989) Protein content and protein synthesis rates of planktonic marine bacteria. *Marine Ecology Progress Series* **51**, 201–213.

Slanina J., Lingerak W.A. & Bergman L. (1976) A fast determination of nitrate in rain and surface waters by means of UV spectrophotometry. *Zeitschrift für Analytische Chemie* **280**, 365–368.

Smith D. & Azam F. (1992) A simple, economical method for measuring bacterial protein synthesis rates in seawater using tritiated-leucine. *Marine microbial food webs* **6**, 107–114.

Sournia A. (Ed). (1978) *Phytoplankton manual*. (Ed. A. Sournia), UNESCO, Paris.

Spijkerman E., Bissinger V., Meister A. & Gaedke U. (2007) Low potassium and inorganic carbon concentrations influence a possible phosphorus limitation in Chlamydomonas acidophila (Chlorophyceae). *European Journal of Phycology* **42**, 327–339.

Stephens D.W. & Krebs J.R. (1987) *Foraging Theory*. Princeton University Press, Princeton, NJ.

Stevens R.J. & Parr M.P. (1977) The significance of alkaline phosphatase activity in Lough Neagh. *Freshwater Biology* **7**, 351–355.

Štrojsová A., Vrba J., Nedoma J., Komárková J. & Znachor P. (2003) Seasonal study of extracellular phosphatase expression in the phytoplankton of a eutrophic reservoir. *European Journal of Phycology* **38**, 295–306.

Tambi H., Flaten G., Egge J., Bødtker G., Jacobsen a & Thingstad T. (2009) Relationship between phosphate affinities and cell size and shape in various bacteria and phytoplankton. *Aquatic Microbial Ecology* **57**, 311–320.

Thingstad T.F., Havskum H., Garde K. & Riemann B. (1996) On the strategy of eating your competitor'': A mathematical analysis of algal mixotrophy. *Ecology* **77**, 2108–2118.

Tittel J., Bissinger V., Gaedke U. & Kamjunke N. (2005) Inorganic carbon limitation and mixotrophic growth in Chlamydomonas from an acidic mining lake. *Protist* **156**, 63–75.

Tittel J., Bissinger V., Zippel B., Gaedke U., Bell E., Lorke A., *et al.* (2003) Mixotrophs combine resource use to outcompete specialists: implications for aquatic food webs. *Proceedings of the National Academy of Sciences of the United States of America* **100**, 12776–81.

Våge S., Castellani M., Giske J. & Thingstad T.F. (2013) Successful strategies in size structured mixotrophic food webs. *Aquatic Ecology* **47**, 329–347.

Vaqué D., Gasol J.M. & Marrasé C. (1994) Grazing rates on bacteria: the significance of methodology and ecological factors. *Marine Ecology Progress Series* **109**, 263–274.

Violle C., Navas M.-L., Vile D., Kazakou E., Fortunel C., Hummel I., *et al.* (2007) Let the concept of trait be functional! *Oikos* **116**, 882–892.

Van Vliet L.J., Boddeke F.R., Sudar D. & Young I.T. (1998) Image detectors for digital image microscopy. In: *Digital image analysis of microbes*. (Eds M.H.F. Wilkinson & F. Schut), pp. 37–63. Wiley, Chichester.

Vrba J., Nedoma J., Kohout L., Kopáček J., Nedbalová L., Ráčková P., *et al.* (2003) Massive occurrence of heterotrophic filaments in acidified lakes: seasonal dynamics and composition. *FEMS microbiology ecology* **46**, 281–294.

Zubkov M. & Tarran G. (2008) High bacterivory by the smallest phytoplankton in the North Atlantic Ocean. *Nature* **455**, 224–U48.

Chapter 4

Is *Cyclotella* spp. a temperature or a nutrient limitation proxy?

AUTHORS

Daniel Diaz de Quijano[a], Marisol Felip[a]

[a]Unitat de Limnologia, Departament d'Ecologia i Centre de Recerca d'Alta Muntanya, CEAB-CSIC-Universitat de Barcelona, Av. Diagonal 643, 08028 Barcelona, Catalonia, Spain.

KEY WORDS

Cyclotella, global warming, phosphatase activity, functional traits, proxy

INTRODUCTION

An increase in the relative abundances of small planktonic *Cyclotella* spp. diatoms has been recurrently registered in nutrient-poor, non-acidified, and non-shallow lakes since the mid-19th century. A meta-analysis of sub-arctic, alpine and temperate lakes from Europe and North America evidenced the consistence and extent of the current paleolimnological event, and detected significant differences in the date when *Cyclotella* spp. took off between high-latitude lakes (median age = AD 1870) and temperate lakes (median age = AD 1970) (Rühland *et al.*, 2008).

The current interpretation of this recent *Cyclotella* spp. increase is that climate warming would be its main driver, whereas other possible causes like acidification, long-range transport of heavy metals and persistent organic pollutants or changes in the nutrient regime would not be relevant (p.e. Rühland *et al.*, 2003, 2008; Rühland & Smol, 2005; Smol *et al.*, 2005). In general, diatom-based transfer functions for temperature show a good and direct correlation between diatom assemblages and temperature (Korhola *et al.*, 2000), and concretely, the amount of literature supporting that *Cyclotella* spp. increases with climate warming is robust for the last centuries (p.e. Catalan *et al.*, 2002; Rühland *et al.*, 2008) and before (p.e. Ampel *et al.*, 2010). Climate warming extends the duration of the ice-free period and the growing season, and in deep enough lakes, it increases the stability and duration of the thermic structure. These limnological changes modify some lake water properties (pH, nutrients, oxygen…) and light availability and especially develop the planktonic habitat that favours planktonic species like *Cyclotella* spp. (Smol, 1988; Battarbee *et al.*, 2002; Sorvari *et al.*, 2002; Rühland *et al.*, 2003).

Nevertheless, it was expectable that an increase in temperature and the consequent development of planktonic habitat could have promoted a general increase in biomass of the different planktonic species and not only of *Cyclotella* spp., as reported. Therefore, we argue that some difference(s) in the functional traits of *Cyclotella* spp. could be the cause of its specific increase. Since many of the lakes surveyed by Rühland and colleagues (Rühland *et al.*, 2008) are precisely situated in areas where the nitrogen atmospheric deposition is sufficiently important to saturate the lakes and induce or enhance a phosphorus limitation of phytoplankton primary production (Elser *et al.*, 2009; Lamarque *et al.*, 2013), we hypothesized that

the functional trait that has recently favoured *Cyclotella* spp. could be related to its autoecology of phosphorus. Concretely, we suggest that the capacity of *Cyclotella* spp. to hydrolyse dissolved organic phosphorus (DOP) using phosphatase activity (PA) could explain its relative advantage to other planktonic species, and finally explain its singular increase in North American and European lakes during the last two centuries.

PHOSPHATASE ACTIVITY: A NUTRIENT SCAVENGING FUNCTIONAL TRAIT

Phosphatase activity is a mechanism used by phytoplankton and other components of the plankton to overcome P limitation. Although inorganic phosphate is directly bioavailable for phytoplankton, it may become limiting in many situations. Then, extracellular or surface-bound PA is a mechanism to access the significant pool of DOP that exists in lakes under the form of organic compounds that otherwise could not be directly transported through microbial cell membranes (Wetzel, 1975; Chróst & Siuda, 2002).

We measured PA as a component of the functional niche of *Cyclotella* and *Fragilaria* planktonic species from the deep chlorophyll maximum (DCM) of fifteen mountain lakes sampled in the Central Pyrenees in July-August 2008. A modification of the Nedoma *et al*. (Nedoma *et al.*, 2003) enzyme labelled fluorescence (ELF) protocol was used to label phosphatase active cells as described by Diaz-de-Quijano & Felip (Díaz-de-Quijano & Felip, 2011). Succinctly, a 10µM solution, final concentration, of the ELF substrate (ELF97-phosphate or ELFP; Molecular Probes E6589) was used to incubate samples in the dark, at *in situ* temperature and pH. Incubations were sampled twice, via gentle filtration (<20KPa), within the incubation phase where there was a linear increase of the reaction product (ELF alcohol or ELFA) (Duhamel *et al.*, 2009). Polycarbonate filters were imaged under a Nikon Eclipse 90i epifluorescence microscope (Nikon, Tokyo, Japan) (see Novotná et al. for further equipment specifications; Novotná *et al.*, 2010). Fluorescence intensity measurements were based on 2D image analysis, and translated to fmol of hydrolysed phosphate (single cell hydrolysed phosphate or SCHP) according to Diaz-de-Quijano *et al*. (Diaz-de-Quijano *et al.*, 2014). The single-cell PA (SCPA) was calculated as the difference of mean SCHP of the population in the final filter minus that of the initial filter, divided by the time lapse between initial and final samplings of the incubation. Diatoms were identified through chloroplast size and shape observed by the chlorophyll

auto-fluorescence. Parallel observations of Lugol fixed subsamples under an inverted light microscope (X600 and X1000 magnifications) facilitated and confirmed diatom identification under the epifluorescence microscope.

The capacity of diatom species to hydrolyse DOP via PA was confirmed: a considerable proportion of labelled cells were observed in all the analysed diatom populations (Fig. 1 a-g). Moreover, previous studies reported PA in *Cyclotella* and/or *Fragilaria* species, including *Fragilaria crotonensis* (Rengefors *et al.*, 2001; Štrojsová *et al.*, 2003, 2005; Wang *et al.*, 2012), *Cyclotella atomus* (Wang *et al.*, 2012), *Cyclotella caspia* (Kuenzler & Perras, 1965), *Cyclotella cryptica* (Kuenzler & Perras, 1965), *Cyclotella meneghiniana* (Wang *et al.*, 2012), *Cyclotella nana* (Kuenzler & Perras, 1965; Fuhs *et al.*, 1972), *Cyclotella ocellata* (Cao *et al.*, 2005), and undefined *Cyclotella* spp. (Kuenzler, 1965; Štrojsová *et al.*, 2003). Thus, PA is a functional trait present in these two diatom genera, and in view of the fact that PA may substantially contribute to satisfy phytoplankton P demands when the enzymatic rates are large enough (Hernández *et al.*, 1996), it was advisable to assess the magnitude of their PA. In the case of the studied mountain lakes the majority of the *Cyclotella* populations presented relatively high PA, whereas only some small *Cyclotella* and the *Fragilaria* populations presented low PA rates (Fig. 1 h). Although the highest PA rate that we recorded was in a small Chrysophyta (41.8 fmol P·cell^{-1}·h^{-1}), it was closely followed by *Cyclotella* sp. 1 (39.0 fmol P·cell^{-1}·h^{-1}). The *Discostella* cf. *pseudostelligera* – previously *Cyclotella* cf. *pseudostelligera*– populations also recorded significantly positive PA rates: 4.3, 2.6 and 1.1 fmol P·cell^{-1}·h^{-1}. Moreover, most *Cyclotella* populations were the maximum phosphatase active agents in their respective lakes (the two mentioned species and *C*. cf. *praetermissa*), as it occurred in previous studies (Cao *et al.*, 2005). In a study where *Cyclotella* sp. was not dominating PA (Štrojsová *et al.*, 2003), it was at least still superior to the other co-occurring diatoms. Then, the possibility that PA conferred an adaptive advantage to the *Cyclotella* spp. in P limited environments appears to be plausible.

The environmental conditions where *Cyclotella*'s PA was maximized informs about its role in the environment and, at last, may be a clue to interpret the *Cyclotella* spp. presence in paleolimnological records. The maximum PA, in *Cyclotella* sp. 1, occurred in an extreme environmental situation in relation to the range of lake conditions where we found *Cyclotella.* It was in the most alkaline extreme (pH 8.82), low TDP and DRSi (94 nM and 13 µatgr,

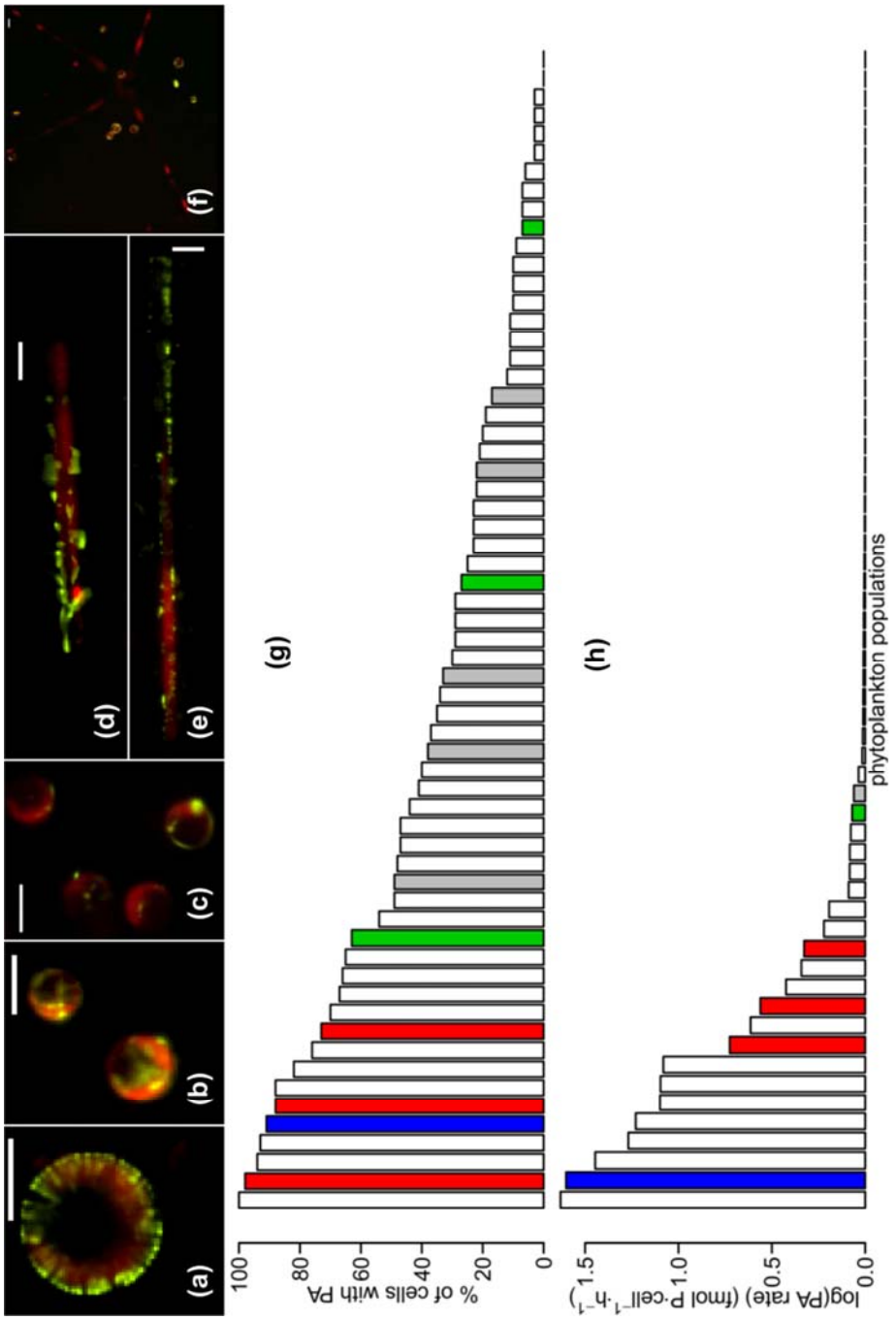

Fig. 1 Epifluorescent microscope microphotographs of PA in different diatoms: (a) *Cyclotella* sp. 1, (b) *Discostella* cf. *pseudostelligera*, (c) *Cyclotella* cf. *polymorpha*, (d and e) *Fragilaria*, (f) labelled *D.* cf. *pseudostelligera* and unlabelled *Asterionella* sp.. Chloroplasts are in red, and PA in green. White bars are 5 µm long. Histograms showing PA (in percentage of active cells (g) and average PA rates (h)) for the

different phytoplankton populations assessed in fifteen high mountain lakes in the Pyrenees. Blue: *Cyclotella* sp. 1, Red: *D.* cf. *pseudostelligera*, Green: other *Cyclotella* spp. (*Cyclotella* cf. *polymorpha* and *Cyclotella* cf. *praetermissa*), Grey: *Fragilaria* spp., White: non-Bacillarophyceae populations.

respectively), and high TDN (Fig. 2), which fits the adaptation of *Cyclotella* spp. to alkaline environments with low silicate described in the literature (Tilman & Kilham, 1976; Whitmore, 1989). Moreover, the tendency that PA increases in higher TDN concentrations is also insinuated in the case of *D.* cf. *pseudostelligera* (Fig. 2 b), which is the second group of Cyclotellas in terms of PA rates. Overall, *D.* cf. *pseudostelligera* and *Cyclotella* sp. 1 seem to increase their PA in relatively high TDN concentrations and low levels of P and silicate. We suggest that this mechanism could partly explain the recent increase in the last two centuries of *Cyclotella* spp. populations in Northern Hemisphere lakes fertilized by atmospheric N deposition (Rühland *et al.*, 2008). In a similar way, a different diatom capable of high PA rates, *Didymosphenia geminata*, became hegemonic in the benthic communities of a lotic ecosystems with low dissolved inorganic phosphate (Ellwood & Whitton, 2007; Miller *et al.*, 2009; Ladrera-Fernández, 2012).

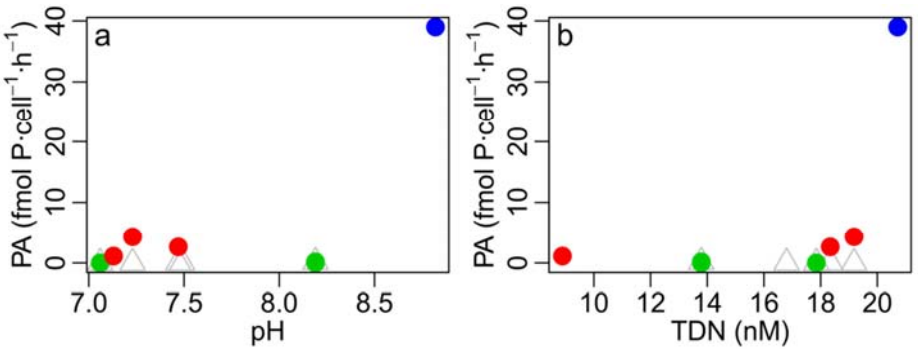

Fig. 2 Phosphatase activity rates of different diatom populations from high mountain lakes against pH (a) and total dissolved nitrogen (b). Blue: *Cyclotella* sp. 1, Red: *Discostella* cf. *pseudostelligera*, Green: other *Cyclotella* spp., Grey: *Fragilaria* spp.

In any case, the PA in *Cyclotella* spp. may be explained by the principle of opportunity of costs (Stephens & Krebs, 1987), where a weakly efficient mechanism is still useful to access wider resource opportunities in scarcity

conditions. This would agree with modest abundances and biomasses recorded here and before in a Pyrenean high mountain lake (Catalan *et al.*, 2002). The kinetic parameters of PA (K_M and Vmax) were determined in eight of the 15 sampled lakes, including the two lakes where PA was dominated by *Cyclotella* sp. 1 and the *D.* cf. *pseudostelligera* population that had a 2.6 fmol $P \cdot cell^{-1} \cdot h^{-1}$ rate. The K_M and Vmax values of these two lakes were 10.2 µM and 1.65 $nM \cdot min^{-1}$, and 2.6 µM and 0.39 $nM \cdot min^{-1}$ respectively, whereas the averages for the eight assessed lakes were 10.7 µM and 1.75 $nM \cdot min^{-1}$. This means *Cyclotella* spp. were presenting intermediate to high affinity phosphatases with intermediate to low maximum rates, which would reflect an adaptation to low DOP concentrations but the impossibility to report extremely high hydrolysed P even in an event of a DOP pulse. According to these data we would not expect *Cyclotella* to hegemonise phytoplankton communities in mountain lakes.

CONCLUSION

The interpretation of a species (or genus) shift in the paleolimnological record is not a trivial question and may be based on at least two different sources of evidence. On the one hand, there are the correlations with other paleoecological variables whose interpretation is already accepted. On the other hand, the knowledge of the ecological niche of the taxon is also essential. This may be based on modern distribution of the taxon along environmental gradients and/or in a biogeographic scope (realised ecological niche), or on experimental data from laboratory cultures (potential and optimum ecological niches). In fact, any change in the relative abundance of a taxon always responds to an n-dimensional set of factors (different environmental factors, interactions with other species, stochastic phenomena like arrival of propagula or extinctions, etc.), and the interpretation of the shift is a logical procedure that attempts to reduce dimensionality for the sake of its understanding that should consider, at least *a priori*, the whole complexity of possible interacting factors.

This kind of interpretation was conducted by Rühland and colleagues (Rühland *et al.*, 2003), who concluded that temperature was the main factor inducing the *Cyclotella* spp. shift in fifty Subarctic lakes without discarding synergistic effects with other factors. Most of those lakes were ultraoligotrophic to oligotrophic (TP <10 $\mu g \cdot l^{-1}$) and modern populations of

Cyclotella spp. were abundant in the lowest range of TP and TN. Additionally, no correlation was found between diatom assemblage changes and TP and TN, so it was generally interpreted that diatom assemblage changes including *Cyclotella* spp. increase were not promoted by a human-induced nutrient increase. Nevertheless, it was not tested how far the stoichiometry between different bioavailable nutrients (in dissolved and generally inorganic form) could contribute to explain the *Cyclotella* spp. shift. We highlight that independently of the total nutrient budget, slight unbalanced stoichiometries where dissolved inorganic phosphorus was limiting could be sufficient to promote phosphatase active species like *Cyclotella* spp. Then, Subarctic and nutrient-poor temperate lakes like those surveyed by Rühland *et al*. (Rühland *et al.*, 2008) could represent both, natural or atmospheric nitrogen deposition-induced situations of phosphorus limitation within the oligotrophic range needed by *Cyclotella* spp.

Thus, the early *Cyclotella* spp. take-off in Subarctic lakes would respond to the especial sensitiveness of these ecosystems to climate warming (Serreze *et al.*, 2000), and should occur under natural phosphorus limitation of primary production because atmospheric nitrogen deposition was low in that area, notably in Subarctic North America (Lamarque *et al.*, 2013). Afterwards, when climate warming arrived to affect nutrient-poor temperate lakes, they would be already phosphorus limited, either naturally or by atmospheric nitrogen deposition. The non-significant positive correlation between atmospheric nitrogen deposition and a detailed record of *Cyclotella* spp. increase during the last decades in a temperate lake (Rühland *et al.*, 2008) could mean that such increase responds rather to a combination of warm temperature and P limiting conditions than to the nitrogen enrichment itself.

Finally, it is worth to note that there may be an interaction between temperature and nutrient availability because the PA mechanism is activated by *Cyclotella* spp. under phosphorus limitation, and the enzymatic rate is temperature dependent. In another scale, increasing temperatures increase nutrient cycling at the lake and watershed levels, and may trigger stoichiometric changes possibly faster than atmospheric nitrogen deposition in Subarctic areas. Then, the *Cyclotella* spp. populations would respond to synergistic effects of warming and changes in the nutrient stoichiometry, as it has recently been suggested for the whole phytoplankton of Subarctic lakes (Bergström *et al.*, 2013).

In conclusion, the detailed study of a functional trait (PA) in *Cyclotella* spp. from high mountain lakes shed some light to the interpretation of the recent paleolimnological records, which responded to climate warming in combination to a phosphorus limiting situation enhanced by atmospheric nitrogen deposition.

BIBLIOGRAPHY

Ampel L, Wohlfarth B, Risberg J, Veres D, Leng MJ, Tillman PK (2010) Diatom assemblage dynamics during abrupt climate change: the response of lacustrine diatoms to Dansgaard–Oeschger cycles during the last glacial period. *Journal of Paleolimnology*, **44**, 397–404.

Battarbee RW, Grytnes JA, Thompson R, Appleby PG, Catalan J (2002) Comparing palaeolimnological and instrumental evidence of climate change for remote mountain lakes over the last 200 years. *Journal of Paleolimnology*, **28**, 161–179.

Bergström A-K, Faithfull C, Karlsson D, Karlsson J (2013) Nitrogen deposition and warming – effects on phytoplankton nutrient limitation in subarctic lakes. *Global Change Biology*, **19**, 2557–2568.

Cao X, Štrojsová A, Znachor P, ZApomělová E, Liu G, Vrba J, Zhou Y (2005) Detection of extracellular phosphatases in natural spring phytoplankton of a shallow eutrophic lake (Donghu, China). *European Journal of Phycology*, **40**, 251–258.

Catalan J, Pla S, Rieradevall M, Felip M, Ventura M (2002) Lake Redo ecosystem response to an increasing warming in the Pyrenees during the twentieth century. *Journal of Paleolimnology*, **28**, 129–145.

Chróst RJ, Siuda W (2002) Ecology of microbial enzymes in lake ecosystems. In: *Enzymes in the environment. Activity, ecology and applications* (eds Burns RG, Dick RP), pp. 35–72. Marcel Dekker, Inc, New York.

Diaz-de-Quijano D, Hornák K, Palacios P, Felip M (2014) 3D restoration microscopy improves quantification of enzyme-labelled fluorescence

(ELF)-based single-cell phosphatase activity in plankton. *Cytometry Part A*. DOI: 10.1002/cyto.a.22486.

Díaz-de-Quijano D, Felip M (2011) A comparative study of fluorescence-labelled enzyme activity methods for assaying phosphatase activity in phytoplankton. A possible bias in the enzymatic pathway estimations. *Journal of microbiological methods*, **86**, 104–7.

Duhamel S, Gregori G, Van Wambeke F, Nedoma J (2009) Detection of Extracellular Phosphatase Activity at the Single-Cell Level by Enzyme-Labeled Fluorescence and Flow Cytometry: The Importance of Time Kinetics in ELFA Labeling. *Cytometry Part A*, **75A**, 163–168.

Ellwood N, Whitton B (2007) Importance of organic phosphate hydrolyzed in stalks of the lotic diatom Didymosphenia geminata and the possible impact of atmospheric and climatic changes. *Hydrobiologia*, **592**, 121–133.

Elser JJ, Andersen T, Baron JS et al. (2009) Shifts in lake N:P stoichiometry and nutrient limitation driven by atmospheric nitrogen deposition. *Science*, **326**, 835–837.

Fuhs GW, Demmerle SD, Canelli E, Chen M (1972) Characterization of phosphorus limited plankton algae (with reflections on the limiting nutrient concept). In: *Nutrients and eutrophication: the limiting nutrient controversy* (ed Likens GE), pp. 113–133. American Society of Limnology and Oceanography.

Hernández I, Hwang SJ, Heath RT (1996) Measurement of phosphomonoesterase activity with a radiolabelled glucose-6-phosphate. Role in the phosphorus requirement of phytoplankton and bacterioplankton in a temperate mesotrophic lake. *Archiv für Hydrobiologie*, **137**, 265–280.

Korhola A, Weckström J, Holmström L, Erästö P (2000) A Quantitative Holocene Climatic Record from Diatoms in Northern Fennoscandia. *Quaternary Research*, **54**, 284–294.

Kuenzler EJ (1965) Glucose-6-phosphate utilization by marine algae. *Journal of Phycology*, **1**, 156–164.

Kuenzler EJ, Perras JP (1965) Phosphatases of marine algae. *Biological Bulletin*, **128**, 271–284.

Ladrera-Fernández R (2012) *Estudio del estado ecológico de los cursos fluviales del Parque Natural Sierra de Cebollera (La Rioja) en base a la comunidad de macroinvertebrados acuáticos*. University of Barcelona.

Lamarque J-F, Dentener F, McConnell J et al. (2013) Multi-model mean nitrogen and sulfur deposition from the Atmospheric Chemistry and Climate Model Intercomparison Project (ACCMIP): evaluation of historical and projected future changes. *Atmospheric Chemistry and Physics*, **13**, 7997–8018.

Miller MP, McKnight DM, Cullis JD, Greene A, Vietti K, Liptzin D (2009) Factors controlling streambed coverage of Didymosphenia geminata in two regulated streams in the Colorado Front Range. *Hydrobiologia*, **630**, 207–218.

Nedoma JJ, Štrojsová A, Vrba J et al. (2003) Extracellular phosphatase activity of natural plankton studied with ELF97 phosphate: fluorescence quantification and labelling kinetics. *Environmental microbiology*, **5**, 462–472.

Novotná J, Nedbalová L, Kopáček J, Vrba J (2010) Cell-specific extracellular phosphatase activity of Dinoflagellate populations in acidified mountain lakes. *Journal of Phycology*, **46**, 635–644.

Rengefors K, Pettersson K, Blenckner T, Anderson DM (2001) Species-specific alkaline phosphatase activity in freshwater spring phytoplankton : Application of a novel method. *Journal of Plankton Research*, **23**, 435–443.

Rühland K, Smol JP (2005) Diatom shifts as evidence for recent Subarctic warming in a remote tundra lake, NWT, Canada. *Palaeogeography, Palaeoclimatology, Palaeoecology*, **226**, 1–16.

Rühland K, Priesnitz A, Smol JP (2003) Paleolimnological evidence from diatoms for recent environmental changes in 50 lakes across Canadian arctic treeline. *Arctic, Antarctic, and Alpine Research*, **35**, 110–123.

Rühland K, Paterson A, Smol J (2008) Hemispheric-scale patterns of climate-related shifts in planktonic diatoms from North American and European lakes. *Global Change Biology*, **14**, 2740–2754.

Serreze MC, Walsh JE, Osterkamp T et al. (2000) Observational evidence of recent change in the northern high-latitude environment. *Climatic Change*, **46**, 159–207.

Smol JP (1988) Paleoclimate proxy data from freshwater arctic diatoms. *Verhundlungen der Internationalen Vereinigung von Limnologen*, **23**, 837–844.

Smol JP, Wolfe AP, Birks HJB et al. (2005) Climate-driven regime shifts in the biological communities of arctic lakes. *Proceedings of the National Academy of Sciences of the United States of America*, **102**, 4397–402.

Sorvari S, Korhola A, Thompson R (2002) Lake diatom response to recent Arctic warming in Finnish Lapland. *Global Change Biol*, **8**, 171–181.

Stephens DW, Krebs JR (1987) *Foraging Theory*. Princeton University Press, Princeton, NJ.

Štrojsová A, Vrba J, Nedoma J, Komárková J, Znachor P (2003) Seasonal study of extracellular phosphatase expression in the phytoplankton of a eutrophic reservoir. *European Journal of Phycology*, **38**, 295–306.

Štrojsová A, Vrba J, Nedoma J, Šimek K (2005) Extracellular phosphatase activity of freshwater phytoplankton exposed to different in situ phosphorus concentrations. *Marine and Freshwater Research*, **56**, 417–424.

Tilman D, Kilham SS (1976) Phosphate and silicate growth and uptake kinetics of the diatoms Asterionella formosa and Cyclotella

meneghiniana in batch and semicontinuous culture. *Journal of Phycology*, **12**, 375–383.

Wang P, Shen H, Xie P (2012) Can hydrodynamics change phosphorus strategies of diatoms?-Nutrient levels and diatom blooms in lotic and lentic ecosystems. *Microbial ecology*, **63**, 369–382.

Wetzel RG (1975) *Limnology*. Saunders, Philadelphia.

Whitmore TJ (1989) Florida diatom assemblages as indicators of trophic state and pH. *Limnology and Oceanography*, **34**, 882–895.

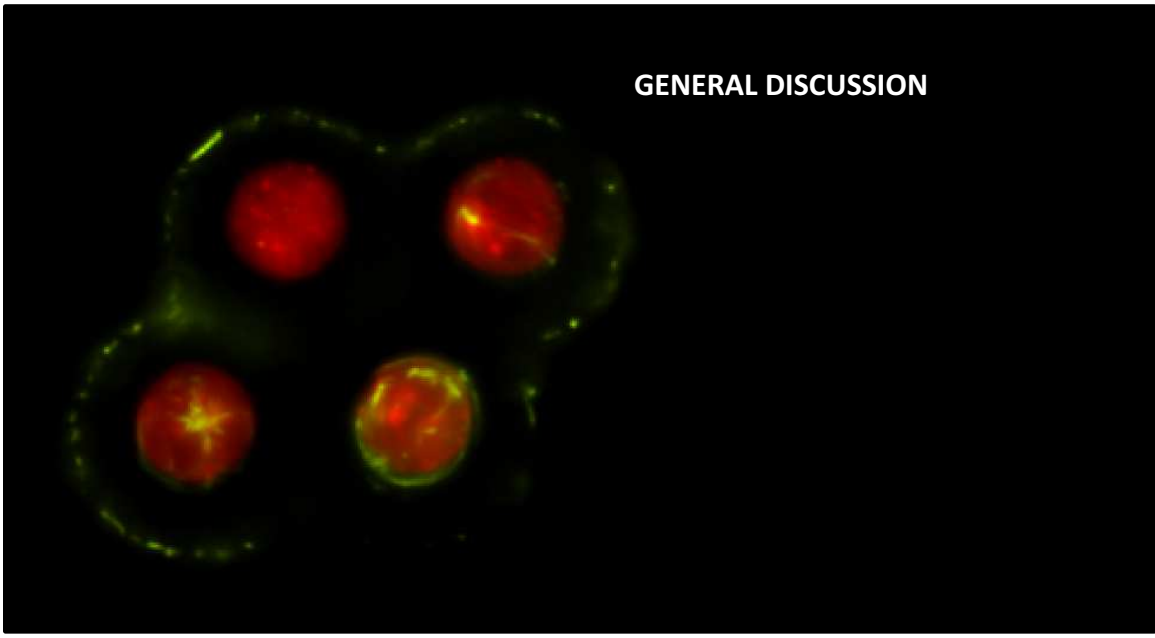

GENERAL DISCUSSION

1. The importance of phosphatase activity (PA)

The present study has assessed PA in the phytoplankton of high mountain lakes in the Pyrenees for the first time. PA values in the bulk summer deep chlorophyll maximum (DCM) were low to intermediate, compared to the literature (Hoppe, 2003; Sawatzky *et al.*, 2005; Nedoma *et al.*, 2006). Nevertheless, their role in supporting the primary production during one of the most productive period of the year in these ecosystems seems to be relevant: Lakes where P mobilisation was high, mobilised up to 3.6 or 26.1 times more organic phosphorus by PA than by bacterivory, and bacterivory magnitudes were always comparable to those reported in many other studied ecosystems (Vaqué *et al.*, 1994; Šimek *et al.*, 1999; Callieri *et al.*, 2006; Comte *et al.*, 2006; Zubkov & Tarran, 2008). Moreover, the dominance of PA as a P scavenging activity was recorded in the extreme pH lakes, clearly in acidic lakes and also in some species of the alkaline extreme lakes. But apart from the role of phosphatases for the bulk primary production in high mountain lakes, we also identified PA as an important functional trait that could have determined the recent expansion of *Cyclotella* spp. (Rühland *et al.*, 2008).

2. The importance of single-cell PA (SCPA) quantification

This thesis contributed to improve the enzyme-labelled fluorescence (ELF) quantification and the ELF protocol via avoiding biases induced by cell-size and out-of-focus light when quantifying fluorescence intensity on 2D images, avoiding possible false negative and false positive results, maximising the labelling of ectophosphatase activity, and minimising the labelling of intracellular PA. The solution (unfixed and liquid incubations, and quantification of deconvolved 3D images) is important because it diminishes the methodological bias in our observations of the nature, but also because a standardization of the protocol is required, together with data bases (Allan *et al.*, 2012) and automatic image acquisition and analysis routines (Zeder & Pernthaler, 2009; Zeder *et al.*, 2010, 2011), to make the ELF technique a high-throughput single-cell enzyme activity technique.

2.1. Intracellular labelling and its consequences

An important contribution of this thesis was the detection of a systematic reactivity of intracellular phosphatases with the ELF substrate (ELFP). The location of the ELF labelling (intracellular, surface-bound or both) depended on the ELF protocol rather than on the phytoplankton species, and although in different extents, all of the tested ELF protocols presented this problem. We confirmed previous observations of intracellular labelling of phosphatases (González-Gil *et al.*, 1998; Dyhrman & Palenik, 1999; Skelton *et al.*, 2006; Ou *et al.*, 2010), extending it for the first time to the case of nonmixotrophic species (mostly Chlorophyceae). We hypothesise that the labelling of intracellular phosphatases may be due to a combination of phagocytosis of particles together with the ELFP substrate, pinocytosis of ELFP (as may be the case of Chlorophyceae like *Chlamydomonas*; Joseph et al., 1995; Tittel et al., 2005; Spijkerman et al., 2007), and cell membrane disruption caused by natural cell death (Bidle & Falkowski, 2004), sample manipulation, and the accumulation of ELFA crystals (the reaction product).

The consequences of such observation are to be discussed. Bulk and single-cell assays of PA, either colorimetric, fluorimetric or radiometric have been thought to react only with ectophosphatases (and dissolved extracellular phosphatases) because most of the substrates are unable to pass through a cell membrane due to their physicochemical properties (Chróst, 1991). The hypothesis that the detection of intracellular labelling was a problem exclusive to the ELF substrate should be experimentally tested in the future. We tend to expect that this might not be the case because previous studies found that ELFP and 4-methylumbelliferyl-phosphate (MUFP) substrates reacted with the same set of phosphatases in natural samples (Štrojsová *et al.*, 2003; Nedoma *et al.*, 2007). Therefore, it is thinkable that most of our knowledge on *extracellular* PA in the environment was biased by the interference of intracellular phosphatases. Finally, it is also conceivable that such interference occurred in the assays of other extracellular enzyme activities (EEA). The weight of the intracellular enzyme bias would probably depend on the ecosystem and the species, but approximately this could represent more than the 10% of particulate aminopeptidase and phosphatase activities (Chróst, 1991; Chróst & Siuda, 2002), or a much higher percentage in certain species (e.g. Dyhrman and Palenik, 1999).

2.2. Other methodological challenges and open questions

Since the seminal paper of Nedoma and colleagues on the ELF technique and its quantification, a couple of caveats were identified (Nedoma *et al.*, 2003). The time-course of the phosphatase reaction with ELFP substrate starts with a lag time, i.e. a period of time when phosphatases hydrolyse ELFP but ELFA fluorescent precipitates are not being formed yet. The length of this lag time is approximately (but imperfectly) proportional to the velocity of the reaction. Despite it has been highlighted that quantifications of the fluorescence labelled enzyme activity (in percentages and rates) should be performed in the stationary phase of linear increase in ELFA precipitate (Nedoma *et al.*, 2003; Duhamel *et al.*, 2009), studies performed in lakes with extraordinarily high PA quantified PA rates based on a single time point in the incubation (e.g. Novotná et al., 2010). In these cases the lag time was neglected arguing that it represented a very short time in relation to the whole incubation time. Since we worked with a range of diverse high mountain lakes, and usually with low to intermediate PA, the diversity of lag-times was an important fact in our quantifications. We took the compromise decision to measure species-specific rates from two time points taken during the increasing linear phase of the bulk phosphatase reaction. Two aspects are worth to mention from our experience. On the one hand, several quantifications within a certain time point did not follow a normal distribution but rather a fat-tailed distribution, which should be considered when estimating centrality and dispersion. In fact, fat-tailed distributions are characteristic for populations with only a few phosphatase active individuals, whereas normal distributions usually correspond to populations with higher percentages of phosphatase active cells (Fig. 1). On the other hand, variability in the central value and dispersion of single-cell hydrolysed phosphorus (SCHP) supposed a problem to the calculation of species-specific PA rates, especially in low activity populations: the standard deviation of the initial and final time points could be very different and their means (or expectations) sometimes decreased instead of increasing, or increased very slightly compared to the bulk fluorimetric rate (Fig. 2 a, b and c). Therefore, taking only two time points (but especially when taking only one time point!) could under- or overestimate PA rates in populations. Overall, increasing the number of time points would probably minimise this problem, but it would multiply the economic and time cost of the assay. Alternatively, quantifying a larger amount of cells per time point (a minimum of 30 individuals per

population and time point was the law of thumb that we and previous studies followed) would be advisable, especially when fat-tailed distributions are found. In order to discard the possibility of any artefact in the incubation (e.g. that manipulating the incubation detached ELFA precipitates from the surface of some cells, decreasing the ELFA in advanced time points of the incubation), it would be interesting to quantify a time-series of images of *in vivo* ELFP incubations in a quiet and a slightly turbulent medium. Such a procedure would be also interesting to assess the possible differences in lag time length between individuals of a population, between species, and between species and the bulk fluorimetric lag time, which we assumed to be not very different. Finally, an abrupt shift of bulk fluorescence in fluorimetric ELF time-course series was occasionally observed (Fig 2 d). We do not have any explanation for this phenomenon (that was not described before) but a quantification of all the ELFA precipitates under the microscope could shed some light into it.

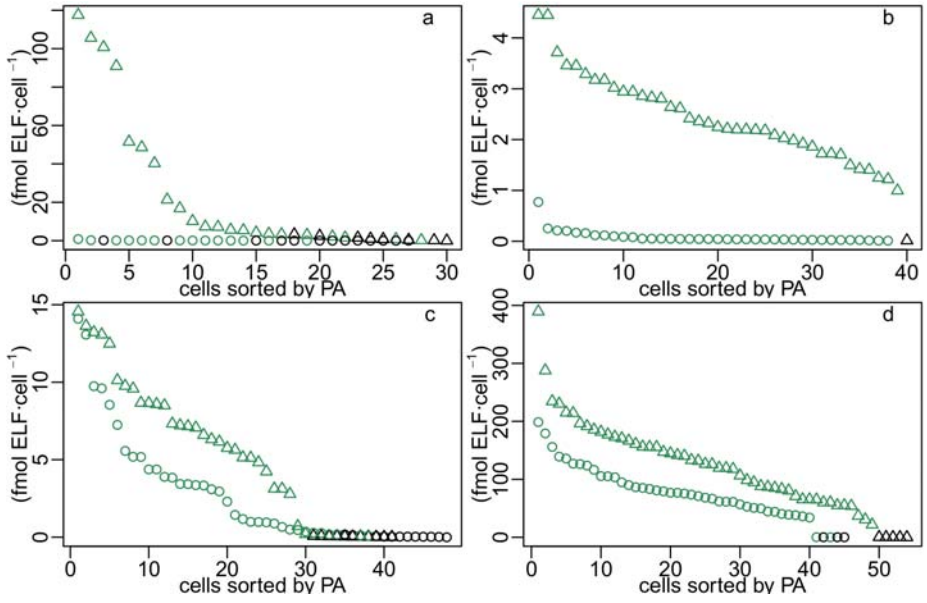

Fig. 1 Distribution of cells ordered by SCPA. Cells belonging to the initial or final incubation times were represented by circumferences and triangles, respectively. Cells that were *de visu* qualified as phosphatase active or inactive were represented by green and black symbols, respectively. a: 8 µm *Amphidinium* sp. in Pica Palomèra; b: *Discostella* cf. *pseudostelligera* in Gerber; c: *Discostella* cf. *pseudostelligera* in Botornàs; d: *Cyclotella* sp. 1 in Filià. Note that different populations may follow fat-

tailed distributions (a, b initial incubation time, and c) or normal distributions (b final incubation time, and d) (Lilliefors test, p-v>0.05).

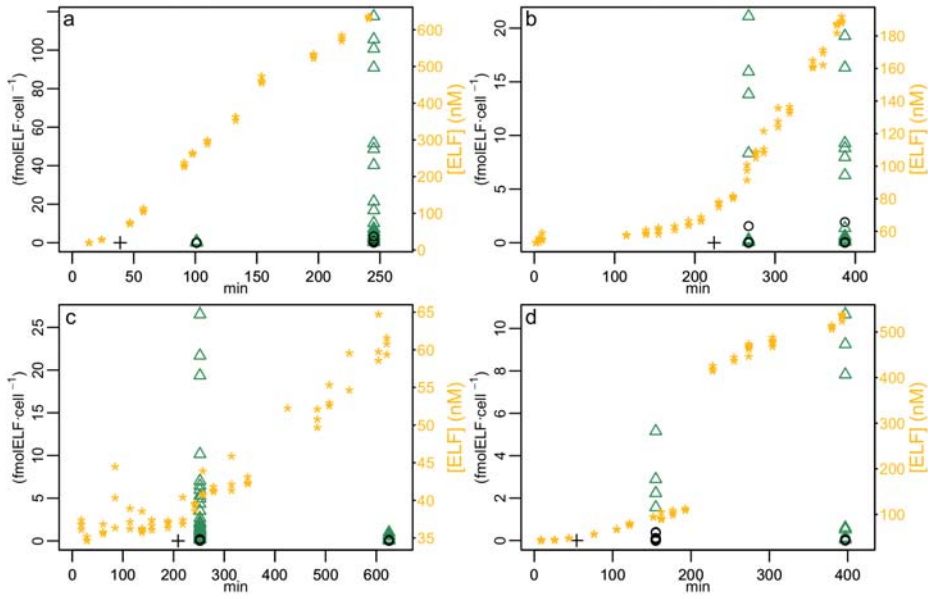

Fig. 2 Time-course of the PA reaction as measured by fluorimeter (yellow), with SCPA measurements at the initial and final incubation times. Black cross indicates the time point considered the breakpoint between lag time and linear increase phase. Cells that were *de visu* qualified as phosphatase active or inactive were represented by green triangles and black circumferences, respectively. a: 8 µm *Amphidinium* sp. in Pica Palomèra; b: 5 µm *Ochromonas* sp. in Bassa d'Òles; c: *Fragilaria* sp. in Botornàs; d: *Chloromonas* sp. in Bassa de les Granotes.

A second topic of interest is the use of a fluorescein standard to perform flat-fielding and get an intersession correction factor (Icf) for the quantification of fluorescence via a microscope (Model & Burkhardt, 2001). In our experience, the protocol appeared basically correct but we ambitioned to improve it. On the one hand, moderate differences in this correction factor could be obtained if measured consecutively within the same session. On the other hand, we deducted that flat-fielding based on fluorescein could suppose some bias if used to quantify ELFA. Flat-fielding is a procedure that corrects for uneven sensitivity of the camera and for uneven spatial illumination. Since the main correction refers to loss of intensity in the edges of the field of view (flat-fielding is also named shading correction), and this

shading in the edges is due to the dispersion of light that penetrates different materials with different optical activity, the properties of the shading depend on the wavelength of the fluorescent light, which makes it is recommendable to perform flat-fielding using a fluorochrome with the same emission wavelength than the light to be quantified in the samples. For this reason, and also in an attempt to find a better alternative for the calibration factor (fmol ELFA·microscope FU $^{-1}$), we tried to use a series of slides with different ELFA concentrations as a standard instead of the fluorescein one. Unfortunately, the fluorescence intensity of the ELFA slides didn't always correlate (positive nor negatively) with the ELFA concentration, and two ELFA slides with the same concentrations prepared and imaged in correlative days could yield substantially different fluorescence intensity values. We firstly hypothesized quenching effect within the ELFA slides but after further experimentation, the irregular behaviour showed that some other phenomena could be also occurring. Moreover, it was very difficult to get rid of exogenous fluorescent debris in the ELFA sample, which challenged the usefulness of ELFA slides as a flat-fielding standard. Despite these problems with ELFA slides, some correct images (sufficiently fluorescent and without debris) could be taken. There we observed that the flat-fielding obtained from fluorescein standard slides improved the raw shading of another wavelength fluorochrome like ELFA but still kept some level of shading at the edges of the field of view, as expected. In any case, this inefficiency of fluorescein standard to flat-field ELFA wavelength was quantitatively tiny. In conclusion, the fluorescein standard is not a perfect way to get intersession calibration factor and to flat-field for our purposes, but our attempts to improve it did not succeed, so we had to accept the fluorescein standard as a useful option.

Since our attempt to develop a cheaper and faster way to get a conversion factor (fmol ELFA·microscope FU^{-1}) did not succeed, we turned back to Nedoma's work (Nedoma *et al.*, 2003). Nedoma and colleagues identified this step as the second most important caveat of the proposed quantification procedure. In this thesis, we suggest that the use of deconvolved 3D images will probably improve this critical step in the ELF technique. As we mentioned in chapter two, current raw 2D images of filters acquired to calculate the conversion factor are focused to the plane with the highest amount of fluorescence, but this compromise undersamples fluorescence for three reasons: only one optical slice of large objects is acquired, only one

optical slice of the out-of-focus light of objects (usually >10 µm deep) is acquired, and not all objects in a frame are usually well focused because some may detach from the filter during sample mounting, and more important, because rippling or mispositioning (not strictly orthogonal) of the filter may occur.

Finally, another important challenge of the ELF technique is to clearly discriminate between very low phosphatase active and phosphatase inactive cells. Basically, the problem lies in the spectral overlap of ELFA with DAPI or degraded phytoplankton pigments, so we suggest that raw 3D images should be deconvolved with an algorithm that, apart from modelling light blur, also modelled the spectral overlap of different fluorochromes (Hoppe *et al.*, 2006). If that was successful, the question why is there a rupture of linearity between the dimmest and the intermediate fluorescence intensities when measured via deconvolved 3D in comparison to the other methods should be addressed. This rupture of linearity seems to be robust because it was not only observed in this thesis but also in Swedlow *et al*. (Swedlow *et al.*, 2002), albeit the authors almost did not mention it.

2.3. Potentialities of the ELF technique

Several authors have mentioned before the potentialities of the ELF technique to be combined with other non-destructive single-cell techniques (e.g. Schade and Lemmer, 2006). In this thesis we suggest to use the deconvolved 3D ELF technique when attempting to combine different single-cell techniques because here the particular value of a concrete cell is important because it corresponds to a certain value in the second assessed variable, and the deconvolved 3D ELF technique improves the accuracy of the single-cell enzyme activity measurements. The most mentioned possible combinations would be with microautoradiography or microautoradiography-fluorescent-in-situ-hybridisation (MAR-FISH) for single-cell nutrient incorporation, and with fluorescence-labelled bacteria (FLBs) or catalysed reported deposition-FISH (CARD-FISH) for single-cell bacterivory assessments. Such technical integrations may provide information about detailed biogeochemical processes such as the link between hydrolytic enzyme activity and nutrient uptake at the cellular level and in close-to-*in situ* conditions, but also about functional shifts in trophic strategies within mixotrophic populations of the microbial loop. In fact, the

combination of different single-cell techniques would represent a step forward into the individual-based (or cellular) ecology in the microbial loop, which is nowadays still to be explored because the available single-cell data are unfortunately merged into a population-level analysis.

Three more potentialities of the ELF technique are also worth to mention. Firstly, the use of quantitative ELF technique would be able to characterise the in situ kinetic and thermodynamic parameters of enzyme activities in natural populations, which would be a nice contribution to the knowledge of EEA in the environment. Secondly, the ELF technique is ideal to assess the identity of heterotrophic flagellate species with PA in the nature, the role of that enzyme activity in heterotrophic protists and the regulation mechanisms that take place in these cases. Finally, the use of the ELF technique has also arisen its own questions: different shapes and patterns of the ELFA precipitates drawn on the cell surfaces of different phytoplankton species have been detected (e.g. linear structures, dots, evenly labelled whole cell surfaces, etc.) (see chapter covers; Štrojsová *et al.*, 2003). It is possible that such patterns corresponded to the physical distribution and degree of mobility of the phosphatases within the cell membrane or wall, which could finally influence in the capacity of enzymes to reach their substrates. In that case, differences between species or eventual differences in the ELF pattern within a same species could be hypothesised to have an adaptive meaning in the evolutionary or physiological level.

3. 5 µm threshold

In this thesis we identified a surface-to-volume ratio (S/V) threshold of 1.24, above which phytoplankton of natural communities decreased its rates and percentage of active cells in PA and bacterivory (chapter 3 Fig. 6 b). This unexpected finding could be explained by the fact that small cells, with high S/V, may be more efficient in the uptake of inorganic P (and other nutrients) (as theoretically and experimentally reported before; Catalan, 2000; Tambi et al., 2009) and therefore less dependent on PA and bacterivory to access organic P.

Model simulations of mixotrophic phytoplankton foraging modes showed a sharp decrease of phagotrophy in the phytoplankton smaller than 5 µm cell diameter, relative to intermediate size phytoplankton, for a wide variety of conditions (Våge *et al.*, 2013). Since a 1.24 S/V corresponds to approximately

a 4.8 µm diameter sphere, the idea of a threshold for nutrient scavenging modes around 5 µm cell diameter is reinforced. Besides, our observations in oligotrophic high mountain lakes also suggest that, additionally to phagotrophy, PA also decreases below the c. 5 µm cell diameter threshold. Thus, it is conceivable that low phagotrophy (and PA) in small cells was rather due to their higher capacity to meet their P requirements via transport of inorganic P than to physical space restrictions to digest particles.

But why should the threshold concretely be 1.24? We attempted to answer this question hypothesising that the relationship between the S/V and the phosphorus critical concentration (PC_{cri}), i.e. the minimum [P] necessary to support maximum exponential growth rate, would change above and below 1.24. The use of P scavenging activites like PA and bacterivory above the PC_{cri} of a population would represent a waste of energy, whereas below that value a range of possibilities are conceivable: submaximal, zero or negative growth supported or not by P scavenging activities. The PC_{cri} was estimated for ideal spherical cells with S/V in the range of S/V found in the high mountain lakes studied in this thesis at 0.10 intervals (calculations were described in the appendix). The 1.24 value, in fact, lied close to the middle value of the observed S/V range (1.11). The increase of constant 0.10 S/V intervals represented smaller steps in PC_{cri} as the S/V value increased but we did not observe any change in this behaviour around the 1.24 S/V (Fig. 3). Therefore, the fact that the threshold was concretely at the value of 1.24 S/V may not be explained by any discontinuity in the PC_{cri} that it implies, and should respond to temperature and inorganic P availability in such systems. For the coldest lakes (for instance Botornàs; 4ºC) the PC_{cri} of a 4.8 µm spherical cell would be 2.58 nM P, in the warmest lake (Bassa d'Òles; 21.8ºC), 7.18 nM P, and in an average lake (9.8ºC), 3.62 nM P. At such P concentrations cells smaller than 5 µm would not need any additional source of P.

As we found the 1.24 S/V threshold for general phytoplankton, we also wondered how different would be the PC_{cri} for different shaped cells with 1.24 S/V, and thus the presumed [P] below which P scavenging activities could take importance. We then calculated the PC_{cri} for a set of ideal cells with different shapes but constant 1.24 S/V (Fig. 4 a). PC_{cri} values depended on temperature and on cell shape. A perfect sphere, the shape with lowest volume, and P demands, had the lowest PC_{cri} (below 5nM P for most of the temperature range) and was closely followed by loosely round shapes (round

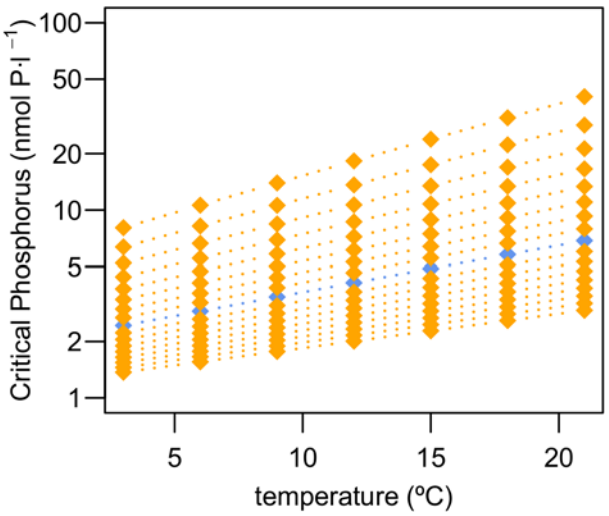

Fig. 3 Critical phosphorus concentrations of ideal spherical cells with S/V between 0.44 and 2.02 at 0.10 steps (yellow) related to temperature. Blue represents the spherical cell with S/V=1.24.

and pointed dinoflagellates, and pointed chryptophytes). PC_{cri} only increased significantly in diatoms: *Cyclotella*-like diatoms had PC_{cri} between 5-10 nM P and *Fragilaria*-like diatoms, one order of magnitude above (Fig. 4 a). Since all the PC_{cri} values, except in *Fragilaria*-like diatoms, stayed below 10 nM P, it seems reasonable that the threshold could not be much higher than 1.24 because it would trigger only modest decreases in PC_{cri} within the narrow range between 0 and 10 nM P (or 0 and 2.58 in the coldest lakes). Finally, the PC_{cri} of a selection of species studied in this thesis were also reported (Fig. 4 b, c and d). In chapter 3, we found that 5 µm *Chromulina-Ochromonas* had a wider range of PA and bacterivory values than the 3 µm, both in specific rates and percentage of active cells. A possible explanation to that would be that since the 5 µm *Chromulina-Ochromonas* has higher PC_{cri}, it is more probable to find it in a more P-limited situation, and then investing in P scavenging activities. In a similar way, *Cyclotella* sp. 1 had a notably higher PC_{cri} and probability to be P limited than *Discostella* cf. *pseudostelligera*, and effectively, we measured per cell PA rates two orders of magnitude higher in *Cyclotella* sp. 1 (Chapter 4).

Regarding the study of the S/V threshold, it must be noted that 1.24 corresponds to relatively small cells, where possible size-induced biases in the measurement of 2D image-based SCPA could more significantly distort our perception. For this reason, the study of this threshold should ideally be based on 3D image-based SCPA. Nevertheless, our results are reliable because the clear-cut threshold was found on the basis of percentage of

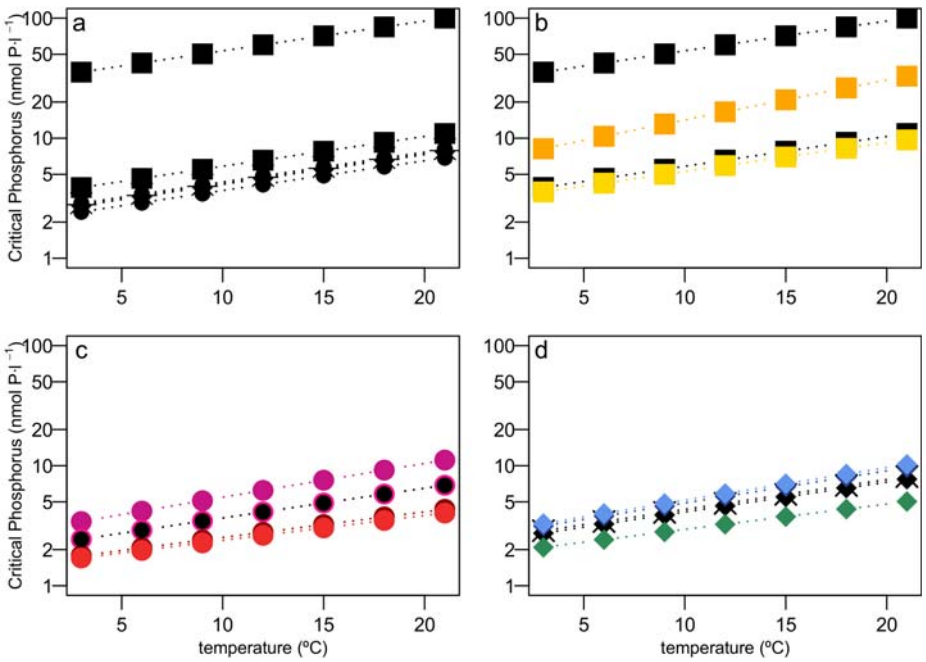

Fig. 4 Critical phosphorus concentrations of ideal shapes with S/V=1.24 (a), and actual phytoplankton species found in Central Pyrenees lakes (b, c and d). Ideal cells with S/V=1.24: sphere (black circle); round dinoflagellate (black rhombus); pointed chryptophyte (black cross); pointed dinoflagellate (black "X"); *Cyclotella*-like (lower black squares); Fragilaria-like (upper black squares). *Discostella* cf. *pseudostelligera* (S/V=1.33; yellow squares); *Cyclotella* sp. 1 (S/V=0.65; orange squares); *Pseudokephyrion* sp. (S/V=1.7; light red circles); 3 µm *Cromulina-Ochromonas* (S/V=1.62; dark red circles); 5 µm *Cromulina-Ochromonas* (S/V=1.24; pink circles); 7 µm *Cromulina-Ochromonas* (S/V=0.96; violet circles); 4 µm *Amphidinium* sp. (S/V=1.65; green rhombuses); 8 µm *Amphidinium* sp. (S/V=1.07; dark blue rhombuses); 8 µm *Gymnodinium* sp. (S/V=1.04; light blue rhombuses).

active cells (chapter 3 Fig. 6 b), and even when rates were considered (chapter 3 Fig. 6 c and d), it should be reminded that size-induced biases were a quantitatively less important source of variability when compared to deconvolution.

4. The trade-off

A novel contribution of the present thesis is the description of a direct trade-off relationship between PA and bacterivory in the phytoplankton of the

summer deep chlorophyll maxima (DCM) of oligotrophic high mountain lakes. Phosphatase activity and bacterivory were scarcely assessed together in the past and consequently we were the first to describe the trade-off relationship between them. We also found it to be a trade-off of direct type because no allometric relationships were found between the selection of the activities (phosphatase or bacetrivory) and cell size, so the trade-off was directly imposed by restrictions in the energetic budget of organisms (optimal allocation principle; Levins, 1968). The discovery of this trade-off opened a series of new questions rather than definitively resolving any previous ecological questions, but our results pointed out some answers (Fig. 5), which are developed below.

- When is this trade-off observable? How general may this trade-off be?

An obvious condition to find this trade-off relationship is the investment of phytoplankton in the two studied activities, which we found to appear and increase, as expected, under conditions of low P availability within an oligotrophic range of lakes. We hypothesise that the fact that PA and bacterivory function as P scavenging activities or as more complex nutrient scavenging activities could influence the presence or not of a trade-off relationship between them. Then, in the case that both activities were intended for the same purpose, let's say the scavenging of P, the individuals and the species would regulate their investment in each activity following the optimum allocation principle until the P demands were met, and this would lead to a trade-off relationship. It is very probable that the main function of PA and bacterivory in the studied conditions (oligotrophy and appropriate light conditions for the photosynthesis) was the scavenging of P, but it has been reported that bacterivory and PA may be a source of organic matter and energy for mixotrophic phytoplankton under poor light regimes (Thingstad *et al.*, 1996; Jones, 2000) and in extreme eutrophic or acidic conditions (Cao *et al.*, 2005, 2009, 2010; Tittel *et al.*, 2005; Spijkerman *et al.*, 2007), respectively. Therefore, it would be interesting to check whether the PA-bacterivory trade-off is also observable in the phytoplankton of hypereutrophic and/or poor-light-regime ecosystems. Assuming that the trade-off relationship was actually affected by changing the function of these activities from P scavenging to others, we would hypothesise different

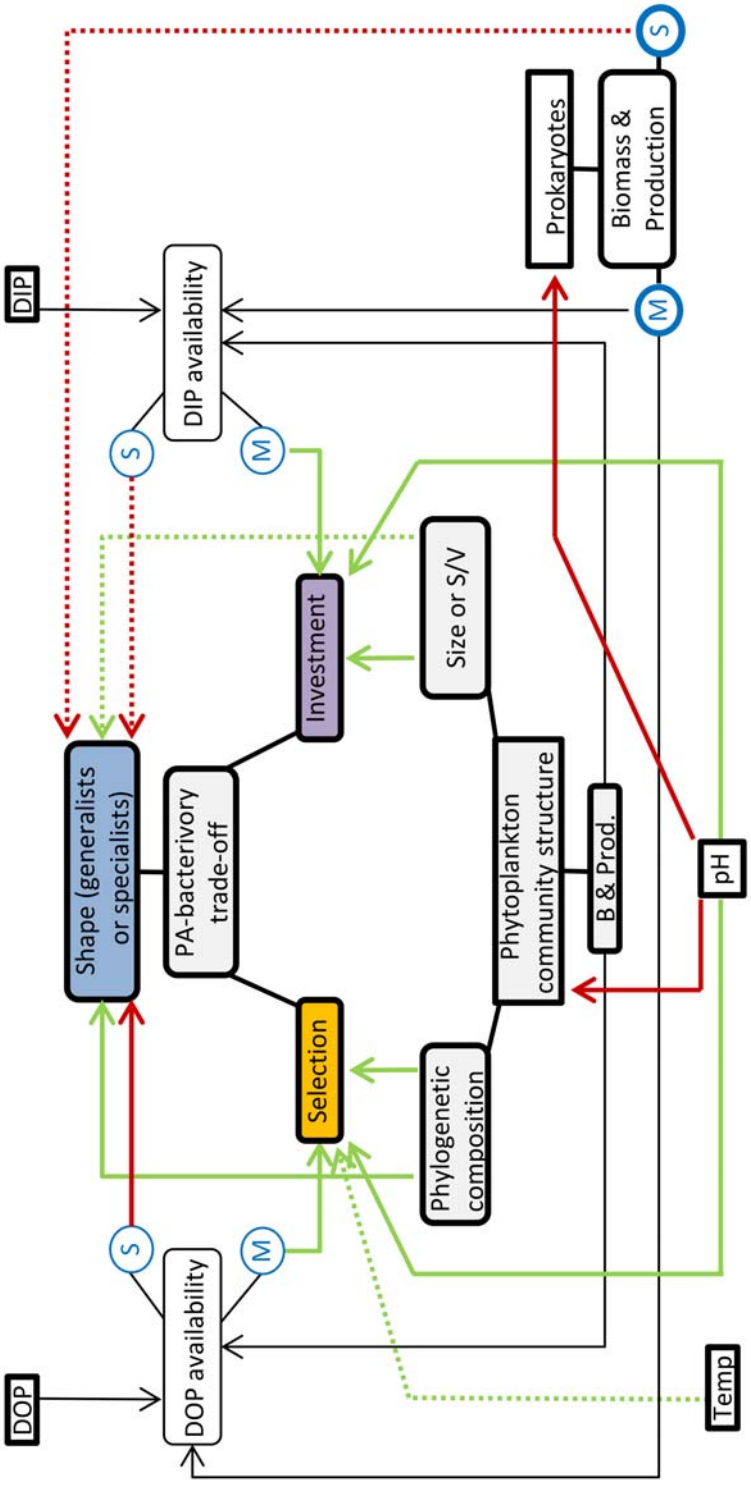
DIP
DIP availability
S
M
Prokaryotes
Biomass & Production
S
M
Investment
Size or S/V
Shape (generalists or specialists)
PA-bacterivory trade-off
Phytoplankton community structure
B & Prod.
pH
Selection
Phylogenetic composition
S
M
DOP
DOP availability
Temp

Fig. 5 Schema of the factors controlling the trade-off between phosphatase activity and bacterivory in phytoplankton. Black arrows show dissolved phosphorus availability, green arrows show processes that have been studied in the present thesis, and red arrows show hypothetic processes. Solid and dotted lines represent probable or more dubious relationships, respectively. Letter *M* in a circle means magnitude, and *S* means temporal stability.

patterns in the loss of trade-off relationship when increasing trophic status or decreasing light regime: According to our findings, PA had a more robust function of P scavenging because it could achieve higher mobilisations of P and correlated to tracers of substrate availability, whereas bacterivory represented a more constant and modest mobilisation of P even when more prey were available (in shallow mountain lakes).

- Is there a relationship between the PA-bacterivory trade-off and the structure of phytoplankton community?

Definitely yes, there is. We identified that two characteristics of the trade-off were related to, or determined by, two characteristics of the phytoplankton community that performed the activities (Fig. 5). On the one hand, investment ceiling in phosphatase and bacterivory decreased linearly above the threshold of 1.24 S/V, connecting the phytoplankton community size structure to the maximum investement in PA and bacterivory. On the other hand, some classes only presented PA (Bacillarophyceae and Chlorophyceae), almost only bacterivory (Chryptophyceae) or a combination of both (Dinophyceae and Chrysophyceae), which also connects the selection between the two activities in the trade-off to the species composition of the phytoplankton community.

- Which factors drive a specialist or a generalist trade-off curve?

A possible hypothesis to test in the future could be that small cells (with high S/V) had more specialist strategies in the choice between PA and bacterivory, i.e. a more convex shape in their specific trade-off curves. The explanation would be that no physical space would be available for both activities in small mixotrophic phytoplankton. In our experience, the hypothesis that the selection of PA or bacterivory was driven by physical space availability was

rejected for general phytoplankton, but there is a possibility that the physical space availability in the cells influenced the trade-off shape because we found clear concave (specialist) trade-off curves in some small species (*Pseudokephyrion* sp. and 5 µm *Chromulina-Ochromonas* sp.).

Alternatively, the trend towards a specialist or a generalist trade-off between PA and bacterivory could also depend on the phytoplankton community phylogenetic composition. We perceived a timid trend at the Class taxonomic level, where Dinophyceae seemed to be more specialists and Chrysophyceae leaned towards generalism, in percentage of active cells. In fact, the two hypothesis, species composition or functional traits, are two possible ways to explain the choice between specialist or generalist behaviours. The modest amount of species and functional traits diversity in our study make it difficult to discern which of both approaches could be more appropriate.

A couple of questions arise from our observations. The fact that a small chrysophyte (the 3 µm *Chromulina-Ochromonas* sp.) did not have a clear specialist trade-off was due to a combination of functional traits (too small compared to 5 µm *Chromulina-Ochromonas* sp. and/or lack of lorica in comparison to *Pseudokephyrion* sp.) or was due to its phylogenetic identity (Chapter 3 Fig. 5 d)? And is the discordance between generalist tendence in the whole set of Chrysophyceae and strong specialist behaviour in some small Chrysophyceae (Chapter 3 Fig. 4 and Fig. 5 d) due to differences when comparing rates and percentage of active cells or are the patterns observed at the Class level a nonsense mixing of different specific behaviours?

Finally, the shape of the trade-off curves may be driven by the principle of opportunity costs (Stephens & Krebs, 1987), enhancing generalist behaviours under conditions of scarce and/or irregular P availability in time, where P availability includes DIP, DOP and bacterial P and the time scale is that of phytoplankton replication. For example, minimum theoretical generation times of the phytoplankton species from high mountain lakes represented in Fig. 4 ranged from 0.47 to 4.39 days, assuming maximum exponential growth). Therefore, generalist trade-offs would be expected under P supply irregularities operating at the time scale of days.

- Is the trade-off restricted to PA and bacterivory or would it be generally observed between phagotrophy and other extracellular

enzymatic activities? In other words, is the trade-off restricted to the P scavenging activities or is it a trade-off between intracellular and extracellular *digestion* of organic matter?

- What is the role of environmental conditions in controlling the trade-off properties?

Our clearest observation was that extreme pH significantly affected the trade-off. Extreme acidic lakes had very high investment in P scavenging activities and also strongly selected PA rather than bacterivory. At the basic extreme of pH, some species also showed very high phosphatase activities (e.g. *Cyclotella* sp. 1 in Filià). Therefore, pH seems to be a crucial factor in the extreme values. For this reason, we think that the dynamics of the trade-off may be altered in abrupt pH increases, for example those caused by algae bloom (Spilling, 2007) whereas we have no evidence to think that the relatively modest acidification of aquatic ecosystems due to increasing atmospheric CO_2 levels (Caldeira & Wickett, 2003; Orr *et al.*, 2005) would yield a clear effect on the P scavenging activities of phytoplankton.

Temperature positively correlated to the selection of PA in the high mountain lakes, but lakes with higher temperatures had also DOC concentrations. We argued that lake type (including temperature and all the other conditions) rather than temperature alone was determining the selection between PA and bacterivory. Nevertheless, it is thinkable that the trade-off selection index varied following the differences in temperature dependence between bacterivory and PA. Previous studies on the dependence of bacterivory and PA on temperature are indicative of how important may temperature be to the trade-off (Jansson *et al.*, 1988; Vaqué *et al.*, 1994; Rose *et al.*, 2009), but further systematic studies would be desirable because slightly discording values, response variables and different temperature ranges assessed in the available literature make it difficult to compare results.

Finally, UV radiation (UVR) is expected to influence the trade-off in many ways. UVR is known to photo-inhibit phytoplankton and prokaryote production, decreasing the photosynthetic P demand, decreasing the prokaryote availability for bacterivory, and modulate bacterivory in mixotrophs (Carrillo *et al.*, 2002; Pérez & Sommaruga, 2007; Navarro *et al.*, 2011). It is also known to photo-hydrolyse P from DOP, and to inhibit or

enhance extracellular phosphatases depending on the presence of dissolved organic matter (Francko & Heath, 1982; Boavida & Wetzel, 1998; Espeland & Wetzel, 2001; Tank *et al.*, 2005). Overall, the ultimate effect of UVR on the trade-off may result from the concrete magnitudes of the positive and negative feedbacks that are involved. Nevertheless, since UVR is not continuous in time (it follows day cycles), it is probable that high UVR destabilised the DIP, DOP and bacteria budgets, favouring a more generalist trade-off.

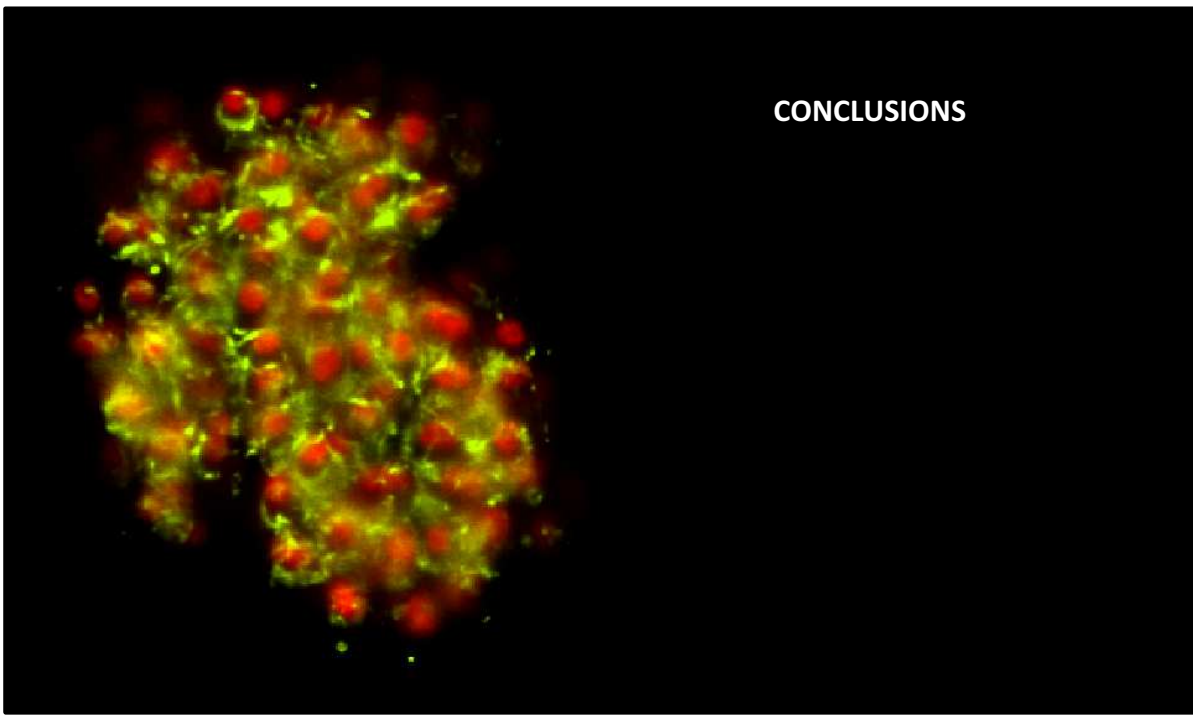
CONCLUSIONS

1. **Unfixed and liquid incubations are devised in the ELF technique protocols**. Amongst the tested protocols, the best trade-offs between signal maximisation and the extracellular location of the signal were the protocols that did not use fixative or that used the LFT fixative after the incubation of the liquid water sample.
2. We demonstrated that the reaction of the ELFP substrate with **intracellular phosphatases** was systematic, including nonmixotrophic species for the first time, which could point out **a source of bias in ectoenzymatic activities measurements** based either on the ELF or classical bulk methods.
3. **Linearity between methods.** We compared, for the first time in the literature, 2D and 3D (raw and deconvolved) fluorescence intensity quantifications, and we found that there was basically a linear relationship between different approaches, excluding only the very dimmest fluorescence magnitudes.
4. **Deconvolved 3D avoids bias associated to out-of-focus light in 2D measurements.** We demonstrated that single-cell ELF quantifications based on 2D image analysis were biased by up to one order of magnitude relative to deconvolved 3D. This was basically attributed to out-of-focus light, and to a lesser extent to object size. Nevertheless, if sufficient cells were measured (25 to 40 cells), biases in individual 2D cell measurements were partially compensated, providing useful and comparable results to deconvolved 3D.
5. **Cell size modulates 2D measurement bias.** Caution should be used when comparing the single-cell enzyme activities of different sized bacterio- and/or phytoplankton populations measured on 2D images because fluorescence intensities may be cell-size-biased in up to 10-20% between common phytoplankton size ranges, and up to 30% when comparing phyto- and bacterioplankton.
6. **Deconvolved 3D is the best estimate.** A novel method based on deconvolved 3D images (wide field restoration microscopy; WFR) was strongly recommended when attempting to improve: the comparison of enzyme activities between different size cells, the discrimination of similar single-cell enzyme activities, the measurement of low fluorescence intensities, the quantification of less numerous species, and the combination of the FLEA technique with other single-cell methods.

7. A direct **trade-off** relationship **between PA and bacterivory** was found in oligotrophic high mountain lakes phytoplankton, both at bulk and species level.
8. In general, **PA and bacterivory** were widely used by the phytoplankton of high mountain lakes, **increased along a gradient of nutrient demand**, **and the selection of one or another depended on the resources availability**, which was determined by the lake type. Phosphatase activity (PA) was preferred in acidic lakes, whereas bacterivory was favoured in deep stratified lakes, with shallow lakes in an intermediate position
9. Communities with relatively high levels of investment in P scavenging activities **mobilized up to 3.6 or 26.1 times more P by PA than by bacterivory**.
10. The use of PA or bacterivory varied between phytoplankton phylogenetic Classes: **Chlorophyceae and Bacillarophyceae only presented PA, Chryptophyceae mostly used bacterivory, and Dinophyceae and Chrysophyceae combined both**.
11. The single-cell analysis of natural phytoplankton populations described diverse relationships between nutrient scavenging activities down to the species (or genus) level.

    11.1. On the one hand, **concave trade-off curves were observed in *Pseudokephyrion* sp. and 5 µm *Chromulina-Ochromonas* populations (with higher specific activities in the loricated *Pseudokephyrion* sp.)**. This indicates that different populations within a same species (or belonging to closely related species) may also invest in either one or another activity.

    11.2. On the other hand, **the trophic niches of three phylogenetically close dinoflagellate species could be distinguished** in terms of specific bacterivory rate.
12. **No allometric relationship was found between surface-to-volume ratio (S/V) and the selection of PA or bacterivory**, which contradicts our initial hypothesis that allocation in PA or bacterivory would be driven by physical space availability on the surface and in the volume of the cell. Therefore, the trade-off between PA and bacterivory is a direct trade-off.
13. We detected **a phytoplankton cell S/V threshold (1.24 μm^{-1})** above which rates and percentage of cells active in PA and bacterivory clearly decreased indicating lower demand on nutrient scavenging

activities in small cells (i.e. approximately in cells below 5 µm of diameter).

14. In spite of the scarce use of phosphatase and bacterivory by these **small-celled populations**, relatively **important rates per biovolume unit** could be reached.
15. A quantitative study of PA in ***Cyclotella* spp.** from high mountain lakes described these diatoms as the main **phosphatase strategist** in most of the phytoplankton communities where it was present. The adaptive advantage that this functional trait confers in P limited environments could explain the ~150-years-old expansion of *Cyclotella* in nutrient-poor, non-acidified, and non-shallow lakes from the Northern Hemisphere, as a response to a combination of climate warming and P limiting conditions partially enhanced by atmospheric nitrogen deposition.

REPORT OF THE THESIS SUPERVISOR

Dra. Marisol Felip i Benach from the Departament d'Ecologia, Universitat de Barcelona, as the supervisor of the PhD thesis entitled **"On the track of cellular ecology. Methodological improvements and contributions of single-cell phosphatase activity on the ecology of phytoplankton in Pyrenean lakes"** submitted by the PhD candidate Daniel Díaz de Quijano i Barbero, informs about the impact factor of the two journals where part of the thesis has been published and of the two potential journals where the remaining manuscripts will be submitted, as well as about the involvement of the PhD candidate in each paper.

Paper 1: "**A comparative study of fluorescence-labelled enzyme activity methods for assaying phosphatase activity in phytoplankton. A possible bias in the enzymatic pathway estimations**" by Daniel Díaz-de-Quijano and Marisol Felip published in *Journal of Microbiological Methods* in year 2011. This journal had an impact factor of 2.161 in 2012 (2012 JCR Science Edition) and of 2.086 in 2011, appears in the third quartile of its corresponding large categories (67 of 116 in MICROBIOLOGY, 43 of 75 in BIOCHEMICAL RESEARCH METHODS), and has one of the highest impact factor in the field of ecological methods. Each paper undergoes an exhaustive peer-reviewing process, which warrants the high quality standards of the manuscripts published in this journal.

In this study we compared published and new protocols for the phosphatase activity assay at the single-cell level in natural phytoplankton communities. The methods were compared using the criterion that extracellular FLEA (fluorescence-labelled enzyme activity) labelling should be maximized and intracellular labelling eliminated. The most interesting aspect of this study is that it considers the presence of intracellular labelling, which none of the tested protocols completely eliminated. This is the first study suggesting that quantification of ectoenzymatic activities might have been biased by intracellular activity.

This publication was the perfect starting point for the PhD candidate, who became the FLEA specialist in our group. All the work was fully under his responsibility. He is the first and corresponding author of this paper and the data presented is not included in any other doctoral thesis.

Paper 2: **“3D restoration microscopy improves quantification of enzyme-labelled fluorescence (ELF)-based single-cell phosphatase activity in plankton"** by Daniel Díaz-de-Quijano, Pilar Palacios, Karel Horňák and Marisol Felip published in *Cytometry Part A* in year 2014 (DOI: 10.1002/cyto.a.22486). This journal has an impact factor of 3.711 (2012 JCR Science Edition) and appears in the first quartile of its corresponding category (17 of 75 in BIOCHEMICAL RESEARCH METHODS). Each paper undergoes an exhaustive peer-reviewing process, which warrants the high quality standards of the manuscripts published in this journal.

This study was initiated during a predoctoral stay of the PhD candidate at the Institute of Hydrobiology of the Academy of Sciences of the Czech Republic under the supervision of Dr. Jiři Nedoma, and its main objective was the improvement of phytoplankton fluorescence quantification. Fluorescence intensity is quantified in 2D and 3D fluorescence microscopy for multiple purposes. Albeit 3D microscopy has been considered superior to 2D, there was not any published comparison between methods. In this study we demonstrate that deconvolved 3D (or wide-field restoration) fluorescence microscopy is the most advisable technique for many applications. Nevertheless, we observed that a sufficiently big sample size compensates for individual biases and makes 2D and deconvolved 3D measurements comparable. Finally, we compared fluorescence quantifications between differently sized bacterio- and/or phytoplankton cells under 2D microscopy. Our improvements in cell enzyme activity measurements will provide a more precise picture of individual species’ behavior in nature, which is essential to properly understand their functional role.

This work was developed in collaboration with some specialists in cytometry (Karel Horňák) and in deconvolution (Pilar Palacios). The PhD candidate did all the microscopy work, the data processing, and wrote the paper. He is the first and corresponding author of this paper and the data presented is not included in any other doctoral thesis.

Paper 3 (manuscript): “**Phytoplankton adaptations to oligotrophy: A Trade-off between two nutrient scavenging activities**” by Daniel Díaz-de-Quijano, Miguel Ballen and Marisol Felip, ready to be submitted to *Freshwater Biology*. This journal has and impact factor of 3.933 (2012 JCR

Science Edition) and appears in the first quartile of its corresponding category (3 of 100 in MARINE AND FRESHWATER BIOLOGY) and has the highest impact factor in the field of Freshwater Biology.

In this study we investigated the relationship between phosphatase and bacterivory activities (considered as tracers of dissolved and particulate organic phosphorus utilization) in phytoplankton communities and species of oligotrophic high mountain lakes. The work is based on detailed measurements of single cell activities, which provide a more precise picture of individual species' behaviour in nature. The approach is very novel and has yielded very interesting results. For instance, a trade-off between phosphatase and bacterivory activities was observed both at bulk community and at inter-specific level; and a cell size threshold (S/V >1.24) on organic P demand was empirically observed.

This paper fits nicely within the scientific topic of the research group. Miguel Ballen worked on bacterivory quantification, whereas the PhD candidate did the phosphatase activity measurements and all the data processing. He participated in drafting/designing the scientific approach and wrote the paper. The PhD candidate is the first and corresponding author of this paper and the data presented is not included in any other doctoral thesis.

Paper 4 (manuscript): "**Is *Cyclotella* spp. a temperature or a nutrient limitation proxy?**" by Daniel Díaz-de-Quijano and Marisol Felip, ready to be submitted as an opinion to *Global Change Biology*. This journal has and impact factor of 6.910 (2012 JCR Science Edition) and appears in the first quartile of its corresponding categories (1 of 40 in BIODIVERSITY CONSERVATION, 9 of 136 in ECOLOGY and 5 of 210 in ENVIRONMENTAL SCIENCES).

This manuscript is a comment of the species shifts interpretation in paleolimnological records. Our detailed study of the phosphatase activity in *Cyclotella* spp. in Pyrenean high mountain lakes, indicates that this can be an important functional trait that sheds some light on the interpretation of the recent paleolimnological records. We suggest that *Cyclotella* spp. responded to climate warming in combination to a phosphorus limitation situation enhanced by atmospheric nitrogen deposition. This work shows the need to

study phytoplankton functional traits and it is a nice example of the skills of the PhD candidate in multidisciplinary research.

This work was fully under the responsibility of the PhD candidate, who devised the scientific idea and elaborated the manuscript. The PhD candidate is the first and corresponding author of this paper and the data presented is not included in any other doctoral thesis.

Barcelona, 23th of May 2014

Marisol Felip i Benach

Departament Ecologia

Universitat Barcelona

BIBLIOGRAPHY

Aaronson S, Patni NJ (1967) The role of surface and extracellular phosphatases in the phosphorus requirement of Ochromonasl. *Limnology and Oceanography*, **21**, 838–845.

Allan C, Burel J-M, Moore J, Blackburn C, Linkert M (2012) OMERO: flexible, model-driven data management for experimental biology. *Nature Methods*, **9**, 245–253.

Allison SD, Treseder KK (2008) Warming and drying suppress microbial activity and carbon cycling in boreal forest soils. *Global Change Biology*, **14**, 2898–2909.

Arnosti C (2011) Microbial Extracellular Enzymes and the Marine Carbon Cycle. *Annual Review of Marine Science (2009)*, **3**, 401–425.

Azam F, Smith DC (1991) Bacterial influence on the variability in the ocean's biogeochemical state: a mechanistic view. In: *Particle analysis in oceanography*, Vol. G27 (ed Demers S), pp. 213–236. Berlin-Heidelberg.

Azam F, Fenchel T, Field JG, Gray JS, Meyer-Reil LA, Thingstad F (1983) The ecological role of water-column microbes in the sea. *Marine Ecology Progress Series*, **10**, 257–263.

De Baar HJW (1994) von Liebig's law of the minimum and plankton ecology (1899–1991). *Progress in Oceanography*, **33**, 347–386.

Baltar F, Arístegui J, Gasol JM, Sintes E, van Aken HM, Herndl GJ (2010) High dissolved extracellular enzymatic activity in the deep central Atlantic Ocean. *Aquatic Microbial Ecology*, **58**, 287–302.

Baltar F, Arístegui J, Gasol JM, Yokokawa T, Herndl GJ (2013) Bacterial versus archaeal origin of extracellular enzymatic activity in the Northeast Atlantic deep waters. *Microbial ecology*, **65**, 277–88.

Beardall J, Young E, Roberts S (2001) Approaches for determining phytoplankton nutrient limitation. *Aquatic Sciences - Research Across Boundaries*, **63**, 44–69.

Bentzen E, Taylor WD (1991) Estimating organic-P utilization by fresh-water plankton using (P-32)ATP. *Journal of Plankton Research*, **13**, 1223–1238.

Bentzen E, Taylor WD, Millard ES, March I (1992) The importance of dissolved organic phosphorus to phosphorus uptake by limnetic plankton. *Limnology and Oceanography*, **37**, 217–231.

Bergström A-K, Jansson M (2006) Atmospheric nitrogen deposition has caused nitrogen enrichment and eutrophication of lakes in the northern hemisphere. *Global Change Biology*, **12**, 635–643.

Bessey OA, Lowry OH, Brock J (1946) A method for the rapid determination of alkaline phosphatase with five cubic millimeters of serum. *J. Biol. Chem.*, **164**, 321–329.

Bidle KD, Falkowski PG (2004) Cell death in planktonic, photosynthetic microorganisms. *Nat Rev Micro*, **2**, 643–655.

Bloom AJ, Chapin FS, Mooney HA (1985) Resource limitation in plants—an economic analogy. *Annual Review of Ecology and Systematics*, **16**, 363–392.

Boavida MJ, Heath RT (1988) Is alkaline phosphatase always important in phosphate regeneration? *Archiv für Hydrobiologie*, **111**, 507–518.

Boavida M-JJ, Wetzel RG (1998) Inhibition of phosphatase activity by dissolved humic substances and hydrolytic reactivation by natural ultraviolet light. *Freshwater Biology*, **40**, 285–293.

Boström B, Persson G, Broberg B (1988) Bioavailability of different phosphorus forms in freshwater systems. *Hydrobiologia*, **170**, 133–155.

Brandt K (1899) Ueber den Stoffwechsel im Meere (Rektoratsrede). *WissenschaftlicheMeeresuntersuchungen, Abteilung Kiel Neue Folge*, **4**, 215–230.

Caldeira K, Wickett ME (2003) Anthropogenic carbon and ocean pH. *Nature*, **425**, 2003.

Callieri C, Corno G, Bertoni R (2006) Bacterial grazing by mixotrophic flagellates and Daphnia longispina: a comparison in a fishless alpine lake. *Aquatic Microbial Ecology*, **42**, 127–137.

Camarero L, Catalan J (2012) Atmospheric phosphorus deposition may cause lakes to revert from phosphorus limitation back to nitrogen limitation. *Nature communications*, **3**.

Cao X, Štrojsová A, Znachor P, Zapomělová E, Liu G, Vrba J, Zhou Y (2005) Detection of extracellular phosphatases in natural spring phytoplankton of a shallow eutrophic lake (Donghu, China). *European Journal of Phycology*, **40**, 251–258.

Cao X, Song C, Zhou Y, Štrojsová A, Znachor P, Zapomělová E, Vrba J (2009) Extracellular phosphatases produced by phytoplankton and other sources in shallow eutrophic lakes (Wuhan, China): taxon-specific versus bulk activity. *Limnology*, **10**, 95–104.

Cao X, Song C, Zhou Y (2010) Limitations of using extracellular alkaline phosphatase activities as a general indicator for describing P deficiency of phytoplankton in Chinese shallow lakes. *Journal of Applied Phycology*, **22**, 33–41.

Carlsson P, Caron DA (2001) Seasonal variation of phosphorus limitation of bacterial growth in a small lake. *Limnology and Oceanography*, **46**, 108–120.

Carrillo P, Medina-Sanchez JM, Villar-Argaiz M (2002) The interaction of phytoplankton and bacteria in a high mountain lake: Importance of the spectral composition of solar radiation. *Limnology and Oceanography*, **47**, 1294–1306.

Catalan J (1987) *Limnologia de l'estany Redó (Pirineu Central). El sistema pelàgic d'un llac profund d'alta muntanya*. Universitat de Barcelona.

Catalan J (1999) Small-scale hydrodynamics as a framework for plankton evolution. *Japanese Journal of Limnology*, **60**, 469–494.

Catalan J (2000) Primary production in a high mountain lake: an overview from minutes to kiloyears. *Atti Associazione Italiana Oceanologia Limnologia*, **13**, 1–21.

Cembella AD, Antia NJ, Harrison PJ (1984a) The utilization of organic and inorganic phosphorus compounds as nutrients by eukaryotic microalgae- A multidisciplinary perspective: Part 1. *Crit.Rev.Microbiol.*, **10**, 317–391.

Cembella AD, Antia NJ, Harrison PJ (1984b) The utilization of organic and inorganic phosphorus compounds as nutrients by eukaryotic microalgae- A multidisciplinary perspective: Part 2. *Crit.Rev.Microbiol.*, **11**, 13–81.

Chang CCY, Kuwabara JS, Pasilis SP (1992) Phosphate and Iron limitation of phytopankton biomass in lake Tahoe. *Canadian Journal of Fisheries and Aquatic Sciences*, **49**, 1206–1215.

Chernin L, Chet I (2002) Microbial enzymes in the biocontrol of plant pathogens and pests. In: *Enzymes in the environment* (eds Dick RP, Burns RG), pp. 171–226. Marcel Dekker, New York.

Chisholm SW, Morel FM (eds.) (1991) What controls phytoplankton production in nutrient-rich areas of the open sea? In: *Limnology and Oceanography*, Vol. 36, pp. 1507–1970.

Chróst RJ (1991) Environmental control of the synthesis and activity of aquatic microbial ectoenzymes. In: *Microbial Enzymes in Aquatic Environments* (ed Chróst RJ), pp. 29–59. Springer-Verlag New York Inc., New York.

Chróst RJ, Siuda W (2002) Ecology of microbial enzymes in lake ecosystems. In: *Enzymes in the environment. Activity, ecology and applications* (eds Burns RG, Dick RP), pp. 35–72. Marcel Dekker, Inc, New York.

Chróst RJ, Siuda W, Halemejko G (1984) Longterm studies on alkaline phosphatase activity (APA) in a lake with fish-aquaculture in relation to lake eutrophication and phosphorus cycle. *Archiv f r Hydrobiologie*, **Supp. 70**, 1–32.

Chróst RJ, Siuda W, Albrecht D, Overbeck J (1986) A method for determining enzymatically hydrolyzable phosphate (EHP) in natural waters. *Limnology and Oceanography*, **31**, 662–667.

Clark LL, Ingall ED, Benner R (1998) Marine phosphorus is selectively remineralized. *Nature*, **393**, 426.

Comte J, Jacquet S, Viboud S, Fontvieille D, Millery a, Paolini G, Domaizon I (2006) Microbial community structure and dynamics in the largest natural French lake (Lake Bourget). *Microbial ecology*, **52**, 72–89.

Cotner JB, Wetzel RG (1991) 5'-nucleotidase activity in a eutrophic lake and an oligotrophic lake. *Applied and Environmental Microbiology*, **57**, 1306–1312.

Diaz-de-Quijano D (2006) *Aproximació a les estratègies tròfiques del microplàncton amb dos mètodes d'anàlisi a nivell unicel·lular*. Universitat de Barcelona.

Dignum M, Hoogveld HL, Matthijs HCP, Laanbroek HJ, Pel R (2004a) Detecting the phosphate status of phytoplankton by enzyme-labelled fluorescence and flow cytometry. *FEMS microbiology ecology*, **48**, 29–38.

Dignum M, Hoogveld HL, Floris V, Gons HJ, Matthijs HCP, Pel R (2004b) Flow cytometric detection of phosphatase activity combined with C-13-CO2 tracer-based growth rate assessment in phytoplankton populations from a shallow lake. *Aquatic Microbial Ecology*, **37**, 159–169.

Duhamel S, Gregori G, Van Wambeke F, Nedoma J (2009) Detection of Extracellular Phosphatase Activity at the Single-Cell Level by Enzyme-Labeled Fluorescence and Flow Cytometry: The Importance of Time Kinetics in ELFA Labeling. *Cytometry Part A*, **75A**, 163–168.

Dungan RS, Frankenberger WT (2002) Enzyme-mediated transformations of heavy metals/metalloids: applications in bioremediation. In: *Enzymes in the environment* (eds Dick RP, Burns RG), pp. 267–284. Marcel Dekker, New York.

Dyhrman ST (2008) Molecular approaches to diagnosing nutritional physiology in harmful algae: Implications for studying the effects of eutrophication. *HABs and Eutrophication*, **8**, 167–174.

Dyhrman ST, Palenik B (1999) Phosphate stress in cultures and field populations of the dinoflagellate Prorocentrum minimum detected by a single-cell alkaline phosphatase assay. *Applied and Environmental Microbiology*, **65**, 3205–3212.

Elser JJ, Kimmel BL (1986) Alteration of phytoplankton phosphorus status during enrichment experiments: implications for interpreting nutrient enrichment bioassay results. *Hydrobiologia*, **133**, 217–222.

Elser JJ, Marzolf ER, Goldman CR (1990) Phosphorus and nitrogen limitation of phytoplankton growth in the freshwaters of North America: A review and critique of experimental enrichments. *Canadian Journal of Fisheries and Aquatic Sciences*, **47**, 1468–1477.

Elser JJ, Bracken MES, Cleland EE et al. (2007) Global analysis of nitrogen and phosphorus limitation of primary producers in freshwater, marine and terrestrial ecosystems. *Ecology letters*, **10**, 1135–42.

Elser JJ, Andersen T, Baron JS et al. (2009) Shifts in lake N:P stoichiometry and nutrient limitation driven by atmospheric nitrogen deposition. *Science*, **326**, 835–837.

Espeland EMM, Wetzel RGG (2001) Complexation, stabilization, and UV photolysis of extracellular and surface-bound glucosidase and alkaline phosphatase: Implications for biofilm microbiota. *Microbial ecology*, **42**, 572–585.

Evans JC, Prepas EE (1997) Relative importance of iron and molybdenum in restricting phytoplankton biomass in high phosphorus saline lakes. *Limnology and Oceanography*, **42**, 461–472.

Falkowski PG, Greene RM, Geider RJ (1992) Physiological limitations on phytoplankton productivity in the ocean. **5**, 84–91.

Falkowski PG, Katz ME, Knoll AH, Quigg A, Raven J a, Schofield O, Taylor FJR (2004) The evolution of modern eukaryotic phytoplankton. *Science*, **305**, 354–60.

Fermi C (1906) The presence of enzymes in soil, water and dust. *Zentralblatt für Bakteriologie und Parasitenkunde*, **26**, 330–334.

Fitzgerald GP, Nelson TC (1966) extractive and enzymatic analyses for limiting or surplus phosphorus in algae. *Journal of Phycology*, **2**, 32–37.

Francko DA, Heath RT (1979) Functionally distinct classes of complex phosphorus compounds in lake water. *Limnology and Oceanography*, **24**, 463–473.

Francko DA, Heath RT (1982) UV-sensitive complex phosphorus : Association with dissolved humic material and iron in a bog lake. *Limnology and Oceanography*, **27**, 564–569.

Freeman C, Fenner N, Shirsat AH (2012) Peatland geoengineering: an alternative approach to terrestrial carbon sequestration. *Philosophical transactions. Series A, Mathematical, physical, and engineering sciences*, **370**, 4404–21.

Frossard A, Mutz M, Gessner MO (2011) Microbial enzyme activities in an early successional stream network. In: *The fourth international conference. Enzymes in the environment: Activity, ecology and applications* (eds Dick RP, Sandeno J), p. 7. Bad Nauheim, Germany.

Frossard A, Gerull L, Mutz M, Gessner MO (2013a) Litter supply as a driver of microbial activity and community structure on decomposing leaves: a test in experimental streams. *Applied and environmental microbiology*, **79**, 4965–73.

Frossard A, Gerull L, Mutz M, Gessner MO (2013b) Shifts in microbial community structure and function in stream sediments during experimentally simulated riparian succession. *FEMS microbiology ecology*, **84**, 398–410.

Fuhs GW, Demmerle SD, Canelli E, Chen M (1972) Characterization of phosphorus limited plankton algae (with reflections on the limiting nutrient concept). In: *Nutrients and eutrophication: the limiting nutrient controversy* (ed Likens GE), pp. 113–133. American Society of Limnology and Oceanography.

García-Ruiz R, Hernández I, Lucena J, Niell FX (2000) Significance of phosphomonoesterase activity in the regeneration of phosphorus in a meso-eutrophic, P-limited reservoir. *Soil Biology and Biochemistry*, **32**, 1953–1964.

Gebbing J (1910) Über den Gehalt des Meeres an Stickstoffnährsalzen. Untersuchungsergebnisse der von der Deutschen Südpolar-Expedition (1901 - 1903) gesammelten Meerwasserproben. *Internationale Revue der gesamten Hydrobiologie*, **3**, 50–66.

Gianfreda L, Bollag J-M (2002) Isolated enzymes for the transformation and detoxification of organic pollutants. In: *Enzymes in the environment* (eds Dick RP, Burns RG), pp. 491–538. Marcel Dekker, New York.

Gilbert PA, De Jong AL (1977) The Use of Phosphate in Detergents and Possible Replacements for Phosphate. In: *Ciba Foundation Symposium 57 - Phosphorus in the Enviroment: Its Chemistry and Biochemistry*, Vol. 57, pp. 253–268. John Wiley & Sons, Ltd.

Gleeson SK, Tilman D (1992) Plant allocation and the multiple limitation hypothesis. *American Naturalist*, **139**, 1322–1343.

Goldman CR (1960) Molybdenum as a factor limiting primary productivity in Castle Lake, California. *Science*, **132**, 1016–1017.

Goldman CR (1972) The role of minor nutrients in limiting the productivity of aquatic ecosystems. In: *Nutrients and eutrophication: the limiting nutrient controversy*, pp. 21–33. ASLO, Lawrence.

González-Gil S, Keafer BA, Jovine RVM, Aguilera A, Lu S, Anderson DM (1998) Detection and quantification of alkaline phosphatase in single cells of phosphorus-starved marine phytoplankton. *Marine Ecology Progress Series*, **164**, 21–35.

Gran HH (1931) On the conditions for the production of plankton in the sea. *Rapports et Proces verbaux des Réunions, Conseil International pour l 'exploration de la Mer*, **75**, 37–46.

Graziano LM, La Roche J, Geiders RJ (1995) Physiological responses to phosphorus limitation in batch and steady-state cultures of Dunaliella tertiolecta (Chlorophyta): a unique stress protein as an indicator of phosphate deficiency. *Journal of Phycology*, **32**, 825–838.

Guildford SJ, Hecky RE (2000) Total nitrogen, total phosphorus, and nutrient limitation in lakes and oceans: Is there a common relationship? *Limnology and Oceanography*, **45**, 1213–1223.

Harvey HW (1925) Oxidation in sea water. *Journal of Marine Biology Association*, **13**, 953–969.

Hassett RP, Cardinale B, Stabler LB, Elser JJ (1997) Ecological stoichiometry of N and P in pelagic ecosystems: Comparison of lakes and oceans with emphasis on the zooplankton-phytoplankton interaction. *Limnology and Oceanography*, **42**, 648–662.

Haupert CL (2000) *Nutrient limitation dynamics of a coastal Cape Cod pond: seasonal trends in alkaline phosphatase activity*. Massachussets institute for technology / WHOI.

Healey FP, Hendzel LL (1979) Fluorimetric measurement of alkaline phosphatase activity in algae. *Freshwater Biology*, **9**, 429–439.

Heath RT (1986) Dissolved organic phosphorus compounds: do they ssatisfy planktonic phosphate demand in summer? *Canadian Journal of Fisheries and Aquatic Sciences*, **43**, 343–350.

Hecky RE, Kilham P (1988) Nutrient limitation of phytoplankton in freshwater and marine environments : A review of recent evidence on the effects of enrichment. **33**, 796–822.

Herbes SE, Allen HE, Mancy, Khalil H (1975) Enzymatic Characterization of Soluble Organic Phosphorus in Lake Water. *Science*, **187**, 432–434.

Hernández I, Hwang SJ, Heath RT (1996) Measurement of phosphomonoesterase activity with a radiolabelled glucose-6-phosphate. Role in the phosphorus requirement of phytoplankton and bacterioplankton in a temperate mesotrophic lake. *Archiv für Hydrobiologie*, **137**, 265–280.

Hill HD, Summer GK, Waters MD (1968) An automated fluorometric assay for alkaline phosphatase using 3-o-methylfluorescein phosphatte. *Analytical Biochemistry1*, **24**, 9–17.

Hoppe HG (2003) Phosphatase activity in the sea. *Hydrobiologia*, **493**, 187–200.

Hoppe AD, Swanson J a., Shorte SL (2006) Three-dimensional FRET microscopy (eds Periasamy A, So PTC). *Proceedings of SPIE--the international society for optical engineering*, **6089**, 1–9.

Huang Z, Terpetschnig E, You W, Haugland RP (1992) 2-(2'-Phosphoryloxyphenyl)-4(3H)-quinazolinone derivatives as fluorogenic precipitating substrates of phosphatases. *Analytical Biochemistry*, **207**, 32–39.

Huang Z, You W, Haugland RP, Paragas VB, Olson NA (1993) A novel fluorogenic substrate for detecting alkaline phosphatase activity in situ. *Journal of Histochemistry and Cytochemistry*, **41**, 313–317.

Ivancić I, Fuks D, Radić T, Lyons DM, Silović T, Kraus R, Precali R (2010) Phytoplankton and bacterial alkaline phosphatase activity in the northern Adriatic Sea. *Marine environmental research*, **69**, 85–94.

Jansson M, Olsson H, Pettersson K (1988) Phosphatases; origin, characteristics and function in lakes. *Hydrobiologia*, **170**, 157–175.

Jones RI (2000) Mixotrophy in planktonic protists: an overview. *Freshwater Biology*, **45**, 219–226.

Joseph EM, Morel FMM, Price NM (1995) Effects of aluminum and fluoride on phosphorus acquisition by Chlamydomonas reinhardtii. *Canadian journal of fisheries and aquatic sciences/Journal canadien des sciences halieutiques et aquatiques. Ottawa ON*, **52**, 353–357.

Jumars PA, Deming JW, Hill PS, Karp-Boss L, Yager PL, Dade WB (1993) Physical constraints on marine osmotrophy in an optimal foraging context. *Marine microbial food webs*, **7**, 121–159.

Karl DM (1999) A Sea of Change: Biogeochemical Variability in the North Pacific Subtropical Gyre. *Ecosystems*, **2**, 181–214.

Kemp PF (1994) A philosophy of methods development: The assimilation of new methods and information into aquatic microbial ecology. *Microbial ecology*, **28**, 159–162.

Kiersztyn B, Siuda W, Chrost RJ (2002) Microbial ectoenzyme activity: Useful parameters for characterizing the trophic conditions of lakes. *Polish Journal of Environmental Studies*, **11**, 367–373.

Killham K, Staddon WJ (2002) Bioindicators and sensors of soil health and the application of geostatistics. In: *Enzymes in the environment* (eds Dick RP, Burns RG), pp. 391–406. Marcel Dekker, New York.

Kjøller AH, Struwe S (2002) Fungal communities, sucession, enzymes, and decomposition. In: *Enzymes in the environment* (eds Dick RP, Burns RG), pp. 267–284. Marcel Dekker, New York.

Kreps E (1934) Organic catalysts or enzymes in sea water. In: *James Johnstone Memorial Volume1*, pp. 193–202. University of Liverpool Press, Liverpool.

Krom MD, Kress N, Brenner S (1991) Phosphorus limitation of primary productivity in the eastern Mediterranean Sea. *Limnology and Oceanography*, **36**, 424–432.

Kuenzler EJ, Perras JP (1965) Phosphatases of marine algae. *Biological Bulletin*, **128**, 271–284.

Lamarque J-F, Dentener F, McConnell J et al. (2013) Multi-model mean nitrogen and sulfur deposition from the Atmospheric Chemistry and Climate Model Intercomparison Project (ACCMIP): evaluation of

historical and projected future changes. *Atmospheric Chemistry and Physics*, **13**, 7997–8018.

Lemke MJ, Churchill PF, Wetzel RG (1995) Effect of substrate and cell-surface hydrophobicity on phosphate utilization in bacteria. *Applied and Environmental Microbiology*, **61**, 913–919.

Levins R (1968) *Evolution in a changing environment*. Princeton University Press, Princeton, NJ.

Von Liebig J (1855) *Die Grundsätze der agricultur-chemie mit Rücksicht auf die in Englend angestellten Untersuchchungen*. Friedrich Vieweg and Sohn, Braunschweig.

Litchman E, Klausmeier CA (2008) Trait-based community ecology of phytoplankton. *Annual Review of Ecology, Evolution, and Systematics*, **39**, 615–639.

Litchman E, Nguyen BL V (2008) Alkaline phosphatase activity as a function of internal phosphorus concentration in freshwater phytoplankton. *Journal of Phycology*, **44**, 1379–1383.

Loladze I, Elser JJ (2011) The origins of the Redfield nitrogen-to-phosphorus ratio are in a homoeostatic protein-to-rRNA ratio. *Ecology letters*, **14**, 244–250.

Lomas MW, Swain A, Shelton R, Ammerman JW (2004) Taxonomic variability of phosphorus stress in Sargasso Sea phytoplankton. *Limnology and Oceanography*, **49**, 2303–2310.

Lund JWG, Mackereth FJH, Mortimer CH (1963) Changes in depth and time of certain chemical and physical conditions and of the standing crop of Asterionella formosa HASS. in the north basin of Windermere in 1947. *Phil. Trans. Roy. Soc. Lond. B Biological Sciences*, **246**, 255–290.

Maas E, Law C, Hall J et al. (2013) Effect of ocean acidification on bacterial abundance, activity and diversity in the Ross Sea, Antarctica. *Aquatic Microbial Ecology*, **70**, 1–15.

Margalef R (1951) Rôle des entomostracés dans la régéneration des phosphates. *Verhundlungen der Internationalen Vereinigung von Limnologen*, **11**, 246–247.

Margalef R (1983) *Limnología*. Ediciones Omega S.A., Barcelona.

Margalef R (1997) *Our biosphere*, Excellence edn. Ecology Institute, Oldendorf, Luhe, Germany.

Marxsen J, Schmidt HH (1993) Extracellular phosphatase activity in sediments of the Breitenbach, a Central European mountain stream. *Hydrobiologia*, **253**, 207–216.

Mateo P, Berrendero E, Perona E, Loza V, Whitton B a. (2010) Phosphatase activities of cyanobacteria as indicators of nutrient status in a Pyrenees river. *Hydrobiologia*, **652**, 255–268.

Model MA, Burkhardt JK (2001) A standard for calibration and shading correction of a fluorescence microscope. *Cytometry*, **44**, 309–316.

Van Mooy B a S, Fredricks HF, Pedler BE et al. (2009) Phytoplankton in the ocean use non-phosphorus lipids in response to phosphorus scarcity. *Nature*, **458**, 69–72.

Navarro MB, Balseiro E, Modenutti B, Navarro Esteban Modenutti, Beatriz MB (2011) UV radiation simultaneously affects phototrophy and phagotrophy in nanoflagellate-dominated phytoplankton from an Andean shallow lake. *Photochemical & photobiological sciences : Official journal of the European Photochemistry Association and the European Society for Photobiology*, **10**, 1318–1325.

Nedoma J, Vrba J (2006) Specific activity of cell-surface acid phosphatase in different bacterioplankton morphotypes in an acidified mountain lake. *Environmental microbiology*, **8**, 1271–1279.

Nedoma J, Štrojsová A, Vrba J et al. (2003) Extracellular phosphatase activity of natural plankton studied with ELF97 phosphate: fluorescence quantification and labelling kinetics. *Environmental microbiology*, **5**, 462–472.

Nedoma J, Garcia JC, Comerma M, Simek K, Armengol J (2006) Extracellular phosphatases in a Mediterranean reservoir: seasonal, spatial and kinetic heterogeneity. *Freshwater Biology*, **51**, 1264–1276.

Nedoma J, Van Wambeke F, Štrojsová A, Štrojsová M, Duhamel S (2007) Affinity of extracellular phosphatases for ELF97 phosphate in aquatic environments. *Marine and Freshwater Research*, **58**, 454–460.

Nelson DM, Tréguer P (1991) Role of silicon as a limiting nutrient to Antarctic diatoms: evidence from kinetic studies in the Ross Sea ice-edge zone. *Marine Ecology Progress Series*, **80**, 255–264.

Nicholson D, Dyhrman ST, Chavez F, Paytan A (2006) Alkaline phosphatase activity in the phytoplankton communities of Monterrey Bay and San Francisco Bay. *Limnology and Oceanography*, **51**, 874–883.

Novotná J, Nedbalová L, Kopáček J, Vrba J (2010) Cell-specific extracellular phosphatase activity of Dinoflagellate populations in acidified mountain lakes. *Journal of Phycology*, **46**, 635–644.

Ohle W (1981) Photosynthesis and chemistry of an extremely acidic bathing pond in Germany. *Internationale Vereinigung fuer Theoretische und Angewandte Limnologie Verhandlungen*, **21**, 1173–1177.

Ommen Kloeke F Van, Geesey GG (1999) Localization and Identification of Populations of Phosphatase-Active Bacterial Cells Associated with Activated Sludge Flocs. *Microbial ecology*, **38**, 201–214.

Ommen Kloeke F, Baty III AM, Eastburn CC, Diwu Z, Geesey GG (1999) Novel method for screening bacterial colonies for phosphatase activity. *Journal of microbiological methods*, **38**, 25–31.

Orr JC, Fabry VJ, Aumont O et al. (2005) Anthropogenic ocean acidification over the twenty-first century and its impact on calcifying organisms. *Nature*, **437**, 681–6.

Ou L, Huang B, Hong H, Qi Y, Lu S (2010) Comparative alkaline phosphatase characteristics of the algal bloom dinoflagellates Prorocentrum donghaiense and Alexandrium catenella, and the diatom Skeletonema costatum. *Journal of Phycology*, **46**, 260–265.

Overbeck J (1991) Early studies on ecto- and extracellular enzymes in aquatic environments. In: *Microbial enzymes in aquatic environments* (ed Chróst RJ). Springer-Verlag New York Inc., New York.

Pérez MT, Sommaruga R (2007) Interactive effects of solar radiation and dissolved organic matter on bacterial activity and community structure. *Environmental microbiology*, **9**, 2200–10.

Pernthaler J (2005) Predation on prokaryotes in the water column and its ecological implications. *Nature Reviews Microbiology*, **3**, 537–546.

Perry MJ (1972) Alkaline phosphatase activity in subtropical Central North Pacific waters using a sensitive fluorometric method. *Marine Biology*, **15**, 113–119.

Petersson K (1980) Alkaline phosphatase activity and algal surplus phosphorus as phosphorus-deficiency indicators in Lake Erken. *Archiv für Hydrobiologie*, **89**, 54–87.

Pettersson K, Jansson M (1978) Determination of phosphatase activity in lake water a study of methods. *Verh.Internat.Verein.Limnol.*, **20**, 1226–1230.

Piontek J, Lunau M, Haendel N, Borchard C, Wurst M (2010) Acidification increases microbial polysaccharide degradation in the ocean. *Biogeosciences*, **7**, 1615–1624.

Pomeroy LR (1974) The ocean's food web, a changing paradigm. *Bioscience*, **24**, 499–504.

Provasoli L (1958) Nutrition and ecology of protozoa and algae. *Annual Review of Microbiology*, **12**, 279–308.

Redfield AC (1934) On the proportions of organic derivations in sea water and their relation to the composition of plankton. In: *James Johnstone Memorial Volume* (ed Daniel RJ), pp. 177–192. University Press of Liverpool.

Reichardt W, Overbeck J, Steubing L (1967) Free dissolved enzymes in lake waters. *Nature*, **216**, 1345–1347.

Reinfelder JR, Kraepiel AML, Morel FMM (2000) Unicellular C4 photosynthesis in a marine diatom. *Nature*, **407**, 996–9.

Rengefors K, Pettersson K, Blenckner T, Anderson DM (2001) Species-specific alkaline phosphatase activity in freshwater spring phytoplankton : Application of a novel method. *Journal of Plankton Research*, **23**, 435–443.

Rengefors K, Ruttenberg KC, Haupert CL, Taylor C, Howes BL, Anderson DM (2003) Experimental investigation of taxon-specific response of alkaline phosphatase activity in natural freshwater phytoplankton. *Limnology and Oceanography*, **48**, 1167–1175.

Reynolds CS (1997) *Vegetation processes in the pelagic: a model for ecosystem theory*, Excellence edn. Ecology Institute, Oldendorf/Luhe, Germany.

Reynolds C (2006) *Ecology of phytoplankton*. Cambridge University Press, Cambridge, UK.

Rhee G-Y (1978) Effects of N : P atomic ratios and nitrate limitation on algal growth, cell composition, and nitrate uptake. *Limnology and Oceanography*, **23**, 10–25.

Rivkin RB, Swift E (1979) Diel and vertical patterns of alkaline phosphatase activity in the oceanic dinoflagellate Pyrocystis noctiluca. *Limnology and Oceanography*, **24**, 107–116.

Romaní i Cornet AM (2001) *Biofilms fluvials. Metabolisme heterotròfic i autotròfic en rius mediterranis*. Institut d'Estudis Catalans, Barcelona.

Rose C, Axler RP (1998) Uses of alkaline phosphatase activity in evaluating phytoplankton community phosphorus deficiency. *Hydrobiologia*, **361**, 145–156.

Rose JM, Vora NM, Countway PD, Gast RJ, Caron D a (2009) Effects of temperature on growth rate and gross growth efficiency of an Antarctic bacterivorous protist. *The ISME journal*, **3**, 252–60.

Rottberger J, Gruber a, Boenigk J, Kroth P (2013) Influence of nutrients and light on autotrophic, mixotrophic and heterotrophic freshwater chrysophytes. *Aquatic Microbial Ecology*, **71**, 179–191.

Rühland K, Paterson A, Smol J (2008) Hemispheric-scale patterns of climate-related shifts in planktonic diatoms from North American and European lakes. *Global Change Biology*, **14**, 2740–2754.

Ryther JH, Dunstan WM (1971) Nitrogen, phosphorus, and eutrophication in the coastal marine environment. *Science*, **171**, 1008–1013.

Sañudo-Wilhelmy SA, Kustka AB, Gobler CJ et al. (2001) Phosphorus limitation of nitrogen fixation by Trichodesmium in the central Atlantic Ocean. *Nature*, **411**, 66–69.

Sañudo-Wilhelmy SA, Tovar-Sanchez A, Fu F-X, Capone DG, Carpenter EJ, Hutchins DA (2004) The impact of surface-adsorbed phosphorus on phytoplankton Redfield stoichiometry. *Nature*, **432**, 897–901.

Sarmiento JL, Slater R, Barber R et al. (2004) Response of ocean ecosystems to climate warming. *Global Biogeochemical Cycles*, **18**, 1–23.

Sawatzky CL, Wurtsbaugh WA, Luecke C (2005) The spatial and temporal dynamics of deep chlorophyll layers in high-mountain lakes: effects of nutrients, grazing and herbivore nutrient recycling as growth determinants. *Journal of Plankton Research*, **28**, 65–86.

Scanlan DJ, Wilson WH (1999) Application of molecular techniques to addressing the role of P as a key effector in marine ecosystems. *Hydrobiologia*, **401**, 149–175.

Schade M, Lemmer H (2006) In situ enzyme activities of filamentous scum bacteria in municipal activated sludge wastewater treatment plants. *Acta Hydrochimica et Hydrobiologica*, **34**, 480–490.

Schelske CL (1962) Iron, Organic Matter, and Other Factors Limiting Primary Productivity in a Marl Lake. *Science*, **136**, 45–46.

Schindler DW (1975) Whole-lake eutrophication experiments with phosphorus, nitrogen, and carbon. *Int. Ver. Theor. Angew. Limnol. Verh.*, **19**, 3221–3231.

Schindler DW (1977) Evolution of Phosphorus Limitation in Lakes. *Science*, **195**, 260–262.

Schindler DW, Series N, May N (1974) Eutrophication and Recovery in Experimental Lakes : Implications for Lake Management. *Science*, **184**, 897–899.

Schlesinger WH (2000) *Boigeoquímica. Un análisis del cambio global*. Ariel, Barcelona.

Sherr EB, Sherr BF (1988) Role of microbes in pelagic food webs. *Limnology and Oceanography*, **33**, 1225–1227.

Šimek K, Kojecká P, Nedoma J, Hartman P, Vrba J, Dolan JR (1999) Shifts in bacterial community composition associated with different

microzooplankton size fractions in a eutrophic reservoir. *Limnology and Oceanography*, **44**, 1634–1644.

Sinsabaugh RL, Antibus RK, Linkins AE, McClaugherty CA, Rayburn L, Repert D, Weiland T (1993) Wood Decomposition : Nitrogen and Phosphorus Dynamics in Relation to Extracellular Enzyme Activity. *Ecology*, **74**, 1586–1593.

Sinsabaugh RL, Carreiro MM, Repert DA (2002) Allocation of extracellular enzymatic activity in relation to litter composition, N deposition, and mass loss. *Biogeochemistry*, **60**, 1–24.

Skelton HM, Parrow MW, Burkholder JM (2006) Phosphatase activity in the heterotrophic dinoflagellate Pfiesteria shumwayae. *Harmful Algae*, **5**, 395–406.

Skujiņš JJ (1978) History of abiontic soil enzyme research. In: *Soil enzymes* (ed Burns RG), pp. 1–49. Academic Press, New York.

Speir T (2011) What role can soil enzymes play – insights from the 21st century? In: *The fourth international conference. Enzymes in the environment: Activity, ecology and applications* (eds Dick RP, Sandeno J), p. 4. Bad Nauheim, Germany.

Speir TW, Ross DJ (2002) Hydrolytic enzyme activities to assess soil degradation and recovery. In: *Enzymes in the environment: activity, ecology, and applications*, pp. 407–431. Marcel Dekker Inc, Hoboken.

Spidlen J, Breuer K, Rosenberg C, Kotecha N, Brinkman RR (2012) FlowRepository: a resource of annotated flow cytometry datasets associated with peer-reviewed publications. *Cytometry. Part A : the journal of the International Society for Analytical Cytology*, **81**, 727–31.

Spijkerman E, Bissinger V, Meister A, Gaedke U (2007) Low potassium and inorganic carbon concentrations influence a possible phosphorus limitation in Chlamydomonas acidophila (Chlorophyceae). *European Journal of Phycology*, **42**, 327.

Spilling K (2007) Dense sub-ice bloom of dinoflagellates in the Baltic Sea, potentially limited by high pH. *Journal of Plankton Research*, **29**, 895–901.

Sprengel CP (1828) Von den Substanzen der Ackerkrume und des Untergrundes. *Journal für Tecnische und Ökonomische Chemie*, 2: 423–474; 3: 42–99, 313–352, and 397–421.

Steiner M (1938) Zur Kenntnis der Phosphatkreislaufes in Seen. *Naturwissenschaften*, **26**, 723–724.

Stephens DW, Krebs JR (1987) *Foraging Theory*. Princeton University Press, Princeton, NJ.

Sterner RW (2008) On the Phosphorus Limitation Paradigm for Lakes. *International Review of Hydrobiology*, **93**, 433–445.

Stevens RJ, Parr MP (1977) The significance of alkaline phosphatase activity in Lough Neagh. *Freshwater Biology*, **7**, 351–355.

Stibal M, Anesio AM, Blues CJD, Tranter M (2009) Phosphatase activity and organic phosphorus turnover on a high Arctic glacier. *Biogeosciences*, **6**, 913–922.

Strickland JD, Solórzano L (1966) Determination of monoesterase hydrolysable phosphate and phosphomonoesterase activity in sea water. In: *Some contemporary studies in marine science* (ed Barnes J), pp. 665–674. Allen and Unwin.

Štrojsová M, Vrba J (2005) Direct detection of digestive enzymes in planktonic rotifers using enzyme-labelled fluorescence (ELF). *Marine and Freshwater Research*, **56**, 189–195.

Štrojsová A, Vrba J (2006) Phytoplankton extracellular phosphatases: Investigation using the ELF (Enzyme Labelled Fluorescence) technique. *Polish Journal of Ecology*, **54**, 715–723.

Štrojsová A, Vrba J (2009) Short-term variation in extracellular phosphatase activity: possible limitations for diagnosis of nutrient status in particular algal populations. *Aquatic Ecology*, **43**, 19–25.

Štrojsová A, Vrba J, Nedoma J, Komárková J, Znachor P (2003) Seasonal study of extracellular phosphatase expression in the phytoplankton of a eutrophic reservoir. *European Journal of Phycology*, **38**, 295–306.

Štrojsová A, Nedoma J, Štrojsová M, Cao XY, Vrba J (2008) The role of cell-surface-bound phosphatases in species competition within natural

phytoplankton assemblage: an in situ experiment. *Journal of Limnology*, **67**, 128–138.

Stumm W, Morgan JJ (1970) *Aquatic chemistry*. Wiley.

Swedlow JR, Hu K, Andrews PD, Roos DS, Murray JM (2002) Measuring tubulin content in Toxoplasma gondii: A comparison of laser-scanning confocal and wide-field fluorescence microscopy. *Proceedings of the National Academy of Sciences*, **99**, 2014–2019.

Swedlow J, Allan C, Burel J-M, Linkert M, Loranger B (2009) The Open Microscopy Environment: Informatics and Quantitative Analysis for Biological Microscopy. *Microscopy and microanalysis*, **15**, 1520–1521.

Talling JF, Lemoalle J (1998) *Ecological dynamics of tropical inland waters*. Cambridge University Press.

Tambi H, Flaten G, Egge J, Bødtker G, Jacobsen a, Thingstad T (2009) Relationship between phosphate affinities and cell size and shape in various bacteria and phytoplankton. *Aquatic Microbial Ecology*, **57**, 311–320.

Tanaka T, Henriksen P, Lignell R, Olli K, Seppälä J, Tamminen T, Thingstad TF (2006) Specific Affinity for Phosphate Uptake and Specific Alkaline Phosphatase Activity as Diagnostic Tools for Detecting Phosphorus-limited Phytoplankton and Bacteria. *Estuaries and Coasts*, **29**, 1226–1241.

Tank SE, Xenopoulos MA, Hendzel LL (2005) Effect of ultraviolet radiation on alkaline phosphatase activity and planktonic phosphorus acquisition in Canadian boreal shield lakes. *Limnology and Oceanography*, **50**, 1345–1351.

Teubner K (2003) Phytoplankton, pelagic community and nutrients in a deep oligotrophic alpine lake: ratios as sensitive indicators of the use of P-resources (DRP:DOP:PP and TN:TP:SRSi). *Water research*, **37**, 1583–92.

Teubner K, Crosbie ND, Donabaum K, Kabas W, Kirschner AKT, Pfister G, Salbrechter M (2003) Enhanced phosphorus accumulation efficiency by the pelagic community at reduced phosphorus supply : A lake experiment from bacteria to metazoan zooplankton. *Limnology and Oceanography*, **48**, 1141–1149.

Thingstad TF, Havskum H, Garde K, Riemann B (1996) On the strategy of eating your competitor'': A mathematical analysis of algal mixotrophy. *Ecology*, **77**, 2108–2118.

Thingstad TF, Zweifel UL, Rassoulzadegan F (1998) P limitation of heterotrophic bacteria and phytoplankton in the northwest Mediterranean. *Limnology and Oceanography*, **43**, 88–94.

Tittel J, Bissinger V, Gaedke U, Kamjunke N (2005) Inorganic carbon limitation and mixotrophic growth in Chlamydomonas from an acidic mining lake. *Protist*, **156**, 63–75.

Våge S, Castellani M, Giske J, Thingstad TF (2013) Successful strategies in size structured mixotrophic food webs. *Aquatic Ecology*, **47**, 329–347.

Vaqué D, Gasol JM, Marrasé C (1994) Grazing rates on bacteria: the significance of methodology and ecological factors. *Marine Ecology Progress Series*, **109**, 263–274.

Vidal M, Duarte CM, Agustí S, Gasol JM, Vaqué D (2003) Alkaline phosphatase activities in the central Atlantic Ocean indicate large areas with phosphorus deficiency. *Marine Ecology Progress Series*, **262**, 43–53.

Vrba J, Vyhnálek V, Hejzlar J, Nedoma J (1995) Comparison of phosphorus deficiency indices during a spring phytoplankton bloom in a eutrophic reservoir. *Freshwater Biology1*, **33**, 73–81.

Vrede T, Tranvik LJ (2006) Iron Constraints on Planktonic Primary Production in Oligotrophic Lakes. *Ecosystems*, **9**, 1094–1105.

Van Wambeke F, Nedoma J, Duhamel S, Lebaron P (2008) Alkaline phosphatase activity of marine bacteria studied with ELF 97 substrate: success and limits in the P-limited Mediterranean Sea. *Aquatic Microbial Ecology*, **52**, 245–251.

Weber M (1905) Die protestantische Ethik und der Geist des Kapitalismus. *Archiv für Sozialwissenschaften und Sozialpolitik*, **20-21**, 1–54 and 1–110.

Wetzel RG (1975) *Limnology*. Saunders, Philadelphia.

Wetzel RG (1991) Extracellular Enzymatic Interactions: Storage, Redistribution and Interspecific Communication. In: *Microbial Enzymes in Aquatic Environments* (ed Chróst RJ), pp. 6–28. Springer-Verlag New York Inc., New York.

Wu J, Sunda W, Boyle EA, Karl DM (2000) Phosphate Depletion in the Western North Atlantic Ocean. *Science*, **289**, 759–762.

Wynne D (1981) The role of phosphatases in the metabolism of Peridinium cinctum, from lake Kinneret. *Hydrobiologia*, **83**, 93–99.

Young CL, Ingall ED (2010) Marine Dissolved Organic Phosphorus Composition : Insights from Samples Recovered Using Combined Electrodialysis / Reverse Osmosis. *Aquatic geochemistry*, **16**, 563–574.

Zeder M, Pernthaler J (2009) Multispot live-image autofocusing for high-throughput microscopy of fluorescently stained bacteria. *Cytometry Part A*, **75A**, 781–788.

Zeder M, Kohler E, Pernthaler J (2010) Automated quality assessment of autonomously acquired microscopic images of fluorescently stained bacteria. *Cytometry. Part A : the journal of the International Society for Analytical Cytology*, **77**, 76–85.

Zeder M, Ellrott a, Amann R (2011) Automated sample area definition for high-throughput microscopy. *Cytometry. Part A : the journal of the International Society for Analytical Cytology*, **79**, 306–10.

Zubkov M, Tarran G (2008) High bacterivory by the smallest phytoplankton in the North Atlantic Ocean. *Nature*, **455**, 224–U48.

APPENDICES

APPENDIX 1

We estimated the P critical concentration using the formula (Catalan, 2000):

$$C_{cri} = \frac{C_{cell} \times r_R \times A_r}{12 \times \pi \times \left(\frac{S}{V}\right)^{-1} \times D}$$

Where C_{cell} is the cell carbon content (mol C·cell^{-1}), A_r is the C:P atomic ratio (mol P·mol C^{-1}), r_R is the replication rate (mol C·mol C^{-1}·s^{-1}), S/V is the surface to volume ratio (m^{-1}), D is the molecular diffusivity (m^2·s^{-1}). C_{cell} was calculated as the product of the cell volume (L·cell^{-1}) by 18.8 mol C·L^{-1} (Reynolds, 2006; page 30), and we used the Redfield ratio C:P 106:1. The r_R (day^{-1}) was calculated using the formula (Catalan, 2000):

$$r_R = 10^{\left(a - \frac{e}{\tau}\right)} \times \left(\frac{S}{V}\right)^{\left(\frac{d}{\tau} - b\right)}$$

Where τ is the absolute temperature (K), and a, b, d and e were experimentally determined as 11.5867, 8.2245, 2505 and 3378 respectively (Reynolds, 1997). The molecular diffusivity of orthophosphate was calculated using the equation (Jumars *et al.*, 1993):

$$D = \frac{k_B \times \tau}{6 \times \pi \times \mu_{fw} \times R_0}$$

Where k_B is the Boltzmann constant (1.38064888·10^{-23} m^2·Kg·s^{-2}·K^{-1}), τ is temperature (K), R_0 is the molecular radius of the solute (2.8 Å in orthophosphate), and μ_{fw} is the fresh water dynamic viscosity, calculated as follows (Jumars *et al.*, 1993):

$$log_{10}\mu_{fw} = \frac{-157.095 - 3.09695T - 0.001827T^2}{89.93 + T}$$

Where T is temperature (ºC), and μ_{fw} units are g·cm^{-1}·s^{-1}.

Journal of Microbiological Methods 86 (2011) 104–107

Contents lists available at ScienceDirect

Journal of Microbiological Methods

journal homepage: www.elsevier.com/locate/jmicmeth

Note

A comparative study of fluorescence-labelled enzyme activity methods for assaying phosphatase activity in phytoplankton. A possible bias in the enzymatic pathway estimations

Daniel Díaz-de-Quijano *, Marisol Felip

Unitat de Limnologia, Departament d'Ecologia i Centre de Recerca d'Alta Muntanya, CEAB-CSIC-Universitat de Barcelona, 645 Diagonal Av. 08028, Barcelona, Catalonia, Spain

ARTICLE INFO

Article history:
Received 26 December 2010
Received in revised form 18 March 2011
Accepted 18 March 2011
Available online 2 April 2011

Keywords:
Phosphatase
Ectoenzyme
Phytoplankton
ELF97-phosphate
Single cell analysis

ABSTRACT

We compared different fluorescence-labelled enzyme activity (FLEA) methods for assaying phosphatase activity in phytoplankton. Unfixed and liquid incubations are devised. We demonstrated that the presence of intracellular labelling was persistent, which could point out a source of bias in ectoenzymatic activities measurements based either on the FLEA or classical methods.

The published protocols of the enzyme-labelled fluorescence (ELF) or FLEA technique differ widely in the fixative used, the way the incubation is performed and the final support of the sample (liquid or filter). These differences have been shown to affect not only cell integrity, but also labelling efficiency (Rengefors et al., 2001; Young et al., 2010). Additionally, the presence of intracellular labelling is a problem that has not yet been solved. We compared published and new protocols for the phosphatase activity assay in natural phytoplankton communities, using the criterion that ectophosphatase (surface-bound) FLEA labelling should be maximised because these are the phosphatases playing the ecological role of catalysing reactions around the lipid boundary, where life and the surrounding environment come into contact.

Phytoplankton communities were sampled from Crous Pond (41°40′37″N, 2°35′2″E) and Redon Lake (42°38′33″N, 0°46′46″E), in Catalonia. We tested several protocols that were defined by a combination of two factors: step order and fixative (Table 1). The step order had two levels: B (Bottle) and F (Filter). B consisted in incubating the sample in a bottle, fixing it and stopping the reaction by filtration. It was based on the protocol devised by Nedoma et al.(2003). F consisted in fixing the sample, filtering it, and incubating the filters in a Petri dish. This was a modification of the protocol drawn up by Lomas et al. (2004). B or F was placed in first position in our protocol code. The fixative factor had five levels, whose initial letters were placed in the second position in our code: $HgCl_2$ (H), no fixative (X), LFT (L), ethanol + DMSO (E), and liquid N_2 (N). $HgCl_2$ 4 mM f.c. was added to samples and immediately filtered. LFT fixation was performed by adding alkaline Lugol 0.5% (vol/vol), formaldehyde 2% f.c. (pH 7) and several drops of 3% sodium thiosulfate (Sherr and Sherr, 1993). Ethanol 70% + DMSO 10% were added to the samples and left for 30 minutes before filtration (Lomas et al., 2004). In the case of the FN protocol, samples were placed in plastic vials and sunk into the liquid N_2, removed, and left to thaw prior to filtration. All the incubations were performed in the dark for 1 hour at room temperature and with a substrate concentration of 20 μM ELF97-phosphate (ELFP) (Molecular Probes, E6589). Three replicates and one negative control (without ELFP) of 30 ml each were filtered through 25 mm diameter and 2 μm pore polycarbonate filters (Millipore). Very gentle pressure (<20 KPa) was used to avoid cell disruption. Filters were left to dry on cellulose paper and stored at −20 °C. Finally, they were thawed and mounted on microscope slides using Citifluor AF1.

The composition of the phytoplankton community was determined by the Utermöhl method. Particular attention was paid to the size and shape of chloroplasts, as these characters would subsequently be used to identify taxa under the epifluorescence microscope. The different FLEA filters were analysed under a Nikon Eclipse E600 epifluorescence microscope and the percentage of ELFA-labelled cells was determined. A cell was only considered positive when a clear ELFA object was observed on or in the cell, whatever its size or intensity. Some of the experimental conditions (FH and BE in the Crous sample) resulted in non-measurable filters (Fig. 1a and b). One replicate per experimental

* Corresponding author at: Present address: Departament d'Ecologia Universitat de Barcelona, 645 Diagonal Av. 08028, Barcelona, Catalonia, Spain. Tel.: +34 93 403 11 90; fax: +34 93 411 14 38.
E-mail address: diazdequijano@ub.edu (D. Díaz-de-Quijano).

0167-7012/$ – see front matter © 2011 Elsevier B.V. All rights reserved.
doi:10.1016/j.mimet.2011.03.010

Table 1
Experimental design and codes used in this study; n = number of available replicates; unc = uncountable filters.

			Fixative				
			$HgCl_2$	No fixative	LFT	Ethanol + DMSO	Liquid N_2
Step order	Bottle	Crous	BH ($n=2$)	BX ($n=2$)	BL ($n=2$)	BE (unc)	–
	Filter		FH (unc)	FX ($n=2$)	FL ($n=2$)	FE ($n=2$)	–
	Bottle	Redon	BH ($n=3$)	BX ($n=3$)	BL ($n=2$)	–	–
	Filter		FH ($n=3$)	FX ($n=3$)	FL ($n=3$)	–	FN ($n=3$)

condition and sample was analysed with a Leica SP II spectral detection confocal microscope to determine the location of ELFA bodies. The percentage of cells with only external labelling (EXT), only internal labelling (INT), and both external and internal labelling (EXT and INT) (Fig. 1c and d, e and f) were determined by counting more than 100 cells per filter. Within each taxon, we discarded location patterns that were based on less than 5% of taxon total counts. One-way and two-way ANOVAs were performed with Statgraphics Plus 5.1 (Statistical Graphics Corp.) and STATISTICA 6.0 (Statsoft, Inc., OK, USA).

The percentage of ELFA-labelled cells in the entire phytoplankton differed significantly between protocols in both Redon (p–$v<0.0000$) and Crous (p–$v=0.0153$) samples. The step order (Crous p–$v=0.035781$ and Redon p–$v=0.001377$) was always more significant than the fixative (Crous was not significant and Redon p–$v=0.0025$) (Fig. 2, first row), and this result was consistent across most of the studied taxa. In all the cases, liquid-incubation protocols (B) significantly maximised ELFA labelling. B and F protocols differed in two factors that could explain this result: (1) the status of cells and enzymes during incubation (alive/unfixed (B) or fixed (F)), and (2) the physical support of the incubation (liquid (B) or on-filter (F)). If we consider the low labelling results of FX protocol, where cells were incubated live but on filter, as in Van Wambeke's method (Van Wambeke et al., 2008), we may conclude that apart from the expected effect of incubating fixed or unfixed samples, a physical obstruction that prevents ELFP from reaching enzymes may occur. Reasonable explanations would be either because in F protocols some phosphatases are in contact with the filter itself, or because ELFP cannot diffuse fast enough within the drop, which creates a low concentration of ELFP in the volume surrounding the cell.

The percentage of ELFA-labelled cells showed four acceptable protocols: BH, BX, BL and FH. Of these options, BH was the best in terms of the percentage of ELFA-labelled cells, but consistently performed the worst in terms of ELFA-labelling location. It was therefore an undesirable option. BX and BL had good percentage of labelled cells and good labelling location in all the cases except that BX had low EXT location in Redon sample and BL had a low percentage of labelled cells in Crous. Finally, FH had good results in both variables when the protocol worked (in Redon), but it could be unreliable as it developed huge particle aggregates in Crous. To sum up, BX and BL would be reasonably good options, BH could provide positive but ecologically uncertain results, and FH seems to be a good but unstable option.

Traditional total enzyme activity substrates (MUF-P, MFP, p-NNP, etc.) have been thought to label dissolved and/or ectoenzymes as they have physical and chemical characteristics that make it impossible for them to get into the cells by membrane transport (Chróst, 1991). The ELF substrate shares the same physical and chemical characteristics. In addition, there is evidence that ELFP and MUFP substrates react with

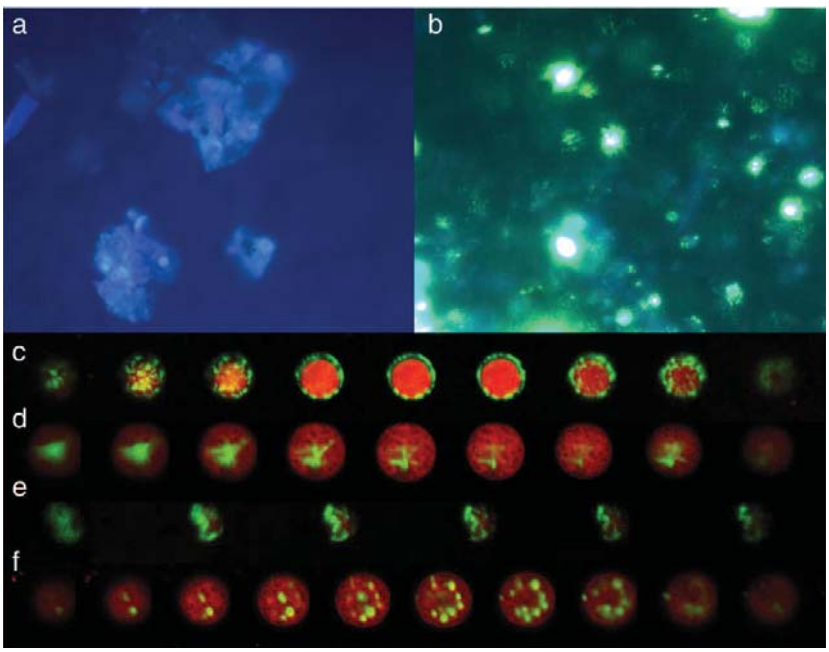

Fig. 1. Colour epifluorescent images: a and b; a) general view of protocol FH, with aggregates (Crous); b) general view of protocol BE, with extremely high unspecific ELFA labelling and non-recognisable chloroplasts (Crous). Pseudocolour optical sections at different depths through a unicellular *S. schroeteri* (c, d and f) or a small flagellated (e). Red is chloroplast and green are ELFA precipitates. c) EXT labelling; d) INT labelling; e and f) EXT & INT labelling.

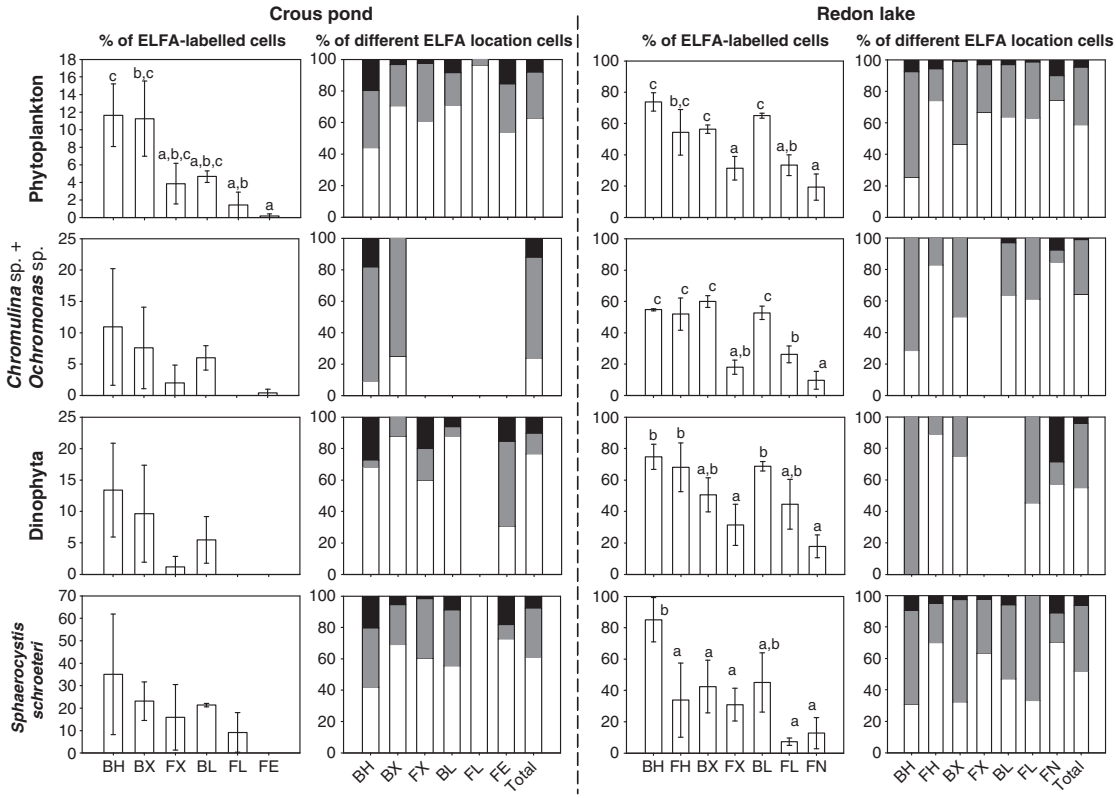

Fig. 2. Simple bars: Percentage of ELFA-labelled cells. Letters on bars (a, b, and c) show homogeneous groups, as found by Tukey HSD multiple range tests (p–v<0.05), when one-way ANOVA showed significant differences (p–v<0.05). Stacked bars: Percentage of different ELFA-labelling location cells. Black = INT labelling, grey = EXT and INT labelling, white = EXT labelling. TOTAL column = sum of all the cells counted in all the protocols.

the same set of phosphatases within a certain sample (Štrojsová et al., 2003; Nedoma et al., 2007). Therefore, we could conclude that the ELF substrate should normally react with ectoenzymes, but not with intracellular enzymes. However, the optical dissection of FLEA-incubated cells by confocal microscopy confirmed that intracellular PA was labelled by any of the tested protocols (Fig. 2, first row), as previously observed (Dyhrman and Palenik, 1999; Skelton et al., 2006; Ou et al., 2010). The extent of INT together with EXT and INT labelling shows that this problem should be taken into consideration. The hypothesis that the detection of intracellular labelling is a problem that is exclusive to ELF substrate should be experimentally tested in the future. If this hypothesis was rejected, all of our substrate reaction-based knowledge about environmental PA, and maybe the general enzymatic pathway, would have been biased to some extent by interaction with intracellular enzymes.

Previous observations have found ELFA labelling patterns to vary in different species (e.g. linear structures, dots, evenly labelled whole cell surfaces, etc.) (Pers. Obs., Štrojsová et al., 2003). Therefore, we expected the location of ELFA labelling to be species-specific. In contrast, we found the taxon effect to be secondary to the protocol effect: the range of variability within protocols was significantly narrower than within taxa (p–v = 0.0003). Nonetheless, more diverse species than those used here (in terms of cell aggregation, morphology, wall properties, etc.) should be considered to generalise this result. In any case, many hypotheses (including taxon-specific ones) could be made to explain intracellular labelling. In Dinophyta and small flagellated Crysophyta intracellular labelling could be due to the internalisation of ELFP together with phagocytosed particles, as these taxa have been described as potential bacterivores (Jones, 2000). However, this does not explain other intracellular labelling, such as that found in *Sphaerocystis schroeteri* (CHOD) (Fig. 2c), *Monoraphidium* sp., *Oocystis parva*, *Stichogloea doederleinii* (SCHMIDLE) (data not shown), which are the first non-mixotrophic phytoplankton observed with intracellular ELFA. In this case, we hypothesise that cell membrane disruption may be the reason for intracellular labelling. There may be three different causes of membrane disruption: natural cell death (Bidle and Falkowski, 2004), sample manipulation, and accumulation of ELFA crystals, which may damage the cell membrane and make it collapse, resulting in ELFA penetrating the cell.

In conclusion, the FLEA technique protocols should incubate unfixed and liquid samples. BX and BL may be the best trade-offs amongst the tested protocols, between FLEA signal maximisation and the EXT location of the signal. The FLEA technique results are mainly determined by the protocol, and the possible taxon dependence is secondary. Finally, we demonstrated the presence of intracellular fluorescence-labelled PA when the FLEA technique is used, which highlights the need to further understand the origin of this signal.

Acknowledgments

We thank Jiři Nedoma for critically reading the manuscript and for valuable suggestions, the Scientific-Technical Services of the University of Barcelona (SCT-UB) for technical assistance in confocal microscopy, and Maria Diaz de Quijano and Eglantine Chappuis for assistance in the field. This research was carried out by the Limnology Group CEAB-UB

and was supported by the Spanish Ministry of Science and Technology, projects CGL2004-02989 and CGL2007-64177/BOS.

References

Bidle, K.D., Falkowski, P.G., 2004. Cell death in planktonic, photosynthetic microorganisms. Nat. Rev. Micro. 2, 643–655.

Chróst, R.J., 1991. Environmental control of the synthesis and activity of aquatic microbial ectoenzymes. In: Chróst, R.J. (Ed.), Microbial Enzymes in Aquatic Environments. Springer-Verlag New York Inc., New York, pp. 29–59.

Dyhrman, S.T., Palenik, B., 1999. Phosphate stress in cultures and field populations of the dinoflagellate prorocentrum minimum detected by a single-cell alkaline.

Jones, R.I., 2000. Mixotrophy in planktonic protists: an overview. Freshwat. Biol. 45, 219–226.

Lomas, M.W., Swain, A., Shelton, R., Ammerman, J.W., 2004. Taxonomic variability of phosphorus stress in Sargasso Sea phytoplankton. Limnol. Oceanogr. 49, 2303–2310.

Nedoma, J., Štrojsová, A., Vrba, J., Komárková, J., Šimek, K., 2003. Extracellular phosphatase activity of natural plankton studied with ELF97 phosphate: fluorescence quantification and labelling kinetics. Environ. Microbiol. 5, 462–472.

Nedoma, J., Van Wambeke, F., Štrojsová, A., Štrojsová, M., Duhamel, S., 2007. Affinity of extracellular phosphatases for ELF97 phosphate in aquatic environments. Mar. Freshwat. Res. 58, 454–460.

Ou, L., Huang, B., Hong, H., Qi, Y., Lu, S., 2010. Comparative alkaline phosphatase characteristics of the algal bloom dinoflagellates *Prorocentrum donghaiense* and *Alexandrium catenella*, and the diatom *Skeletonema costatum*. J. Phycol. 46, 260–265.

Rengefors, K., Pettersson, K., Blenckner, T., Anderson, D.M., 2001. Species-specific alkaline phosphatase activity in freshwater spring phytoplankton: application of a novel method. J. Plankton Res. 23, 435–443.

Sherr, E.B., Sherr, B.F., 1993. Preservation and storage of samples for enumeration of heterotrophic protists. In: Kemp, P.F., Sherr, B.F., Sherr, E.B., Cole, J.J. (Eds.), Handbook of Methods in Aquatic Microbial Ecology. Lewis Publishers, Boca Raton, Florida U.S.A., pp. 207–212.

Skelton, H.M., Parrow, M.W., Burkholder, J.M., 2006. Phosphatase activity in the heterotrophic dinoflagellate *Pfiesteria shumwayae*. Harmful Algae 5, 395–406.

Štrojsová, A., Vrba, J., Nedoma, J., Komárková, J., Znachor, P., 2003. Seasonal study of extracellular phosphatase expression in the phytoplankton of a eutrophic reservoir. Eur. J. Phycol. 38, 295–306.

Van Wambeke, F., Nedoma, J., Duhamel, S., Lebaron, P., 2008. Alkaline phosphatase activity of marine bacteria studied with ELF 97 substrate: success and limits in the P-limited Mediterranean Sea. AME 52, 245–251.

Young, E.B., Tucker, R.C., Pansch, L.A., 2010. Alkaline phosphatase in freshwater Cladophora-epiphyte assemblages: regulation in response to phosphorus supply and localization. J. Phycol. 46, 93–101.

Cytometry PART A
Journal of the International Society for Advancement of Cytometry

MIFlowCyt

3D Restoration Microscopy Improves Quantification of Enzyme-Labeled Fluorescence-Based Single-Cell Phosphatase Activity in Plankton

Daniel Diaz-de-Quijano,[1]* Pilar Palacios,[2] Karel Horňák,[3,4] Marisol Felip[1]

[1]Unitat de Limnologia, Departament d'Ecologia i Centre de Recerca d'Alta Muntanya, CEAB-CSIC-Universitat de Barcelona, 08028 Barcelona, Catalonia, Spain

[2]Department of Microbial Biotechnology, Centro Nacional de Biotecnología-CSIC, Darwin 3, Campus de Cantoblanco, 28049 Madrid, Spain

[3]Department of Aquatic Microbial Ecology, Biology Centre of the Academy of Sciences of the Czech Republic, Institute of Hydrobiology, Na Sádkách 7, CZ-370 05 České Budějovice, Czech Republic

[4]Limnological Station, Institute of Plant Biology, University of Zurich, Seestrasse 187, CH-8802 Kilchberg, Switzerland

Received 17 June 2013; Revised 22 January 2014; Accepted 30 April 2014

Grant sponsor: Spanish Ministry of Science and Technology; Grant numbers: ECOFOS (CGL2007-64177/BOS); GRACCIE (CDS2007-00067); NITROPIR (CGL2010-19373).

Additional Supporting Information may be found in the online version of this article.

Present address of D. Diaz de Quijano: Departament d'Ecologia Universitat de Barcelona, Av. Diagonal 643, 08028 Barcelona, Catalonia, Spain

*Correspondence to: D. Diaz de Quijano, Departament d'Ecologia Universitat de Barcelona, Av. Diagonal 643, 08028 Barcelona, Catalonia, Spain. E-mail: diazdequijano@ub.edu

ISAC
International Society for Advancement of Cytometry

Abstract

The ELF or fluorescence-labeled enzyme activity (FLEA) technique is a culture-independent single-cell tool for assessing plankton enzyme activity in close-to-*in situ* conditions. We demonstrate that single-cell FLEA quantifications based on two-dimensional (2D) image analysis were biased by up to one order of magnitude relative to deconvolved 3D. This was basically attributed to out-of-focus light, and partially to object size. Nevertheless, if sufficient cells were measured (25–40 cells), biases in individual 2D cell measurements were partially compensated, providing useful and comparable results to deconvolved 3D. We also discuss how much caution should be used when comparing the single-cell enzyme activities of different sized bacterio- and/or phytoplankton populations measured on 2D images. Finally, a novel method based on deconvolved 3D images (wide field restoration microscopy; WFR) was devised to improve the discrimination of similar single-cell enzyme activities, the comparison of enzyme activities between different size cells, the measurement of low fluorescence intensities, the quantification of less numerous species, and the combination of the FLEA technique with other single-cell methods. These improvements in cell enzyme activity measurements will provide a more precise picture of individual species' behavior in nature, which is essential to understand their functional role and evolutionary history.

Key terms

3D fluorescence microscopy; deconvolution; ELF phosphate; phosphatase activity; phytoplankton

PHOSPHORUS recycling in ecosystems is driven by different processes involving various enzyme activities. Phosphatases (including phosphoesterases, nucleases and nucleotidases) hydrolyse oxygen–phosphorus bonds in phosphoesters, the dominant form of dissolved organic phosphorus (1–4), whereas C-P lyases and hydrolases hydrolyse carbon–phosphorus bonds in phosphonates (5). These enzymes may play a key role in those ecosystems in which P is temporarily or permanently a limiting factor, as is the case of some freshwater, marine and terrestrial ecosystems (6–10). Notably, P limitation is expected to increase as the deposition of atmospherically transported anthropogenic N modifies the N:P stoichiometry of ecosystems all over the world (11). A number of studies have already assessed the shifts in environmental enzyme activity driven by anthropogenic atmospheric N deposition (12,13) and by other parameters related to climate change that can modulate enzymatic activity, such as pH (14,15), temperature (16,17), and UV radiation (18–21). These studies have demonstrated the importance of enzyme activity in the response of ecosystems to global climate change. However, a more accurate characterization of the link between taxonomic identity and *in situ* enzymatic activity is essential to understand and to predict enzyme dynamics in nature.

Published online 00 Month 2014 in Wiley Online Library (wileyonlinelibrary.com)
DOI: 10.1002/cyto.a.22486

Phosphomonoesterases are one of the most widely studied enzymes in aquatic ecosystems, and to date the only ones that can be assessed using the enzyme-labelled fluorescence-phosphate (ELFP) substrate, via the so-called FLEA technique. Upon enzymatic hydrolysis, the ELFP substrate is converted to a fluorescent ELF alcohol (ELFA) that precipitates at the site of enzyme activity (22). Therefore, the FLEA technique constitutes a powerful and culture-independent tool with which to study the contribution of this functional trait to the species trophic strategy (23,24) at the single-cell level, and in close-to-*in situ* conditions. Simultaneously, this technique also enables the preservation of useful cell structures required for adequate taxonomic identification (autofluorescent chloroplasts and stained DNA), mainly in phyto- and bacterioplankton communities (25–28). Moreover, Nedoma et al. (29) developed a method to quantify the ELFA precipitate based on epifluorescence microscopy and 2D image analysis. Thus, the FLEA technique has provided the opportunity to open the "black box" of environmental enzyme activity in phyto- and bacterioplankton. Knowledge of single-cell enzymatic activity, if accurate enough, is essential for the proper definition of functional niches, the reconstruction of the evolution of functional traits associated with certain trophic strategies (30,31), and better modelling and understanding of the dynamics of enzyme activity in nature (32). Nonetheless, the 2D images on which most quantifications have been based to date are distorted representations of real 3D cells. Therefore, we hypothesized that (i) 2D image-based measurements might be significantly biased, and (ii) cell size might modulate this bias, which could invalidate comparisons between different size cells, such as phytoplankton and bacterial cells.

To test these hypotheses, a 3D imaging system was required. Amongst the different modalities of fluorescence microscopy (wide-field, structured light illumination, confocal, and confocal-derived techniques), 3D wide-field restoration microscopy (WFR) was chosen for several reasons. Blurring of light is a common phenomenon in all the above-mentioned 3D microscopy techniques but it is especially important in 3D wide-field microscopy, where light blurs mainly along the Z axis and more moderately in the XY plane (33). This problem may be solved in one of two ways or via combination of approaches. On the one hand, mechanical devices may be used to reduce the amount of out-of-focus light (confocal and structured light illumination microscopy). On the other hand, out-of-focus light may be considered informative light and any of the mentioned techniques, including wide-field, may be combined with image restoration by deconvolution to relocate out-of-focus light to its source (34). Second, the WFR imaging system requires a wide-field microscope with a motorized *Z* axis, a cooled digital CCD camera and deconvolution software for image restoration. This WFR set up is cheaper than that required for the other techniques and makes it affordable for a larger number of laboratories. Moreover, WFR microscopy is the most suitable technique for our fluorescence intensity quantification purposes and for microplankton samples (thin and with no or small amounts of fluorescent material out of focus). This technique has a higher signal-to-noise ratio (SNR) than laser scanning confocal microscopy (LSCM) for samples <30 μm thick (33,35), and uses CCD detectors with a quantum efficiency of $\sim$60%, contrasting with that of photomultiplier (PMT) detectors normally used in confocal microscopy which used to have a quantum efficiency of $\sim$10% (36). WFR microscopy also has the shortest acquisition time, which makes this technique a better option for fluorescence quantification and the imaging of living cells, as photobleaching of fluorophores and cell damage are minimized. Finally, WFR microscopy has also been found to be more sensitive and accurate than LSCM when measuring low fluorescence intensity objects (35,36), although ELFA labelings are usually intense enough for both techniques. So, although structured light illumination could be an alternative option [it meets most of the requirements mentioned above and has been reported to be reliable (37)], WFR is an appropriate choice for fluorescence quantification in phyto- and bacterioplankton samples.

In WFR, image formation can be described by the 3D mathematical model:

$$\text{Image} = \text{object} \otimes \text{psf} \quad (1)$$

where image is the acquired image, object is the real specimen, and psf is the point spread function of the microscope (all the elements in the equation are 3D arrays). The psf describes the way an infinitely small point would be imaged, and distorted, by the microscope (in fact, it is a 3D photograph of a subresolution fluorescent bead) (38). By the mathematical operation of convolution ($\otimes$), i.e. by applying the psf to every single point in the real 3D object, we would get the blurred image. Inversely, an estimate of the object can be calculated by deconvolution of the distorted image. Two kinds of deconvolution algorithms have been implemented: deblurring and restoration algorithms (38–40). The first operate separately on each focal plane of the 3D image to estimate and eliminate its blur. In contrast, restoration algorithms consider all the 3D data simultaneously to reassign light to its source in its original in-focus plane. The result in both cases is a contrast improvement but only the latter algorithms respect all the acquired information and are, therefore, suitable for improving fluorescence intensity measurements (33,35,41).

In this study, we describe and propose a novel method for accurate FLEA quantification in phytoplankton cells based on WFR. We characterize the improvement in performance and accuracy of the proposed imaging system, and we compare, for the first time in the literature, 2D and 3D WFR fluorescence intensity quantifications. This is an important

contribution because on the one hand 3D fluorescence microscopy is considered superior to 2D and is thus widely used for many different purposes (41–43), but on the other hand, 2D imaging may still be used given its various advantages: simplicity, faster acquisition and analysis times, cheaper equipment and lower storage memory requirements. With this in mind, we describe the errors associated with the current 2D wide-field method and the relative distorting effect of cell size on these measurements, and discuss how to correctly interpret 2D-based data.

Materials and Methods

Study Sites and Sampling

Data were collected from phytoplankton cells from eight high mountain lakes of the Central Pyrenees in order to have a wide range of phosphatase activity and cell sizes.

FLEA Phosphatase Protocol

Samples were sieved in the field to remove zooplankton and processed upon arrival at the laboratory (always within 6 h after sampling in summer and within 18 h in winter and spring). An aliquot per sample was fixed with alkaline Lugol for phytoplankton determination. The FLEA technique was performed as previously described by Diaz-de-Quijano and Felip (44). Liquid samples were incubated in the dark, at *in situ* temperature, buffered at *in situ* pH with 0.1M HCl/Tris, citric or acetic acid buffers depending on sample pH, and using 10 μM of ELFP (Molecular Probes, E6589) substrate to achieve a compromise concentration above K_M for almost all samples. The time courses of the incubations were always monitored by fluorimeter to ensure that we sampled the incubation during its linear phase, as previously recommended (29). Incubation of the samples was stopped by gentle filtration (<20 KPa) through 2 μm pore polycarbonate filters, following which the samples were stored at −20°C until they were mounted with CitiFluor AF1, and covered with 0.17 μm thick cover slides for microscope analysis.

Beads

Different sets of fluorescent beads were quantified: 2.5 μm diameter fluorescence intensity calibrated beads (In Speck™ Green (505/515) Microscope Image Intensity Calibration Kit, 2.5 μm, Invitrogen, Molecular Probes, I7219), 6 μm beads (FocalCheck Fluorescent Microspheres Kit, 6 μm, Slide C, Invitrogen, Molecular Probes, F24633), and 15 μm beads (FluoSpheres polystyrene microspheres, 15 μm, yellow-green fluorescent (505/515), Invitrogen, Molecular Probes, F8844). A drop of each intensity and size set of beads was spread separately on a slide, air-dried, and mounted with CitiFluor AF1 as in the case of phytoplankton cells except for the 6 μm beads, which were commercially mounted in optical cement.

Beads were used to check for size and intensity effect. First, we measured 193 fluorescent 2.5 μm diameter latex beads stained with six different calibrated intensities ranging between three orders of magnitude by flow cytometry (as a reference) and by quantitative microscopy (2D raw, and 3D raw or deconvolved). We compared differences in relative fluorescence measurements between the different methods and checked for linearity of the fluorescence intensity measurements using simple linear regression, within the R environment. The percentages of FU were log transformed to meet the assumptions of normality and homoscedasticity. Secondly, we used linear regression to relate 2D and 3D measurements of different size beads. Sample sizes were $n = 30$ for 15 μm beads, $n = 52$ for 6 μm beads, and $n = 140$ for 2.5 μm beads. We estimated the regression slopes and calculated their two-sided and nonparametric bootstrapped 95% confidence intervals with the boot.ci function in R, based on 10,000 replicates (samplings of data) each. The bias-corrected accelerated percentile (BCa) interval type was chosen (45,46).

Flow Cytometry

Intensity calibrated fluorescent beads (as detailed above) diluted in 1 ml of fresh 0.2 μm-filtered Milli-Q water were measured using the FACSCalibur flow cytometer (Becton Dickinson, USA) equipped with an air-cooled argon ion laser (15 mW, 488 nm). Beads were identified based on their fluorescent intensity signatures in a plot of 90° angle light scatter versus green fluorescence (515 nm) using the flow cytometry analysis software CELLQuest Pro (Becton Dickinson) (the gating strategy is shown as Supporting Information). To avoid particle coincidence, the rate of particle passage was kept at <1,000 events s^{-1} during analyses.

Image Acquisition

Samples were imaged with a Huygens restoration microscope (Scientific Volume Imaging b. v., Hilversum, The Netherlands) built around a Nikon Eclipse 90i epifluorescence microscope (Nikon, Tokyo, Japan). The microscope was equipped with a monochromatic Vosskühler COOL-1300Q CCD camera with a pixel size of 6.45 μm^2 (Vosskühler GmbH, Osnabrück, Germany) and a Xenon-arc illumination. Bead images were acquired with a Plan Apo 40X/1.0 NA oil immersion objective lens and a fluorescein filter block (ex. 450–490 nm, em. >515 nm). Cell images were acquired using a Plan Fluor 20X/0.75 NA MI objective lens with the collar adjusted to immersion with oil, and two different filter blocks: an ELFA-specific filter block (ex. 360–370 nm, em. 520–540 nm) and a chlorophyll-specific filter block (ex. 510–550 nm, em. >590 nm) for species determination. A 9.4% w/v fluorescein standard solution was used for shading correction, and to determine an inter-session correction factor (*Icf*) (47). Gain was fixed to 1 but exposure time was modified for each image acquisition to avoid image clipping (no voxel saturation was allowed) and also to collect as much information as possible from weakly bright voxels. Modulation of exposure time between images did not hinder comparability because CCDs generate a linear response over time (48). The three parameters were recorded in metadata for further calculations. Collected 3D images were a stack composed of 35 2D slides spaced at a distance similar to the depth of field (DOF) (1.4 μm at the 20× objective and 0.7 μm at the 40× objective), and had the object of interest centred on the *Z* axis.

Deconvolution

Image restoration (deconvolution) was performed using the Classic Maximum Likelihood Estimation algorithm implemented in Huygens Professional 3.3.2p1, which includes a batch processor. Images were translated from nd2 to ICS file format to import them into the deconvolution software. They were cropped, respecting the volume dimensions of out-of-focus light, to speed up deconvolution. A set of images with known SNR of 40, 30, 20, and 10 was visually compared with our raw images to determine their SNR index. A SNR index of 35 was used according to our data, the maximum number of iterations was set to 40, and bleaching correction was activated. To select a point spread function (PSF) we deconvolved an image of a 2.5 μm fluorescent bead using both, experimental and theoretical PSF. The latter was able to reconstruct the known spherical shape of the fluorescent bead whereas the former produced a distorted shape (double banana-shaped artifact at the top and bottom edges). Moreover, the grey values of the deconvolved images showed a quantitatively more efficient deconvolution when using theoretical PSF (minimum, mean, and maximum) (0, 38.03, 40807) than experimental PSF (0.002, 16.55, 13481). Therefore, we decided to use the theoretical PSF for both reasons: it triggered a better shape and fluorescence intensity restoration. The output format file had to be scaled 16 bit TIFF because the NIS-Elements software used to quantify the images only supports up to 16 bit images, whereas voxel intensities reached values above 16 bits after deconvolution.

Image Analysis and Calculations

Fluorescence intensity was measured using NIS-Elements AR 2.34 software (Laboratory Imaging, Praha, Czech Republic). We used two macros to semi-automate the quantification routine: the macro described by Nedoma et al. (29) for 2D images, and an adapted version for 3D images. In the latter macro, the user is able to set an optimum contrast enhancement and move across the different slides of the stack to properly select the area of the object and the area of the background to be measured. These areas are projected across the whole stack defining two irregular prisms (the Volumes of Interest, VOIs). Finally, the macro measured the following variables per slide in the stack: area of the object (*Area*; μm^2), mean grey value of the object (*Mgv*; dimensionless), and mean grey value of the background (*BgMgv*; dimensionless). These measurements were automatically exported to an Excel file for semiautomated calculation together with the following metadata: distance between slides in a stack (*Zstep*; μm), number of slides (*ns*; dimensionless), camera exposure time (*expT*; ms), camera gain (*Gain*; dimensionless), intersession correction factor (*Icf*; dimensionless), and image file identity. The relative fluorescence of the object (*RFobject*; fluorescence units—FU) was calculated as follows:

$$RFobject = \frac{Icf}{\exp T \times \mathrm{Gain}} \times \sum_{i=1}^{ns} \mathrm{Area} \times Zstep \times (Mgv_i - BgMgv_i) \quad (2)$$

A conversion factor to relate the amount of ELFA to FU (*ConvF*; fmol ELFA·FU^{-1}) was obtained from the comparison of fluorimeter and microscope raw 2D measurements. The increase in ELFA fluorescence of several phosphatase incubations from an independent set of samples was measured by both methods in parallel. Microscope measurements were expressed in FU whereas fluorimeter measurements were translated to fmol ELFA using a calibration line based on a dilution of commercially available ELFA standard. See Nedoma et al. (29) for more details. To obtain the *ConvF* for the raw 3D and deconvolved 3D modes, we compared the fluorimeter measurements (fmol ELFA) and predicted raw and deconvolved 3D fluorescence intensity values corresponding to the raw 2D measurements of the independent set of samples. This prediction was based in two partial regressions (built on the 212 raw, or 175 deconvolved, cells measured in this study) that related raw 2D fluorescence intensity and object area to the raw (or deconvolved) 3D fluorescence intensity. *ConvF* values were 0.013553 fmol ELFA·FU^{-1} (raw 2D), 0.000124 fmol ELFA·FU^{-1} (raw 3D), and 0.000014 fmol ELFA·FU^{-1} (deconvolved 3D). In the case of phytoplankton cells, the single cell hydrolysed phosphate (*SCHP*; fmol ELFA·$cell^{-1}$) was calculated as:

$$\mathrm{SCHP} = RFobject \times ConvF \quad (3)$$

Finally, the single cell phosphatase activity (SCPA; fmol ELFA·$cell^{-1}$·h^{-1}) was calculated by dividing SCHP by the number of hours in the linear phase before incubation was stopped.

Statistics

Linear least-squares regression, partial correlation, partial regression, graphics and variation partitioning were carried out in the R environment (49). Comparison of least-squares regression slopes and comparison of slopes to a theoretical value for the different intensity beads were performed using GraphPad Prism 5.01 for Windows (GraphPad Software, San Diego, CA). K-means analysis was performed within the Ginkgo multivariate analysis system (http://biodiver.bio.ub.es/ginkgo/index.html, Barcelona, Catalonia).

We used an iterative approach in the R environment to find the minimum number of cells that must be counted in raw 2D to obtain the most similar results to deconvolved 3D. For each group (a species or a set of several species), the first loop involved removing one cell per iteration, sampled stochastically without replacement, and testing if the new set of sampled data: (i) maintained the homogeneity of variances between raw 2D and deconvolved 3D, and (ii) had the same difference in raw 2D and deconvolved 3D means as calculated using all observations. The macro recorded the number of remaining cells (sample size) when conditions (i) or (ii) were not met. The second loop restarted the first one 10,000 times and recorded the results. For each species (or set of several species), we considered the minimum sampling size to be the number of cells that did not significantly alter the original mean and SD results in 99.99% of iterations.

Results

Measurement of Beads of Different Fluorescence Intensity

We measured 193 fluorescence intensity calibrated latex beads of 2.5 μm diameter using three image analysis (IA)

Table 1. Average fluorescence intensities of the different groups of fluorescence intensity standard beads

N	MANUFACTURER FLUORESCENCE INTENSITY (%)	FLOW CYTOMETRY FLUORESCENCE INTENSITY (%)	RAW 2D FLUORESCENCE INTENSITY (FU) AND (SD)	RAW 2D FLUORESCENCE INTENSITY (%)	RAW 3D FLUORESCENCE INTENSITY (FU) AND (SD)	RAW 3D FLUORESCENCE INTENSITY (%)	DECONVOLVED 3D FLUORESCENCE INTENSITY (FU) AND (SD)	DECONVOLVED 3D FLUORESCENCE INTENSITY (%)
37	100	100	19,719 (1879)	100	202,750 (26,123)	100	18,226,411 (16,718,390)	100
29	38	36	6068 (541)	30.11	64,803 (6,959)	30.91	9,467,089 (1,966,014)	29.47
36	14	13	2110 (172)	10.57	22,033 (1,828)	10.66	2637021.8 (1,333,435)	9.83
22	3.3	3.1	547 (28.3)	2.75	5,739 (431)	2.81	6,36,586 (4,37,252)	2.73
36	0.96	0.9	157 (14.7)	0.79	1,679 (149)	0.82	1,68,243 (1,14,843)	0.75
33	0.25	0.22	25.6 (4.9)	0.18	371 (49.1)	0.18	65,583 (32,185)	0.24

Values are in percentage relative to the most fluorescent group, and in fluorescence units (FU). Note that values, in FU, increase one order of magnitude from raw 2D to raw 3D, and two orders of magnitude more from raw 3D to deconvolved 3D. The statistics of flow cytometry measurements are available as Supporting Information.

methods: raw 2D, raw 3D and deconvolved 3D (Table 1). These measurements were compared with flow cytometry measurements with adjusted R-squared values between 0.994 and 0.9969 and slopes between 0.9830 and 1.0199. These slopes were significantly different from 1 (P value$<$0.05), but approached 1 in 3D imaging (raw or deconvolved). Therefore, the tested quantitative microscopy methods provided comparable but slightly different relative fluorescence intensity measurements to those obtained by flow cytometry (Fig. 1a).

We also compared the previously used raw 2D IA method to the two 3D methods. Raw 3D provided the same relative fluorescence measurements as raw 2D (slope = 1, $\alpha = 0.05$) (Fig. 1b). Deconvolved 3D did not fit a linear regression (runs test P value < 0.0001) but did fit a quadratic one when low intensity beads were included (Fig. 1c). This was due to a difference between the two methods when measuring low intensity objects. If the latter objects were excluded, the relationship became linear (Fig. 1d). Deconvolved 3D measurements provided the most similar percentage fluorescence to that obtained by flow cytometry in these dimmest fluorescent beads (although not in the intermediate intensity beads) (Table 1).

Measurement of Different Size Fluorescent Beads

Fluorescence intensities of 2.5, 6, and 15.4 μm diameter beads were quantified by the raw 2D, raw 3D and deconvolved 3D methods. The slopes of simple regression lines that related 2D and 3D methods increased along with the diameter of the bead, which suggests that object size might determine the relationship between the raw 2D and the 3D measurements. This tendency was clearer when comparing raw 2D vs. raw 3D than raw 2D vs. deconvolved 3D, because the 95% confidence intervals of the regression's slopes overlapped in the latter case (Table 2).

Measurement of Phytoplankton Cells

We quantified SCHP (fmol·cell^{-1}) in lake phytoplankton cells using the previously outlined quantitative microscopy methods. Cells were divided into three size groups by a K-means analysis. The plots relating the current method (raw 2D) to the 3D methods (Figs. 2a and 2b) confirmed the results obtained by measuring different size beads. The relationship between raw 2D and 3D gave regression lines for the different cell size groups with clearly different intercepts (Fig. 2a), whereas that of raw 2D against deconvolved 3D was not as clearly affected by cell size. In this case, the increase in dispersion may mask any eventual cell size effect.

To understand the dispersion difference between Figures 2a and 2b we may consider an ideal cell (Fig. 2 right). Three-dimensional measurements are based on the sum of voxel intensities within a volume of interest (VOI). This volume is a prism whose irregular base is user-defined following the silhouette of the cell projected on the XY plane. Besides, the restoration algorithm that we used respects the total amount of energy that belonged to a cell in the raw image and simply relocates it to its source, in such a way that the sum of energy inside ($_i$) and outside ($_o$) the VOI before ($_r$) and after deconvolution ($_d$) is identical, i.e.:

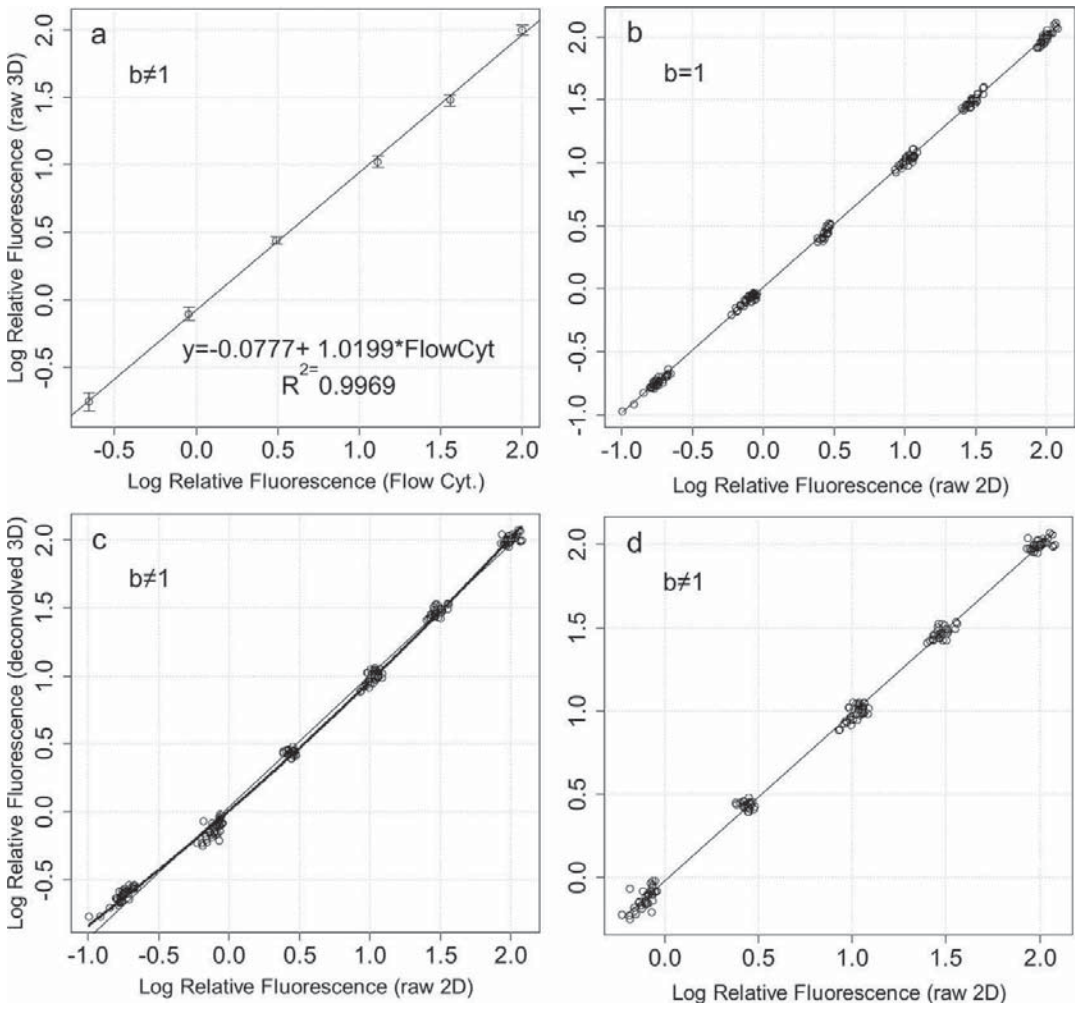

Figure 1. Comparison of standard flourecence intensity bead measurements performed using different methods (flow cytomtry and quantitative microscopy: raw 2D, raw 3D, and deconvovled 3D). Thin lines are linear regessions, thick line in Figure c is quadratic regression. Figure **d** presents the same data as **c**, but excluding the lowest intensity flourescent beads.

$$E_{ir} + E_{or} = E_{id} + E_{od} \quad (4)$$

which can be expressed as:

$$E_{or} - E_{od} = E_{id} - E_{ir} \quad (5)$$

The dispersion difference between Figures 2a and 2b indicates that for two cells with a very similar raw 2D measurement, the difference for each cell between deconvolved 3D (E_{id}) and raw 3D (E_{ir}) values may be quite substantial. Taking into account Eq. (5), this dispersion difference also means that the difference of energy outside the VOI in the raw image

Table 2. Slopes of linear regressions relating 2D and 3D measurements of fluorescent beads of different sizes

SLOPES	2.5 μm	6 μm	15.4 μm
Raw 2D vs. Raw 3D	10.23 (10.09, 10.41)	15.31 (13.98, 16.92)	20.77 (20.51, 21.04)
Raw 2D vs. Dec. 3D	18.92 (18.07, 19.71)	23.98 (16.43, 30.99)	43.31 (22.53, 56.88)

In brackets are the bootstrapped 95% confidence intervals of these slopes. The bootstrapped confidence intervals are of the bias-corrected accelerated percentile (Bca) type and are based on 10,000 bootstrap replicates (see Materials and Methods for more detail).

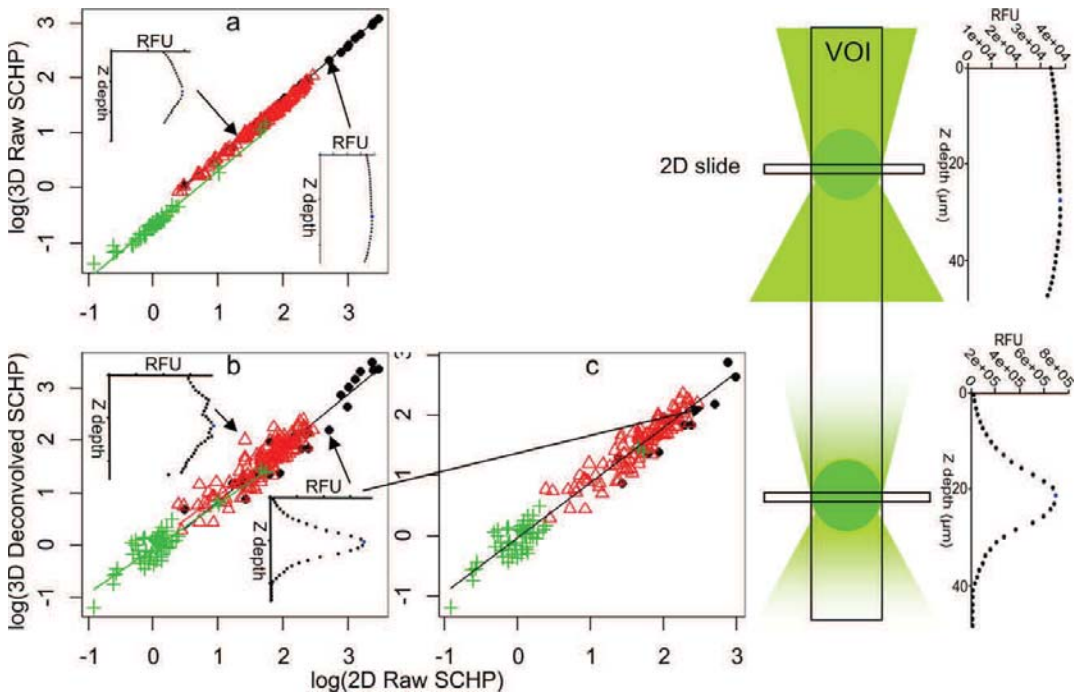

Figure 2. Right: Schema of the lateral view of a raw cell (top) and a well deconvolved cell (bottom), and their respective intensity profiles. Horizontal rectangles represent in-focus 2D slides, the vertical one represents the volume of interest (VOI) for 3D fluorescence measurements. Left: Comparison of three different IA fluorescence quantification methods using the log of SCHP (fmol ELFA·cell^{-1}) of phytoplankton cells (**a** and **b**). Graph c is the same as graph b but excludes inefficient deconvolved cells. Small (green cross), medium (red triangle), and large cells (black circle). The intensity profiles of a well deconvolved cell and an inefficiently deconvolved cell are embedded in graphs a (raw) and b (deconvolved profiles). The arrows point out the position of these two example cells. [Color figure can be viewed in the online issue, which is available at wileyonlinelibrary.com.]

(E_{or}) minus energy outside the VOI in the deconvolved image (E_{od}) differs between cells. Because the first element of the difference (E_{or}) is proportional to the degree of out-of-focus light and the second (E_{od}) is inversely proportional to the efficiency of deconvolution, we argue that the increase in dispersion observed when deconvolving could be due to either the original amount of acquired out-of-focus light, the efficiency of deconvolution or a combination of both. To further deepen our knowledge on this subject, we conducted a cell-by-cell inspection of the intensity profile of their VOI along the *Z* axis (Fig. 2). Only cells with sharp profiles, indicative of efficient deconvolution, were considered while those with inefficient deconvolution were excluded from the analysis (Fig. 2c). (A total of 175 cells out of 212 were analyzed). Thus, the increase in dispersion can be caused by actual differences in the amount of out-of-focus light between individual cells and not by any artifact introduced by deconvolution. As the magnitude of dispersion was virtually identical (Figs. 2b and 2c), we were able to confirm that for a given value in raw 2D (or 3D), a range of values spanning one order of magnitude was recorded by deconvolved 3D. Therefore, raw SCHP measurements (used to calculate the population averages reported in recent studies) may be biased by up to one order of magnitude since out-of-focus light was not taken into account.

Because we used mismatching immersion oil ($n = 1.516$ at 23°C) and embedding Citifluor AF1 ($n = 1.4628$ at 22°C), it could be hypothesized that the increase in dispersion observed between raw and deconvolved results (Figs. 2a and 2b) was also explained by the fact of having imaged under spherical aberration (SA) conditions. SA implies both, a strong decay in signal intensity as the focal plane is moved into the sample (depth aberration) and a challenge to efficient deconvolution. Nevertheless, only the former effect was to be taken into account because efficient deconvolutions triggering sharp and symmetric fluorescence intensity profiles where achieved thanks to a series of pre-deconvolution treatments (accurate image cropping to accommodate all the out-of-focus light, instable illumination correction, and correction of bleaching- and SA-induced fluorescence intensity decline in depth) together with a SA correction mechanism in Huygens Professional software (where the PSF was resized, and the whole image stack was splitted into a series of bricks along the *Z* axis to be able to apply different PSF to them). In the case that such dispersion was induced by SA the cells with high

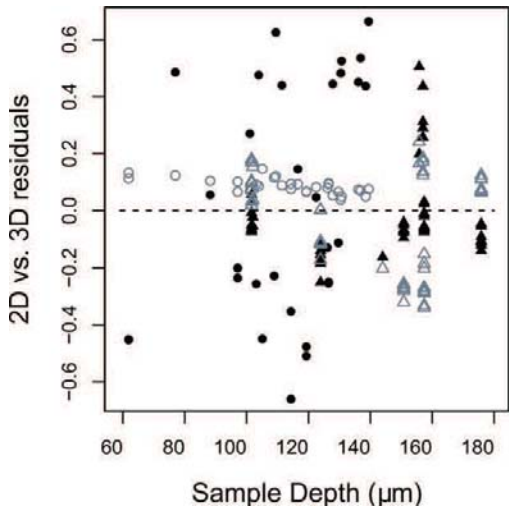

Figure 3. Relationship between sample depth (or distance to the coverslide) of 2.5 μm (triangles) and 15 μm (circles) fluorescent beads, and the residuals of linear regressions relating their raw 2D and raw 3D (grey) or raw 2D and deconvolved 3D (black) fluorescence intensities. [Color figure can be viewed in the online issue, which is available at wileyonlinelibrary.com.]

residuals in the 2D vs. deconvolved 3D regression should be those closer to the coverslide because the loss of fluorescence intensity with depth is steeper there, and hence the predeconvolution bleaching (and SA) correction may increase more the whole 3D image intensity. Sample depth was recorded just for big and small beads, and we found that fifteen µm fluorescent beads also showed this increase in dispersion when deconvolved but there wasn't any significant correlation between sample depth and the residuals (Fig. 3). Therefore, difference in the dispersion between raw and deconvolved data does not seem to be caused by SA, either.

Additionally, we compared beads and cells to check whether morphology could be responsible for some of the unexplained variation. The adjusted R-squared of linear regressions relating 2D and 3D measurements decreased when 3D was deconvolved, i.e. the unexplained variation increased. Concretely, the unexplained variation increase was high for 15 µm beads, intermediate in the three populations of cells (large, medium, and small) with diverse morphology (including diatoms, dinoflagellates, chrysophytes, and chlorophytes), and small in the case of 2.5 µm beads. Hence, morphology might not be an important driver of unexplained variation.

To assess the impact of the cell area on the relationship between 2D and 3D fluorescence intensity measurements, we developed a specific model. Because 2D and 3D measurements are different ways of measuring fluorescence intensity, these variables were highly correlated. Log of area vs. log of raw 3D fluorescence intensity and log of area vs. log of deconvolved 3D fluorescence intensity had partial correlation coefficients of 0.997 and 0.93, respectively. Because of this high degree of collinearity, partial regression was selected as the best approach to forecast raw ($Raw3D_0$) or deconvolved ($Dec3D_0$) 3D measurements from new area ($Area_0$) and 2D measurements ($Raw2D_0$). The e subindices ($_e$) correspond to estimated intermediate variables necessary to resolve the equation system. The functions we obtained, as the log of area (μm^2) and log of fluorescence intensity expressed as SCHP (fmol ELFA·cell^{-1}), were:

$$\begin{aligned} Raw2D_e &= Raw2D_0 - (-1.482449 + (1.329476 \cdot Area_0)) \\ Raw3D_e &= 1.255279 \cdot 10^{-17} + (1.026991 \cdot Raw2D_e) \\ Raw3D_0 &= Raw3D_e + (-2.406128 + (1.514223 \cdot Area_0)) \end{aligned} \quad (6)$$

And in the case of deconvolved 3D:

$$\begin{aligned} Raw2D_e &= Raw2D_0 - (-2.259155 + (1.725148 \cdot Area_0)) \\ Dec3D_e &= 2.037851 \cdot 10^{-17} + (8.952034e\text{-}01 \cdot Raw2D_e) \\ Dec3D_0 &= Dec3D_e + (-2.145553 + (1.600514 \cdot Area_0)) \end{aligned} \quad (7)$$

Then, we calculated adjusted R-squared to clarify whether the addition of object size (*Area*) provided any improvement in the explanation of variation relative to a simple linear regression that excluded object size. The results showed that for the forecast of raw 3D, we explained 99.5% of the variation when using a linear regression without the *Area* variable, whereas the explained variation increased to 99.7% when the *Area* variable was included in the partial regression. In contrast, for the forecast of deconvolved 3D, the inclusion of the *Area* variable slightly decreased the explained variation (from 95.4 to 95.3%). The partitioning of variation is summarized in Table 3, and confirms the results based on different size beads: object size slightly biases raw 2D measurements when compared to raw 3D, but this size effect is masked when compared to deconvolved 3D because the increase in unexplained variation (4.5–0.2), which is attributable to deconvolution, is almost 150 times greater than the variation explained by object size alone (0.03).

Here again, we could hypothesize that the slight impact of the cell area on the relationship between 2D and 3D fluorescence intensity measurements (Fig. 2a) was influenced by

Table 3. Proportions of variation of raw and deconvolved 3D values (R^2)

	VARIATION EXPLAINED BY RAW 2D	VARIATION EXPLAINED BY RAW 2D AND AREA	VARIATION EXPLAINED BY AREA	UNEXPLAINED VARIATION
Raw 3D	33.5%	66.1%	0.2%	0.2%
Deconvolved 3D	28.9%	66.6%	0.03%	4.5%

Table 4. Percentage between the apparent raw 2D SCHP simulated for five ideal spherical cells (from 2 to 32 μm diameter) with the same deconvolved 3D SCHP value

	32 μm	16 μm	8 μm	4 μm	2 μm
32 μm	100	109	119	130	142
16 μm	92	100	109	119	130
8 μm	84	92	100	109	119
4 μm	77	84	92	100	109
2 μm	71	77	84	92	100

The table is to be read from columns to rows. For instance: in raw 2D SCHP values, a 2 μm diameter cell seems to have a 142% of the ELFA of a 32 μm cell with the same deconvolved 3D SCHP value. Inversely, a 32 μm cell seems to have the 71% of the ELFA of a 2 μm cell with the same deconvolved 3D SCHP value.

the fact of having imaged under SA conditions. To test this hypothesis, we used *in silico* modeling. The behavior of the ratio between raw 2D and raw 3D fluorescence intensity values (2D/3D) was observed for typical intensity profiles of small and big objects at different distances to the coverslide. As we mentioned above, the decline of fluorescence intensity in depth caused by SA is steeper in the first micrometers and more moderate at deeper positions in the sample. This triggered two observable phenomena: (i) the 2D/3D was slightly smaller than in the cases where the decline was lineal or where there wasn't any decline, and (ii) the 2D/3D relationship diminished more intensely when the non-aberrated intensity profile of the object was flatter (not sharply unimodal), but mainly diminished when the imaged object was closer to the coverslide (steeper loss of intensity). Because big cells usually have flatter intensity profiles than small cells, it was expectable that big cells had smaller 2D/3D than small cells (as it was observed in Fig. 2a), and especially when the cells were close to the coverslide. Therefore, it is possible that SA contributed to some extent to the apparent size effect, although it would be quantitatively modest according to the model (to a maximum of about 5% in an extreme case).

To assess the bias induced by cell size in raw 2D single-cell enzyme activity measurements, raw 2D SCHP were determined for five ideal spherical cells ranging from 2 to 32 μm diameter and having the same deconvolved 3D SCHP value by using Eq. (7). The different raw 2D values of these cells were compared in pairs and the comparison was expressed as a percentage (Table 4). If cells with 2 and 32 μm in diameter were compared in raw 2D (the most extreme case), it could seem that the larger cell had 71% of the SCHP of the small cell (i.e., the small cell had 142% of the SCHP of the large cell), while they would have the same value in deconvolved 3D according to our model.

Species Level Analysis

In the analysis of natural populations or species, it is interesting to assess the population- or species-specific functional variability as well as the average SCPA. Three selected species of lake phytoplankton were analyzed for SCHP to estimate enzymatic functional variability by the three techniques (raw 2D and raw or deconvolved 3D) (Fig. 4). Similar dispersions were recorded and the homogeneity of variances between raw 2D and deconvolved 3D measurements was statistically confirmed using Levene's test (Table 5). Although the medians were similar in raw 2D and deconvolved 3D, the means were significantly different in most cases (Wilcoxon test; Table 5). Raw 3D provided clearly lower values (Fig. 4). The mean SCPA measured by the classic raw 2D method was 17.23 fmol·cell^{-1}·h^{-1} in *Amphidinium* sp., 0.3786 fmol·cell^{-1}·h^{-1} in *Cyclotella* sp.1, and 32.43 fmol·cell^{-1}·h^{-1} in *Cyclotella* sp.2.

Discussion

Deconvolved 3D is the Best Estimate

Deconvolved 3D was considered our best estimate of fluorescence intensity because it generally improved the management of out-of-focus light (which significantly increases the total measured fluorescence intensity) without introducing any detectable error. On the one hand, the biggest difference driven by deconvolution in fluorescence intensity measurements was a substantial increase in the dispersion of 2D vs. 3D measurements (Fig. 2b relative to 2a). Therefore, dealing with out-of-focus light (performing restorative deconvolution) is more important than correcting the eventual size effect or using raw 3D microscopy alone. The contribution of out-of-focus light to total variation in the 2D vs. 3D measurements was visibly more important (changes in overall dispersion from Fig. 2a relative to 2b) than that due to size effect (changes in 2D to 3D relationship between size groups in Figs. 2a and 2b). Specifically, out-of-focus light may account for 4.3% of the total variation on top of the 0.03 or 0.2% due to object size. On the other hand, we showed that this difference in dispersion mainly reflected real changes in the amount of out-of-focus light per cell and therefore should not be regarded as a deconvolution artifact or a spherical aberration effect (Figs. 2b, 2c, and 3). In summary, absolute and relative values (magnitude and dispersion) obtained by deconvolved 3D should be considered as the most reliable estimate of real values.

Raw 2D and Deconvolved 3D are Equivalent Methods in the Case of Population Characterization

We found that since current raw 2D quantifications do not take out-of-focus light into account, they may produce single-cell measurements that are half an order of magnitude above or below our best estimate of fluorescence intensity via deconvolved 3D. Nevertheless, these individual errors in raw 2D measurements were partially compensated when we attempted to describe mean cell activity and functional variability of one or several species (Fig. 4) or groups of cells (Fig. 2). If 25–40 cells per species were measured in raw 2D, the obtained SD did not differ significantly from that of deconvolved 3D, and the slight (but significant) difference in means was not significantly affected by sample size either, with a confidence level of 99.99% (Table 5) (see methods for more detail). A minimum of 141 cells had to be measured to achieve

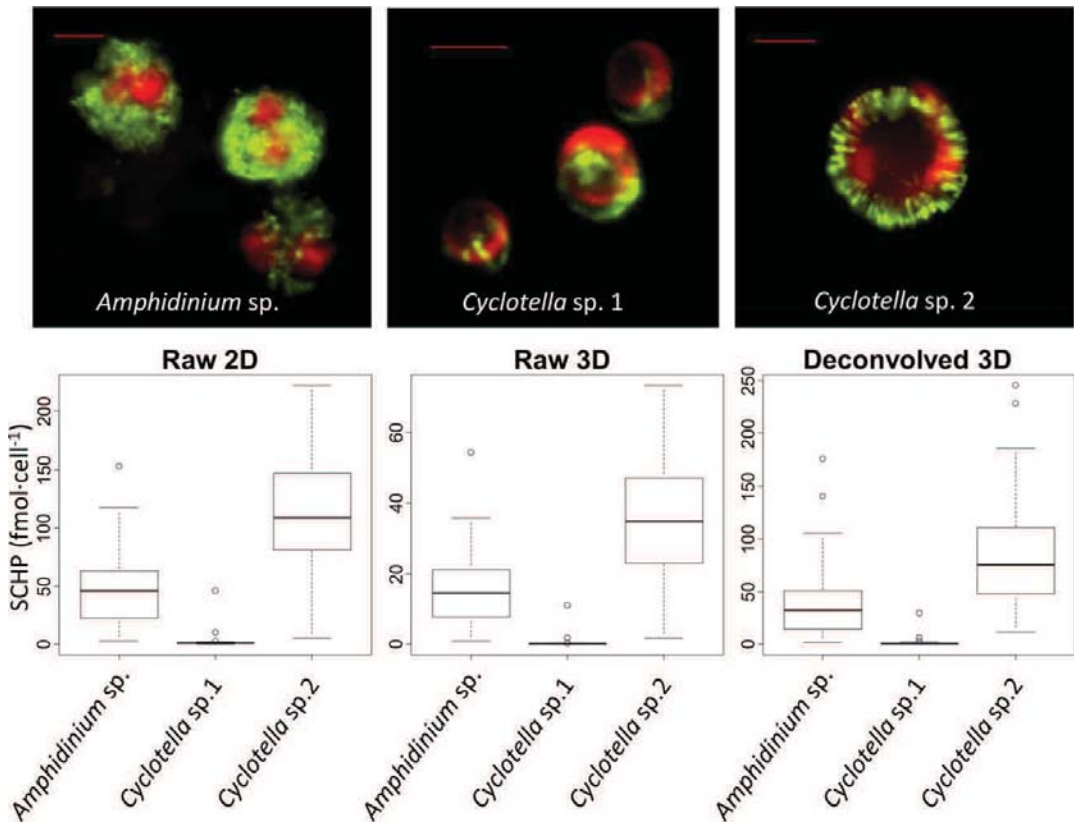

Figure 4. Epifluorescence microimages of three phytoplankton species. Red: chloroplasts; Yellow-green: ELFA precipitates indicating phosphatase activity. Scale bars are 5 μm long. Single cell hydrolysed phosphate (SCHP) of the three separate phytoplankton populations, measured using the three IA quantification methods. [Color figure can be viewed in the online issue, which is available at wileyonlinelibrary.com.]

a reliable result in groups of more heterogeneous cells (like a community). Thus, the measurement in raw 2D of a minimum of 25–40 cells per species provides sufficiently similar average values and ranges to deconvolved 3D.

Cell Size Modulates 2D Measurement Bias

Although deconvolved 3D was the best method tested, the results from raw 3D are also interesting since they show that cell size contributed substantially to the overall bias recorded by the raw 2D method. When object size was introduced into the model of raw 3D depending on raw 2D, adjusted R-squared (total explained variability) improved from 0.995 to 0.997. This suggests that object size modulates the raw 2D bias in relation to raw 3D. The apparent paradox is that when we modelled deconvolved 3D depending on raw 2D, the inclusion of object size did not increase the adjusted R-squared. As pointed out in the first paragraph of the discussion, we interpret this as showing that

Table 5. Wilcoxon and Levene tests for comparison of means and homogeneity of variances between raw 2D and deconvolved 3D fluorescence intensity measurements in the three selected species and the whole set of efficiently deconvolved cells

N	SPECIES	SIZE	MEAN (P-V)	SD (P-V)	MINIMUM SAMPLING SIZE (NUMBER OF CELLS)
175	All	All	$\neq (3.075 \times 10^{-14})$	$= (0.4598)$	141
53	*Amphidinium* sp.	Medium (14 µm)	$\neq (0.0004)$	$= (0.8421)$	39
54	*Cyclotella* sp.1	Small (~6 µm)	$= (0.0761)$	$= (0.6858)$	37
35	*Cyclotella* sp.2	Medium (14 µm)	$\neq (1.106 \times 10^{-9})$	$= (0.1360)$	26

object size contributes to the fluorescence intensity bias measured in raw 2D but is clearly a less important source of variability when compared to deconvolution. These observations were essentially not undermined by having imaged under SA. According to our partial regression, comparison of raw 2D ELFA values of different species or populations of different cell sizes should be carefully interpreted: for instance, a 16 μm diameter cell could appear to have 84% of the ELFA of a 4 μm cell in raw 2D, while they would be identical in deconvolved 3D (Table 4).

If we take raw 3D as a reference (Fig. 2a), we can graphically observe the effect of object size on 2D fluorescence intensity measurements even when we consider this variable in discrete groups of small, medium and large cells. The simple regression lines of the three size groups showed different intercepts (relationship between 2D and 3D measurements depended on cell size). Moreover, we observed a nonlinearity in this size effect: the distance between the intercepts of the regression lines of small and medium cells was greater than that between the medium and large cells (∼6, 14, and 40 μm of object diameter respectively). (Note that object sizes—the projection in the XY plane of the defined VOI—are always proportional but slightly larger than the actual cell size). Having said that object size was not the major biasing factor, we must note that most of the phytoplankton cells in oligotrophic marine and freshwater systems are frequently of small to medium size (50–52), a range in which object size bias might be more important.

Finally, deconvolution did not affect all cell sizes in the same way. When we deconvolved, the simple linear regression intercepts of all three size groups moved towards zero, but the smaller the cell, the bigger the effect of deconvolution. In this respect, the percentage of inefficient deconvolutions was the highest in larger cells. These results suggest that deconvolution may be more efficient for small and medium cells than for very large ones. Nevertheless, after checking for deconvolution efficiency, all the values of efficiently deconvolved cells were equally reliable whatever their size.

Future Quantification of Cells with Low Phosphatase Activity

The fluorescence intensity measurements of weakly fluorescent objects were the most affected by deconvolution. This resulted in a quadratic relationship between deconvolved 3D and raw 2D (Figs. 1c and 1d), but deconvolved 3D was the method that measured the most similar values to flow cytometry and manufacturer values for the standard 0.22% (weak fluorescence) intensity beads (Table 1). Deconvolved 3D was also reported as the most accurate quantification method for low intensity objects in the literature (35), although we did not observe such improvement. In practice, the 0.22% intensity beads recorded average fluorescence intensities (FU) like those that would produce the low ELFA amounts of: 0.35 ± 0.07 fmol in raw 2D, 0.05 ± 0.01 fmol in raw 3D, or 0.92 ± 0.45 fmol in deconvolved 3D (0.071 ± 0.014 fmol·μm^{-2}, 0.010 ± 0.002 fmol·μm^{-2}, and 0.187 ± 0.092 fmol·μm^{-2}, respectively). Therefore, non-linearity is a phenomenon that is restricted to the smallest values of SCHP, which constitutes a minor problem in the current state-of-the-art. Although reported SCHP values ranged from 0 to 1831 fmol·cell^{-1} (53), including the nonlinear range of fluorescence intensity, in current state-of-the-art, small amounts of fluorescence originating from fluorochromes in the sample other than ELFA (DAPI, degraded chlorophyll autofluorescence, etc.) may show overlap of their emission tails with the ELFA emission peak window and may account for a significant proportion when object ELFA intensity is very low. Therefore, the cells with the lowest amount of activity cannot be accurately quantified nor distinguished from completely inactive cells when DAPI or degraded chlorophyll is present in the sample. To avoid this problem, we suggest that raw 3D images should be deconvolved with an algorithm that, apart from modeling light blur, also models the spectral overlap of different fluorochromes (41). In that scenario, the question why is there a rupture of linearity between the dimmest and the intermediate fluorescent beads when measured via deconvolved 3D in comparison to the other methods should be addressed. Such phenomenon seems to be robust because it was not only observed in this study but also in Swedlow et al. (35).

Improvement of the FLEA Technique

One of the weaknesses that Nedoma et al. detected in the FLEA technique (29) was the intercalibration of a microscope with a fluorimeter, i.e., the conversion of microscope FU to fmols of ELFA. The conversion factor is the slope of a linear regression that relates the rate of ELFA formation during the linear phase of an incubation measured by a fluorimeter (in fmol·l^{-1}·h^{-1}, on the *X* axis) and by raw 2D image analysis (in FU·l^{-1}·h^{-1}, on the *Y* axis). Thus, each point on the graph represents a single incubation. The problem is that the r^2 of the regression line is about 0.65. Because the range of ELFA formation rates is already quite wide, we argue that there are other sources of the dispersion of the different incubations in the mentioned graph. First, quantitative microscopy may underestimate ELFA particles <0.2 μm because the incubated sample is filtered by polycarbonate (PC) filters of the same pore size, whereas ELFA particles of all sizes are measured by fluorimetry. Thus, dispersion could be due to differences in the proportion of small ELFA particles between different incubated samples. Second, using raw 2D images may be another source of variability. Current raw 2D images of filters acquired to calculate the conversion factor (ConvF) are focused to the plane with the highest amount of fluorescence, but this compromise undersamples fluorescence for three reasons: only one optical slice of large objects is acquired, only one optical slice of the out-of-focus light of objects (usually >10 μm deep) is acquired, and not all objects in a frame are usually well focused because some may detach from the PC filter during sample mounting, and more important, because rippling or mispositioning (not strictly orthogonal) of the PC filter may occur. The proposed deconvolved 3D method for FLEA quantification is expected to significantly improve this critical step in the FLEA technique.

In conclusion, deconvolved 3D FLEA measurements provide superior analytical power and are recommended to distinguish cells with SCPA differing by less than an order of magnitude. They also avoid problems of comparability between different size cells and, finally, they are the most appropriate option in those cases where the value of each single cell is important rather than the average of a population of cells. This is the case for measurements of activity in less numerous species and in the combination of the FLEA technique with other single-cell techniques. The deconvolved 3D FLEA technique alone will provide accurate information about a relevant component of trophic strategy, the enzymatic pathway, which should be incorporated into studies of biological traits that could be important for the fitness of species (54). This will aid in reconstructing the evolutionary history of the trophic strategy, defining the functional niche of many microplanktonic species, and better understanding and modeling of the dynamics of enzyme activity in nature. In addition, the deconvolved 3D FLEA technique improves the accuracy of the FLEA technique at the cell level enough to make it combinable with microautoradiography or MAR-FISH for single-cell nutrient incorporation, and with FLBs or CARD-FISH for single-cell bacterivory assessments. Such technical integrations may provide information about detailed biogeochemical processes such as the link between hydrolytic enzyme activity and nutrient uptake at the cellular level and in close-to-*in situ* conditions, but also about functional shifts in trophic strategies within mixotrophic populations of the microbial loop.

Acknowledgments

This research involved collaboration between the Limnology Group (CEAB-UB) and the Aquatic Microbial Ecology Department (HBI, CAS). The authors thank Dr. Jiři Nedoma for technical support during image acquisition and image analysis, and Mrs. Mireia Utzet and Dr. Francesc Carmona for statistical advice. All the authors state that they do not have any conflict of interests to declare.

Literature Cited

1. Clark LL, Ingall ED, Benner R. Marine phosphorus is selectively remineralized. Nature 1998;393:426.
2. Kolowith LC, Ingall ED, Benner R. Composition and cycling of marine organic phosphorus. Limnol Oceanogr 2001;46:309–320.
3. Reitzel K, Ahlgren J, Gogoll A, Jensen HS, Rydin E. Characterization of phosphorus in sequential extracts from lake sediments using P-31 nuclear magnetic resonance spectroscopy. Can J Fish Aquat Sci 2006;63:1686–1699.
4. Bai X, Ding S, Fan C, Liu T, Shi D, Zhang L. Organic phosphorus species in surface sediments of a large, shallow, eutrophic lake, Lake Taihu, China. Environ Pollut 2009;157:2507–2513.
5. Luo H, Zhang H, Long R, Benner R. Depth distributions of alkaline phosphatase and phosphonate utilization genes in the North Pacific Subtropical Gyre. Aquat Microb Ecol 2011;62:61–69.
6. Schindler DW. Evolution of phosphorus limitation in lakes. Science 1977;195:260–262.
7. Thingstad TF, Rassoulzadegan F. Nutrient limitations, microbial food webs, and biological C-pumps—Suggested interactions in a P-limited Mediterranean. Mar Ecol Prog Ser 1995;117:299–306.
8. Perry MJ. Phosphate utilization by an oceanic diatom in phosphorus-limited chemostat culture and in the oligotrophic waters of the central North Pacific. Limnol Oceanogr 1976;21:88–107.
9. Vidal M, Duarte CM, Agustí S, Gasol JM, Vaqué D. Alkaline phosphatase activities in the central Atlantic Ocean indicate large areas with phosphorus deficiency. Mar Ecol Prog Ser 2003;262:43–53.
10. Reich PB, Oleksyn J. Global patterns of plant leaf N and P in relation to temperature and latitude. Proc Natl Acad Sci USA 2004;101:11001–11006.
11. Elser JJ, Andersen T, Baron JS, Bergström A-K, Jansson M, Kyle M, Nydick KR, Steger L, Hessen DO. Shifts in lake N:P stoichiometry and nutrient limitation driven by atmospheric nitrogen deposition. Science 2009;326:835–837.
12. Sinsabaugh RL, Carreiro MM, Repert DA. Allocation of extracellular enzymatic activity in relation to litter composition, N deposition, and mass loss. Biogeochemistry 2002;60:1–24.
13. Edwards I, Zak D, Kellner H, Eisenlord S, Pregitzer K. Simulated atmospheric N deposition alters fungal community composition and suppresses ligninolytic gene expression in a Northern Hardwood forest. PLoS One 2011;6:1–10.
14. Yamada N, Tsurushima N, Suzumura M. Effects of seawater acidification by ocean CO(2) sequestration on bathypelagic prokaryote activities. J Oceanogr 2010;66:571–580.
15. Piontek J, Lunau M, Haendel N, Borchard C, Wurst M. Acidification increases microbial polysaccharide degradation in the ocean. Biogeosciences 2010;7:1615–1624.
16. Sardans J, Penuelas J, Estiarte M. Seasonal patterns of root-surface phosphatase activities in a Mediterranean shrubland. Responses to experimental warming and drought. Biol Fertil Soils 2007;43:779–786.
17. Wallenstein M, Allison S, Ernakovich J, Steinweg JM, Sinsabaugh R. Controls on the temperature sensitivity of soil enzymes: A key driver of in situ enzyme activity rates. Soil Biol 2011;22:245–258.
18. Boavida M-JJ, Wetzel RG. Inhibition of phosphatase activity by dissolved humic substances and hydrolytic reactivation by natural ultraviolet light. Freshw Biol 1998;40:285–293.
19. Espeland EMM, Wetzel RGG. Complexation, stabilization, and UV photolysis of extracellular and surface-bound glucosidase and alkaline phosphatase: Implications for biofilm microbiota. Microb Ecol 2001;42:572–585.
20. Tank SE, Xenopoulos MA, Hendzel LL. Effect of ultraviolet radiation on alkaline phosphatase activity and planktonic phosphorus acquisition in Canadian boreal shield lakes. Limnol Oceanogr 2005;50:1345–1351.
21. Steen AD, Arnosti C. Long lifetimes of beta-glucosidase, leucine aminopeptidase, and phosphatase in Arctic seawater. Mar Chem 2011;123:127–132.
22. González-Gil S, Keafer BA, Jovine RVM, Aguilera A, Lu S, Anderson DM. Detection and quantification of alkaline phosphatase in single cells of phosphorus-starved marine phytoplankton. Mar Ecol Prog Ser 1998;164:21–35.
23. Lauro F, McDougald D, Thomas T, Williams T, Egan S. The genomic basis of trophic strategy in marine bacteria. Proc Natl Acad Sci USA 2009;106:15527–15533.
24. Christie-Oleza JA, Piña-Villalonga JM, Bosch R, Nogales B, Armengaud J. Comparative proteogenomics of twelve Roseobacter exoproteomes reveals different adaptive strategies among these marine bacteria. Mol Cell Proteom 2012;11:1–12.
25. Ou L, Huang B, Lin L, Hong H, Zhang F, Chen Z. Phosphorus stress of phytoplankton in the Taiwan Strait determined by bulk and single-cell alkaline phosphatase activity assays. Mar Ecol Ser 2006;327:95–106.
26. Carlsson P, Caron DA. Seasonal variation of phosphorus limitation of bacterial growth in a small lake. Limnol Oceanogr 2001;46:108–120.
27. Nedoma J, Vrba J. Specific activity of cell-surface acid phosphatase in different bacterioplankton morphotypes in an acidified mountain lake. Environ Microbiol 2006;8:1271–1279.
28. Duhamel S, Gregori G, Van Wambeke F, Nedoma J. Detection of extracellular phosphatase activity at the single-cell level by enzyme-labeled fluorescence and flow cytometry: The importance of time kinetics in ELFA labeling. Cytom A 2009;75A:163–168.
29. Nedoma JJ, Štrojsová A, Vrba J, Komárková J, Šimek K, Strojsova A, Komarkova J, Simek K. Extracellular phosphatase activity of natural plankton studied with ELF97 phosphate: Fluorescence quantification and labelling kinetics. Environ Microbiol 2003;5:462–472.
30. Litchman E, Klausmeier CA. Trait-based community ecology of phytoplankton. Annu Rev Ecol Evol Syst 2008;39:615–639.
31. Litchman E, Klausmeier CA, Schofield OM, Falkowski PG. The role of functional traits and trade-offs in structuring phytoplankton communities: Scaling from cellular to ecosystem level. Ecol Lett 2007;10:1170–1181.
32. Allison SD. A trait-based approach for modelling microbial litter decomposition. Ecol Lett 2012;15:1058–1070.
33. Andrews PD, Harper IS, Swedlow JR. To 5D and beyond: Quantitative fluorescence microscopy in the postgenomic era. Traffic 2002;3:29–36.
34. Verveer PJ, Gemkow MJ, Jovin TM. A comparison of image restoration approaches applied to three-dimensional confocal and wide-field fluorescence microscopy. J Microsc 1999;193:50–61.
35. Swedlow JR, Hu K, Andrews PD, Roos DS, Murray JM. Measuring tubulin content in *Toxoplasma gondii*: A comparison of laser-scanning confocal and wide-field fluorescence microscopy. Proc Natl Acad Sci USA 2002;99:2014–2019.
36. Murray JM, Appleton PL, Swedlow JR, Waters JC. Evaluating performance in three-dimensional fluorescence microscopy. J Microsc 2007;228:390–405.
37. Barlow AL, Guerin CJ. Quantization of widefield fluorescence images using structured illumination and image analysis software. Microsc Res Tech 2007;70:76–84.
38. Wallace W, Schaefer LH, Swedlow JR. A workingperson's guide to deconvolution in light microscopy. Biotechniques 2001;31:1076–1097.
39. McNally JG, Karpova T, Cooper J, Conchello JA. Three-dimensional imaging by deconvolution microscopy. Methods 1999;19:373–385.
40. Swedlow JR. Quantitative fluorescence microscopy and image deconvolution. Methods Cell Biol 2007;81:447–465.

41. Hoppe AD, Swanson JA Shorte SL. Three-dimensional FRET microscopy Periasamy A, So PTC, editors. Proc SPIE Int Soc Opt Eng 2006;6089:1–9.
42. Selinummi J, Niemisto A, Saleem R, Carter G, Aitchison J, Yli-Harja O. A case study on 3D reconstruction and shape description of peroxisomes in yeast. 2007 IEEE International Conference on Signal Processing and Communications (ICSPC 2007), 24-27 November 2007, Dubai, United Arab Emirates 2008:672–675.
43. Huang K, Murphy RF. From quantitative microscopy to automated image understanding. J Biomed Opt 2004;9:893–912.
44. Diaz-de-Quijano D, Felip M. A comparative study of fluorescence-labelled enzyme activity methods for assaying phosphatase activity in phytoplankton. A possible bias in the enzymatic pathway estimations. J Microbiol Methods 2011;86:104–107.
45. Davison AC, Hinkley D V. Bootstrap Methods and their Application. Cambridge: Cambridge University Press; 1997. p 582.
46. Crawley MJ. Regression: Bootstrap with Regression. Chichester: Wiley; 2007. p 418–421.
47. Model MA, Burkhardt JK. A standard for calibration and shading correction of a fluorescence microscope. Cytometry 2001;44:309–316.
48. Hiraoka Y, Sedat JW, Agard DA. The use of a charge-coupled device for quantitative optical microscopy of biological structures. Science 1987;238:36–41.
49. R_Development_Core_Team. R: A language and environment for statistical computing team RDC, editor. R Found Stat Comput 2011;1:409.
50. Duarte CM, Agustí S, Canfield DE. Size plasticity of fresh-water pytoplankton: Implications for community structure. Limnol Oceanogr 1990;35:1846–1851.
51. Sarmento H. New paradigms in tropical limnology: The importance of the microbial food web. Hydrobiologia 2012;686:1–14.
52. Chen B, Liu H. Relationships between phytoplankton growth and cell size in surface oceans: Interactive effects of temperature, nutrients, and grazing. Limnol Oceanogr 2010;55:965–972.
53. Novotná J, Nedbalová L, Kopáček J, Vrba J. Cell-specific extracellular phosphatase activity of Dinoflagellate populations in acidified mountain lakes. J Phycol 2010;46:635–644.
54. Green JL, Bohannan BJM, Whitaker RJ. Microbial biogeography: From taxonomy to traits. Science 2008;320:1039–1043.